UNIVERSITY OF SOUTHAMPTON

FACULTY OF MEDICINE, HEALTH & LIFE SCIENCES

School of Medicine

The molecular mechanisms involved in rhinovirus-induced asthma exacerbation and its potential therapy

by

Nicole Bedke

Thesis submitted for the degree of Doctor of Philosophy

January 2010

UNIVERSITY OF SOUTHAMPTON

ABSTRACT

FACULTY OF MEDICINE, HEALTH & LIFE SCIENCES

SCHOOL OF MEDICINE

Doctor of Philosophy

THE MOLECULAR MECHANISMS INVOLVED IN RHINOVIRUS-INDUCED ASTHMA EXACERBATION AND ITS POTENTIAL THERAPY

by Nicole Bedke

Rhinovirus (RV) infection is a major cause of asthma exacerbation in children and adults. Previous studies have shown that primary bronchial epithelial cells (PBECs) obtained from asthmatic subjects have a deficient interferon (IFN) response against RV infection, the molecular mechanism of which is unknown (Wark *et al* 2005; Contoli *et al* 2006).

Initially it was hypothesised that this deficiency is inherent to other cell types in the airway, such as bronchial fibroblasts. In a rhinovirus infection model, it was shown that fibroblasts respond with a vigorous pro-inflammatory response. However this response was accompanied by no significant IFN response. Fibroblasts produced IFN when we treated with a synthetic double-stranded RNA. However, no differences were observed between normal and asthmatic cells, indicating that the deficient innate immune response in asthmatic epithelium is not inherent to other cell types. We suggest that *in vivo*, bronchial fibroblasts may contribute to the inflammatory state in asthma when infected with RV. This might occur when an epithelial cell barrier with disrupted tight junctions might allow penetration and infection of the underlying mesenchymal cell layer.

To investigate the innate immune response of asthmatic PBECs we hypothesised that the anti-inflammatory cytokine transforming growth factor beta (TGF-β) dampened the innate immune response against rhinovirus infection. It has been shown previously that TGF-β is elevated in asthmatics. It was found that PBEC cultures from asthmatic subjects produce significantly more endogenous TGF-β_2 compared to healthy controls. When PBECs from healthy donors were treated with exogenous TGF-β_2 it promoted RV replication, which was coupled with a decreased IFN response. Conversely, treatment of PBECs from asthmatic subjects with a neutralizing antibody against TGF-β decreased RV replication. These observations provide an interesting link between an anti-inflammatory environment in the asthmatic airways contributing to a defective innate immune response in asthma.

To understand the TGF-β-mediated effect on RV replication, the importance of src kinases as one of the upstream signaling molecules in TGF-β-dependent alterations of cellular physiology was investigated. We found that inhibitors of src, in particular the SU6656 compound, were very potent in inhibiting RV replication. Inhibition by SU6656 was coupled with a significant increase in IFN response. These findings may pave the way towards designing compounds of similar structure, which are able to augment the IFN response and therefore provide a new form of therapy against asthma exacerbation.

Table of Contents

Table of Contents 3
List of Figures 5
Acknowledgement 10
Abbreviations 11
Chapter 1: Introduction 14
Asthma: Definition and Features 14
Airway remodeling 15
Transforming Growth Factor –beta (TGF-β) 18
Asthma Therapy 22
Asthma Genetics 24
Asthma Exacerbation 26
Innate immune response against viral infection 28
Deficient innate immune response in asthma 35
Hypothesis 36
Chapter 2: Materials and Methods 37
Materials 37
Methods 40
Establishment of primary bronchial epithelial cells from bronchial brushings 40
Culture of primary bronchial fibroblasts 40
Patient characteristics of primary bronchial epithelial cell samples 41
Patient characteristics of primary bronchial fibroblasts samples 43
Growth of rhinovirus stocks 44
Rhinovirus inactivation using UV-irradiation 45
Infection of primary bronchial epithelial cells with rhinovirus-1B stock and treatment with reagents 45
Infection of primary bronchial fibroblasts with rhinovirus-1B stock 46
End point Dilution Assay 46
Treatment of primary epithelial cells and fibroblasts with inhibitors and Poly I: PolyC (Poly(I:C)) 47
Lactate Dehydrogenase (LDH) Assay 48
Interleukin-8 (IL-8) ELISA 48
TGF-β_2 ELISA 49
IFN-β ELISA 51
IL-29 ELISA 52

RNA extraction and reverse transcription 53
Real time-Quantitative PCR Analysis (RT-qPCR) 54
Protocols used for RT-qPCR 55
Gene Sequences of Primers and Probes 56
Transfection of small interfering RNAs (siRNAs) into PBECs 57
SDS-PAGE and Western Blotting 59
SDS-PAGE Western Blotting Buffers 61
Native Immunoprecipitation with RIPA Buffer 63
Co-immune precipitation Buffers 64
Caspase 3/7 Assay 65
Immunofluorescence staining of PBECs in chamber slides 65
Zenon labeling β 1 integrin antibody 66
Bacterial propagation of pUCT7-HRV16 66
Plasmid digestion with *SacI* and clean-up 68
Agarose gel electrophoresis 68
Generation of T7-HRV16 replicon transcripts 69
Electroporation of HeLa cells with HRV16 T7 transcripts 70
Statistical analysis 71
Chapter 3: Results 72
Contribution of bronchial fibroblasts to the anti-rhinoviral response in asthma 72
Chapter 4: Results 91
TGF-β promotes Rhinovirus-1B (RV1B) replication in Primary Bronchial Epithelial Cells (PBECs) by modulating the innate immune response 91
Chapter 5: Results 113
Neutralizing endogenous TGF-β in asthmatic PBECs reduces RV replication 113
Chapter 6: Results 137
Small molecule chemical inhibitors of src kinases inhibit rhinovirus replication through possible modulation of the innate immune response 137
Possible mechanisms by which the src kinase inhibitor SU6656 modulates the innate immune response 160
Chapter 7 178
Final Discussion and Future Work 178
Reference List 188

List of Figures

Figure 1-1. Pathological effects of different severities of asthma on the airways 15
Figure 1-2. Chronic allergic inflammation and tissue remodeling in asthma. 17
Figure 1-3. The TGF-β signaling pathway 21
Figure 1-4. The epithelial-mesenchymal trophic unit in asthma 22
Figure 1-5. Factors influencing the development of atopy and allergic inflammation 26
Figure 1-6. Chart peak flow recording and respiratory symptom scores 29
Figure 1-7. Structural analysis of the rhinovirus and its replication cycle 30
Figure 1-8. Type I IFN induction, signalling and action 34
Table 2.2-1. Patient characteristics for primary bronchial epithelial cells 41
Table 2.2-2. Patient characteristics for primary bronchial fibroblasts 43
Figure 2-1. Ohio Hela cells infected with RV-1B for 24 hours 45
Figure 2-2. IL-8 Standard curve 49
Figure 2-3. TGF-β_2 Standard curve 51
Figure 2-4. IFN-β Standard curve 52
Figure 2-5. IL-29 Standard curve 53
Table 2.2-3. Target sequences of siRNAs targeting Human src 58
Table 2.2-4. Target sequences of siRNAs targeting Human RNaseL 58
Table 2.2-5. Primary Antibodies used for Western Blotting 60
Table 2.2-6. Secondary Antibodies used for Western Blotting 61
Figure 2-6. pUCT7-HRV16 vector map. 67
Figure 2-7. pUCT7 plasmid vector linearized with *Sac I*. 69
Figure 2-8. T7 RNA transcripts visualized on a MOPS formaldehyde gel 70
Figure 3-1. Characterization of the responses of primary bronchial fibroblasts to RV infection. 73
Figure 3-2. The effects of RV1B on IL-8 and LDH released are time- and dose-dependent. 74
Table 3.1-1. Percentage inhibition of IL-6 and IL-8 mRNA by LY294002. 76
Figure 3-3. Viral replication in normal and asthmatic fibroblasts. 77
Figure 3-4. Induction of proinflammatory genes in response to RV1B infection. 78
Figure 3-5. Induction of TNF-α mRNA in response to RV1B infection. 79
Figure 3-6. Induction of RANTES and IFN-β in response to RV1B infection. 80
Figure 3-7. Kinetics and dose responses to Poly I:C. 82
Figure 3-8. IFN-β protects against RV1B infection. 85

Figure 3-9. Model for the contribution of bronchial fibroblasts to inflammation during a viral-induced asthma exacerbation. 86
Figure 4-1. Photomicrographs of PBECs from one healthy volunteer at 24 hours post-infection with RV1B in the presence or absence of TGF- β_2. 93
Figure 4-2. Photomicrographs of PBECs from one healthy volunteer at 48 hours post-infection with RV1B in the presence or absence of TGF- β_2. 94
Figure 4-3. Viral mRNA and $TCID_{50}$/ml from PBEC infected with RV1B and treated with TGF-β 96
Figure 4-4. $TCID_{50}$/ml of PBECs from healthy volunteers pre-treated for 24 hours with TGF-β followed by infection with RV1B 98
Figure 4-5. $TCID_{50}$/ml of PBECs from asthmatic patients were pre-treated with 10 ng/ml TGF- β_2 and infected with RV1B (MOI=0.01) as described in Figure 4-4. 99
Figure 4-6. Immunofluorescent staining of PBECs treated with TGF-β 101
Figure 4-7. Collagen I mRNA of PBECs from one healthy volunteer were infected with RV (MOI=0.01) and incubated for 24 in the presence or absence of TGF-β. 102
Figure 4-8. Caspase 3/7 activity of RV-infected PBECs in the presence or absence of TGF-β. 104
Figure 4-9. IFN-β protein levels were measured by ELISA from RV-infected PBECs after 48 hours p.i in the presence or absence of 10 ng/ml TGF-β (A). 106
Figure 4-10. IL-29 protein levels were measured by ELISA from RV-infected PBECs after 48 hours p.i in the presence or absence of 10 ng/ml TGF-β (A). 107
Figure 4-11. Control samples from normal and asthmatic PBEC cultures were analysed for baseline TGF- β_2. 108
Figure 5-1. Viral titres of infected PBECs from asthmatic patients that were pre-treated with 10 μg/ml neutralizing anti-TGF-β antibody for 24 hours. 114
Figure 5-2. Photomicrographs of PBEC from asthmatic patient at 24 hours post-infection with RV1B in the presence or absence of neutralizing pan anti-TGF-β antibody. 115
Figure 5-3. Photomicrographs of PBEC from asthmatic patient at 48 hours post-infection with RV1B in the presence or absence of neutralizing pan anti-TGF-β antibody. 116
Figure 5-4. LDH Assay of PBECs from one asthmatic subject were infected with RV (MOI=0.05) and incubated for 24 and 48 hours in the presence or absence of TGF-β or neutralizing TGF-β antibodies. 117

Figure 5-5. IFN-β protein levels relative to virus particles measured 48h p.i. in supernatants from RV-infected asthmatic PBECs that were treated with neutralizing anti-TGF-β antibodies or an IgG1 isotype control. 118
Figure 5-6. IFN-β and IL-29 protein levels of PBECs from 6 asthmatic donors that were treated with 0.1-10 μg/ml polyIC in the presence of neutralizing anti-TGF-β antibodies or an IgG isotype control and incubated for 24 hours. 119
Figure 5-7. The Smad3 and JNK/p38 pathway illustrating which signaling molecules we targeted using the Specific Inhibitor of Smad3 40 and p38 inhibitor (SB203580). Adopted from Zhang *Cell Research* 2009 120
Figure 5-8. Levels of infectious virus particles measured by an end-point dilution assay called $TCID_{50}$/ml of PBECs from 3 asthmatic donors were pre-treated for 1 hour with 1 or 5 μM Smad3 inhibitor SIS3 followed by infection with RV1B (MOI=0.01). 121
Figure 5-9. Viral RNA of PBECs from 3 asthmatic donors pre-treated with Smad-3 inhibitor 40 for 1 hour followed by infection with RV (MOI=0.01) and incubated for 8, 24 or 48 hours in the presence or absence of the inhibitor. 122
Figure 5-10. IFN-β mRNA of PBECs from 3 asthmatic donors pre-treated with Smad-3 inhibitor 40 for 1 hour followed by infection with RV as described in Figure 4-21. 123
Figure 5-11. Levels of infectious virus particles measured by an end-point dilution assay called $TCID_{50}$/ml from PBECs from 3 asthmatic donors were pre-treated for 1 hour with 1 or 5 μM p38 MAPK inhibitor (SB203580) followed by infection with RV1B (MOI=0.01). 124
Figure 5-12. Viral mRNA of PBECs from 3 asthmatic donors pre-treated with p38 inhibitor (SB203580) for 1 hour followed by infection with RV as described in..... 125
Figure 5-13. IFN-β mRNA of PBECs from 3 asthmatic donors pre-treated with p38 inhibitor (SB203580) for 1 hour followed by infection with RV as described in..... 126
Figure 5-14. IFN-β protein (A) and IL-29 protein levels (B) of PBECs from 5 asthmatic donors pre-treated with 5 μM SIS3 or SB203580 for 1 hour followed by treatment with polyIC at a concentration of 0.1 or 1 μg/ml and incubated for 24 hours. 128
Figure 5-15. Co-immuneprecipitation of STAT-1 protein with anti PIAS-1 antibodies using asthmatic PBECs treated with neutralizing anti-TGF-β antibodies or and isotype control. 131
Figure 5-16. STAT-1 and PIAS-1 protein bands from Figure 5-15 were quantified by densitometry and plotted as a ratio of STAT-1 to PIAS-1. 132

Figure 5-17. Co-immuneprecipitation of STAT-1 protein with anti PIAS-1 antibodies using non-asthmatic PBECs treated with exogenous TGF-β_2. 133
Figure 6-1. Beta -1 integrin staining of PBECs from a healthy donor in the presence or absence if TGF-β 138
Figure 6-2. The linear structure of c-src..... 140
Table 6.1-1. Potencies of different src inhibitors (Bain et al 2007). 141
Figure 6-3. Viral titres measured using the end-point dilution assay in the presence or absence of src inhibitors graphed as $TCID_{50}$/ml 142
Figure 6-4. Viral titres measured using the end-point dilution assay in the presence or absence of src inhibitors graphed as $TCID_{50}$/ml. 143
Figure 6-5. Viral titres measured using the end-point dilution assay in the presence or absence of src inhibitors graphed as $TCID_{50}$/ml. 145
Figure 6-6. Viral titres measured using the end-point dilution assay in the presence or absence of src inhibitors graphed as $TCID_{50}$/ml. 146
Figure 6-7. Photomicrographs of PBEC infected with 0.1-0.5 MOI RV1B in the presence or absence of 10μM SU6656. 147
Figure 6-8. Ohio Hela cells were electroporated with RNA transcripts generated from an *in vitro* T7 transcription reaction of a GFP-tagged HRV construct. 148
Figure 6-9. Viral RNA from RV-infected PBECs in the presence of absence of src kinase inhibitors. 150
Figure 6-10. Viral RNA from RV-infected PBECs in the presence or absence of src kinase inhibitors. 151
Figure 6-11. Photomicrographs of PBECs were infected with RV1B at MOI=0.01-0.1 and incubated for 16 hours. 152
Figure 6-12. RV1B and IFN-β mRNA from RV-infected PBECs in the presence or absence of SU6656..... 153
Figure 6-13. IFN-β mRNA of RV-infected PBECs in the presence or absence of src kinase inhibitors. 155
Figure 6-14. IFN-β mRNA and protein levels in polyIC-treated PBECs treated with SU6656 or DMSO..... 156
Figure 6-15. Phosphorylation status of src protein kinase in RV-infected PBECs in the presence or absence of SU6656. 158
Figure 6-16. Protein bands from Figure 6-15 were quantified by densitometry using Image J analysis software. 159
Figure 6-17. The classical RNA interference (RNAi) pathway in Drosophila. 161

Figure 6-18. Immunofluorescent photographs of PBEC from a healthy control volunteer..... 163
Figure 6-19. Cyclophilin B mRNA PBEC from a healthy volunteer were transfected with siRNA targeted against Cyclophilin B and incubated for 24 (A) and 48 (B) hours.164
Figure 6-20. Src mRNA levels from 2 asthmatic subjet after transfection with src siRNA 165
Figure 6-21. RV1B mRNA and virus titre in PBECs transfected with src siRNA. 167
Figure 6-22. IFN-β from asthmatic PBECs transfected with src siRNAor followed by infection with RV1B at MOI=0.01 for 8 hours. 168
Figure 6-23. Src protein levels in PBECs after transfection with siRNAs targeted to src kinase protein. 170
Figure 6-24. Src mRNA levels from 3 subjects after transfection with src siRNA and RV1B infection. 171
Figure 6-25. RV1B and IFN-β mRNA levels from 3 subjects after transfection with src siRNA and RV1B infection. 172
Figure 6-26. Viral titres from PBECs transfected with src siRNA and infected with RV1B. 173
Figure 6-27. RNaseL mRNA in PBECs transfected with RNAseL siRNA..... 174
Figure 6-28. RV1B mRNA and virus titre in PBECs transfected with RNAseL siRNA 175
Figure 7-1. Immunological effects of viral infection in atopic lung. Figure was obtained from a review written by Tauro et al 2008 *Microbes and Infection* 184
Figure 7-2. A summary of the different studies pursued during this project. 186

To John

Abbreviations

A2	phospholipase A2
BEGM	Bronchial epithelial growth medium
BHR	Bronchial hyperresponsiveness
BSA	Bovine serum albumin
cDNA	complementary DNA
CPE	cytopathic effect
CBP	CREB-binding protein
CREB	cAMP response element binding
Ct	Cycle threshold
DAPI	4',6-diamidino-2-phenylindole
DMEM	Dulbecco's Modified Eagle Medium
DNA	Deoxyribonucleic acid
dNTPs	Deoxyribonucleotide triphosphate
dsRNA	double-stranded RNA
ELISA	Enzyme-linked immunosorbent assay
EMT	Epithelial-to-mesenchymal transition
FBS	Fetal bovine serum
GFP	Green fluorescent protein
GAPDH	Glyceraldehyde 3-phosphate dehydrogenase
HRP	Horseradish peroxidase
HRV	Human rhinovirus
IFN-α	Interferon-alpha
IFN-β	Interferon-beta
IFN-γ	Interferon-gamma
IFN-λ	Interferon-lambda
IL-1R	Interleukin-1 receptor
IL-6	Interleukin-6
IL-8	interleukin-8
IP-10	IFN-γ-induced protein 10
IPS-1	Interferon-β promoter stimulator 1
IRF-1	Interferon regulatory factor-1
IRF-3	Interferon regulatory factor-3
IRF-7	Interferon regulatory factor-7

IRF-E	IRF-binding elements
IKK	IκB kinase
LDH	Lactate dehydrogenase
MAVS	Mitochondrial antiviral signalling molecular
Mda-5	Melanoma differentiation-associated gene-5
MMP	Matrix metalloproteinase
MOI	Multiplicity of infection
PBEC	Primary bronchial epithelial cells
PBS	Phosphate buffered saline
PCR	Polymerase Chain Reaction
PIAS-1	Protein inhibitor of activated STAT-1
PolyIC	polyinosinic:polycytidylic acid
PRR	Pattern recognition receptor
RANTES	Regulated on Activation, Normal T cells expressed and secreted
ROS	Reactive oxygen species
Treg	Regulatory T-cells
Rig-I	Retinoic acid inducible gene-I
RIPA	Radio Immuno Precipitation Assay
RNA	Ribonucleic acid
RPMI	Roswell Park Memorial Institute
RSV	Respiratory syncytical virus
RT-qPCR	Reverse transcription-quantitative PCR
siRNA	Small interfering RNA
Smad3	Mothers against decapentaplegic homolog 3
Src	Sarcoma
STAT-1	Signal Transducers and Activators of Transcription-1
TANK	Traf family member-associated NF-κB activator
TBK-1	TANK-binding kinase-1
$TCID_{50}$	Tissue culture infectious dose 50
TGF-β	Transforming Growth Factor Beta
TSP-1	Thrombospondin-1
TLR	Toll-like receptor
TMB	Tetra-Methyl Benzidine
TNF-α	Tumour necrosis factor alpha
TRIF	TIR-domain-containing adapter-inducing interferon-β

UBC	Ubiquitin C
UV	Ultraviolet

1 Chapter 1: Introduction

1.1 Asthma: Definition and Features

Asthma is a chronic inflammatory disease of the airways, affecting up to 10-33 % of children and 5-10% of adults in the Western world. It is estimated that 7% of Americans and >15% of the population in the UK are affected and about 300 million people worldwide, with more boys than girls afflicted, then after puberty, more women than men. It is characterized by recurrent episodes of airway obstruction and wheezing due to airway narrowing, which is partially or totally reversible (Cohn et al., 2004),(Kay, 2001b). Wheezing typically occurs as a high-pitched whistling or squeaking originating from the chest (Fanta, 2009). The symptoms of asthma include cough, shortness of breath, chest tightness and wheeziness due to airway smooth muscle constriction and inflammation of the bronchi (Fanta, 2009). Although similar in clinical features, atopic or allergic asthma account for majority of asthma cases compared with non-atopic/intrinsic asthma, which afflicts individuals later in life (Kay, 2001b).

The pathogenic features of asthma include goblet cell hypertrophy/hyperplasia, which results in mucus hypersecretion; sloughing of airway epithelial cells, and bronchial hyperresponsiveness (BHR) (Cohn et al., 2004). Th2 lymphocytes have also been shown to play a distinct role in asthma pathogenesis as shown by data demonstrating a higher detection of Th2 cytokines IL-4, IL-5 and IL-13 in BAL samples from asthmatic samples (Robinson et al., 1997). Studies have shown that transgenic mice overexpressing IL-13, IL-9 and IL-5 show increased AHR and collagen deposition in the airways (Cohn et al., 2004). It has been shown that in asthmatics, there is increased levels of CD4+ T-cells that express activation markers including CD25 and MHC class II (Corrigan et al., 1988; Walker et al., 1991). Although chronic inflammation is a major feature of asthma, it is likely that it is not to be the only cause as treatment of asthmatics with corticosteroids does not alleviate TGF-β mediated collagen deposition which is a feature of airway remodeling in asthma (Chakir et al., 2003). Th2 lymphocytes promote inflammation and allergic airway disease, and chronic exposure to Th2 cytokines may induce airway remodeling. However, studies in children have also shown that airway remodeling occurs even before asthma diagnosis (Pohunek et al., 2005).

This disease is also characterized by IgE production, airways smooth muscle (ASM) and, eosinophil, neutrophil and mononuclear cell infiltration into submucosal

layer of the airways, mast cell and macrophage activation, (Figure 1-1) (Hansbro et al., 2008). Studies in mouse models of ovalbumin-induced airway inflammation, mouse knock-out for IL-5 showed decreased eosinophilia, lung damage and airway hyperreactivity from the allergen challenge (Pohunek et al., 2005). However, studies with anti-IL-5 antibodies in humans failed to demonstrate key role. For example, treatement with Mepolizumab, resulted in decreased eosinophil maturation in the bone marrow (Menzies-Gow et al., 2003) and eosinophil depletion from the peripheral blood (Flood-Page et al., 2003), but did not change late asthmatic reaction or airway hyperresponsiveness to histamine treatment (Leckie et al., 2000)

Figure 1-1. Pathological effects of different severities of asthma on the airways. Taken from the National Institute of Allergy and Infectious Disease.

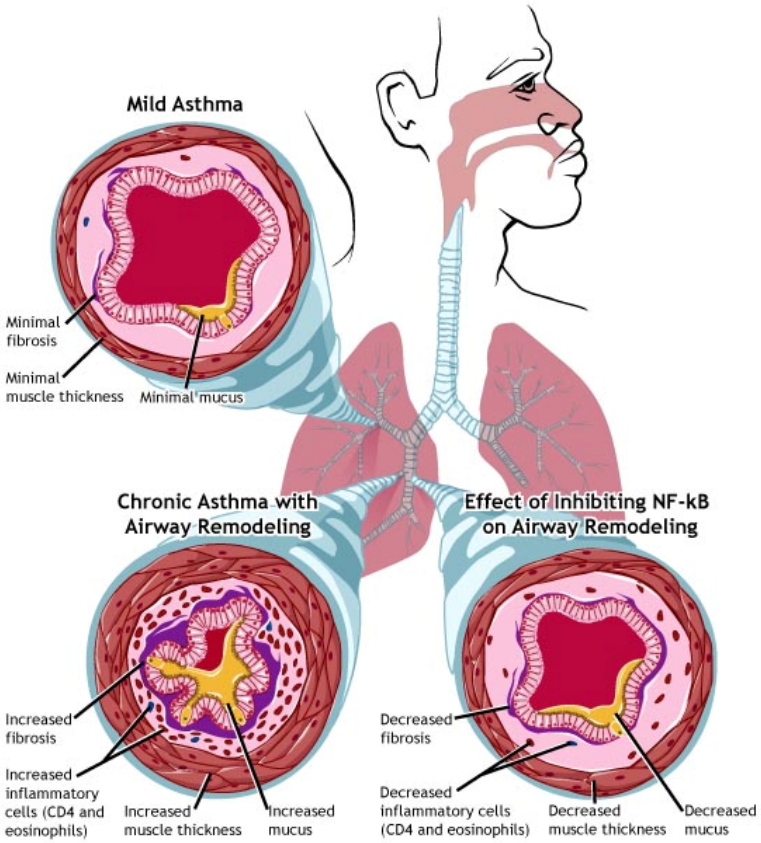

1.2 Airway remodeling

One of the characteristics of asthma is airway wall thickening due to epithelial dysplasia, thickening of the lamina reticularis, increased blood vessels, increased extracellular matrix (ECM) deposition, and increased airway smooth muscle (ASM) mass (Burgess, 2009). In chronic asthma, changes in the airway also include changes in

fibroblasts, increased development of myofibroblasts, increased vascularity and increased thickness of the muscular layer of the airways with increased size, number and function of smooth muscle cells (Galli et al., 2008). Asthma is characterized by reversible airway obstruction although full reversibility in some asthmatic patients may be prevented due to tissue remodeling (Burgess, 2009). The ECM is a reservoir of growth factors such as insulin-like growth factor, fibroblast growth factor (FGF), transforming growth factor (TGF-β) and hepatocyte growth factor, which are rapidly released from the ECM to allow for rapid extracellular signaling (Burgess, 2009). Examples of proteins found in the ECM, include collagen I, II, III and IV, fibrobronectin, laminin, versican. ASM cells obtained from asthmatics have been shown to produce increased perlecan and collagen I, and less laminin a1 and collagen IV than cells obtained from non-asthmatics (Johnson et al., 2004). Collagen I is a major component of the ECM and has pro-remodelling properties. It is produced by ASM cells and fibroblasts after stimulation with TGF-β (Johnson et al., 2006). It is made as precursor procollagen chains α1 and α2 in the endoplasmic reticulum (ER)(Prockop and Kivirikko, 1995).

Figure 1-2. Chronic allergic inflammation and tissue remodeling in asthma. Tissue sections from the airway of a non-asthmatic person (A) and a patient with severe asthma (B) are shown. In (A) a normal bronchus is shown with few goblet cells (black arrows inset) in the epithelium. The basement membrane and underlying lamina reticulartis (asterisk) are normal. In (B), a small bronchus from an asthmatic patient is filled with mucus (M). There are many goblet cells (black arrows in inserts). The lamina reticularis is thickened. Green arrows point to eosinophils. The image was obtained and modified from (Galli et al., 2008).

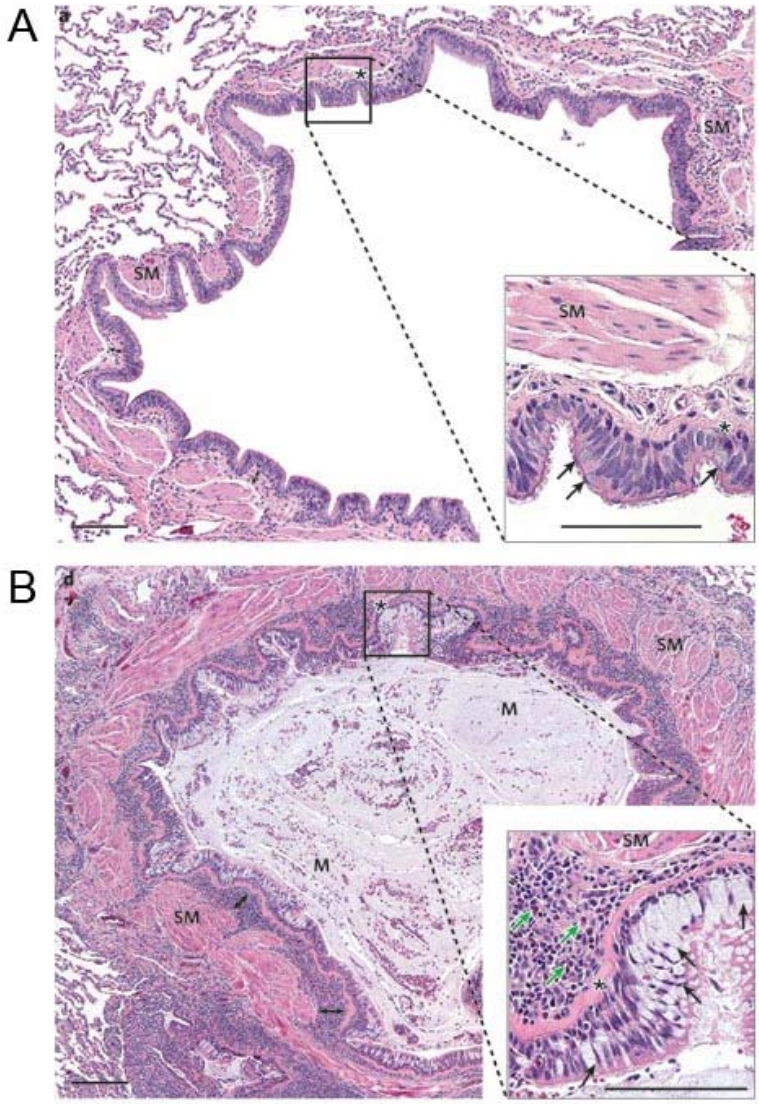

1.2.1 Transforming Growth factor –beta (TGF-β)

One of the key candidates that stands out as both being relevant in asthma and having pro-remodelling and immunomodulatory roles is transforming growth factor-β (TGF- β). TGF-β is a profibrogenic cytokine produced by eosinophils, platelets, macrophages, epithelial cells and ASM cells in an inactive latent form, which is sequestered by the ECM (Burgess, 2009). It has previously been reported than TGF-β augments the production of ECM proteins by ASM cells and fibroblasts and is able to induce the expression of matrix metalloproteases (MMPs). It induces connective tissue growth factor (CTGF) mRNA expression and protein synthesis in fibroblasts and ASM cells.

Ex vivo studies using immunohistochemistry showed that there is elevated TGF-β in the asthmatic epithelium, while i*n vivo* studies have shown that there are increased TGF-β levels in BAL fluid, and increased gene expression in bronchial tissue from asthmatic subjects (Aubert et al., 1994; Chu et al., 1999; Vignola et al., 1997; Redington et al., 1997). It has been hypothesized that TGF- β released by epithelial cells can act on underlying fibroblasts in the airways and induce the synthesis and release of extracellular matrix, thus promoting the deposition of widespread subepithelial extracellular matrix deposition that is characteristic of chronic allergic inflammation and may contribute to the thickening of airway tissue (Holgate et al., 2006a; Makinde et al., 2007). TGF-β can induce the proliferation of fibroblasts and the survival of ASM cells. It has also been shown that TGF- β enhances subepithelial fibrosis, goblet cell proliferation and mucus hyper-secretion (Makinde et al., 2007). It also regulates airway inflammation and Th2-cytokine induced release of RANTES, IL-8, eotaxin and fractalkine from ASM cells (Burgess, 2009). TGF-β regulates angiogenesis and can stimulate endothelial cells migration, differentiation and tubule formation, although some models have shown that TGF-β also inhibits endothelial cell proliferation (Burgess, 2009).

There are 23 genes coding for the TGF-β superfamily which consists of at least 5 different isoforms, 3 of which have been described in mammals (Clark and Coker, 1998). The TGF-β superfamily consists of the TGF-β isoforms (TGF-β1-3), activins, nodals, bone morphogenetic proteins (BMPs), growth and differentiation factor (GDF), and Mullerian inhibitory substance (Rahimi and Leof, 2007). The TGF-β isoforms share a common structural motif and their *in vitro* effects are indistinguishable (Schiller et al., 2004). However knock-out studies for the different isoforms in mice have produced different phenotypes suggesting non-redundant roles for these isoforms. For example,

early studies in mice that were homozygous for the mutated TGF- β_1 allele showed that they developed a dysregulated immune response leading to organ failure and death implicating TGF- β as an immune suppressor. (Shull et al., 1992; Kulkarni et al., 1993). Further studies in TGF-β_2 knockout mice showed that these animals have severe developmental defects including cardiac, lung, limb, and spinal column defects (Sanford et al., 1997). While TGF-β_3 knockout mice develop a cleft palate due to impaired adhesion of the apposing medial edge epithelia of the palatal shelves and subsequent elimination of the mid-line epithelial seam, suggesting that TGF-β_3 is important for epithelial differentiation in palatal development (Proetzel et al., 1995). Bronchial biopsies obtained from asthmatic subjects showed increased staining for the TGF-β_2 isoform compared to non-asthmatic subjects and treatment with TGF-β_2 but not TGF-β_1 increased mucin expression in PBECs, suggesting that TGF-β_2 may be more important in this disease (Chu HW, 2008).A number of studies have been dedicated to studying the effects of TGF- β on the development and function of immune cells, particularly regulatory T-cells (Treg) and Th17 cells (Wahl, 2007). Data suggest that TGF-β regulates activation of T-cells independently of regulatory Treg, although this area still remains controversial (Wan and Flavell, 2007).

The multiple effects of TGF-β on cellular function may be explained by the pleiotropic nature of this cytokine. It is a superfamily of signalling proteins that has been shown to induce a variety of cellular responses including cell proliferation, apoptosis and differentiation depending on cell type and stimulation context (Rahimi and Leof, 2007). For example, it can cause cell cycle arrest and apoptosis in epithelial cells, but also induce epithelial-to-mesenchymal transition (EMT) and mediate fibroblast activation (Siegel and Massague, 2003). It is initially synthesized as a precursor protein, which is proteolytically processed into its inactive form, which is bound to a latency associated peptide (LAP) (Rahimi and Leof, 2007). Latent TGF- β can be activated by proteases such as plasmin or MMP-2, the matricellular protein thrombospondin-1 (TSP-1), cell surface receptors such as integrins, reactive oxygen species (ROS), or acidic pH (Annes et al., 2003).

Active TGF-β can then initiate signaling by interacting with two receptor serine/threonine kinases, the type I and type II receptors (Rahimi and Leof, 2007). This results in the formation of a heterotetrameric complex where constitutively active type II receptor phosphorylates the glycine-serine rich domain in the juxtamembrane region of the type I receptor (Rahimi and Leof, 2007). One of the most characterized mechanisms by which TGF-β initiates intracellular signaling is by phosphorylation of a

family of transcription factors called Smad proteins, which accumulate in the nucleus where they bind to other transcription factors to regulate gene transcription (Massague and Wotton, 2000; Rahimi and Leof, 2007). Type I receptors recognize receptor-activated Smads (R-Smads), which include Smad-2 and -3 (recognized by TGF-β and Activin receptors) and Smad-1,-5 and -8 (recognized by BMP receptors (Figure 1-3) (Massague and Wotton, 2000). This interaction between the receptor and Smads is facilitated by the membrane-bound scaffold protein Smad anchor for receptor activation (SARA) and the adaptor molecule Dab2 (Ross and Hill, 2008). Following activation and on the way to the nucleus, R-Smads associate with Co-Smads (Smad-4 and -4β) which are required for the formation of functional transcriptional complexes (Massague and Wotton, 2000). The R-Smad and Co-Smad complex can then participate in DNA binding and recruitment of transcriptional co-factors to initiate gene expression (Massague and Wotton, 2000). A third class of Smad proteins, the inhibitory Smads (I-Smads), e.g. Smad-6 and -7, negatively regulate the TGF-β signaling pathway in a feedback loop by inactivating the receptor complex through the recruitment of the ubiquitin ligases Smurf 1/2 or protein phosphatase I (Ross and Hill, 2008). I-Smads can also interfere with the formation of the R-Smad/Co-Smad complex, inhibit co-activator recruitment by R-Smads or interfere with Smad-DNA complex formation (Ross and Hill, 2008).

Figure 1-3. The TGF-β signaling pathway. TGF-β ligands bind to the hetero TGF-β receptor complex. Phosphorylation of the type I receptor by the type II receptor, enables it to phosphorylate the R-Smads. Phosphorylated R-Smads then form complexes with Co-Smads (Smad4), which accumulate in the nucleus and associate with other transcription factors (TF) to regulate gene transcription. Taken from a review by Padgett and Reiss et al 2007 (Padgett and Reiss, 2007).

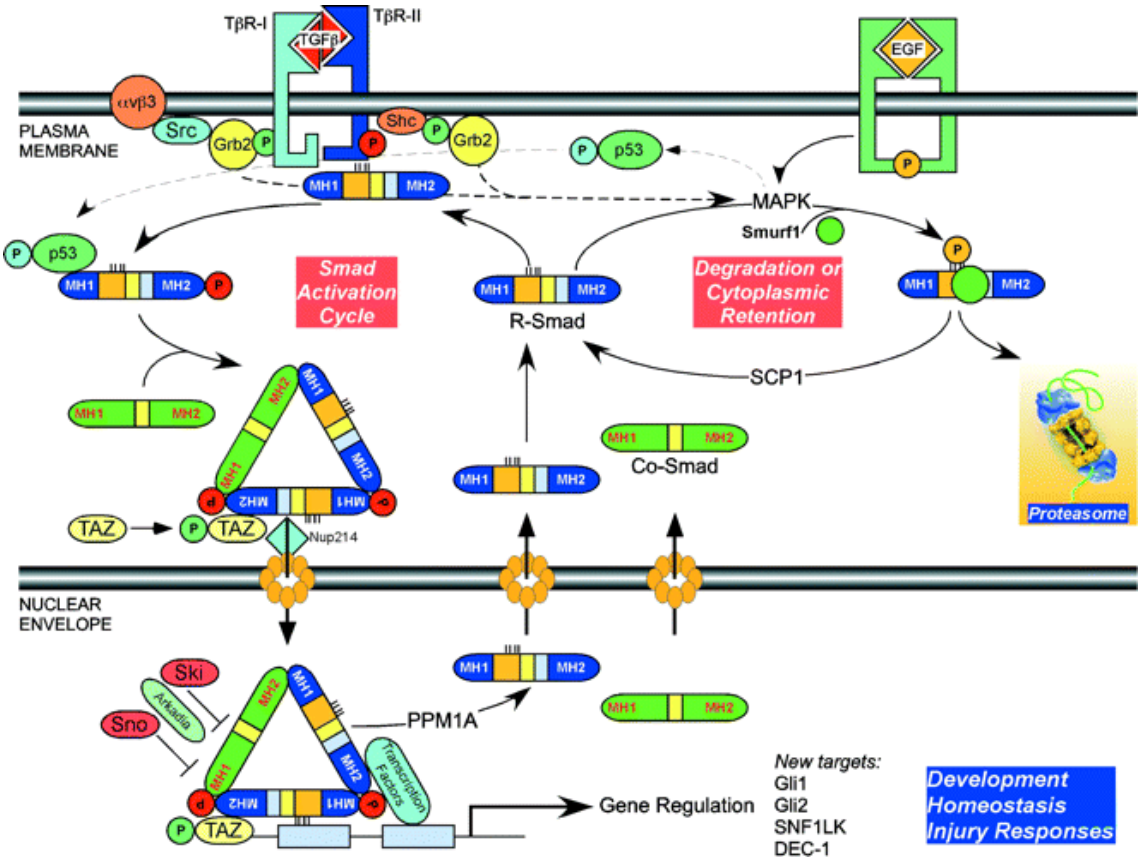

1.2.2 The epithelial-mesenchymal trophic unit

In recent years the view of asthma being a disease of "chronic wound" repair has been favoured, recognizing the contributory role of the various different cell types in the airways. Central to this idea is that the airway epithelium in asthma is functionally abnormal and that there is increased susceptibility to environmental injury, impaired repair mechanisms, and the activation of the epithelial-mesenchymal unit (EMTU) (Figure 1-4) (Holgate, 2008). The EMTU consists primarily of the epithelium, fibroblasts, myofibroblasts and smooth muscle.

The epithelial barrier integrity is maintained by tight junction proteins, such as zona occludin (ZO)-1-3, occludin, claudin-1-5 and transmembrane adhesion proteins (β-catenin, E-cadherin, JAM) (Holgate, 2008). A normal epithelium responds to injury by a

repair mechanism involving EGFR binding to ligands (EGF, amphiregulin, HB-EGF) to promote cell migration, proliferation and differentiation (Holgate, 2008). However, in asthma there is an impaired proliferation of basal cells which is evidenced by reduced nuclear expression of cell cycle marker Ki67 and proliferating cell nuclear antigen (PCNA), as well as increased nuclear expression of cell cycle inhibitors such as $p21^{waf}$ (Holgate, 2008). In asthma, there is also evidence of an impaired epithelial cell barrier and of physical damage to the columnar cells layer, which may lead to the penetration of tissue damaging agents and infectious particles (Holgate, 2008; Knight, 2002; Knight and Holgate, 2003)

Figure 1-4. Schematic representation of the interaction between immune, inflammatory and structural cells through the epithelial-mesenchymal trophic unit (EMTU) in asthma pathogenesis. Figure was obtained from a review written by S.T. Holgate 2008 Allergology International (Holgate, 2008).

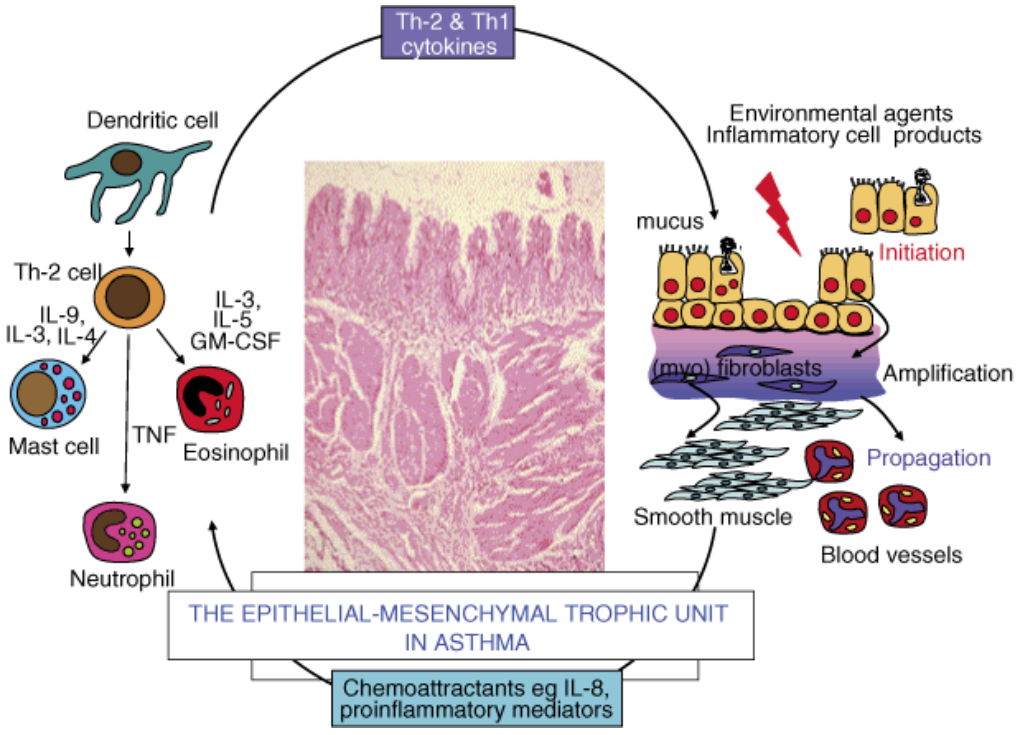

1.3 Asthma Therapy

The traditional classification of asthma treatment was to classify drugs as either bronchodilators, which were used to relax airway smooth muscle, or anti-inflammatory drugs, used to suppress airway inflammation (Fanta, 2009). Today asthma medication are classified as quick relief or long-term treatment. Quick-acting β-adrenergic agonists are examples of quick relief medication and provide the most effective therapy for rapid

reversal of airflow obstruction and relief of asthma symptoms (Fanta, 2009). Examples include short-acting β_2 selective adrenergic agonists such as salbutamol, levalbuterol or pirbuterol (Fanta, 2009). Their onset of action is 5 minutes, with peak effect at 30-60 minutes and the duration of action is 4-6 hours. Short-acting β_2 agonists are recommended only to use for the relief of symptoms or before exposure to asthmatic triggers (Fanta, 2009).

Examples of asthma medication for long-term control include inhaled corticosteroids, which are effective treatment against asthma. They have multiple anti-inflammatory activities, including effects on gene transcription of cytokines. Biopsy specimens obtained from asthmatic patients have shown that prolonged treatment with inhaled corticosteroids resulted in decreased histological abnormalities, including fewer mast cells, eosinophils, T-lymphocytes and dendritic cells in the mucosa and submucosa, reduced goblet cell hyperplasia and epithelial cell injury (Lundgren et al., 1988), and decreased vascularity (Feltis et al., 2007). Treatment with inhaled corticosteroids also resulted in decreased airway inflammation, bronchial hyperresponsiveness (BHR), fewer asthmatic symptoms, increased lung function, improved asthma-specific quality of life, fewer asthma exacerbation, including attacks that result in hospitalization or death (Fanta, 2009). However, there is evidence that neutrophilic inflammation and genetic differences in patients predispose them to unresponsiveness to treatment with inhaled corticosteroids (Fanta, 2009).

Long-term control of asthma symptoms are also dependent on inhaled long-acting β-agonists, which include salmeterol and formoterol. These are potent bronchodilators and provide sustained activity for more than 12 hours. They have fewer side effects due to their β_2 adrenergic receptor specificity and can provide sustained improvement in lung function (Fanta, 2009). It is suggested that combination therapies that include long-acting β-agonists and inhaled corticosteroids within a single inhaler, are the most useful as *in vitro* studies have shown that corticosteroids improve β-receptor-mediated signaling in the lung and β-agonists enhance transcription of genes under the influence of corticosteroids (Fanta, 2009).

Leukotriene modifiers or cysteinyl leukotrience-receptor antagonists such as montelukast, zafirlukast and pranlukast block the action of leukotriene C_4, D_4, E_4 at the type 1 cysteinyl leukotreine receptor (Fanta, 2009). Leukotrienes are bioactive mediators with proinflammatory effects that play an important role in the pathophysiology of asthma. Cysteinyl leukotrienes (CysLT) C_4, D_4, and E_4 originally termed as “slow reacting substance of anaphylaxis” are produced by mast cells,

eosinophils, neutrophils, monocytes and basophils and are mediators of bronchocontriction in allergic asthma (Dahlen et al., 1980; Peters-Golden and Henderson, Jr., 2007). Leukotrienes are generated from arachidonic acid and other polyunsaturated fatty acids and bind to specific receptors of the rhodopsin class, located on the outer plasma membrane of structural and inflammatory cells (Dahlen et al., 1980; Kanaoka and Boyce, 2004; Tager and Luster, 2003). In the normal human lung, expression of CysLT receptors has been shown to be confined to smooth muscle cells and tissue macrophages (Lynch et al., 1999). It was shown that leukotriene C_4 and leukotriene D_4 exert contractile activity on isolated human bronchi (Dahlen et al., 1980). Antagonists to type 1 cysteinyl leukotriene receptor have been shown to be effective against asthma (Peters-Golden and Henderson, Jr., 2007). Bronchodilation through this medication occurs within hours of the first dose and is maximal within the first few days after administration. Administration of leukotriene receptor antagonist has been shown to decrease levels of circulating blood eosinophils (Fanta, 2009).

Another anti-asthma treatment that has been developed is anti-IgE therapy, commercially available as Omalizumab. It is an anti-IgE monoclonal antibody that binds to the portion of IgE and recognizes its high-affinity receptor on the surface of mast cells and basophils. It is given intravenously and has been found to reduce circulating IgE levels by 95% (Fanta, 2009). It also down-regulates expression of FcεR1 on the surface of mast cells, basophils monocytes and dendritic cells (Fanta, 2009).

1.4 Asthma Genetics

Asthma is a complex disease caused by both genetic and environmental factors and their interaction with each other (Figure 1-5). It is, however, suggested that there are four groups of candidates genes responsible for increased susceptibility to this disease: 1. Genes associated with innate immunity and immunoregulation, 2. Genes associated with Th2-cell differentiation effector functions, 3. Genes associated with epithelial biology and mucosal immunity, 4. Genes associated with lung function, airway remodeling and disease severity (von, 2009).

Examples of candidate genes are the IL-4 gene cluster (which include *IL-3*, *IL-4*, *IL-5*, *IL*-9, *IL-13*), granulocyte macrophage colony-stimulating factor (*GM-CSF*) which lie on chromosome 5, β_2-adrenergic receptor (*ADRB2*) (Holgate et al., 2006a). IL-4 is a cytokine that induces naïve T-cells to switch to a Th2 phenotype, while IL-13 is able to induce IgE isotype switching, airway inflammation and remodeling (Holgate et al.,

2006a). Polymorphism in the promoter region of *IL-13* influences its expression, while changes in an *IL-13* exon results in alteration in its structure and influences IL-13 interaction with its receptor (Holgate et al., 2006a). SNPs in the intronic and promoter regions of *ADRB2* are associated with hyperresponsiveness and increase in total serum IgE (Holgate et al., 2006a).

Other candidate genes that have been linked to asthma are genes encoding HLA class II molecules. *HLA* haplotypes have been associated with IgE responses to antigen derived from ragweed (Holgate et al., 2006a). On chromosome 11, polymorphisms in the gene encoding the β-subunit of the high affinity IgE receptor (*FcεRIβ*) has been predictive of atopy (Holgate et al., 2006a). FcεRIβ variants, alter the activity of the IgE receptor. IgE expression levels on the surface of mast cells are modulated by generating an intracellular truncated decoy that lacks function (Holgate et al., 2006a).

Another asthma susceptibility gene is *ADAM-33* (a disintegrin and metalloprotease domain 33), a member of a family of membrane-anchored proteins playing a role in proteolysis, adhesion, intracellular signaling, cell-to-cell and cell-matrix interactions (Holgate et al., 2006b). *ADAM-33* was discovered in 2002 to be significantly linked to incidences of asthma and bronchial hyperresponsiveness (Van et al., 2002). However, when *ADAM33*-knockout mice were generated, these mice did not show aberrant allergen-induced airway responsiveness (Chen et al., 2006). It has now been suggested that ADAM33 might play a role in angiogenesis and tissue remodeling and that a gain-of-function makes it an asthma susceptibility gene (Puxeddu et al., 2008).

Figure 1-5. Factors influencing the development of atopy and allergic inflammation mediated by Th2 cells (Kay, 2001).

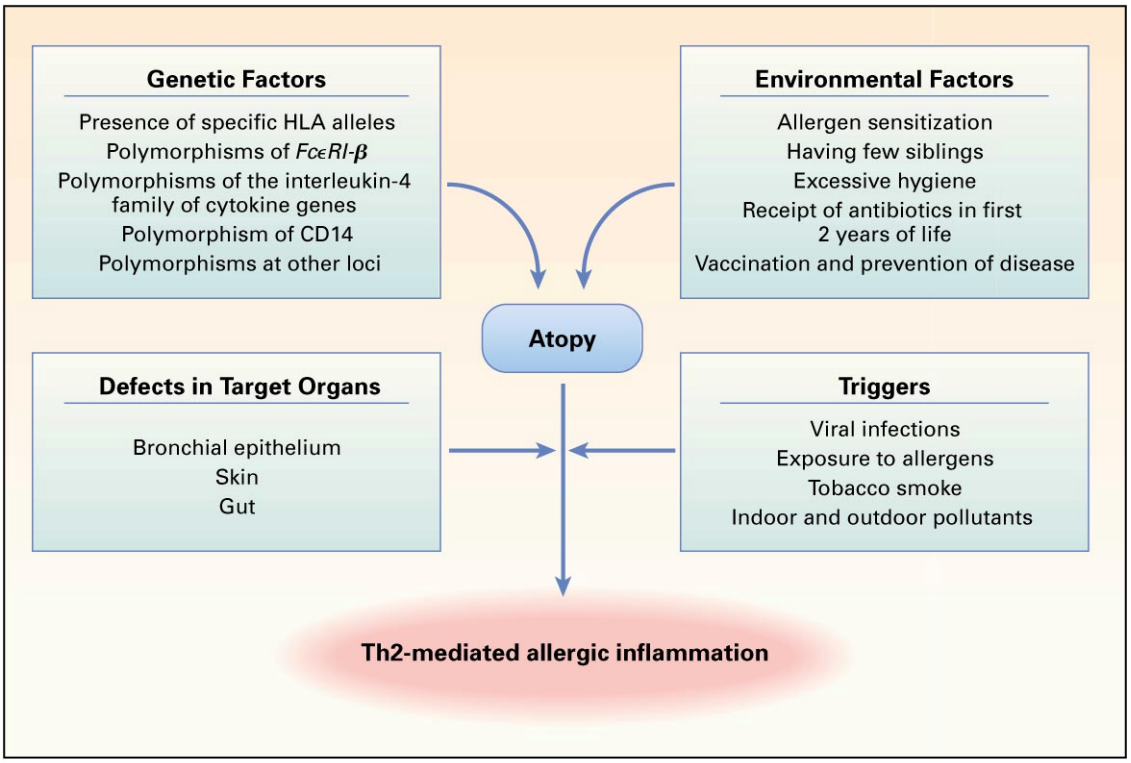

1.5 Asthma exacerbation

Acute exacerbations are a major cause of morbidity and mortality, which still remain at very high levels, despite the use of preventative therapy (Johnston, 2005). Severe exacerbation of asthma is defined as "acute or subacute episodes of progressively worsening shortness of breath, cough, wheezing, and chest tightness or a combination of these symptoms" (Dougherty and Fahy, 2009). It is characterized by decreases in expiratory airflow and lung function tests, such as spirometry and peak flow, and the need for treatment with corticosteroids, hospital admission or emergency treatment (Dougherty and Fahy, 2009). A number of factors are used to phenotype an "exacerbation-prone" subset of asthmatics, which include cigarette smoking, medication non-compliance, gastroesophageal reflux disease, rhinosinusities, obesity and intolerance to non-steroidal anti-inflammatory medications (Dougherty and Fahy, 2009). In 2004, it is estimated that asthma exacerbations accounted for 14.7 million outpatient visits, 1.8 million emergency room visits, 497 000 hospitalizations and 4 055 deaths in the US (Dougherty and Fahy, 2009). Asthma exacerbations lead an increased burden on health care resources, loss of work and school attendance. According to the Nationwide Inpatient Sample (NIS) in the US, from 2000 there were 65,381 admissions

for asthma from ages >5 years. There were 2,770 intubations for respiratory failure associated with severe asthma (Dougherty and Fahy, 2009). Mortality due to asthma exacerbation increases with increasing age: for children and adolescents it being 0.02%, and for elderly 1.9% for ages >75 years (Dougherty and Fahy, 2009).

Asthma exacerbations cause airway obstruction due to concentric smooth muscle contraction, airway wall edema, and luminal obstruction with mucus (Dougherty and Fahy, 2009). They can be triggered by viruses, allergens (dust mite, pollen, animal dander), occupational exposures (grains, flours, cleaning agents, metals, irritants, woods), hormones, drugs, exercise, stress and pollutants (Dougherty and Fahy, 2009). Upper respiratory tract viruses, especially human rhinoviruses (HRV) are the most common triggers of asthma exacerbations and asthma-related death (Hansbro et al., 2008; Dougherty and Fahy, 2009).

1.5.1 Viral Triggers of Asthma exacerbation

Different viruses, such as influenza, HRV, and coronaviruses, can cause asthma exacerbations. Asthmatics do not have more colds but are more susceptible to viral infections leading to increased lower respiratory tract (LRT) infection and hospitalization (Corne et al., 2002). In children and adults, the most commonly occurring viral triggers of asthma are human rhinovirus (HRV) and influenza while in early childhood respiratory syncytial virus (RSV) and parainfluenza are more prevalent. One study showed that RSV-infected children tended to be around 3 years old, whereas those infected with influenza A tended to be slightly older at around 5 years old (Zhao et al., 2002). It was also shown that in RSV-infected children, eosinophil counts in nasopharyngeal secretions were higher is severe asthmatics (Zhao et al., 2002). Another study showed by PCR methods, that in samples obtained from infants with acute bronchiolitis, in majority of the cases (72 %) RSV was detected compared to HRV (29%) (Papadopoulos et al., 2002). Further studies have shown that the most common virus detected in nasal washes of children admitted to the hospital with acute bronchiolotis was RSV (Xepapadaki et al., 2004). A recent study involving community-based samples from 22 countries showed that respiratory infection in childhood may seriously affect the development and persistence of respiratory disease in adulthood (Dharmage et al., 2009). Another study suggests that children born in winter months are likely to be at a higher risk of contracting winter virus infection which may impact later development of asthma (Wu et al., 2008). In terms of disease susceptibility, it is

suggested that virus-induced wheezing in children may later develop into asthma (Hansbro et al., 2008). It seems that RSV is the predominant virus detected during winter months, while HRV is common during the rest of the year (Heymann et al., 2004). Children more than 3 years of age seem also to be more likely to test positive for HRV during wheezing episodes (Heymann et al., 2004). Rhinovirus-induced exacerbations can occur throughout the year, though are especially prevalent in late spring (April-May) and Fall (September-November). The highest rate of hospital mortality from asthma occurs in the winter months (January-March), which is possibly connected to higher rates of influenza infection (Dougherty and Fahy, 2009). During a 13-month community based study of school children in Southampton conducted by Johnston et al in 1989-1990, it was found that during 80-85% of asthma exacerbations and respiratory symptoms, evidence of virus infection was detected by PCR-based methods, most notably rhinovirus in 50% of the cases (Figure 1-6) (Johnston et al., 1995). HRV infection increases neutrophil-dominated bronchial inflammation and increases lower airway inflammation and bronchial hyperresponsiveness (Martin et al., 2006; Holgate et al., 2006a).

Figure 1-6. Chart peak flow recordings and respiratory symptom scores of 3 children taking part in a 13-month study to determine the association of upper and lower respiratory viral infections with acute exacerbations of asthma in schoolchildren (Johnston et al., 1995).

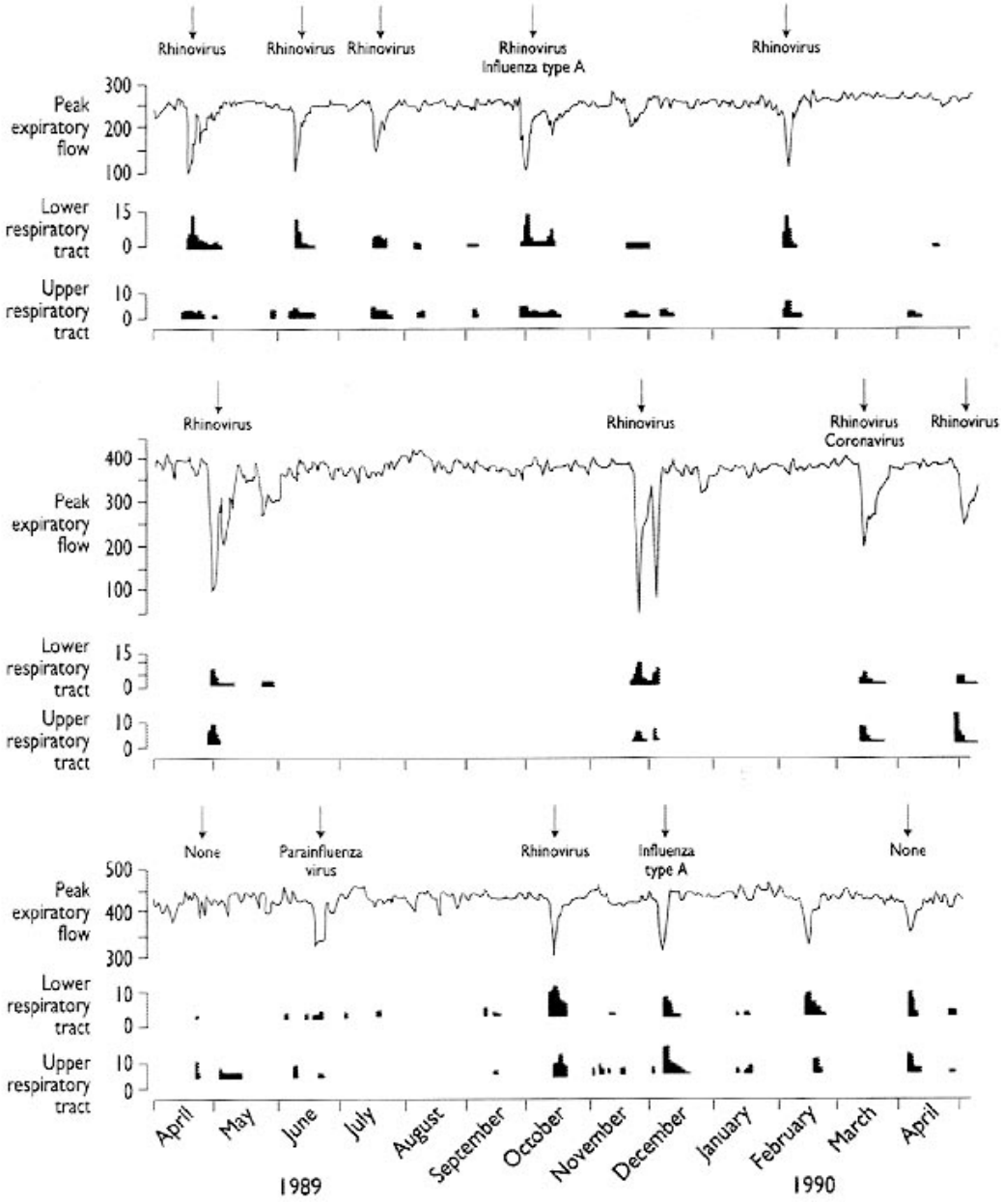

1.5.2 Human rhinoviruses

Human rhinoviruses (HRV) are small (approximately 15-30 nm in diameter), non-enveloped viruses with a single stranded RNA genome and belong to the Picornaviridae family (Dreschers et al., 2007). Rhinoviruses are the most diverse of all picornaviruses with over 100 different serotypes. They have been classified into two major groups according to their receptor-binding properties: major group HRV utilize the host cells' ICAM-1 receptor, whereas minor group HRV utilize the very low density

lipoprotein (vLDL) receptor (Dreschers et al., 2007). The viral capsid consists of 4 different viral proteins (VP): VP1-VP4 (Figure 1-7). The 5' end of the viral genome is joined to the small viral protein Vpg, which is needed for the synthesis of negative strand RNA as a template for replication (Figure 1-7 B) (Dreschers et al., 2007). The 5'end also contains an internal ribosomal entry site (IRES) after which there is a long open reading frame (ORF) for structural or capsid forming proteins (P1 unit) and non-structural proteins, such as viral protease and RNA-dependent RNA polymerase (P2/P3 units) (Dreschers et al., 2007). Protease 2A is coded by the P2 unit, and is needed for the proteolytic cleavage of the P1 and P2/P3 units (Dreschers et al., 2007). The first proteolytic cleavage by protease A occurs during translation of the viral RNA, separating structural proteins from those required for replication (P1 and P2/3). Further cleavage occurs during virion maturation, wherein VP0 is cleaved into mature VP2 and VP4 (Figure 1-1 C).

Figure 1-7. Structural analysis of the rhinovirus and its replication cycle. The structural model of rhinoviruses evaluated from cryoelectron microscopic data (A). A schematic drawing showing the position of the proteins VP1-P3 in the rhinoviral capsid (B). The map of the rhinoviral polyprotein represents the localization of compounds forming the capsid (structural proteins P1) and nonstructural proteins exhibiting function in proteolytic maturation or replication (P2-P3). This figure has been taken from (Dreschers et al., 2007).

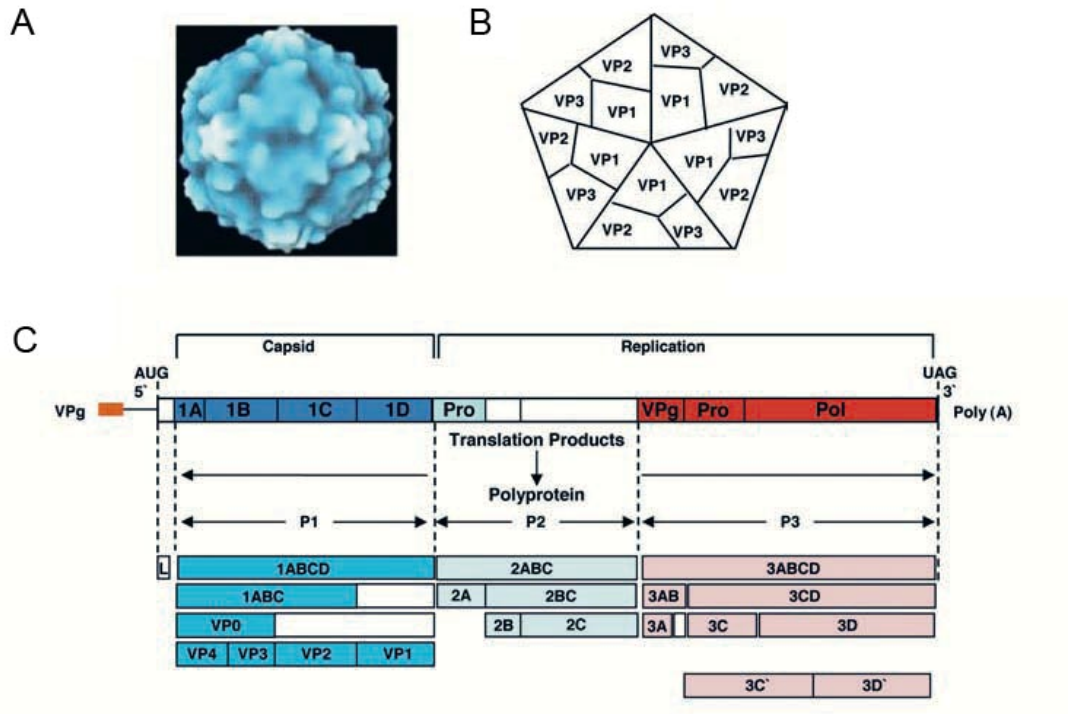

1.6 Innate immune response against viral infection

HRV targets the bronchial epithelium where its replication can eventually lead to cytopathic cell death and release of infectious virions. Infection with HRV normally elicits an innate immune response which is characterized by the expression of proinflammatory mediators and the induction of antiviral proteins, such as interferons. The proinflammatory response is characterized by production of an array of chemokines and cytokines including IFN-γ–induced protein 10 (IP-10, CXCL10), regulated on activation, normal T cells expressed and secreted (RANTES, CCL-5), interleukin-6 (IL-6) and Interleukin-8 (IL-8) (Wark et al., 2007a). During viral infection, the rapid induction of apoptosis is important for an effective antiviral response, in order to limit viral replication and promote phagocytosis of infected cells (Wark et al., 2005a). This is mediated by interferons (IFNs), which are antiviral agents discovered in the 1950s and later described in the 1990s (Isaacs and Lindenmann, 1957; Nakao et al., 1999). The IFN system represents an early host defense and has been classified into several groups: Type I IFNs, also known as viral IFNs include IFN-α, IFN-β, and IFN-ω. They are induced in response to virus infection and are synthesized by most types of virally infected cells. Type I interferons have a direct antiviral effect on infected and neighboring cells, while also promoting acquired antiviral immune responses (Wark et al., 2005a). By contrast, type II IFN, also known as immune IFN (IFN-γ), is induced by mitogenic or antigenic stimuli and only synthesized by certain cells of the immune system including natural killer (NK) cells, CD4 Th1 cells, and CD8 cytotoxic suppressor cells (Samuel, 2001). The newly described interferon lambda family (IFN-λ1/2/3) are also induced during viral infection and, like type-1 IFNs, display significant anti-viral activity (Jordan et al., 2007). Infected cells secrete mainly IFN-β as an initial response to infection but switch to IFN-α during subsequent amplification phase of the IFN response (Marie et al., 1998a). IFN-λ seems to be co-produced with IFN-β in virus infection models as well as treatment with TLR ligands, as to date no study has shown selective production of either interferon (Ank et al., 2006; Berghall et al., 2006; Chi et al., 2006; Uze and Monneron, 2007).

Virus-associated molecules such as genomic DNA and RNA or double-stranded RNA (dsRNA) produced in virally infected cells can be recognized by host-pattern-recognition receptors (PRRs) expressed in innate immune cells, such as dendritic cells (DCs) (Iwasaki and Medzhitov, 2004; Theofilopoulos et al., 2005). There are two major cellular signal transduction pathways that cells use to sense viruses and activate their

type I IFN genes. Most cells including fibroblasts, hepatocytes and conventional dendritic cells (cDCs) use the so-called classical pathway. These cells have intracellular PRRs that, upon infection, detect viral components in the cytoplasm and activate the main interferon regulatory transcription factors IRF-3 and IRF-7, which undergo nuclear translocation and subsequently bind to IRF-binding elements (IRF-Es) in the IFN-α/β promoter (Takaoka and Yanai, 2006). In HRV-infected cells, a signalling chain is activated by double-stranded RNA (dsRNA) molecules which are generated as intermediates of viral transcription. Two intracellular RNA helicases, RIG-I (Yoneyama et al., 2004) and MDA-5 (Andrejeva et al., 2004), act as viral ds RNA detectors. Rig-I_ binds dsRNA but also recognizes single-stranded RNA that is triphosphorylated at the 5' end (Pichlmair et al., 2006). In the detection of picornaviruses, like HRV, it has recently been found that Mda-5 is likely to be more important in the recognition process (Kato et al., 2006). Coupling of RIG-I and MDA5 signals to downstream factors requires IPS-1 (Interferon-β promoter stimulator 1) or MAVS (Mitochondrial antiviral signalling molecule). IPS-1/MAVS leads indirectly to activation of the IRF-3 kinases (Figure 1-8) (Kawai and Akira, 2006; Seth et al., 2005). Two IκB kinase (IKK)-related kinases, IKKε and TANK-binding kinase-1 (TBK-1) are known to phosphorylate the transcription factor IRF-3 (Fitzgerald et al., 2003; Sharma et al., 2003). IRF-3 is a member of the IFN regulatory factor (IRF) family and plays a central role in the activation of the IFN-β promoter (Lin et al., 1998; Schafer et al., 1998; Wathelet et al., 1998; Weaver et al., 1998; Yoneyama et al., 1998). Phosphorylated IRF-3 homodimerizes and moves into the nucleus where it recruits the transcriptional coactivators p300 and CREB-binding protein (CBP) to initiate IFN-β mRNA synthesis (Hiscott et al., 1999; Suhara et al., 2002). In addition, NF-κB and AP-1 are recruited in a dsRNA-dependent way (Chu et al., 1999). Together these transcription factors strongly up-regulate IFN-α/β gene expression.

In contrast, the TLR pathway uses Toll-like receptors (TLRs), such as TLR-3, expressed in intracellular compartments in dendritic cells and epithelial cells to sense dsRNA, an intermediate product of intracellular virus replication (Hiscott et al., 2006). Additional studies have suggested that TLR-3 is expressed on the cell surface of fibroblasts (Matsumoto et al., 2002a). It is suggested that they are unable to sense viruses once these have entered the cytosol (Either from the cell exterior or from endosome) and initiated replication to produce dsRNA (Kawai and Akira, 2006; Kawai and Akira, 2007c), which may account for the presence of additional intracellular receptors (Rig-I and Mda-5). However, the release of viral dsRNA upon cell lysis may

be recognized by TLR-3 on the cell membrane. The cytoplasmic intracellular tail of TLRs, which is highly homologous to the interleukin-1 receptor (IL-1R), mediates the signal transduction. TLR-3 is associated with an adaptor molecule TRIF/TICAM-1, which can directly associate with TBK-1 and TRAF6, a ubiquitin ligase (Hiscott et al., 2006; Sato et al., 2003) following virus infection. This will lead to the activation of the canonical IKK complex (IKKα/IKKβ/NEMO) and NF-κB, which upregulates the transcription of IL-6, IL-1β and TNF-α. The recruitment of TBK-1 to the C-terminal region of TRIF initiates a signalling cascade that results in IRF-3 activation and the induction of IFN- β, RANTES and IP-10 (Hiscott et al., 2006). IFN- β will then bind to IFN- β receptors of neighbouring cells which will induce apoptosis or the expression of antiviral genes to create an "antiviral state" in order to contain the infection (Takaoka and Yanai, 2006). IFN-α/β interacts with the IFN-α/β receptor (IFNAR), which consists of two subunits: IFNAR-1 and IFNAR-2 (Darnell, Jr. et al., 1994; Novick et al., 1994; Stark et al., 1998; Uze et al., 1990). IFNAR-1 and IFNAR-2 have intracellular domains that associate with Janus protein tyrosine kinases (Jak PTKs) Tyk2 and Jak1 respectively. Signalling with type II interferon occurs when IFN-γ binds to IFN-γ receptor complex (IFNGR) consisting of IFNGR-1 and IFNGR-2. IFNGR-1 subunit is constitutively associated with Jak-1, whereas IFNGR-2 is associated with Jak-2 (Bach et al., 1997; Stark et al., 1998). Binding of IFN receptors to their ligands activates the Jak PTKs which phosphorylate signal transducers and activators of transcription (STAT), namely STAT-1 and STAT-2 (Darnell, Jr. et al., 1994; Ihle and Kerr, 1995). STAT phosphorylation results in the formation of IFN-α activated factor (AAF) (or IFN-γ activated factor (GAF)) (Decker et al., 1991), and IFN-stimulated gene factor 3 (ISGF3). AAF/GAF is a complex of phosphorylated STAT-1 homodimers, mainly resulting from type II IFN signaling, whereas ISGF3 is a complex of phosphorylated STAT-1/STAT-2 heterodimers resulting from type I IFN signaling (Bluyssen et al., 1996). These complexes then translocate into the nucleus, where AAF will bind to IFN-γ activated sequences (GAS) (Decker et al., 1991). ISGF3 binds to the IFN-stimulated regulatory element (ISRE) (Kessler et al., 1990). Stimulation of promoters containing GAS or ISRE results in transcriptional activation of IFN-stimulated genes (ISG), such as those involved in antiviral activity.

Interestingly, it has been suggested that fibroblasts, splenocytes, bone-marrow derived macrophages and dendritic cells constitutively produce IFN-α/β at a low level, which will increase to higher levels upon viral infection. IRF-3 is mainly responsible for the initial inefficient induction of IFN- β expression, while IRF-7 plays a critical role in

the maximal induction of IFN- β through the cooperation with constitutively expressed IRF-3 (Grandvaux et al., 2002; Levy et al., 2002; Marie et al., 1998b; Sato et al., 2000; Taniguchi and Takaoka, 2001). This hypothetic model of 'revving-up' system allows a homeostative regulation and prevents the dysregulation of the immune response (Takaoka and Yanai, 2006).

Figure 1-8. Type I IFN induction, signalling and action (Haller et al., 2006). Viral infection of host cells results in the synthesis of a double-stranded RNA (dsRNA) intermediate. DsRNA binds to intracellular signalling molecules (TLR-3, Rig-I, PKR) to initiate a signaling cascade and activation of the IFN-β transcription factor IRF-3. Activated IRF-3 localizes to the nucleus and binds to the IFN-β promoter to initiate IFN-β gene transcription. IFN-β protein released from infected cells will bind to its own IFNAR receptor or receptors of neighbouring cells to induce the JAK/STAT pathway. Activation of transcription factors STAT-1 results in hetereodimerization with STAT-2 and binding to interferon stimulated response elements (ISRE), to initiate transcription of interferon stimulated genes (ISG) involved in the pro-apoptotic and anti-viral machinery.

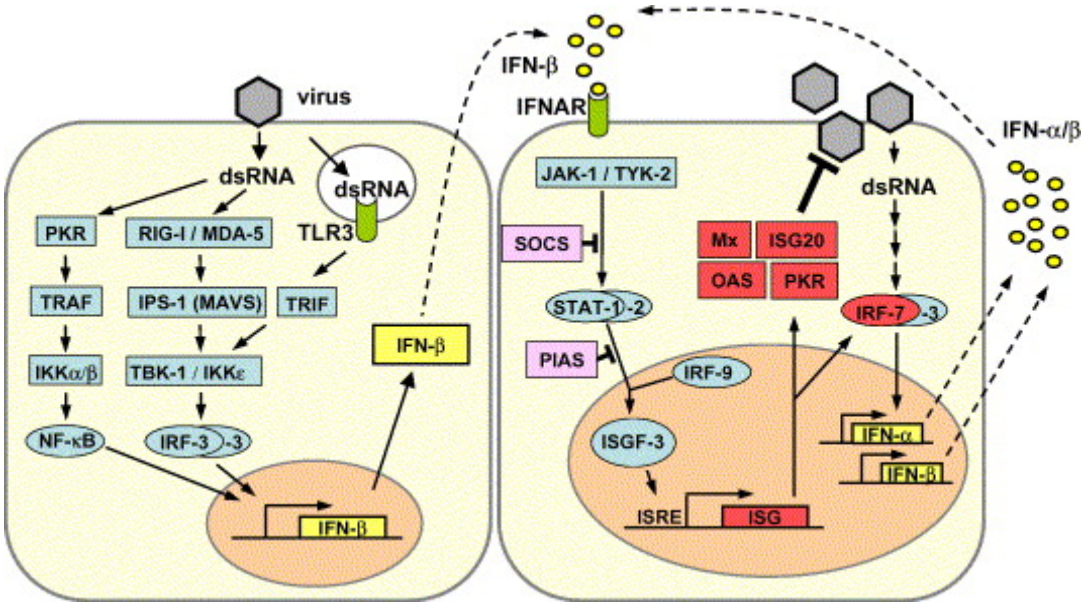

1.7 Deficient innate immune response in asthma

In order to understand the mechanisms underlying virus-induced exacerbation in asthmatic patients, several studies have sought to understand innate differences in the behaviour of asthmatic and non-asthmatic cells to infection. It is likely that there is not one cause but a complex interplay of several different events that contribute to an exacerbation event triggered by viral infection. It is also important to consider these reported findings in the *in vivo* context where different cells in the respiratory tract are likely to be involved. In a study with RV-infected PBMC it was shown that decreased IFN-γ production was associated with increased asthma severity (Brooks et al., 2003). Although the authors mention no significant IL-5 was produced, this decreased IFN response might be due to an increased Th2 cytokine response in asthmatic cells. Data by Wark et al. showed that asthmatic cells have an abnormal innate response to RV-16 infection, with increased viral replication due to a deficiency in IFN-β and reduced cell apoptosis (Wark et al., 2005a). This observation was subsequently reversed when exogenous IFN-β was introduced to asthmatic cultures, which induced apoptosis and reduced virus replication (Wark et al., 2005a). Additionally, a different group has found significantly lower IFN-λ levels in response RV16-infected bronchial epithelial cells from asthmatics compared to normals (Contoli et al., 2006b). This deficiency was also observed in alveolar macrophages (Contoli et al., 2006b). This deficiency in the innate immune response in asthma raises questions whether there are genetic mechanisms that regulate the innate immune response or whether there are environmental factors that contribute to this deficiency in response to infection. It was, therefore, decided to investigate whether other structural cells from the asthmatic airways, such as bronchial fibroblasts exhibit a similar deficient innate immune response to RV infection to determine whether the defect is genetic.

Within this project, it was also considered whether exposure of cells to cytokines that are abundant in asthmatic airways, such as TGF-β, could dampen the innate immune response with its anti-inflammatory properties. It was previously reported that TGF-β reduces the IFN response of bronchial fibroblast to RV infection (Thomas et al., 2009). Furthermore a group reported a TGF-β-mediated enhancement of respiratory syncytial virus (RSV) replication in PBECs (McCann and Imani, 2007). Although, levels of IFN- β expression failed to decrease significantly, these findings suggest that the TGF- β might be an important player in dampening the innate immune response in asthma (McCann and Imani, 2007).

1.8 Hypothesis

The hypothesis for this study was that the deficiency in the innate immune response to rhinovirus infection in asthma is due to genetic or environmental factors that affect the ability of cells in the airways to induce the expression of IFNs and antiviral pathways. One of the aims of this project was to determine whether this deficiency is genetic and thus would also be observed in other structural cells in the airways such as fibroblasts. Additionally, it was decided to investigate the contribution of TGF-β in RV-1B expression in normal and asthmatic bronchial epithelial cells (PBECs) and the mechanism behind the effect of this cytokine on RV replication.

The aims and objectives of this project were:

1. To establish a rhinovirus infection model in primary bronchial fibroblasts
2. To compare and characterize the responses of primary bronchial fibroblasts from asthmatic and non-asthmatic subjects to rhinovirus infection
3. To study the effects of cytokines previously identified to be relevant in asthma (eg. TGF-β) on cellular responses to rhinovirus infection in primary bronchial epithelial cells (PBECs).
4. To elucidate the mechanisms of TGF-β-mediated signaling in rhinovirus-infected PBECs following treatment with exogenous TGF-β
5. To study potential novel modulators of the IFN response to rhinovirus infection

2 Chapter 2: Materials and Methods

2.1 Materials

Alexa Fluor 647 Zenon label (Invitrogen, Paisley, UK # Z25008)

β1 integrin antibody (Abcam, Cambridge, UK # ab24693)

BEBM basal medium (Cambrex, Basel, Switzerland # CC-3171)

Biofuge fresco-Heraeus

Bovine Serum Albumin (Sigma, Dorset, UK # A3059)

Bronchial Epithelial Medium BEGM® (Cambrex, Basel, Switzerland CC-3170)

Caspase 3/7 reagent (Promega, Dorset, UK # G8090)

Chloroform (Sigma, Dorset, UK #C2432)

Collagen I (INAMED, CA, USA)

Complete protease inhibitor cocktail tablets (Roche, West Sussex, UK # 04 693 116 001)

rCTP, rATP, rUTP, rGTP (100 mM each) (Promega, Dorset, UK #E6000)

Cyto Tox 96® Non-radioactive Cytotoxicity Assay (Promega, Dorset, UK # G1780)

Disposable Needle (0.6x25 23G NHS supplies #FTR266)

DMEM (Invitrogen, Paisley, UK #11960044)

DNA-*free*™ reagent (Applied Biosystems, Warrington, UK# 1906)

DNA-free RNA kit (Zymo Research, Cambridge UK# R1013)

Dulbecco A tablet/ phosphate buffered saline (Oxoid, Basingstoke, UK #RR00146)

ECL Plus Western Blotting Detection System (Amersham, Buckinghamshire, UK # RPN2132)

EndoFree Plasmid Maxi Kit (Qiagen, West Sussex, UK #12362)

Ethanol (Riedel-de Haen#32221)

EZview Red Protein G Affinity Gel beads (Sigma, Dorset, UK #E3403)

Fetal bovine serum (Invitrogen, Hertfordshire, UK #10108165)

Filter unit (Millipore, Watford, UK #SLGPO33RS)

Fluorescence microscope (Leica DMI 6000B)

Fotospeed DV10 Varigrade Print Developer

Fotospeed FX20 Rapid Fixer

Goat IgG (Santa Cruz Biotechnology, Heidelberg, Germany # sc2028)

HBSS (Hanks Balanced Salt Solution without Ca^{2+} or Mg^{2+} (Invitrogen, Paisley, UK #14170-0880)

HEPES (Sigma, Dorset, UK)

Hybond P (PVDF) transfer membranes (Amersham, Buckinghamshire, UK # RPN303F)

Hyperfilm cassette (Amersham, Buckinghamshire, UK)

Human Transforming Growth Factor – β_2 (Hu TGF-β_2) (Peprotech, London, UK # 100-35)

Hu IL-8 Cytoset Kit (Biosource, Solingen, Germany # CHC1304)

IL-29 ELISA (PBL Interferon Source, NJ, USA # 61825-1)

Imager Gel Doc System (Biorad, Hertfordshire, UK)

Insulin transferrin selenium (ITS) (Sigma, Dorset, UK # I3146)

Hu IFN-β ELISA kit (PBL Interferon Source, NJ, USA # 41410)

Gene Pulser II electroporator (Biorad, Hertfordshire, UK)

Gene Pulsert Cuvette, 0.4 cm (Biorad, Hertfordshire, UK)

L-Glutamine (Invitrogen, Hertfordshire, UK #25030-024)

Luminescence counter (Topcount NXT-Packard)

MEM Earle's+ GlutaMAX^{TM} I (Invitrogen, Hertfordshire, UK #41090-028)

Microcon YM-10 filter units (Millipore, Watford, England # 42406)

Mini see-saw rocker (Stuart SSM4)

Mini Protean II system (Biorad, Hertfordshire, UK)

MOPS-EDTA-Sodium Acetate Buffer (Sigma, Dorset, UK # M5755-1L)

Multifuge 3S-R

Multiskan Ascent plate reader (Lab systems)

Oligofectamine transfection reagent (Invitrogen, Hertfordshire, UK # 12252-011)

Orbital shaker (Stuart Scientific SO1)

96-well PCR plates (Biorad, Hertfordshire, UK)

Penicillin G Sodium/ Streptomycin sulphate (Invitrogen, Hertfordshire, UK #25030-024)

Phalloidin-Alexa Fluor 488 (Invitrogen, Hertfordshire, UK #A12379)

anti-PIAS1 (Santa Cruz Biotechnology, NJ, USA #sc-8152)

PhosSTOP Phosphatase Inhibitor Cocktail Tablets (Roche, West Sussex, UK # 04 906 837 001)

Poly(I:C) (Invivogen, Wiltshire, UK #tlrl-pic)

PonceauS solution (Sigma, Dorset, UK # P7170-1L)

Power pack (Biorad power Pac 300, Hertfordshire, UK)

PP2 (Calbiochem, Nottingham, UK# 529573)

Precision™ qPCR (Primer Design, Southampton, UK)

Prolong Antifade (Invitrogen, Hertfordshire, UK #P36934)

2-Propanol (Sigma, Dorset, UK # I9516)

Protein molecular weight markers (Biorad, Hertfordshire, UK # 161-0375)

Q-step 4 DNA ladder (Yorkshire Bioscience, York, UK# M4042)

Reverse Transcription kit (Primer Design, Primer Design, Southampton)

RNA Marker (Promega, Southampton, UK# G3191)

RNA secure reagent (Ambion, Warrington, UK# AM7005)

RNAsin Plus RNase inhibitor (Promega, Southampton # N2611)

RPMI 1640 (Invitrogen, Hertfordshire, UK #31870025)

1x siRNA buffer (Dharmacon, Northumberland, UK # B002000-UB-100)

Sac I (New England Biolabs, Herts UK# R0156S)

SB 203580 (Calbiochem, Nottingham, UK #559389)

Sigma Laborzentrifugen 3-10

Sodium Bicarbonate (Sigma, Dorset, UK)

Soniprep 150 Sanyo

Src Kinase Inhibitor I (Calbiochem, Nottingham, UK # 567805)

SU6656 (Calbiochem, Nottingham, UK #572636)

5ml syringe (NHS supplies #FWC306)

T7 RNA Polymerase (New England Biolabs, Herts UK # M0251S)

TAE Buffer (Biorad, Hertfordshire, UK)

anti-TGF-β1, β-2, β-3 antibody (R&D, Abingdon, UK# MAB1835)

TMB solution (Sigma, Dorset, UK # T0440)

TGF-β_2 E_{max}® Immunoassay System (Promega, Southampton, UK# G7600)

Transforming Growth Factor-β_2 (TGF- β_2) (Peprotech, London, UK# 100-35)

Triton-X-100 (Pharmacia Biotech# 17-1315-01)

0.05% Trypsin EDTA (Invitrogen, Hertfordshire, UK #15400054)

TRIzol® reagent (Invitrogen, Hertfordshire, UK #15596-018)

UV Crosslinker (CL-1000 UVP Inc.)

Whatman filter paper (3MM CHR Cat.No. 3030672)

8-well chamber slides (Nunc)

White bottomed 96-well plates (Perkin Elmer)

X-ray film (Amersham Hyperfilm™ ECL, Buckinghamshire, UK #28906837)

X-tremeGENE siRNA Transfection Reagent (Roche, West Sussex, UK # 04 476 093 001)

2.2 Methods

2.2.1 Establishment of primary bronchial epithelial cells from bronchial brushings

Bronchial brushings were obtained from asthmatic or healthy volunteers and collected in 5 ml sterile PBS. 5 ml RPMI 1640 with 2 mM L-Glutamine, 5 units/ml Penicillin G Sodium and 50 µg/ml Streptomycin sulphate, and 20% Fetal Bovine serum were added to samples. Cell samples were then centrifuged for 5 minutes, at 167 x g room temperature. Supernatants were removed and cells resuspended in 3 ml of Bronchial Epithelial Medium BEGM®, which was prepared using 500 ml BEBM Basal medium supplemented with the following components: 0.1 % (v/v) Hydrocortisone, 0.1% (v/v) Retinoic acid, 0.4% (v/v) Bovine pituitary extract, 0.1% (v/v) human recombinant epidermal growth factor, 0.1% (v/v) Epinephrine, 0.1% (v/v) Transferrin, 0.1% (v/v) Gentamycin sulfate amphotericin-B, 0.1% (v/v) TrIIodothyronine (T3), and 0.1% (v/v) Insulin. Cells were passed through a Disposable Needle with a disposable 5ml syringe. Cell suspensions were dispensed in equal volumes into T25 tissue culture flasks, precoated with Collagen I at 29 µg/ml for 30 mins in a total volume of 4 ml. Cells were incubated at 37^0C, 5% CO_2 for about 1 week until confluent. Cells were then washed twice with HBSS, trypsinized for 1-2 minutes with 0.05% Trypsin EDTA and resuspended in 10% DMEM (with 10% FBS, (1x) non essential amino acids, 1mM sodium pyruvate, 2 mM L-Glutamine, 5 units/ml Penicillin G Sodium and 50 µg/ml Streptomycin sulphate and harvested by centrifugation at 167 g, room temperature for 5 minutes. Supernatants were removed and cells resuspended in 3 ml BEGM® and passed through a needle as described previously. Cells were transferred into collagen-coated T75 flasks and cultured until confluent. When cells reached confluency, these were trypsinized and seeded into collagen-coated 12-well plates at a cell density $0.4x10^5$ cells per well. PBECs were then used at 90% confluency for infection experiments.

2.2.2 Culture of primary bronchial fibroblasts

All plasticware were coated with 5.8 µg/ml collagen I for all fibroblast culture. Primary bronchial fibroblasts were grown from bronchial biopsies obtained from normal and asthmatic donors (kindly donated by Dr. Sarah Puddicombe) (Table 2.2-2). This involved taking bronchial biopsies which were chopped and scored into a Petri dish. Fibroblasts that grew out from the attached tissue pieces were cultured in T75 flasks in DMEM with 10% FBS,non essential amino acids, 1mM sodium pyruvate, 2 mM L-

Glutamine, 5 units/ml Penicillin G Sodium and 50 µg/ml Streptomycin sulphate. At 90% confluence, cells were trypsinized and seeded at a density of 0.5 x 10^5 cells for 24-well plates or 3 x 10^5 for 6-well plates. Cells were incubated at 37^0C, 5% CO_2. Cells were used at 90% confluency.

2.2.3 Patient characteristics of primary bronchial epithelial cell samples

Table 2.2-1 shows the characteristics of each volunteer from which primary bronchial epithelial cells were obtained from. (M=Male; F=Female; N=No; Y=Yes; BDP= Beclomethasone dipropionate)

Patient ID	Age	Sex	Atopic	% Predicted FEV_1	PC_{20} (mg/ml)	Medication		
						SABA (Salbutamol)	ICS (BDP equivalen) µg/day	LABA
Normal								
SYNA40	22	M	Y	94	n/a	------	------	------
SYNA61	21	F	N	96	n/a	------	------	------
SYNA64	20	F	N	96	n/a	------	------	------
SYNA65	20	M	Y	98	n/a	------	------	------
SYNA70	22	F	N	119	n/a	------	------	------
SYNA73	20	M	Y	102	n/a	------	------	------
SYNA74	33	M	Y	105	n/a	------	------	------
SYNA75	32	F	N	133	n/a	------	------	------
SYNA77	27	M	Y	110	n/a	------	------	------
SYNA92	21	F	N	90	n/a	------	------	------
SYNA95	25	F	Y	111	n/a	------	------	------
DS49	38	F			17	------	------	------
DS50	27	F			17	------	------	------
DS56	20	M		102.4	17	------	------	------
DS58	21	F		104	17	------	------	------
DS62	24	M	Y	83		------	------	------
DS63	24	M	N	83		------	------	------
BG183	36	M	Y	102		------	------	------
BG227	55	F	N	116		------	------	------
BG228	31	F	Y	110		------	------	------
VK001	21	M	N	100.65	n/d	------	------	------

VK007	28	M	Y	106.9	n/d	------	------	------
VK008	38	F	N	94.49	n/d	------	------	------
VK017	21	F	N	97.47	n/d	------	------	------
VK018	23	F	N	104.48	n/d	------	------	------
VK021	36	F	Y	124.3	n/d	------	------	------

(Mean Age=40.23; Mean % predicted FEV_1=103.44%)

Asthma								
SYNB32	51	F	Y	132	15.53	Y		
SYNB33	23	M	Y	103	n/d	Y		
SYNC25	52	F	Y	102	1	Y		
SYNC43	30	F	Y	110	2.07	Y		
SYNC48	23	M	Y	94	2.23		200	
SYNC49	21	M	Y	97	0.07		250	
SYNC50	19	F	Y	98	11.42	Y	200	
SYND10	35	M	Y	65	n/d	Y		
SYND13	24	F	Y	58	n/d	Y		
DS45	64	F		69.3			200	N
DS47	27	F		102.9	17		0	N
DS48	26	M		113.4	17		0	N
DS52	36	F		95.5	0.42		0	N
DS53	42	M		68.7	1.69		800	Y
BG110	44	F	N	82	n/d		1600	
BG111	49	F	N	68	n/d		1000	
BG088	60	M	Y	70	n/d		1080	
BG113	56	M	N	70	n/d		3600	
BG132	22	F	Y	113	n/d		1200	
BG144	46	F	Y	89	n/d			
BG157	41	F	Y	80	n/d		2400	
BG158	57	M	N	65	n/d		2000	
BG128	62	F	N	87	n/d		2000	
BG169	47	F	Y	91.4	n/d		2000	
BG172	35	F		80	n/d		1400	

BG178	55	F	Y	19.8	n/d		1600	
BG180	52	F	N	29.7	n/d		4000	
BG189	41	F	N	109	n/d		2000	
BG221	70	F	N	101	n/d		1000	
BG224	58	M	Y	64.9	n/d		1600	
VK002	35	M	Y	99.5	n/d			
VK004c	26	M	Y	86.3	n/d			
VK009	23	F	Y	87.8	n/d			
VK016	36	M	Y	103.15	n/d			
VK020	20	M	Y	95.45	n/d			

(Mean Age=40.23; Mean % predicted FEV_1=85.74%; GeoMean PC_{20}=2.55 mg/ml)

2.2.4 Patient characteristics of primary bronchial fibroblasts samples

Table 2.2-2 shows the characteristics of each volunteer from which primary bronchial fibroblasts were obtained from. (M=Male; F=Female; N=No; Y=Yes; BDP= Beclomethasone dipropionate)

Patient ID	Age	Sex	Atopic	% Predicted FEV_1	PC_{20} (mg/ml)	Medication		
						SABA (Salbutamol)	ICS (BDP equivalent) µg/day	LABA
Normal								
1	30	F	N	102	>16	N	none	N
2	38	M	N	107	>16	N	none	N
3	37	M	N	105	Not done	N	none	N
4	25	M	N	121	Not done	N	none	N
5	21	M	N	112	>16	N	none	N
6	21	F	N	83	>16	N	none	N
7	20	M	N	112	>16	N	none	N
8	22	M	N	92	>16	N	none	N
9	22	M	N	98	>16	N	none	N
10	21	F	N	96	>16	N	none	N

(Mean Age=22; Mean % predicted FEV_1=103%)

Asthma								
1	18	F	Y	103	10.76	Y	none	N
2	33	M	Y	131	3.22	Y	none	N
3	21	F	Y	104	11.81	Y	400	N
4	59	M	Y	92	4.86	Y	1000	N
5	21	F	Y	86	1.92	Y	400	Y
6	50	F	Y	114	5.79	Y	200	N
7	34	M	Y	97	0.96	Y	400	N
8	22	M	Y	97	0.70	Y	200	N
9	31	M	Y	83	3.12	Y	200	N
10	35	M	Y	65	Not done	Y	1000	Y

(Mean Age=32; Mean % predicted FEV_1=97%; GeoMean PC_{20}=3.3)

2.2.5 Growth of rhinovirus stocks

Rhinovirus stocks were obtained from Prof. Sebastian Johnston (Imperial College, London). Ohio HeLa cells were cultured and passaged in MEM Earle's+ GlutaMAX^{TM} I with 10% FBS, (1x) non essential aminoacids, 5 units/ml Penicillin G Sodium, and 50 µg/ml Streptomycin sulphate. For infection with rhinovirus-1B (RV-1B), cells were cultured to 80% confluency, washed twice with HBSS and incubated with virus stocks in infection media consisting of MEM Earle's+ GlutaMAX^{TM} I with 4% FBS, 16 mM HEPES, 0.075% Sodium Bicarbonate, (1x) non-essential amino acids, 0.118% w/v Tryptose phosphate broth solution, 30 µM Magnesium Chloride, 5 units/ml Penicillin G Sodium and 50 µg/ml Streptomycin sulphate. Ohio Hela cells were incubated with virus for 1 hour, at room temperature on a mini see-saw rocker, with half the final volume (4 ml for T25 flasks and 10 ml for T75 flasks) of infection media used. After 1 hour post-infection, the rest of the medium was added and cells were incubated at 33^0C, 5% CO_2 for 24 hours. Cells were then analysed the next day for cytopathic effects (CPE). (Figure 2-1). Cells were freeze-thawed twice at 80^oC and the culture media spun at 306 x g. Viral supernatants were filtered through a 0.22 µm Syringe driven filter unit, aliquoted in 1 ml volumes and stored in liquid nitrogen to be used as virus stocks. Viral titres were detemined by End-Point dilution assays (see End point Dilution Assay).

Figure 2-1. Ohio Hela cells were infected with RV-1B stock for 24 hours. Photomicrographs show increased cytopathic effects (CPE) in samples infected with RV-1B. Dead or dying cells are indicated with arrows as rounded and yellow.

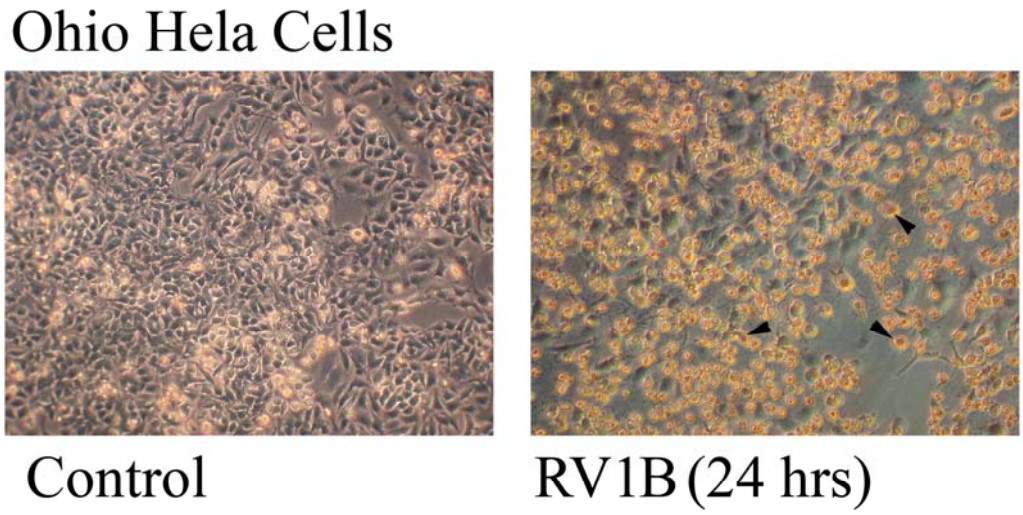

2.2.6 Rhinovirus inactivation using UV-irradiation

1 ml of virus stock was dispensed on an open 12-well plate on ice inside a UV Crosslinker. Virus was exposed to 1200μJ/cm^2 UV light for 50 minutes. UV-inactivation was confirmed by $TCID_{50}$. Irradiated virus was stored at -80^{0}C until use.

2.2.7 Infection of primary bronchial epithelial cells with rhinovirus-1B stock and treatment with reagents

Primary bronchial epithelial cells were cultured in collagen-coated 12-well plates until 90% confluent. Cells were then starved for 24 hours in BEBM basal medium supplemented with 0.1% (w/v) Bovine Serum Albumin 1% (v/v) ITS. During the starvation period, cells were pre-treated with the appropriate concentrations of the following reagents: Recombinant Human Transforming Growth Factor –β_2 (TGF-β_2) or monoclonal anti-TGF-β1, β-2, β-3 antibody. After 24 hours, the starvation medium was removed, and cells in 1 well counted to determine the volume of virus to be used for a Multiplicity of Infection (MOI) of 0.01 or 0.05. This was done for every experiment to control for differences in cell numbers from different subjects. The rest of the wells were used for infection experiments and treatments. Immediately prior to infection, the

culture media were removed from the cells. Cells were then incubated with the appropriate volume of virus supplemented with starvation media to a final volume of 200 µl, on a mini see-saw rocker at 20 oscillations per minute for 1 hour at room temperature. Control cells were treated the same way, but were incubated without virus (media only) or UV-irradiated virus. After infection, cells were washed twice with prewarmed HBSS, and incubated in 1 ml starvation media for a period of 8, 24 and 48 hours at 37^0C, 5% CO_2 in the presence of Transforming Growth Factor-β_2 (TGF- β_2), anti TGF- β1, β2, β3 antibody, SB 203580, Src Kinase Inhibitor I, SU6656 or PP2. Appropriate isotype control antibodies or DMSO were added to control samples. At 24 and 48 hours, cell supernatants were removed, centrifuged at 16 060 g, for 5 minutes, 4^0C. Supernatants were transferred into a clean tube and stored at -80^0C, while pellets were combined with cells that were harvested with TRIzol reagent. 0.5 ml of TRIzol® reagent was added to the cells and transferred into a clean RNAse-free Eppendorf tube and stored at -80^0C for RNA extraction.

2.2.8 Infection of primary bronchial fibroblasts with rhinovirus-1B stock

RV-1B was diluted to the desired MOI (0.01-0.08) in infection medium (DMEM with 2% FBS, (1x) non essential amino acids, 1mM sodium pyruvate, 2 mM L-Glutamine, 5 units/ml Penicillin G Sodium and 50 µg/ml Streptomycin sulphate, 25 mM HEPES, 0.075 % Sodium Bicarbonate) to a final volume of 1 ml in 6-well plates , 0.2 ml in 12-well plates or 0.1 ml in 24-well plates, and incubated for 1 hour at room temperature on a mini see-saw rocker. After 1 hour, the medium was then removed and cells washed twice with infection media. Culture media (DMEM+2% FBS was added to the cells and incubated for the appropriate time period at 37^0C, 5% CO_2 until harvesting.

2.2.9 End point Dilution Assay

Tissue culture infectious dose is the dilution of virus at which virus-infected supernatant will infect 50% of cell monolayers ($TCID_{50}$). Assays were performed using Hela cells infected with virus stocks to confirm virus titres according to the Spearman-Karber formula. HeLa cells were cultured in DMEM with 10% FBS, 2 mM L-Glutamine, 5 units/ml Penicillin G Sodium and 50 µg/ml Streptomycin sulphate until confluent. Cells were trypsinized and seeded into 96-well plates to a density of 1.3 x 10^5 cells, and incubated for 3 hours at 37^0C, 5% CO_2. After 3 hours, the medium was

removed and replaced with DMEM with 2% FBS. A 10-fold serial dilution of viral supernatants was performed on these cells in 200 µl final volume. Cells were incubated for 1 hour at room temperature on a mini see-saw rocker. Cells were then incubated at 37^0C, 5% CO_2 for 5 days. After this time, 50 µl of Crystal violet (0.13% w/v crystal violet, 5% v/v formaldehyde, 5% ethanol in (1x) PBS) was added to cells and incubated at room temperature for 30 minutes in the dark. Wells were then carefully washed with tap water and dried. Cells stained with Crystal violet were recorded as live cells, and clear wells were counted as cytopathic events. The number of cytopathic events were then used in the following formula to calculate the $TCID_{50}$.

Log_{10} $TCID_{50}$ = l-d(s-0.5) for volume of virus stock added to wells.

Where l = Log_{10} of lowest dilution (eg x1 = 0)

d = Log_{10} of difference of stepwise dilutions (eg x10=1)

s = no of rows of wells including undiluted with CPE (each infected well counts as 0.25).

1 $TCID_{50}$ is that which will produce evidence of infection in 50% of cell cultures, is considered to contain 1 infectious unit of virus

1 Multiplicity of infection (MOI) is strictly a cell culture situation where 1 virion infects each cell.

For a given MOI, the $TCID_{50}$ value and total cell number in a well of tissue culture plate was used in order to determine the volume of rhinovirus stocks for each experiment.

2.2.10 Treatment of primary epithelial cells and fibroblasts with inhibitors and Poly I: PolyC (Poly(I:C))

Primary cells were grown until 90% confluent. Cells were then starved for 24 hrs in starvation media (BEBM basal medium supplemented with 0.1% (w/v) Bovine Serum Albumin, 1% (v/v) ITS for PBECs; DMEM+2% FBS for fibroblasts). Appropriate concentrations of TGF- β_2 or anti TGF- β_1, β_2, β_3 antibody were added to the starvation medium. After 24 hrs, media were removed and replaced with fresh starvation media containing TGF- β_2 or anti TGF- β_1, β_2, β_3 antibody. Cells were then stimulated appropriate concentrations of Poly(I:C) and harvested at the time points stated in results.

2.2.11 Lactate Dehydrogenase (LDH) Assay

LDH was measured using a Cyto Tox 96® Non-radioactive Cytotoxicity Assay according to the manufacturer's instructions. The percentage of LDH released was determined by the ratio of LDH detected in the conditioned media only to total LDH in cell lysates and conditioned media. Total LDH was obtained by freeze-thawing cells at -80^{0}C with the media to release intracellular LDH. The supernatant containing LDH was obtained by centrifuging samples for 5 mins, at 16060 g , 4^{0}C and discarding the cell pellet containing debris. 50 µl of conditioned media or total LDH (conditioned media+cell lysate) were dispensed in a 96-well plate. Media only controls were added at the same volume. 50 µl of reconstituted substrate mix in assay buffer were added to each of the samples. The 96-well plate was covered with foil and incubated for 30 minutes at room temperature. After 30 minutes, 50 µl of Stop Solution was added to each of the sample. Absorbance was recorded on a Multiskan Ascent plate reader at 492 nM within 1 hour of addition of Stop Solution. Background values obtained from "media only" controls were subtracted from sample readings. The percentage of LDH released was calculated as:

% LDH released =

$$\frac{OD_{492} \text{ of conditioned media} - OD_{492} \text{ media only}}{OD_{492} \text{ of total LDH (Condition media+cell lysate)} - OD_{492} \text{ media only}} \times 100$$

2.2.12 Interleukin-8 (IL-8) ELISA

To determine the level of IL-8 released from virus-infected cultures, conditioned media were analysed for IL-8 protein by Enzyme-linked Immunosorbent Assay (ELISA) using the Biosource Hu IL-8 Cytoset Kit. NUNC Maxisorb 96-well plates were coated overnight at 4^{0}C with capture antibody (1µg/ml) in coupling buffer (Sodium carbonate 0.159% w/v, Sodium Bicarbonate 0.293% w/v, Sodium Azide 0.02% w/v). Wells were then washed 4 times with wash buffer (1x PBS/ 0.05% v/v Tween 20) before blocking residual binding sites using blocking buffer (Sodium chloride 10% w/v, Sodium Dihydrogen Orthophosphate 2% w/v, Potassium Phosphate 0.25% w/v, BSA 6.25% w/v) for 2 hours at room temperature. Doubling dilutions of IL-8 standards were prepared in assay buffer (1x Blocking buffer/ 0.1% Tween 20). Conditioned media were diluted 1:10 in assay buffer. After blocking, the ELISA plates were washed 4 times with Wash buffer. 100 µl of samples or standards were added to

wells in duplicate. Detection antibody was diluted 0.1 µg/ml in assay buffer added to wells.

Plates were incubated for 2 hours at room temperature and then washed 4 times as above. 100 µl of streptavidin-HRP conjugate diluted 1 in 2500 in assay buffer was added to each well, and incubated for 30 minutes at room temperature. Plates were then washed 4 times with wash buffer. Chromagen solution was prepared by adding 200 µl Tetra-Methyl Benzidine and 1.2 µl (30%) H_2O_2 to 12 ml of 13.6% w/v Sodium Acetate/Citric Acid/ pH 6. 100 µl of Chromagen solution was added to each well and incubated for 30 minutes at room temperature. 50 µl of 2M H_2SO_4 was added to each well to stop the reaction and the absorbance read on a Multiskan Ascent plate reader at 450 nM with a 630 nM reference filter. Figure 2-2 shows a typical IL-8 Standard curve derived from doubling dilutions of a 1ng/ml stock IL-8 solution.
(Limit of detection: OD_{450} 0.06=15 pg/ml)

Figure 2-2. IL-8 Standard Curve

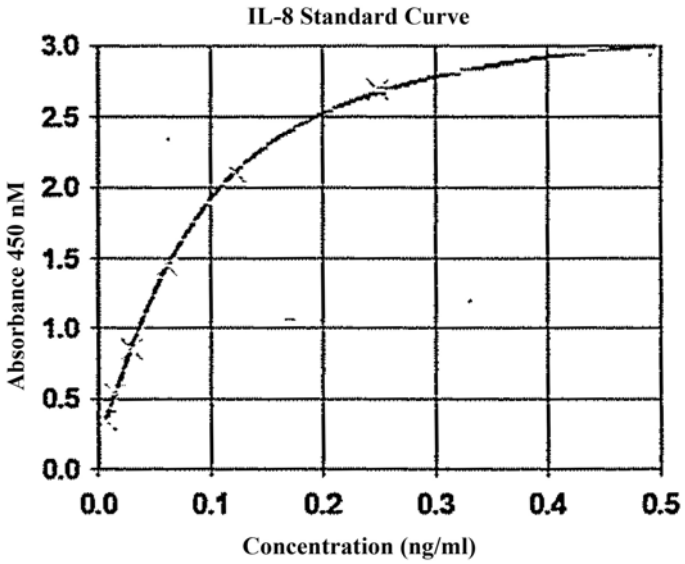

2.2.13 TGF-β_2 ELISA

In order to determine the amount of active and inactive TGF-β_2 released from primary epithelial cells, cell culture supernatants were analysed using the TGF-β_2 $E_{max}^{®}$ Immunoassay System. To analyse active TGF-β_2 culture supernatants were left untreated, however to determine the amount of total TGF-β_2 (both active and latent TGF-β_2) a portion of each sample was acid treated as follows: Samples were first diluted by adding 4 volumes of PBS, then 1 µl of 1 M HCl was added for each 50 µl of

diluted sample and mixed. Samples were then incubated for 15 minutes at room temperature. Samples were neutralized by adding 1 µl of 1M NaOH per 50 µl of sample.

For every 96 well plate, coating antibody solution was prepared by adding 10 µl of TGF-β_2 Coating antibody to 10 ml of sterile carbonate coating buffer (0.025 M Sodium bicarbonate, 0.025M sodium carbonate, pH 9.2). The plate was sealed and incubated overnight at 4^0C. The next day, the plate was allowed to warm to room temperature for 15 minutes. The contents were removed and 270 µl of 1x TGF-β Block Buffer was added to each well. The plate was sealed and incubated at 37^0C for 35 minutes without shaking. The contents were then removed and a serial 2-fold dilution of TGF-β standard in TGF-β sample buffer was performed on the plate from 1,000-15.6 pg/ml. Buffer only was used as a control. 100 µl of the acid-treated and unprocessed samples were added to remaining wells. The plate was then sealed and incubated for 1.5 hours at room temperature on a mini orbital shaker with shaking at 50 rpm. Wells were then washed with TBST wash buffer (20mM Tris-HCl pH 7.6, 150 mM NaCl, 0.05% (v/v) Tween® 20) 5 times. 100 µl of diluted Anti- TGF-β_2 antibody (1:2000 in TGF-β sample buffer) was then added to wells. The plate was sealed and incubated for 2 hours at room temperature on a mini orbital shaker at 50 rpm. Wells were then washed 5 times as previously described. 100 µl of diluted TGF-β HRP antibody conjugate (1:100) was added to each of the well and incubated for 2 hours at room temperature with shaking. After washing 3 times, 100 µl of TMB One Solution was at room temperature added to each of the wells and incubated at room temperature for 15-45 minutes depending on room temperature without shaking. The reaction was stopped by addition 100 µl of 1 M hydrochloric acid to the wells. The absorbance was read at 450 nm using the Multi Skan plate reader. Figure 2-3 shows a typical standard curve obtained from doubling dilutions of TGF-β_2 standards. (Limit of detection OD_{450} 0.03 =31 pg/ml)

Figure 2-3. TGF-β_2 Standard Curve

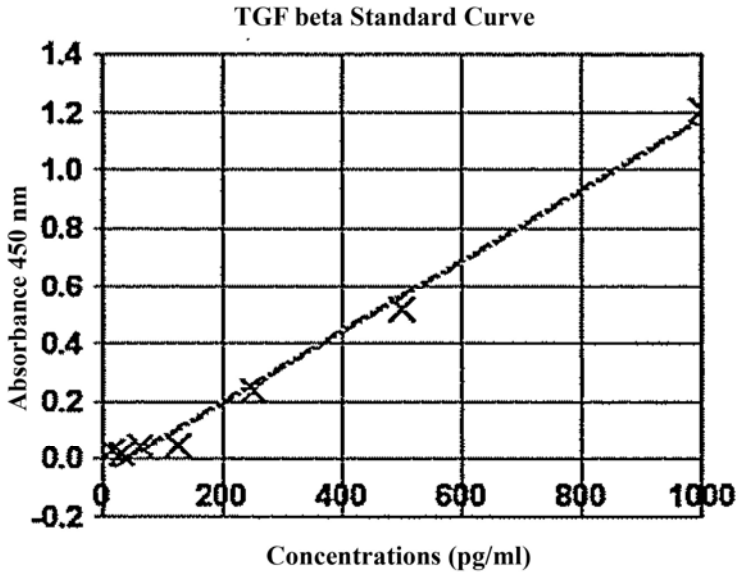

2.2.14 IFN-β ELISA

Cell culture supernatants from fibroblasts were concentrated using the Microcon YM-10 filter units, which allowed protein >10 kDa to be collected as a retentate and this was used for analysis of IFN-β protein. Samples were added directly to filter units and spun at 14 000 x g, 4^0C for 1 hour. Filters were then inverted into clean microfuge tubes and the retentate was collected by centrifuging for 3 mins at 1000 x g, 4^0C. Cell culture supernatants from epithelial cells were analysed without concentrating. Samples were analysed using the Human IFN-β ELISA kit.Samples were diluted in Sample Diluent, provided by the manufacturer, to a final volume of 210 µl. A Human IFN-β Standard was diluted in sample diluent to provide a standard curve from 2000-25 pg/ml. Antibody and HRP solutions were diluted in concentrate diluent according to the manufacturer's specifications. Solutions were kept on ice until use. 100 µl of samples and IFN-β standard were added to pre-coated microwell strips, which were covered and incubated for 1 hour at room temperature. The contents of the plate were then emptied and the plate washed three times with diluted wash buffer, provided by the manufacturer. 100 µl of diluted antibody solution was then added to all wells, covered and incubated for 1 hour at room temperature. After this time, the contents of the plate were emptied and the well washed three times with diluted wash buffer. 100 µl of diluted HRP solution was added to all wells, covered and incubated for 1 hour at room

temperature. TMB substrate solution was pre-warmed to room temperature. After 1 hour, the contents of the plate were emptied and the wells washed three times with diluted wash buffer. 100 µl of TMB Substrate Solution was added to each well, incubated in the dark for 15 minutes without sealing the plate. After 15 minutes, 100 µl of Stop solution was added to each well. The absorbance was determined at 450 nm within 5 minutes after the addition of the Stop solution using a Multiskan Plate reader. Figure 2-44 shows a typical IFN-β standard curve.
(Limit of detection:OD_{450} 0.04=65 pg/ml)

Figure 2-4. IFN-β Standard curve

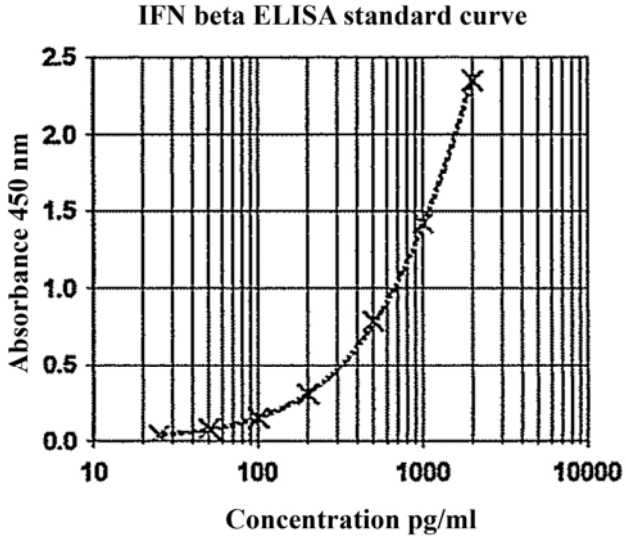

2.2.15 IL-29 ELISA

IL-29 protein levels in cell supernatants were measured using an IL-29 ELISA according to the manufacturer's protocol. Plates were coated with mouse anti-human IL-29 capture antibody in PBS at a working concentration of 1 µg/ml and incubated overnight at 4^0C. The next day, wells were washed with wash buffer (0.05% Tween 20 in PBS, pH 7.2-7.4) three times. Plates were then blocked by adding 300 µl Reagent Diluent (1% BSA in PBS, pH 7.2-7.4, 0.2 µm filtered) and incubated at room temperature for 1 hour. Wells were then washed with wash buffer three times. 100 µl of samples or standards in reagent diluent were added to wells. Samples were diluted 1:2. An IL-29 standard curve was constructed from IL-29 standards diluted two-fold with a highest concentration of 4000 pg/ml. Plates were then incubated for 2 hours at room temperature. Wells were then washed with wash buffer three times. 100 µl of detection

antibody diluted in reagent diluent at a working concentration of 400 ng/ml was added to each well and incubated for 2 hours at room temperature. Wells were then washed three times with wash buffer. 100 µl of Streptavidin-HRP diluted 1:200 in reagent diluent was added to the wells and incubated in the dark for 3 minutes at room temperature. Wells were then washed three times with wash buffer. 100 µl of TMB solution was added to wells and incubated for 20 mins in the dark until a blue colour appeared. 50 µl of Stop solution (2 M H_2SO_4) was then added to wells. The optical density (OD) was then determined using a microplate reader set to 450 nm. OD was also read at 570 nm and readings were subtracted from OD_{450}. Figure 2-5 shows a typical IL-29 standard curve obtained.

Figure 2-5. IL-29 Standard curve.

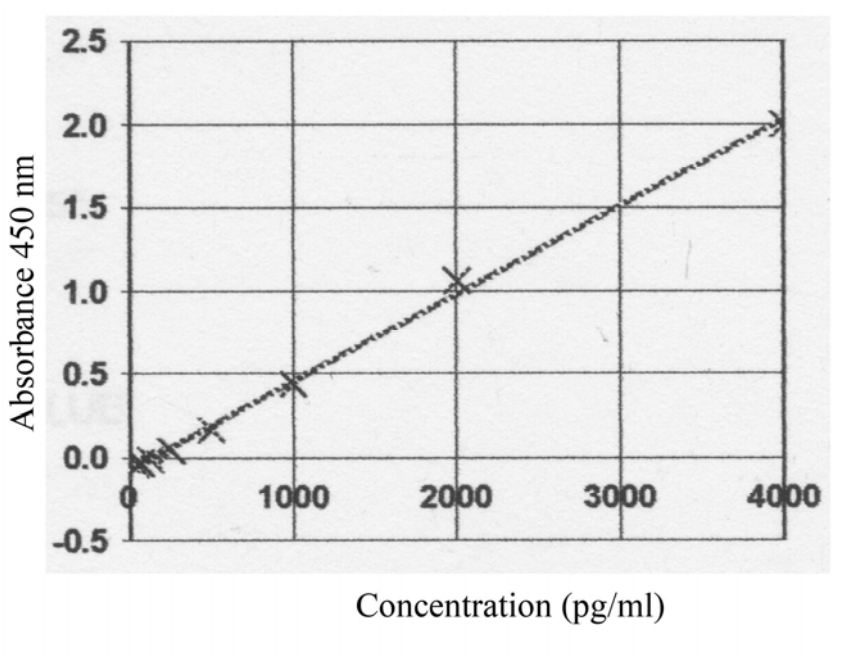

2.2.16 RNA extraction and reverse transcription

Cells in 12-well plates and 6-well plates were harvested with 0.5 and 1 ml TRIzol® reagent, respectively, and incubated for 5 minutes at room temperature. 100 or 200 µl of Chloroform was added to the samples and shaken for 15 seconds. Samples were incubated for 10 minutes at room temperature, then centrifuged for 15 minutes, at 12 000 g, 4^0C. The aqueous phase was carefully removed and transferred into a clean RNase-, DNase-free Eppendorf tube. 0.5 ml of 2-Propanol was added to each sample and briefly shaken. Samples were stored overnight at -80^0C. The next day, samples were

incubated at room temperature for 15 minutes and then vortexed for 15 seconds. RNA samples were then centrifuged at 16 060 g, for 30 minutes, 4^0C. The supernatants were carefully decanted and 75% Ethanol added to each pellet. Samples were spun for 5 minutes at 5660 g, 4^0C. The supernatants were carefully decanted and the pellets were pulse-spun for 10 seconds. Residual ethanol was carefully removed and RNA pellets air dried for 15-20 minutes. RNA samples were DNAse-treated for 1 hour at 37^0C using DNA-*free*™ reagent (Ambion# 1906), using the following amounts per sample: 1 unit rDNase I, 1x DNAse Buffer (10 mM Tris-HCl, pH 7.5, 2.5 mM $MgCl_2$, 0.5 mM $CaCl_2$), 17 µl nuclease-free water. After 1 hour, 5 µl of DNAse Inactivation Reagent was added to each sample, mixed gently, and incubated for 2 minutes at room temperature. Samples were then spun for 2 minutes at 16 060 g rpm, 4^0C and the supernatant collected. Approximately 1 µg (for fibroblasts) and 3 µg (for epithelial cells) of RNA was reverse transcribed using the following reagents and conditions: 1 µl random Hexamers , 1 µl oligodT, 1 mM dNTPs and 2 µl nuclease-free water was added to the RNA and incubated for 5 minutes at 65^0C. Samples were then cooled on ice. The following reagent were then added to each sample: 200 units MMuLV enzyme, 1x MMLV Buffer, 0.2 µl nuclease-free water. Samples were then incubated for 15 minutes at 37 ^{0}C, then for 1 hour at 42 ^{0}C. cDNA samples were then diluted 1 in 6 before quantitative PCR analysis.

2.2.17 Real time-Quantitative PCR Analysis (RT-qPCR)

cDNA samples from the previous section were used as a template for analysing single genes by qPCR reaction in 96-well PCR plates using the following amounts: 1 µl Primers and Probe, 2.5 µl cDNA, 7.5 µl *Precision*™ qPCR Mastermix containing 2x reaction buffer, 0.025 U/µl Taq Polymerase, 5 mM $MgCl_2$, 200 µM of each dNTP, 4 µl nuclease-free water. For multiplex reactions the following amounts were used: 1 µl Primers and Probe, 2.5 µl cDNA, 12.5 µl *Precision*™ qPCR Mastermix and 9 µl nuclease-free water.

Genes of interest were normalized to the geometric means of Ubiquitin C (UBC) and phospholipase A2 (A2) for fibroblast samples, or Glyceraldehyde 3-phosphate dehydrogenase (GAPH) and UBC for epithelial cell samples, using the delta Ct method. Within group comparisons were normalized to one control sample of a single patient using the delta delta Ct method. Between groups comparison were only conducted

where conditions were the same and normalized to the value of a control sample of a single normal patient by the delta delta Ct method.

2.2.18 Protocols used for RT-qPCR

A. Housekeeping genes Multiplex (Perfect Probe)

Cycle 1: (1X)	**Temperature**	**Time (min:sec)**
Step 1:	95.0ºC	for 08:00
Cycle 2: (50X)		
Step 1:	95.0ºC	for 00:15
Step 2:	50.0ºC	for 00:45
Data collection and real-time analysis enabled.		
Step 3:	72.0ºC	for 00:10

B. Singleplex (Perfect Probe)

Cycle 1: (1X)		
Step 1:	95.0ºC	for 08:00
Cycle 2: (52X)		
Step 1:	95.0ºC	for 00:10
Step 2:	50.0ºC	for 00:20
Data collection enabled.		
Step 3:	72.0ºC	for 00:10

C. Singleplex (Taqman Probe)

Cycle 1: (1X)		
Step 1:	95.0ºC	for 08:00
Cycle 2: (52X)		
Step 1:	95.0ºC	for 00:15
Step 2:	60.0ºC	for 01:00
Data collection enabled.		

2.2.19 Gene Sequences of Primers and Probes all are human genes unless otherwise stated)

RANTES (Perfect Probe) (forward) 5'AACCCAGCAGTCGTCTTTGTC3',
(reverse) 5' AGCAAGCAGAAACAGGCAAAT 3';
Probe 5'CCCGAAAGAACCGCCAAGTGTGTGCCAACttcggg

IFN β1 (Perfect Probe) (forward) 5' TTACTTCATTAACAGACTTAC AG GT 3',
(reverse) 5' TACATTAGCCATCAGTCACTT AA AC 3';
Probe 5'CCTCCGAAACTGAAGATCTCCTAGCCTGTGCCaagtttcg 3'

TLR 3 (Perfect Probe) (forward) 5' GTGTGAAAGTATTGCCTGGTTTGT 3'
(reverse) 5' ATGATAGTGAGGTGGAGTGTTGC 3'
Probe 5' ACGAGACCCATACCAACATCCCTGAGC 3'

IL-6 (Taqman Probe) (forward) 5' AACAACCTGAACCTTCCAAAG AT G 3',
(reverse) 5' CCAACTCCAAAAGACCAGTGATG AT 3';
Probe 5' TCACCAGGCAAGTCTCCTCATTGAATCCA 3'

IL-8 (Taqman Probe) (forward) 5' AAGGAACCATCTCACTGTGTGTAAAC 3',
(reverse) 5' TTAGCACTCCTTGGCAAA ACTG 3'
Probe 5'CTGCCAAGAGAGCCACGGCCA G 3'

TNF-α (Taqman Probe) (forward) 5' AAGAGGGAGAGAAGCAACTAC AGA 3',
(reverse) 5' GGTGGAGCCGTGGGTCAG 3'
Probe 5' AAACAACCCTCAGACGCCAATCCCCT

RV-1B (Taqman) (forward) 5' TGGGTGTTGTACTCTGTTATTCC 3',
(reverse) 5' TTGCCTACTATTGGTCTTGTGTT 3'
Probe 5' TCCCTCCCTCCCCATCCTTTTACGTAAC 3'

Src (Perfect Probe) (forward) 5' ACTTTGTCCCGTGGCATTTC 3'
(reverse) 5' CCGCTTAGGCACTCTTTTCC
Probe 5' ACCCTGTTCTCCTCCCCAAGTCGGCAGGGT 3'

RNaseL (Perfect Probe) (forward) 5' CTACACAAAACTACAGAACACAGAA 3'

(reverse) 5’ CCACCAGCTCCATCACACT 3’

Probe 5’ CCCCAAACCCACAGTCCAAACAAGCCTTTGGGG 3’

2.2.20 Transfection of small interfering RNAs (siRNAs) into PBECs

A pool of four siRNAs targeting either the *src* or *RNaseL* genes were purchased as a lyophilized product from Dharmacon. Table 2.2-3 and Table 2.2-4 show target sequences of the four different siRNAs targeting human src and human RNAseL. Tubes containing siRNA were briefly centrifuged, resuspended in 1x siRNA buffer to a stock concentration of 20 µM and stored at -80^{0}C until further use. Prior to transfection, stock siRNAs were diluted to 2 µM with 1x siRNA Buffer.

Primary epithelial cells were cultured and seeded into 24-well plates as previously described. Cells were incubated until 60-80% confluent. Medium was removed and replaced with 400 µl of starvation medium. Calculated amounts of siRNA (15-100 nM siRNA per well) were diluted in 50 µl Opti-MEM-I and incubated for 5 mins at room temperature. Appropriate amounts of X-tremeGENE siRNA Transfection Reagent were diluted in 50 µl Opti-MEM-I and incubated for 5 mins at room temperature: 1 µl transfection reagent was used per 0.4 µg of siRNA). The solutions containing diluted siRNA and transfection reagent were then combined and incubated for 20 mins at room temperature. siRNA-transfection reagent complexes were then added to the cells and incubated for 24 and 48 hrs (37^{0}C, 5 % CO_2). After 24 and 48 hrs, cells were harvested with 250 µl TRIzol® and RNA extracted, DNAse –treated, reverse transcribed and gene expression of *src* and *RNAseL* were analyzed by RT-qPCR.

Since no significant reduction in target protein levels were observed when cells were transfected with siRNA using the X-tremeGENE siRNA transfection reagent, it was decided to try an alternative method of transfection by using Oligofectamine transfection reagent. PBECs were grown in 24-well plates in 500 µl BEGM until 50% confluent. Media were removed and replaced with 400 µl fresh BEGM. Oligofectamine (2.5 µl per well) transfection reagent was mixed with 12 µl Opti-MEM-I and incubated for 5 mins at room temperature. At the same time, 25 µl of a 2 µM siRNA stock was diluted with 50 µl Opti-MEM-I and incubated for 5 mins at room temperature. The diluted transfection reagent and siRNA were then mixed together and incubated for 20 mins at room temperature. After 20 mins, the complexes were added drop-wise to cells and incubated for 24 hours at 37^{o}C, 5% CO_2. After 24 hours, media were replaced with 500 µl basal medium (BEBM/ITS/BSA).

For infection of siRNA-transfected PBEC, one well of transfected cells was counted and used as a basis to determine the virus inoculum to be used for infection. This was to take into account any cell death cause by siRNA transfection. Virus infection was performed as described in section 2.2.7. Infected cells were incubated for 8 and 24 hours, after which supernatants were removed and stored at -80^0 until further analysis. Adherent cells were harvested with TRIzol®.

Table 2.2-3. Target sequences of siRNAs targeting Human Src

ON-TARGETplus SMARTpool L-003175-0005, Human SRC, NM_198291
ON-TARGETplus SMARTpool siRNA J-003175-13, SRC Target Sequence: GCAGUUGUAUGCUGUGGUU
ON-TARGETplus SMARTpool siRNA J-003175-14, SRC Target Sequence: GCAGAGAACCCGAGAGGGA
ON-TARGETplus SMARTpool siRNA J-003175-15, SRC Target Sequence: CCAAGGGCCUCAACGUGAA
ON-TARGETplus SMARTpool siRNA J-003175-16, SRC Target Sequence: GGGAGAACCUCUAGGCACA

Table 2.2-4. Target sequences of siRNAs targeting Human RNaseL

ON-TARGETplus SMARTpool L-005032-00-0005, Human RNaseL,NM_021133
ON-TARGETplus SMARTpool siRNA J-005032-07, RNaseL Target Sequence: CAUGGAAGCCGCUGUGUAU
ON-TARGETplus SMARTpool siRNA J-005032-8, RNaseL Target Sequence: GUAAACGCCUGUGACAAUA
ON-TARGETplus SMARTpool siRNA J-005032-09, RNaseL Target Sequence: GAACACAGAAUAUAGAAAG
ON-TARGETplus SMARTpool siRNA J-005032-10, RNaseL Target Sequence: GCAUAACGCAGUACAAAUG

2.2.21 SDS-PAGE and Western Blotting

A Mini Protean II system was used to cast two 1 mm thick gels for SDS-PAGE. 10 ml of separation gel mix (see section 2.2.22) was prepared, poured into casting plates and overlayed with water-saturated isopropanol. Gels were left to polymerize for approximately 1 hour. Isopropanol was removed with blotting paper. 5 ml of stacking gel mix was prepared and poured over the separation gel. A 10-well comb was inserted into the stacking gel mix which was left to polymerize for 1 hour. Once polymerized, the comb was removed from the gel and wells briefly rinsed with water. The gel cassette was placed into the electrode assembly, which was placed into a mini tank containing 1x running buffer. 20 µl of cell lysates were prepared in SDS-PAGE sample buffer or 10 µl of Protein molecular weight markers were loaded onto the gel. The mini tank was covered with a lid connected to a power pack. Electrophoresis was carried out at 80V for about 40 mins until the bromophenol blue dye front reached the separating gel, after which the voltage was increased to 160V. Once the dye front reached the bottom of the gel, gels were removed and prepared for electrophoretic transfer onto Hybond P (PVDF) transfer membrane..

Precut PVDF membranes (pre-wetted with methanol), Whatman filter and scotchbrite pads were presoaked in transfer buffer for at least 15 mins. On a transfer cassette, a pad of scotchbrite, 5 layers of Whatman filter paper were placed on the black side of the cassette, followed by the gel and membrane. Air bubbles were removed using a falcon tube rolled over the membrane and the cassette sandwich was completed with 5 layers of filter paper and a scotchbrite pad. The cassette was inserted into the Transblot tank containing transfer buffer, with the membrane (i.e. clear side of cassette) nearest the anode (+ red) and gel (black side of cassette) nearest the cathode (- black), to ensure transfer of proteins onto the membrane. A magnetic flea and ice cartridge were placed into the tank and topped up with transfer buffer. The tank was the placed into a tray filled with ice on a magnetic stirrer. Electrophoretic transfer was achieved using a constant voltage of 120 for 90 mins. After transfer, PVDF membranes were removed and air-dried. To confirm transfer of protein to the membrane, they were stained using PonceauS. This involved soaking the membrane in methanol for 1 min, drying and then resoaking in methanol, rinsing in dH_2O and soaking in PonceauS solution for 2-3 mins. Membranes were then rinsed in dH_2O and stained protein bands were photographed. To prepare the membranes for Western Blotting, they were then rinsed in 1x PBS for 15 mins, followed by incubation with Blocking Buffer for 1 hour on an orbital shaker.

Blocking buffer was then removed and fresh blocking/antibody buffer was added with diluted primary antibody (see Table 2.2-5) and incubated overnight on an orbital shaker at 4^0C. The next day, membranes were briefly rinsed twice with wash buffer and incubated for 10 min in wash buffer with shaking at room temperature . This step was then repeated twice. Membranes were then incubated in 2^o Antibody buffer with diluted secondary antibody conjugated to horseradish peroxidase (HRP) (seeTable 2.2-6) and incubated for 2 hrs on an orbital shaker at room temperature. After 2 hrs, membranes were rinsed twice with wash buffer and then incubated in wash buffer for 10 mins with shaking at room temperature. This step was repeated twice. Membranes were the incubated in 1x PBS for 10 mins with shaking at room temperature. Specific antibody binding was visualized using enhanced chemiluminescence according to the manufacturer's instructions. This involved placing the blots were placed onto tissue papers to remove excess wash buffer before covering them with 2ml of ECL Plus solution (2 ml solution A+50 µl solution B) for 5 mins. Membranes were again placed on tissue paper briefly to remove excess solution and then placed onto cling film fixed into the inside of a hyperfilm cassette with tape. Membranes were covered with cling film. X-ray films (Amersham) were exposed to the membrane in the dark. Films were developed immediately in developing solution (30 ml Developer+270 ml dH_2O) for 1 min, followed by incubation in Fixative solution (75 ml Fixer+225 ml dH_2O) for 1 min. X-ray films were then air-dried and analyzed.

Table 2.2-5: Primary Antibodies used for Western Blotting

Antibody	Species	Company	Catalogue No.	Dilution
PIAS1	Goat	Santa Cruz Biotech, Inc	Sc-8152	1:500
Stat1	Mouse	Santa Cruz Biotech, Inc	Sc-464	1:500
Stat1 ($pSer^{727}$)	Rabbit	Calbiochem	569383	1:1000
Stat1 ($pTyr^{701}$)	Rabbit	Cell Signalling Technology	9171	1:1000
Src ($pTyr^{416}$)	Rabbit	Cell Signalling Technology	2101	1:1000
Src	Rabbit	Cell Signalling Technology	2108	1:1000
PIAS1	Rabbit	Abcam	Ab77231	1:5000

Table 2.2-6: Secondary Antibodies used for Western Blotting

Antibody	Species	Company	Catalogue No.	Dilution
α-Mouse-HRP	Rabbit	Dako Cytomation	P0260	1:1000
α-Rabbit-HRP	Donkey	Amersham	NA9340V	1:5882
α-Goat-HRP	Rabbit	Dako Cytomation	P0449	1:1000

2.2.22 SDS-PAGE Western Blotting Buffers

Separation Gel Stock Solution	**10 %**	**12.5 %**
30% (w/v) acrylamide/ 0.8% (w/v) bis acrylamide	30 ml	37.5 ml
1.5M Tris-HCl, pH 8.8	22.5 ml	22.5 ml
dH_2O	37.1 ml	29.6 ml
20% (w/v) SDS	0.45 ml	0.45 ml

Stacking Gel Stock	
30% (w/v) acrylamide/ 0.8% (w/v) bis acrylamide	12.5 ml
0.5M Tris-HCl, pH 6.8	25.0 ml
dH_2O	62.0 ml
20% (w/v) SDS	0.50 ml

Separation gel mix **(for two 1mm thick mini gels)**	
Separation gel stock	10 ml
10% (w/v) ammonium persulphate	100 µl
TEMED	5.0 µl

Stacking Gel mix	
Stacking gel stock	5 ml
10% (w/v) ammonium persulphate	50 µl
TEMED	3.8 µl

5x Phosphate Buffered Saline (PBS)	
727 mM NaCl	425 g
45 mM Na_2HPO_4	64 g
5.7 mM $NaH_2PO_4 \cdot H_2O$	7.8 g
dH_2O	10 L

5x Sample Buffer	
0.3125M Tris-HCl pH 6.8	10.41 ml; 1.5M
50% glycerol	25 ml
25% 2-mercaptoethanol	12.5 ml
10% SDS	5 g
0.01% bromophenol blue	5 mg

Complete protease inhibitor cocktail tablets were dissolved in 1ml dH_2O per tablet and added to 1x Sample buffer for a final dilution of 1:50.

PhosSTOP Phosphatase Inhibitor Cocktail Tablets dissolved in 1ml dH_2O per tablet and added to 1x Sample buffer for a final dilution of 1:10.

1x Running Buffer, pH 8.3	1 L
0.025 M Tris	3.03 g
0.192 M Glycine	14.4 g
0.1 % (w/v) SDS	5 ml

Transfer Buffer (pH 8.0-8.3)	5 L
25 mM Tris	15.15 g
192 mM glycine	72 g
20 % (v/v) methanol	1000 ml

Wash Buffer	1 L
1 x PBS	1000 ml
0.1 % Tween 20	1 ml

1^{o} Antibody Buffer & Blocking Buffer	100 ml
1 x PBS	100 ml
0.05 % Tween 20	50 µl
5% (w/v)Non-fat milk powder (Marvel)	5 g

2^{o} Antibody Buffer	100 ml
1 x PBS	100 ml
0.1 % Tween 20	100 µl
5% (w/v)Non-fat milk powder (Marvel)	5 g

2.2.23 Native Immunoprecipitation with RIPA Buffer

PBECs were seeded into collagen coated 6-well plates at $0.8x10^5$ cells per well. Cells were cultured until 90% confluent in 2ml of medium. Cells were then starved for 24 hrs in BEBM/ITS/BSA. After 24 hrs, cells were treated with poly (I:C) and incubated at 37^0C, 5% CO_2. Cells were then harvested after 8 hrs of treatment. 1 ml of supernatant was removed and stored at -80^0C until further analysis. The rest of the supernatant was discarded. Cell monolayers were then washed twice with 1 ml of ice-cold Wash buffer (as described in section 2.2.24). The 6-well plates containing the cell monolayers were then placed on ice and incubated with 300 µl/well of ice cold RIPA buffer with protease and phosphatase inhibitors for 30 mins. The cell monolayer was then scraped off with a cell scraper and cell lysates were transferred into pre-chilled microfuge tubes. Cell lysates were freeze-thawed at -80^0C. Samples were then sonicated for 15 sec on ice and clarified by centrifuging for 10 min at 16 000 x g at 4^0C.

For co-immunoprecipitation experiments, samples were pre-cleared using 1 µg of species specific IgG (goat IgG for PIAS1 pull-down) which was added to clarified cell lysates and incubated at 4^0C for 30 mins on a rotator (Voss of Madon). 40 µl of EZview Red Protein G Affinity Gel beads were removed and transferred into 0.5 ml microtubes. 0.5 ml ice-cold RIPA buffer were added to beads and vortexed briefly. Beads were centrifuged for 30 seconds at 8 200 x g. This washing step was repeated and beads set on ice. After 30 mins incubation, lysates were pulse-spun and transferred into

tubes containing beads. Samples were then incubated for another 30 mins on a rotator at 4^0C. After 30 mins, samples were centrifuged for 30 seconds at 8 200 x g. Supernatants were then transferred into clean, pre-chilled 0.5 ml microtubes. 5 µg of goat anti-PIAS1 antibodies were added to the cell lysates and incubated overnight on a rotator at 4^0C. Control goat IgG were added at the same concentration to a separate sample as a control. The next day, immune complexes were captured by addition of 40 µl of pre-washed EZview Red Protein G Affinity Gel beads to samples and incubated on a rotator at 4^0C. After 1 hour, samples were centrifuged for 30 seconds at 8, 200 x g, at 4^0C and supernatants were discarded. The beads were then washed with pre-chilled RIPA Buffer containing protease and phosphatase inhibitors on ice (300 µl /wash) and incubated for 5 mins on ice on an orbital shaker. Samples were then centrifuged for 30 seconds at 8200 x g, at 4^0C. This washing step was repeated 3 more times. Supernatants were carefully removed and beads were re-suspended in 40 µl SDS-PAGE sample buffer and boiled for 5 mins. 20 µl portions of the sample were loaded on an SDS-PAGE gel and analysed by Westerm blotting.

2.2.24 Co-immune precipitation Buffers

RIPA Buffer	100 ml
Dul A PBS	1 tablet
1% (v/v) NP40	1 ml
0.5% (w/v) deoxycholate acid, sodium salt	0.5 g
0.1% (w/v) SDS	0.1 g

Complete protease inhibitor cocktail tablets were dissolved in 1ml dH_2O per tablet and added to RIPA buffer for a final dilution of 1:50.

PhosSTOP Phosphatase Inhibitor Cocktail Tablets 2 tablets were added to 20 ml RIPA buffer.

Wash Buffer	40 ml
1x PBS	40 ml

Complete protease inhibitor cocktail tablets were dissolved in 1ml dH_2O per tablet and added to Wash buffer for a final dilution of 1:50.

PhosSTOP Phosphatase Inhibitor Cocktail Tablets 4 tablets were added to 40 ml Wash buffer.

2.2.25 Caspase 3/7 Assay

Primary bronchial epithelial cells were cultured and seeded in collagen-coated white bottomed 96-well plates, compatible with use in a luminometer. Cells were seeded at a density of 20 000 cells/ well, in duplicate for each condition. Cells were left to adhere overnight and incubated at 37^0C, 5% CO_2. The next day, the medium was replaced with starvation media in the absence or presence of 10 ng/ml TGF-β_2. After 24 hrs, the media were removed and cells were infected with RV1B at 0.05 MOI for 1hour. After 1 hour, the virus inoculum was removed and cells washed twice with pre-warmed HBSS. 100 µl of starvation medium was added back to cells and incubated further for 4, 8, and 24 hrs with or without TGF-β_2, at 37^0C, 5% CO_2. After each time point, the plate was allowed to equilibrate briefly to room temperature and 100 µl of Caspase 3/7 reagent was added to each well according to the manufacturer's instruction. The plate was placed on a plate shaker with shaking (300-500 rpm) for 30 seconds and incubated in the dark for 1 hour. Luminescence was measured and recorded with a microplate scintillation and luminescence counter. A negative control was included which consisted of Caspase 3/7 reagent and cells only. A blank control was also included which consisted of Caspase 3/7 reagent and tissue culture medium only. Fold-increase in caspase 3/7 activity was calculated relative to "cells only" controls.

2.2.26 Immunofluorescence staining of PBECs in chamber slides

Primary bronchial epithelial cells were cultured as described in Section 2.2.1 and seeded into collagen-coated 8-well chamber slides at 20 000 cells per well. Cells were grown until 90% confluent at 37^0C, 5% CO_2. Cells were then starved and pre-treated using 10 ng/ml TGF-β_2 for 24 hrs. Media were removed and replaced with fresh starvation media and further incubated for 48 hrs in the presence or absence of TGF-β_2. After 48 hrs, the media were removed and cells were washed once with 1x PBS. Cells were then fixed for 15 mins at room temperature with 4% (w/v) paraformaldehyde (TAAB laboratories). Cells were washed three times with 1x PBS for 5 mins each wash. Cells were then permeabilized with 0.1% (v/v) Triton-X-100 / PBS for 5 mins at room temperature. The permeabilized cells were blocked with 1% BSA (w/v)/ 0.1% (v/v) Triton-X-100/ PBS for 30 mins at room temperature. For staining with beta 1 integrin

antibody, Zenon-labeled β_1 integrin antibody was diluted 1:1000 in 1% w/v BSA/ PBS and added to cells. Hoechst 33342 (Invitrogen) nuclear stain was diluted 1:200 (v/v) in 1% BSA (w/v)/ 0.1% (v/v) Triton-X-100/ PBS, and added to cells at a final concentration of 0.05 mg/ml and incubated for 1 hour in the dark, at room temperature. Cells were washed once with 1x PBS for 5 mins. Cells were then fixed again with 4% (w/v) paraformaldehyde for 15 mins at room temperature. Cells were then washed twice with 1x PBS for 5 mins each wash. Cell samples were incubated with Phalloidin-Alexa Fluor 488 for 20 mins diluted in 1% BSA (w/v)/ 1x PBS to a final concentration of 5 units/ml. Cells were washed 3x with 1x PBS for 5 mins each wash. Chambers were then carefully removed and separated from the slide. One drop of Prolong Antifade was placed on cells and covered with a cover slip. Cells were then analysed with a fluorescence microscope using the GFP channel for visualizing Phalloidin or β_1 integrin staining and the DAPI-channel to visualize the Hoechst nuclear staining.

2.2.27 Zenon labeling β 1 integrin antibody

1 µg of mouse monoclonal β1 integrin antibody was removed and transferred to a clean microtube. The same amount of mouse IgG1 isotype control was labeled separately. 5 µl of Alexa Fluor 647 Zenon label was added to each 15 µl antibody solution and incubated for 5 mins at room temperature. 5 µl Zenon blocking reagent was added to the reaction mixture according to manufacturer's protocol and incubated for 5 mins at room temperature. Labelled antibody solution was immediately used for immunofluorescence staining.

2.2.28 Bacterial propagation of transformed E.coli containing pUCT7-HRV16 vector and plasmid clean-up

500 ml of sterile Luria broth (25 g/ 1 litre water) containing 100 µg/ml ampicillin were inoculated with E.coli transformed with a pUCT7-HRV16 vector (a gift from Dr. Tobias Tuthill) containing an ampicillin-resistance gene (Figure 2-6). The culture was incubated overnight at 37^{o}C with vigorous shaking at 300 rpm. Bacteria were then harvested by centrifugation at 6000 x g for 15 mins at 4^{o}C. For subsequent steps, the buffers used were all supplied by the same manufacturer of a DNA plasmid Max prep kit (Qiagen). The bacterial pellet was then resuspended in 10 ml of Buffer P1. 10 ml of Buffer P2 was then added and mixed thoroughly by inverting the sealed tube

containing bacterial cells 4-6 times and incubated at room temperature for 5 mins. 10 ml of chilled Buffer P3 was added and mixed immediately and thoroughly by vigorously inverting the sealed tube 4-6 times. Lysates were then poured into the barrel of a QIAfilter Cartridge and incubated at room temperature for 10 mins. A plunger was then inserted into the QIAfilter Maxi Cartridge and lysates filtered into a 50 ml falcon tube. 2.5ml of Buffer ER was added to the filtered lysates, mixed by inverting the tube 10 times and incubated on ice for 30 mins. A QIAGEN-tip 500 was equilibrated by applying 10 ml of Buffer QBT and the column was allowed to empty by gravity flow. The filtered lysates were then applied to the QIAGEN-tip and allowed to enter the resin by gravity flow. The QIAGEN-tip was the washed twice with 30 ml Buffer QC. Plasmid DNA was then eluted with 15 ml Buffer QN. DNA was then precipitated by adding 10.5 ml room-temperature isopropanol to the eluted DNA, mixed and centrifuged at 13 000 rpm for 1 h at 4 ^{o}C. The supernatant was then carefully decanted and discarded. The DNA pellet was then washed with 5 ml 70% ethanol and centrifuged at 13 000 rpm for 20 mins. The supernatant was carefully decanted and discarded. The DNA pellets were then air-dried for 5-10 min and redissolved in DNase- RNAse-free water. The DNA was the quantified using a Nanodrop machine.

Figure 2-6. pUCT7-HRV16 vector map.

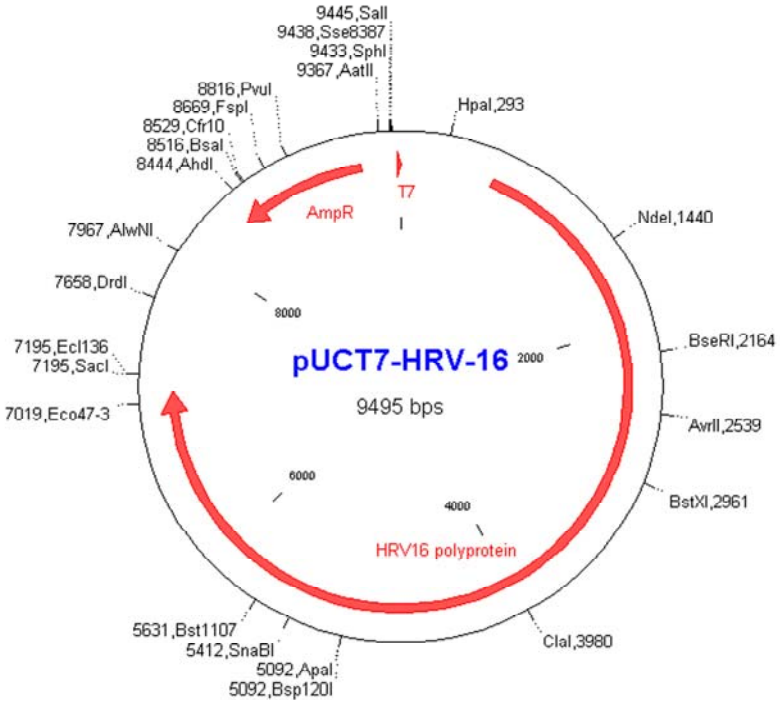

2.2.29 Plasmid DNA digestion with *SacI* and clean-up

In a 1.5 ml Eppendorf tube, the following reagents were dispensed for enzymatic digestion of plasmid DNA: 6 µg of plasmid DNA from section 2.2.28, 5 µl (10x) enzyme buffer, 1 µl SacI enzyme (20 units), 0.5 µl BSA (provided by manufacturer), 23.5 µl water. The digestion reaction was incubated for 1h, in a 37^{o}C water bath. After 1h, 50 µl of Phenol:Chloroform:Isoamyl alcohol (25:24:1) was added to digestion reaction and vortexed for 10 sec. The samples were then centrifuged for 5 mins at 16 060 x g, 4^{o}C. From the samples, the upper aqueous phase was then removed and transferred into a clean, RNase-free tube. 50 µl Chlorofrom was then added and vortexed for 30 sec. Samples were then centrifuged for 5 mins at 16 060 x g and the upper aqueous phase removed and transferred into a clean RNase-free tube. 0.1 Volumes of 3 M sodium acetate (pH 5.2) and 2 volumes of 100% ethanol were added, mixed and left on ice for 20 mins. Samples were the centrifuged for 30 mins at 16 060 x g. Supernatants were then removed and discarded. To the DNA pellet, 70% ethanol was added and centrifuged for 5 mins at 16 060 x g. The supernatant was then removed and discarded. DNA pellets were then air-dried for 15-20 mins and resuspended in 20 µl RNse, DNase free water. Digested plasmid DNA was then visualized using agarose gel electrophoresis as described below.

2.2.30 Agarose gel electrophoresis

Digested plasmid DNA prepared as described in section 2.2.29 was visualized using SYBR-green after electrophoresis on an agarose gel. 0.8% w/v of agarose powder in 1x TAE (40 mM Tris, pH 8.0/ 20 mM Acetic Acid/1 mM EDTA) buffer was heated until dissolved and poured into a gel chamber with a comb inserted, and left to polymerize. The comb was then removed and 1x TAE buffer was poured into the gel tank until the gel was covered with buffer. 0.5-1 µl of *Sac I* DNA digests, as well as undigested DNA were diluted with 3 µl water, 1.5 µl loading buffer and 1 µl SYBR-green and loaded onto the gel. DNA markers were also loaded and samples electrophoresed for 30-40 mins at 120 V in the dark. The agarose gel was then visualized under UV light using an Imager Gel Doc system (Figure 2-7).

Figure 2-7. A pUCT7 plasmid vector containing the gene for the HRV16 polyprotein was linearised with *Sac I* and analysed by agarose gel electrophoresis.

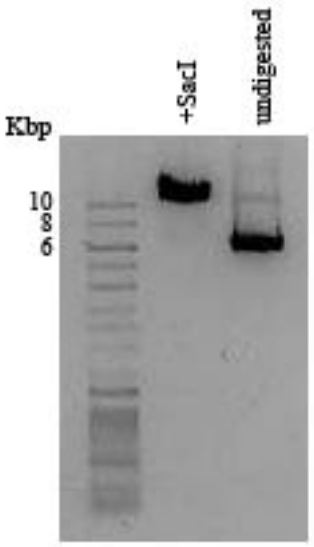

2.2.31 Generation of T7-HRV16 replicon transcripts

DNA digests prepared as described in section 2.2.29 were used to generate T7-HRV16 replicon transcripts by setting up the following reaction: 5 µg linearized DNA, 5 µl T7 Buffer, 5 µg BSA, 2.5 µl RNA secure, water to a final total volume of 43.8 µl. The reaction was then heated to 60^{o}C for 10 mins and cooled on ice. The following reagents were then added to the reaction mixture: 1 µl T7 polymerase, 4 µl of rNTPs (1 µl each), and 1.2 µl RNAsin. The mixture was then mixed and incubated at 30^{o}C for 3-4 hrs. 2.5 µl of DNA-free reagent was then added to the reaction and incubated at 37^{o}C for 30 mins. T7 RNA transcripts were then purified using a DNA-free RNA kit according to the manufacturer's instructions. Purified RNA transcripts were then quantified using a nanodrop machine and RNA integrity assessed by visualizing transcripts on a MOPS-formaldehyde gel (Figure 2-8). To prepare the gel, 0.9% w/v agarose was dissolved in 1x MOPS buffer by heating. 30 ml of agarose solution was then cooled to about 50^{o}C, and 2 ml of 37% formaldehyde added in a fume cupboard, mixed and poured into an agarose casting block. The gel was then allowed to set before removing from the fume cupboard and overlayed with 1x MOPS buffer. In a microfuge tube, 10 µl of MOPS-formaldehyde loading buffer (240 µl formamide, 50 µl 10x MOPS buffer, 87 µl formaldehyde, 15 µl 0.1% bromophenol blue, 25 µl glycerol) was added to 1-3 µl RNA sample and heated to 85^{o}C for 5 mins before cooled on ice. Samples were then loaded on the gel and run for 20-30 mins at 120 V. The gel was then soaked in

buffer containing SYBRgreen for approximately 1 hour, in the dark. The gel was then visualized under UV light using an Imager Gel Doc system,

Figure 2-8. T7 RNA transcripts visualized on a MOPS-formaldehyde gel.

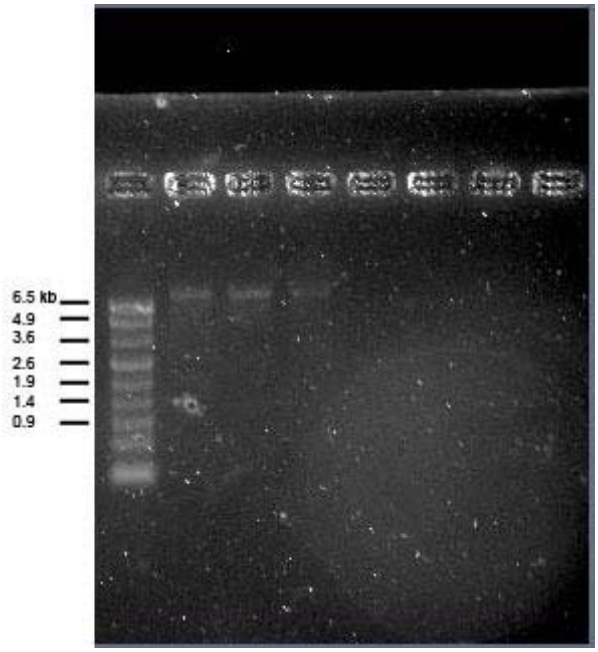

2.2.32 Electroporation of HeLa cells with HRV16 T7 transcripts

HeLa cells were grown until confluent, detached using trypsin-EDTA and resuspended in fresh growth media. Cells were counted to determine volumes needed for electroporation and were put aside ($4x10^6$ cells per electroporation). Cells were centrifuged at 1800 rpm for 3 mins, at 4^oC and resuspended in 10 ml ice cold, sterile DEPC-treated PBS. Cells were again centrifuged at 1800 rpm for 3 mins, at 4^oC and resuspended in 400 µl ice cold, sterile DEPC-treated PBS. 2-5 µg of HRV T7 transcripts generated from section 2.2.31 were dispensed into a pre-chilled microfuge tube to which 400 µl of the cell suspension were added and mixed gently by pipetting up and down. The RNA/Cell sample was then transferred into a prechilled 0.4 cm eletroporation cuvette and immediately pulsed in an electroporator at 960 µF, 270 V. Electroporated cells were then immediately dispensed into cell culture media into 2 wells of a 6-well plate. Cells were then treated with 10 µM src kinase inhibitor-1 or the equivalent volume of DMSO and analysed under time lapse microscopy.

2.2.33 Statistical analysis

Data sets were initially tested for normality. Within group comparisons were performed using paired *t*-test or its non-parametric equivalent Wilcoxon signed Rank test, if data were not normally distributed. Between group comparisons using student's *t*-test for normally distributed data or Mann-Whitney U test if data were not normally distributed. $P<0.05$ was considered significant; where statistical significance was observed, p-values are displayed.

3 Chapter 3: Results

3.1 Contribution of bronchial fibroblasts to the anti-rhinoviral response in asthma

Rationale:

Human rhinoviruses (RV) are a major cause of asthma exacerbations and hospitalization. Studies using primary cultures suggest that this may be due to impaired production of Type I and III interferons by asthmatic bronchial epithelial cells. Although epithelial cells are the main target for RV infection, RV can be detected in the subepithelial layer of bronchial mucosa from infected subjects by *in situ*-hybridization. Therefore, it was postulated that submucosal fibroblasts are also involved in the innate anti-viral response to RV infection in asthma. The aims of this project were to establish a rhinovirus infection model in primary bronchial fibroblasts and to compare and characterize the responses of fibroblasts from asthmatic and non-asthmatic subjects to RV infection.

3.1.1 Characterization of the responses of primary bronchial fibroblasts to RV infection

To optimize the model for infection of primary bronchial fibroblasts with RV1B, fibroblasts from one normal donor were infected with increasing amounts of RV1B *in vitro*. Using phase-contrast microscopy, it was observed a dose-dependent cytopathic effect due to RV1B replication. Infection using MOIs of 0.01-0.08 (1-8 infectious particles per 100 cells) caused a low level of CPE at 9 hours following the first round of viral replication, reflecting the expected level of infection. This increased at 24 hours and 48 hours. No virus-dependent CPE was observed when cells were incubated with UV-irradiated virus (Figure 3-1). Infection also elicited a time and dose-dependent increase in IL-8 production (Figure 3-2 A). In contrast with previous observations with airway epithelial cells (Wark et al., 2005b), a significant increase in IL-8 production was observed even in the fibroblast cultures exposed to UV-irradiated RV1B, which was used to assess the dependency of the response on viral replication.

The cytopathic effect of RV1B was assessed by measuring cytosolic LDH release into the culture supernatant. At 24 hours post-infection (p.i.) less than 10% cell death was observed in RV1B -infected cells (Figure 3-2B). However at 48 hours p.i., a

dose-dependent increase in cell death was observed with more than 40% cell death at the highest dose of RV1B. The amount of cell death seen with UV-irradiated virus was comparable to control samples (Figure 3-2 B). The increase in cytopathic cell death caused by RV1B was associated with a time and dose-dependent increase in release of infectious virus particles; no infectious viral particles were produced from cells incubated with UV-irradiated virus (Figure 3-2 C and D).

Figure 3-1. Characterization of the responses of primary bronchial fibroblasts to RV infection. In order to optimize the model for infection of primary bronchial fibroblasts with RV1B, fibroblasts from one normal donor were infected with increasing amounts of RV1B. Using phase-contrast microscopy at 24h, we observed a dose-dependent cytopathic effect (CPE, rounded cells) due to RV1B replication. No virus-dependent CPE was observed when cells were incubated with UV-irradiated virus**.**

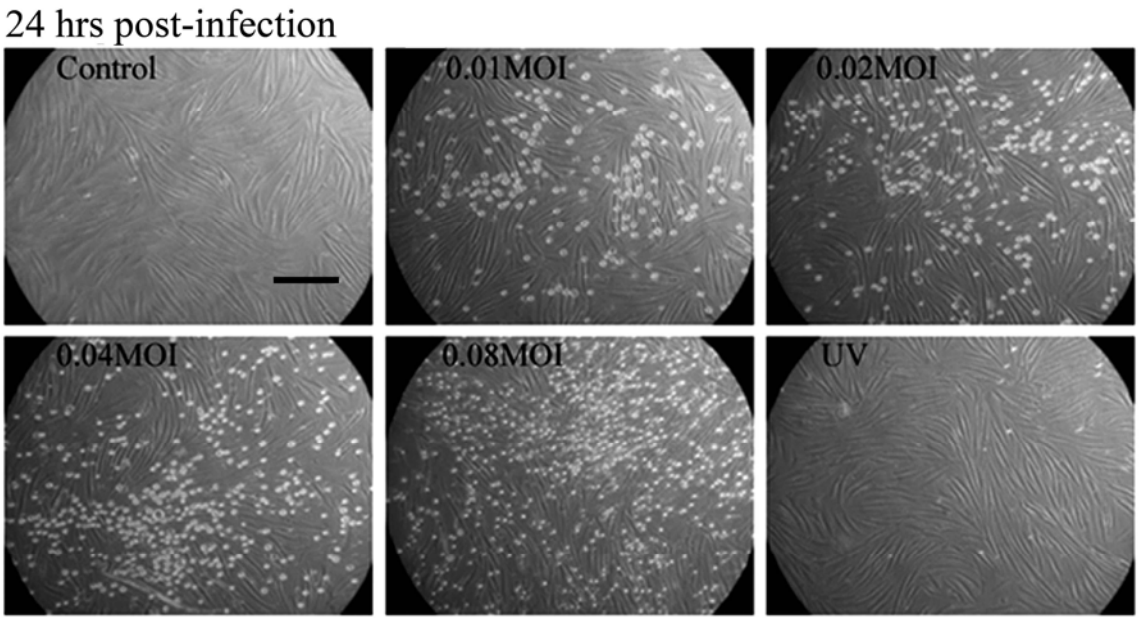

Figure 3-2. The effects of RV1B on IL-8 and LDH released are time- and dose-dependent. Primary bronchial fibroblasts were infected with RV1B at the doses shown for 24 and 48h. The proinflammatory response caused by infection was assessed as IL-8 release measured by ELISA (A); The cytopathic effect of the virus was measured at % LDH release (B); Release of infectious virus particles into culture supernatants was measured by HeLa cell titration at 24h p.i. (C) and 48h p.i. (D). Results are mean±SEM of 3 independent experiments conducted with fibroblasts from one normal donor.

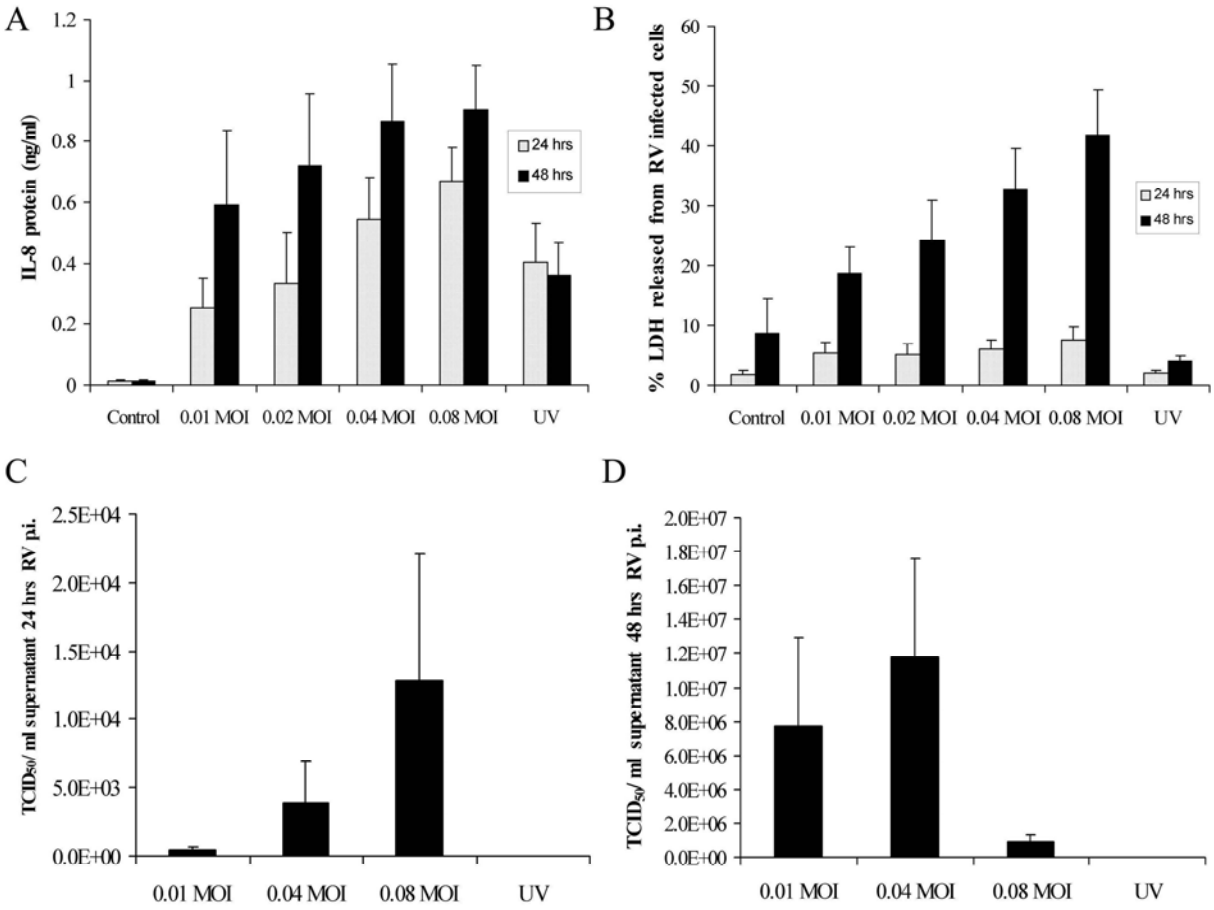

3.1.2 Normal and asthmatic primary bronchial fibroblasts respond to RV1B infection with an immediate pro-inflammatory response

In view of the sensitivity of the fibroblasts to RV1B infection, subsequent experiments using an MOI of 0.05 were performed in order to profile gene expression occurring as an immediate response to RV1B infection, without the complications of CPE and secondary infection. Therefore, cultures from 10 normal and 10 asthmatic donors were infected with RV1B and harvested at 2-8 hours p.i. RV1B transcripts were detectable as early as 2 hours p.i., and increased over 8h p.i. No transcripts were detected with UV-irradiated RV1B. No statistical difference in viral replication was observed between normal and asthmatic groups (Figure 3-3).

To assess proinflammatory mediator production, expression of IL-6, -8, TNF-α and RANTES mRNA was quantified by RT-qPCR. IL-6 and IL-8 were significantly induced by RV1B in both normal and asthmatic fibroblasts at 2 hours p.i. (Figure 3-4 A and B), but had returned to baseline levels by 8h p.i.. Similar transient kinetics were observed for TNF-α gene expression (Figure 3-5). At 24 hours, IL-6 and IL-8 proteins were also significantly elevated in cultures of asthmatic fibroblasts infected with RV1B; normal fibroblasts responded similarly, except induction of IL-8 failed to achieve statistical significance (Figure 3-4 C and D). There was no significant disease-related difference between the proinflammatory responses of the fibroblasts to RV1B. As found in the initial dose-finding studies, IL-8 as well as IL-6 mRNA expression were significantly induced in cells incubated with UV-irradiated virus (UVi). However at the protein level, this only reached statistical significance in the case of IL-6 release from asthmatic fibroblasts.

Previous studies have shown that IL-8 gene expression in BECs infected with RV-39 is independent of viral replication, being triggered by viral endocytosis and activation of phosphatidylinositol 3-kinase (PI 3-kinase) (Newcomb et al., 2005). Pretreatment of bronchial fibroblasts with the PI 3-kinase inhibitor, LY294002, for 1 hour before infection inhibited expression of IL-8 or IL-6 induced by either RV1B or UVi-RV1B (Table 3.1-1). In these experiments, LY294002 dose-dependently blocked the induction of IL-8 mRNA in response to UV-irradiated RV1B but was less potent against RV1B induced IL-6 expression. These data suggest that at least a proportion of the proinflammatory response is due to mechanisms linked to viral endocytosis and is independent of viral replication.

Table 3.1-1. Percentage inhibition of IL-6 and IL-8 mRNA by LY294002.
Pre-treatment of RV1B-infected fibroblasts with PI 3-kinase inhibitor, LY294002 caused partial inhibition of viral induced IL-8 and IL-6 mRNA expression. Fibroblasts from a normal donor were pre-treated for 1 hour with the inhibitor, followed by RV1B infection as described in Materials and Methods. Cells were harvested 2 hrs p.i. and analysed for IL-8 and IL-6 mRNA expression. ND= not done. *= P<0.05 versus RV1B or UVi RV1B treated controls.** = P <0.01

	1 μM LY (±SEM)	10 μM LY (±SEM)	25 μM LY (±SEM)
RV1B IL-6	18 (± 29)	28 (± 33)	29 (± 4)**
RV1B IL-8	27 (± 28)	42 (± 17)	61 (± 13)*
UVi IL-6	ND	53 (± 13)*	40 (± 13)
UVi IL-8	ND	64 (± 9) **	80 (± 3)**

In contrast with the induction of IL-6 and IL-8 mRNA, RANTES expression was dependent on viral replication, since no induction was seen with UV-irradiated virus (Figure 3-6). Induction of RANTES mRNA also showed a different kinetic profile to that seen with IL-6, IL-8 and TNF-α. In this case, induction was significant at 4 hours p.i. in both normal (p=0.012) and asthmatic (p=0.029) fibroblasts (Figure 3-6), and was sustained to up to 8h p.i.. There was no significant difference between normal and asthmatic fibroblasts in the mRNA expression of this cytokine. Even though RANTES mRNA had been induced, no significant levels of RANTES protein were detected in either healthy or asthmatic fibroblasts infected in RV, suggesting that although there was detection of dsRNA leading to increased gene transcription, this did not lead to accumulation of RANTES protein.

Figure 3-3. Viral replication in normal and asthmatic fibroblasts. Primary bronchial fibroblasts from normal and asthmatic donors (n=7-10 per group) were infected with RV1B (0.05 MOI) for 2, 4 and 8h. Total RNA was extracted and analysed for presence of RV1B vRNA. Values were calculated relative to housekeeping genes UBC and A2 and normalized to each other; the individual data points are superimposed on a box plot showing median and IQR.

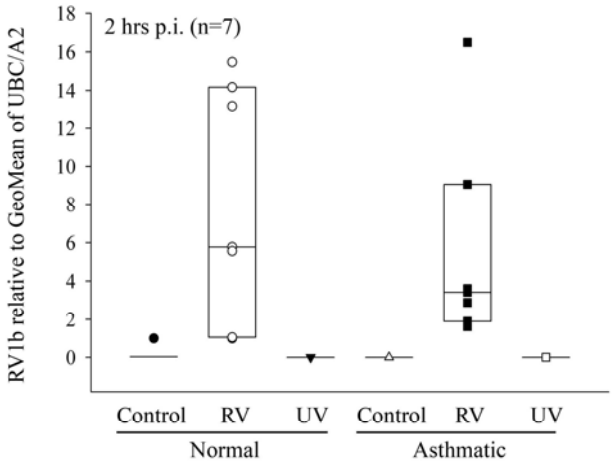
2 hrs p.i. (n=7)
RV1b relative to GeoMean of UBC/A2
18
16
14
12
10
8
6
4
2
0
Control
RV
UV
Control
RV
UV
Normal
Asthmatic

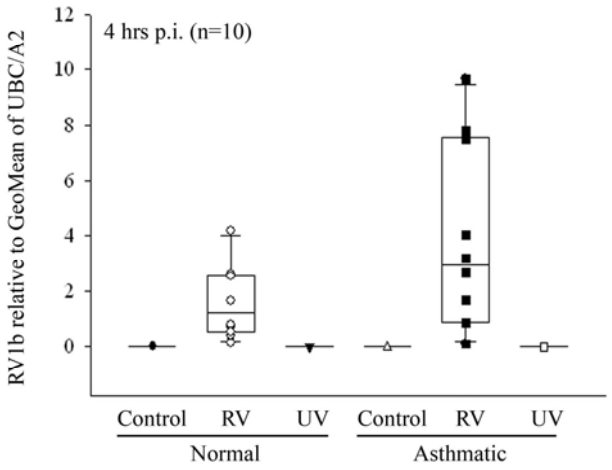
4 hrs p.i. (n=10)
RV1b relative to GeoMean of UBC/A2
12
10
8
6
4
2
0
Control
RV
UV
Control
RV
UV
Normal
Asthmatic

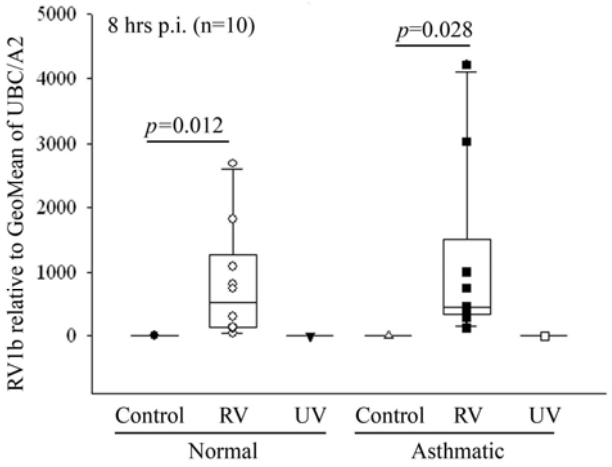
8 hrs p.i. (n=10)
p=0.028
p=0.012
RV1b relative to GeoMean of UBC/A2
5000
4000
3000
2000
1000
0
Control
RV
UV
Control
RV
UV
Normal
Asthmatic

Figure 3-4. Induction of proinflammatory genes in response to RV1B infection. Fibroblasts were treated as in Figure 3 and RT-qPCR and ELISA were used to measure mRNA expression (2h p.i.) and protein release (24h p.i.) respectively of IL-6 (A, C) and IL-8 (B, D). mRNA expression data were analyzed and presented as in figure 3-3.

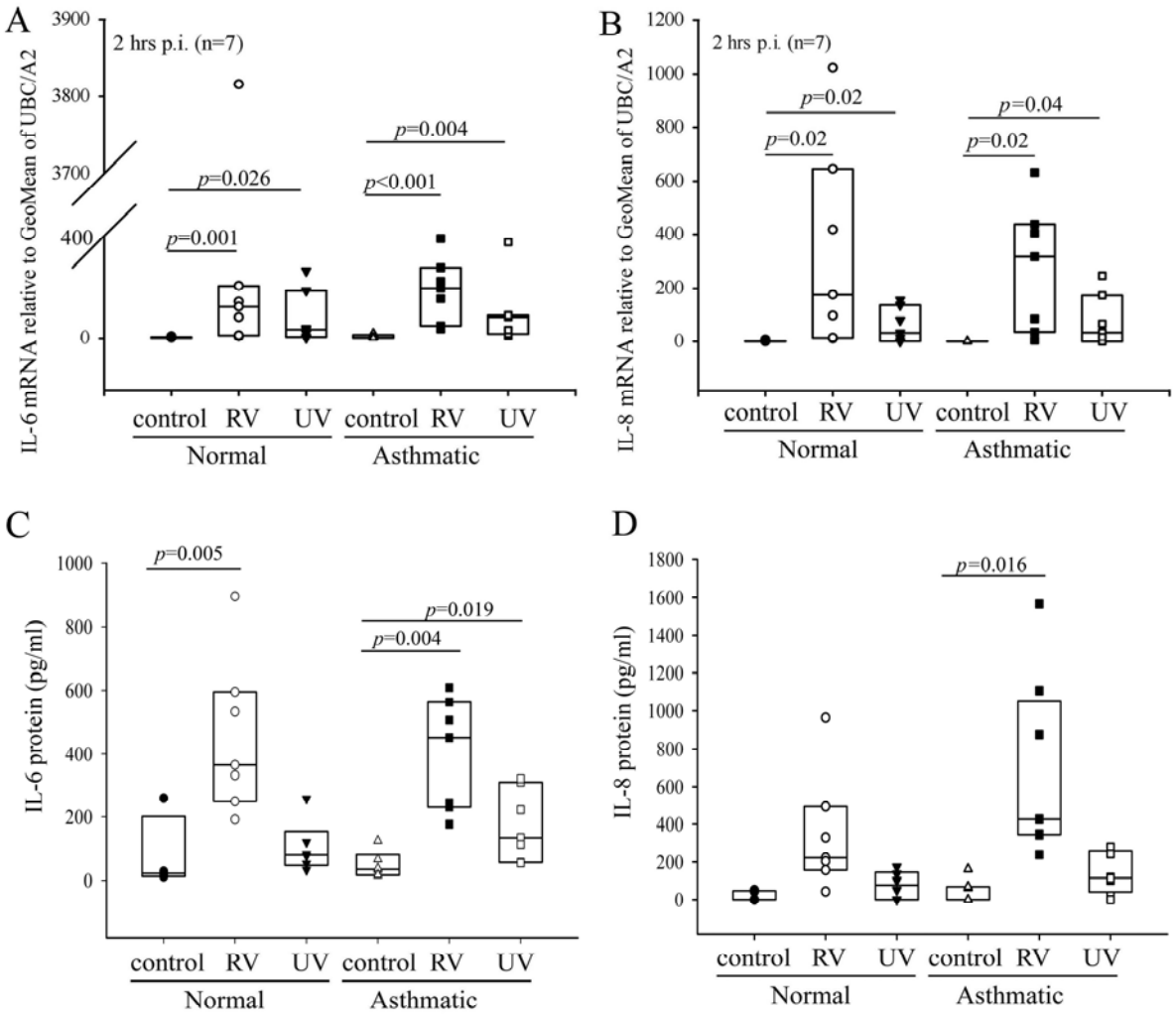

Figure 3-5. Induction of TNF-α mRNA in response to RV1B infection. Fibroblasts were treated as in Figure 3 and RT-qPCR used to measure mRNA expression of TNF-α.

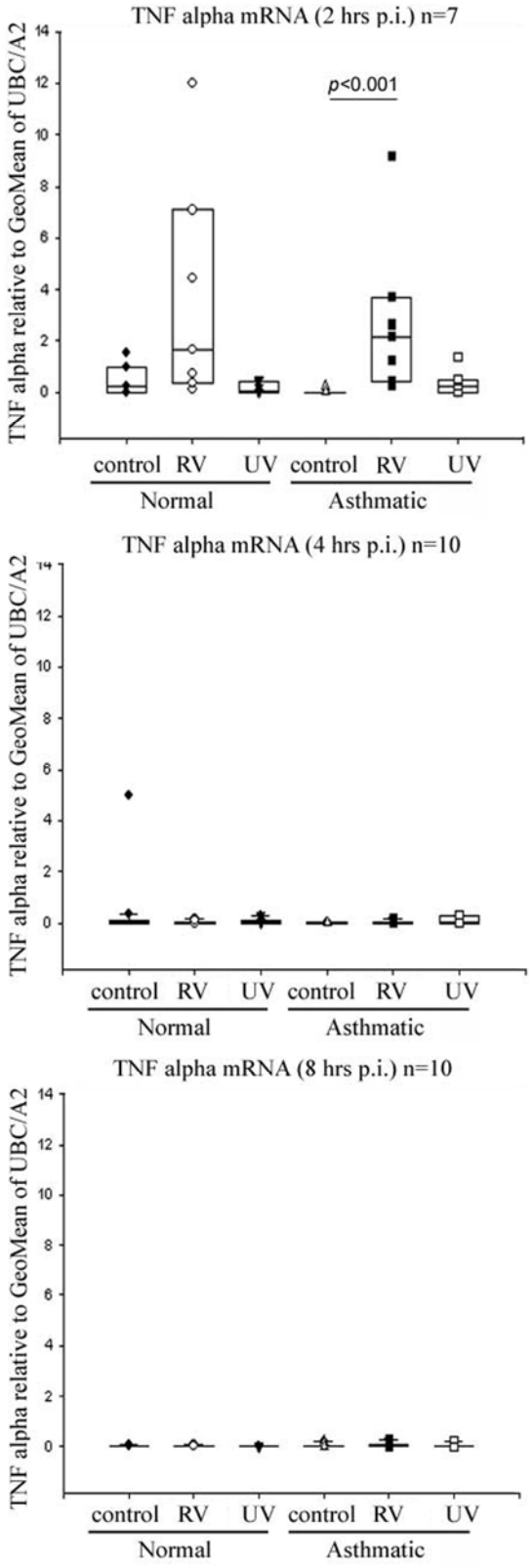

Figure 3-6. Induction of RANTES and IFN-β in response to RV1B infection. Fibroblasts were treated as in Figure 3 and RT-qPCR used to measure mRNA expression of RANTES (A) and IFN-β (B) at 4h p.i.. Data were analyzed and are presented as in figure 3-3.

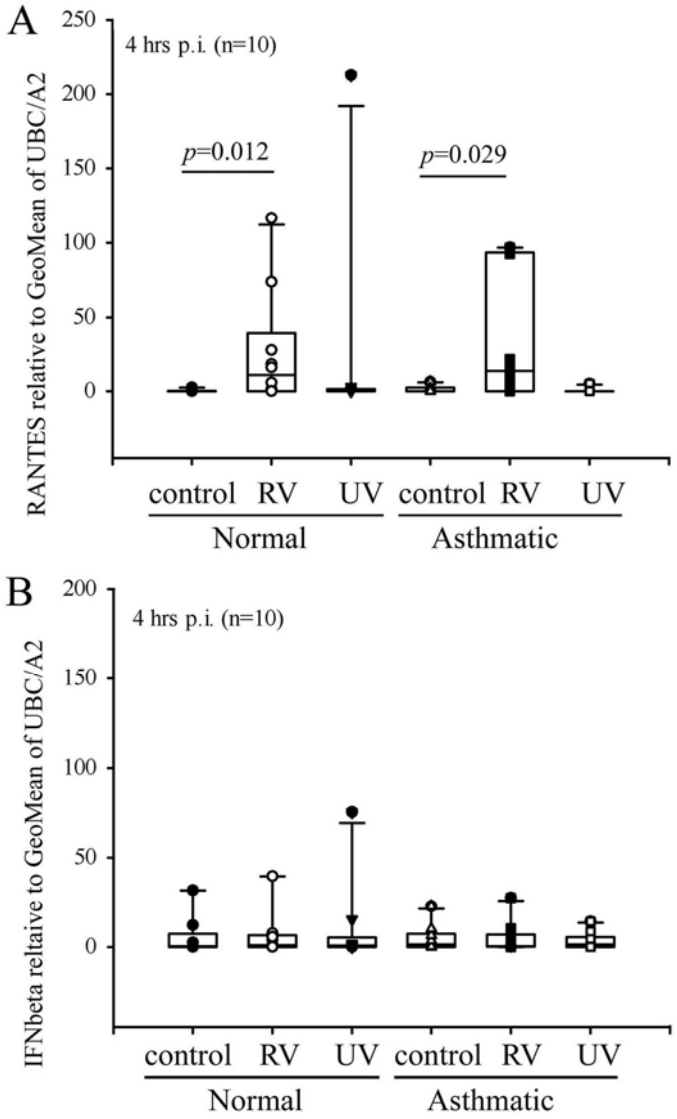

3.1.3 IFN-β was not significantly induced by RV1B in fibroblasts but was rapidly induced by treatment with double-stranded RNA

Even though vRNA was detectable in the infected cultures and expression of RANTES had been triggered in a replication-dependent manner, no significant induction of IFN-β transcription after RV1B infection was found (Figure 3-6 B). Although a few subjects in the normal control group showed some IFN-β expression at 8 hours, no IFN-β protein was detected in any fibroblast cultures at 24 hours p.i.(n=9 normals, n=5 asthmatics); in these experiments, parallel infection of two BEC cultures with RV1B at the same MOI (0.05) yielded detectable IFN-β (2.49 and 2.2 ng/ml) 24 hours p.i.

As no IFN-β was detected in response to RV infection, fibroblasts were treated with synthetic double stranded RNA (polyI:C), a toll-like receptor 3 (TLR3) agonist, which allows the measurement of IFN-β mRNA induction in the absence of cytopathic cell death. This agonist caused high and sustained levels of RANTES and IL-8 expression (Figure 3-7A). IFN-β mRNA was also rapidly induced during the first 2 hours of exposure but decayed 8 hours post-treatment (Figure 3-7B). Interestingly, the induction of IL-8 and RANTES was maximal at ≤10μg/ml polyI:C, whereas the IFN-β response continued to rise at all doses tested. Thus, it appeared that the sensitivity of the Type I interferon response was lower than that of the proinflammatory response, consistent with that observed in response to RV infection.

Since polyI:C stimulation led to induction of IFN-β expression, responses of normal and asthmatic fibroblasts were compared in this model. Both the kinetics and dose response were examined for the induction of IFN-β using fibroblasts from 6 normal and 6 asthmatic volunteers to ensure that any differences in sensitivity or magnitude of response were uncovered. IFN-β mRNA was induced in a dose-dependent manner in normal and asthmatic fibroblasts, however no significant differences between the groups at 2, 4, 8 and 24 hours were observed at all concentrations of polyI:C tested (Figure 3-7 C). IFN-β protein released from normal and asthmatic fibroblasts treated with 1 and 10 μg/ml polyI:C were also measured, but no significant differences were found between the two groups (Figure 3-7 D). As with IFNβ, RANTES protein was detected following stimulation with polyIC.

Figure 3-7. Kinetics and dose responses to Poly I:C. Fibroblasts were exposed to poly I:C for up to 24h. Total RNA was extracted and RT-qPCR used to measure expression of RANTES and IFN-β. Data were analyzed as in Figure 3-3. In (A and B), the graphs show mean values for RANTES (A) and IFN-β (B) mRNA expression at 2 and 8h post treatment with poly I:C; data were obtained in 3 independent experiments using fibroblasts of one normal subject. Plot (C) shows median values for IFN- β mRNA expression by fibroblasts from 6 normal (●) and 6 asthmatic (■) subjects 2 hours post-treatment with polyI:C. The box plots in (D) show data for IFN-β protein release from 6 normal and 6 asthmatic fibroblasts measured 24h post exposure to 1 or 10μg/ml poly I:C. The limit of detection was 25 pg/ml. The 3 data points marked with an asterisk were below the limit of detection and were given a value of 25 pg/ml for analysis. Data were analyzed using Kruskal Wallis or Mann Whitney U test.

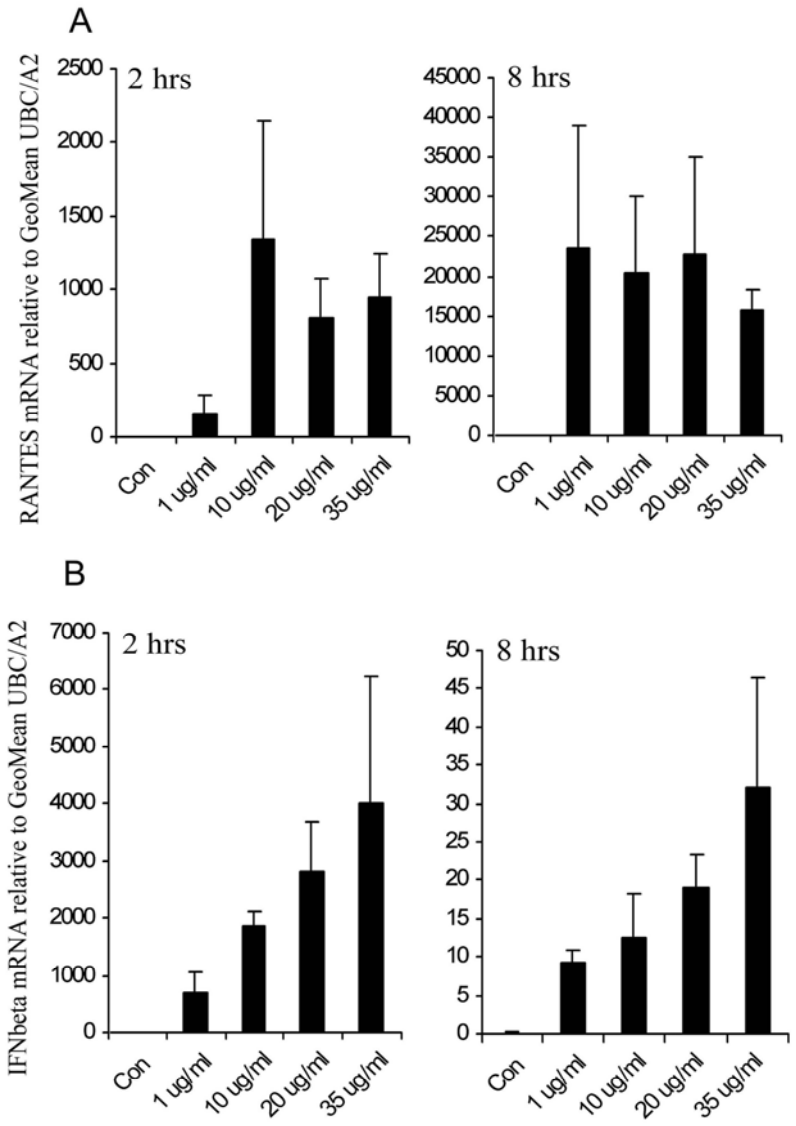

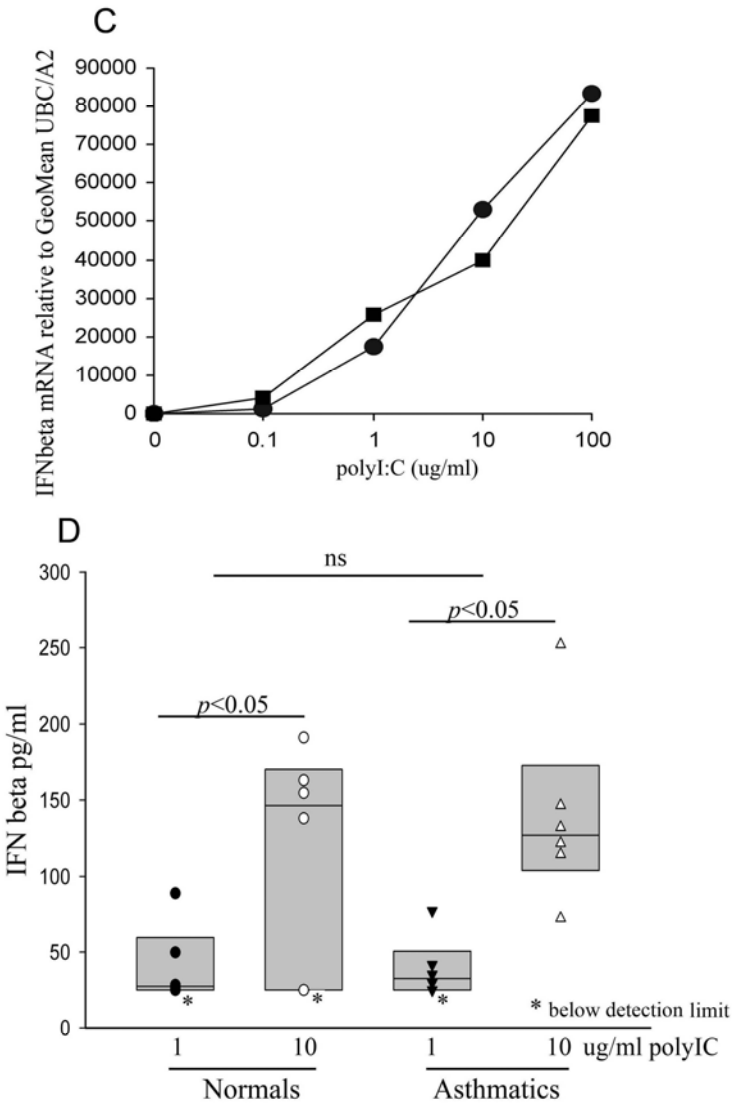
C
IFNbeta mRNA relative to GeoMean UBC/A2
90000
80000
70000
60000
50000
40000
30000
20000
10000
0
0
0.1
1
10
100
polyI:C (ug/ml)
D
IFN beta pg/ml
300
250
200
150
100
50
0
ns
p<0.05
p<0.05
* below detection limit
1
10
1
10 ug/ml polyIC
Normals
Asthmatics

3.1.4 Exogenous IFN-β protects primary bronchial fibroblasts from RV1B infection

Given the lack of endogenous IFN-β production by bronchial fibroblasts during early stages of RV-infection, it was postulated that this may account for their high susceptibility to RV infection. Therefore, fibroblasts were pre-treated with IFN-β for 24 hours and subsequently infected with RV1B (MOI=0.05) for 8 hours. Phase-contrast pictures show clear CPE in cells infected with RV1B in the absence of IFN-β; in contrast, no CPE was observed in RV1B infected cells in the presence of IFN-β (Figure 3-8 A). In parallel, RV1B vRNA was significantly reduced in the presence of IFN-β in the normal group ($p=0.028$), as well as in the asthmatic group ($p=0.001$) (Figure 3-8 B). There was also a significant decrease in RV1B virus particles released into the culture medium in the presence of IFN-β ($p=0.002$) (Figure 3-8 C). Since RV1B induced pro-inflammatory cytokines production in the absence of replication, it was also determined whether the presence of IFN-β had an impact on the production of IL-8. In these experiments, fibroblasts were pre-treated with IFN-β for 24 hours before being infected with RV1B. Expression of IL-8 mRNA was not significantly induced by IFN-β treatment alone but was significantly increased at 8 hours p.i. with RV1B (ie. after 32 hours of IFN-β treatment) in cultures of normal (but not asthmatic) fibroblasts (Figure 3-8D). However, IFN-β pre-treatment did not augment IL-8 production in response to RV1B infection (Figure 3-8E).

Figure 3-8. IFN-β protects against RV1B infection. Fibroblasts were pre-treated for 24h with 1000 IU/mL IFN-β and then infected with 0.05 MOI RV1B in the presence and absence of IFN-β. Phase-contrast photomicrographs comparing the extent CPE in cells infected with RV1B without IFN-β (left panel) or with (right panel) IFN-β (A). The effect of IFN-β on RV1B vRNA (B) or IL-8 mRNA (D) expression in normal or asthmatic fibroblasts at 8h p.i. was measured by RT-qPCR. The effect of IFN-β on release of infectious viral particles(C) or IL-8 protein (E) at 8h p.i., as determined by HeLa cell titration assay or ELISA, respectively.

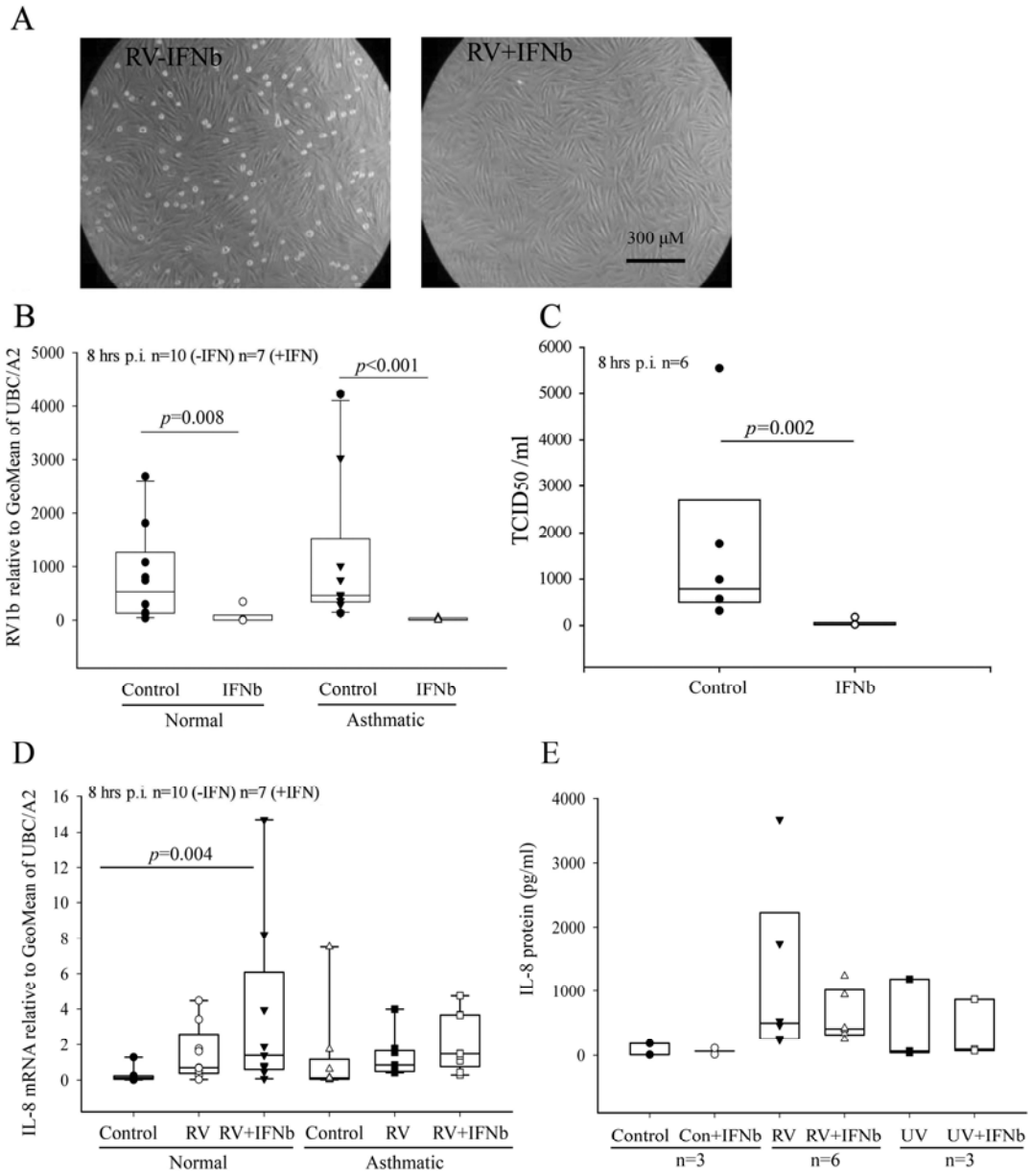

Figure 3-9. Model for the contribution of bronchial fibroblasts to inflammation during a viral-induced asthma exacerbation. Airway fibroblasts may be susceptible to infection in asthma due to epithelial disruption which facilitates entry of virus to the submucosa. Once infected, the lack of an antiviral IFN-β response by the fibroblasts coupled with a deficient protective epithelial innate immune response in asthma renders the cells permissive for viral replication leading to prolonged infection. However, the ability of the fibroblasts to respond to rhinovirus with a proinflammatory response exacerbates existing airway inflammation to contribute to an exacerbation.

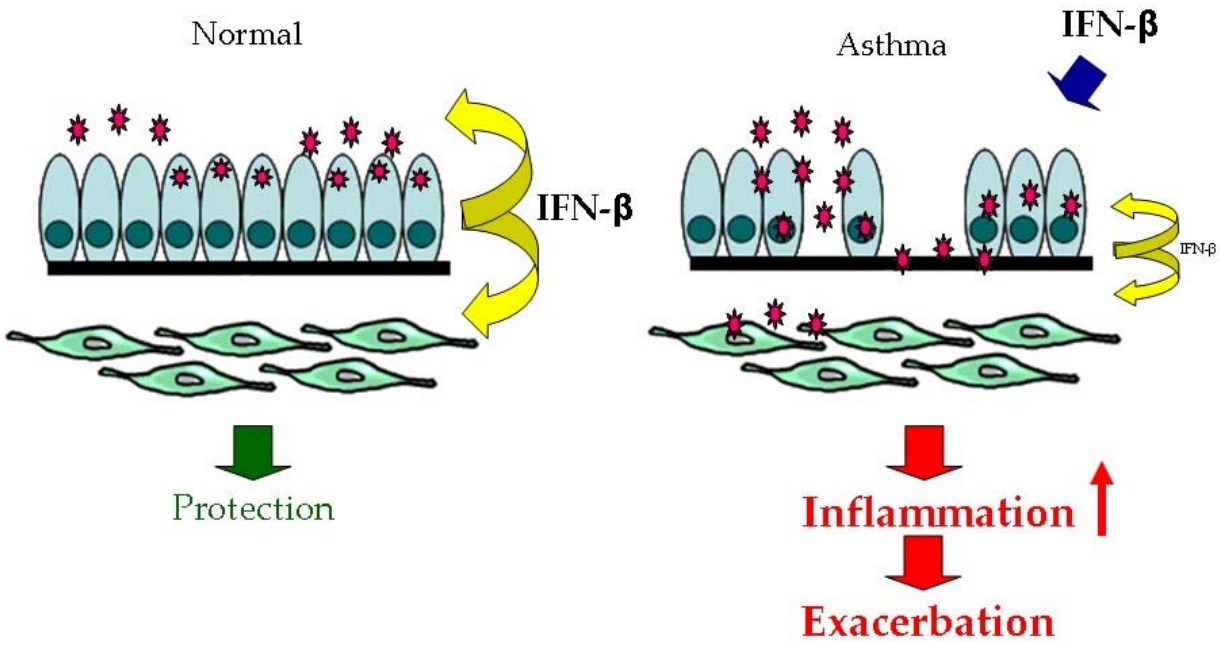

Discussion

These studies have demonstrated that infection of primary bronchial fibroblasts with RV1B *in vitro* induced a rapid proinflammatory response in the absence of any significant induction of IFN-β. Consequently, the cells were permissive for viral replication and were highly susceptible to virus-induced CPE, which was shown could be prevented by treatment with exogenous IFN-β. Although the fibroblasts failed to make IFN-β in response to RV1B, treatment with synthetic double-stranded RNA induced a rapid IFN-β response demonstrating their capability to make IFN-β in the presence of a danger signal. However, no difference in the ability of normal or asthmatic fibroblasts to make IFNβ mRNA was observed in response to poly I:C. These findings do not support the hypothesis that the defective innate immune response previously reported in asthmatic bronchial epithelial cells (Wark et al., 2005c) is mirrored in other structural cells from the asthmatic airway, as a consequence of a common underlying genetic mechanism.

The susceptibility of bronchial fibroblasts to RV1B was striking. RV1B - specific vRNA was demonstrable as early as 2 hours p.i. with RV1B (MOI=0.05) and was dependent on viral replication, as no readout was detectable in cells incubated with UV-irradiated virus. Although there was a trend for higher viral replication in the asthmatic fibroblasts at 4h which may have reached statistical significance if more fibroblasts were tested, it is unlikely that this small relative difference would have much biological relevance since it is clear that the normal fibroblasts were also highly susceptible to infection by RV1B at the later time point. Infection caused a low level of CPE at 9 hours following the first round of viral replication, reflecting the expected level of infection. Following subsequent rounds of viral replication, CPE increased at 24 and 48 hours with large-scale cell death being evident. These findings are consistent with the fact that diploid fibroblast cell lines are used for propagation of HRV and are more efficient than HeLa cells for recovery of HRVs from clinical isolates (Cooney and Kenny, 1977), further underlining their permissiveness for RV replication. However, these results contrast with a previous study in which lung fibroblasts were infected with RV at an MOI of 10 yet infection of only 5-15% of cells observed (Ghildyal et al., 2005). In a small study comparing fibroblasts from 2 normal and 2 asthmatic donors, it was also observed that higher doses of RV16 were required for infection. However, no significant induction of IFNβ by either group of fibroblasts was seen. As RV16 is a major group virus which uses ICAM-1 to infect cells, whereas RV1B is a minor group

virus that uses the low density lipoprotein receptor for entry, the observed difference in susceptibility may reflect differences in receptor levels. However, as ICAM1 is up-regulated by pro-inflammatory cytokines such as TNFα (Boero et al., 2007), it would be of interest to evaluate the susceptibility of primary fibroblasts to RV16 infection after treatment with TNFα to up-regulate ICAM-1 expression.

In view of their susceptibility to the cytopathic effects of RV1B, the kinetics of the fibroblast responses at early time points (0-8 hours p.i.) were examined in order to determine primary responses to viral infection, before significant cell death occurred. Messenger RNA expression of the pro-inflammatory cytokines IL-8, IL-6 and TNF-α was rapidly induced by RV1B infection, but no disease-related differences were observed, similar to our findings with primary BECs (Wark et al., 2005d; Wark et al., 2007b). No significant differences in RV-1B induced IL-8 and IL-6 protein release were found. These data contrast with the findings of Oliver et al. who found that human airway smooth muscle (HASM) cells from asthmatic subjects have significantly increased IL-6 and IL-8 production in response to RV infection which was attributed to differences in transcriptional regulation of the cytokines (Oliver et al., 2006). This difference between fibroblast and HASM cells may reflect cell-type specific responses.

In contrast with previous studies in BECs where proinflammatory cytokine gene expression was dependent on viral replication (Wark et al., 2005e; Wark et al., 2007c), induction of IL-6 and IL-8 by bronchial fibroblasts in the presence of UV-irradiated virus was observed. This indicates that the mechanisms of signal transduction leading to cytokine production can differ depending on cell type. However, in their studies of HASM cells, Oliver et al also reported that IL-6 and IL-8 release were induced by both RV16 and UV-irradiated RV16 (Oliver et al., 2006), which is consistent with our findings. This suggests that, in mesenchymal cells, at least a part of the expression of IL-6 and IL-8 occurs independently of viral replication. It seems highly unlikely that this response is due to the presence of endotoxin, as the media that were used were endotoxin-free and there was no evidence of bacterial infection in any of our cultures. It is most likely that the fibroblasts are responding to cytokines or damage-associated molecular patterns (DAMPs) released by the HeLa cells during propagation of the virus. In related studies, it was found that conditioned media from RV-infected bronchial epithelial cells elicits a marked proinflammatory response when applied to bronchial fibroblasts (Ribbene A et al., 2007).

Previous studies have shown that RV-39 (a major group virus) induced IL-8 expression in epithelial cells occurred by ICAM binding and activation of PI 3-kinase

(Bentley et al., 2007; Newcomb et al., 2005). In these studies, it was also found that inhibition of PI 3-kinase down-regulated both IL-8 and IL-6 mRNA induced by RV1B. This suggests that a minor group virus also activates PI 3-kinase and therefore that activation of PI 3-kinase is not directly dependent on ICAM binding. Other studies have also suggested that IL-8 release from virally infected fibroblasts involves stimulation of reactive oxygen species at the cell surface via a flavoprotein that may act in concert with p47-phox (Kaul et al., 2000). This pathway may control residual IL-8 and IL-6 expression in our model.

Although increases in fibroblast RANTES mRNA expression 4-8 hours post-infection were observed, indicating their ability to sense active viral replication, there was no significant induction of IFN-β expression in response to viral infection up to 8 hours p.i. This suggests that the signals leading to RANTES and IFN-β expression are distinct. Such a proposal would also explain why induction of RANTES and IFN-β by synthetic dsRNA (poly I:C) showed a different dose response (Figure 3-7). Several mechanisms have been identified for detection of dsRNA, including TLR3, retinoic acid-inducible gene I (RIG-I), melanoma differentiation-associated gene 5 (MDA-5), all of which lead to activation of interferon response factor -3 (IRF-3), as well as double-stranded RNA-dependent protein kinase (PKR) which utilizes NFκB for control of transcription (Kawai and Akira, 2007b). Studies using BECs have suggested that RANTES expression is mediated by PKR (Gern et al., 2003), although the detection of double-stranded RNA by host cells is known to occur in a cell-type- and pathogen-type-specific manner. A recent study by Kotla et al (Kotla et al., 2008) has reported a deficient IFN-β response to RV14 infection in a lung alveolar epithelial cell line which was shown to be due to lack of IRF-3 activation following RV14 infection. In these studies, inhibition of viral protein synthesis resulted in an increase in IFN-β mRNA levels suggesting that a virally encoded factor prevented activation of the type I interferon response. Whether a similar anti-interferon mechanism can be employed by RV1B in fibroblasts remains to be determined.

Even though no significant induction of IFN-β mRNA in bronchial fibroblasts in response to RV1B was observed, its expression was elicited using double stranded RNA. This difference may be due to the cellular location of TLR-3, a key sensor of dsRNA that controls IFN-β expression (Kawai and Akira, 2007a). While TLR-3 is predominantly localized in endosomes in epithelial cells (Matsukura et al., 2006), it has been found on the surface of fibroblasts (Matsumoto et al., 2002b). Extracellular localization of TLR3 could explain the slow kinetics of IFN-β expression in response to

RV, as activation would be dependent on detection of dsRNA released by lysis of infected cells. It may also account for the occasional detection of IFN-β mRNA in normal fibroblast cultures 8 hours p.i. However, no significant IFN-β protein at 24 hours was detected, suggesting that insufficient induction of IFN-β mRNA expression had occurred to result in an increase in protein synthesis. *In vivo*, localization of TLR-3 on the surface of fibroblasts would allow them to detect extracellular dsRNA released from infected epithelial cells and as a consequence serve as sensors of infection in the epithelial-mesenchymal trophic unit (EMTU), propagating and amplifying signals to the immune system (Holgate et al., 2007).

The high susceptibility of fibroblasts to rhinovirus infection has potential implications for asthma exacerbations. In asthmatic airways, it is known that the bronchial epithelium is damaged (Puddicombe et al., 2000) and that epithelial shedding occurs (Montefort et al., 1992). This may increase the probability that the underlying fibroblasts are accessible to rhinovirus during an infection. The poor ability of fibroblasts to mount their own innate immune response implies that local IFN production is essential for triggering an antiviral response in these cells. However, it has already been demonstrated that asthmatic BECs have a deficient innate immune response (Wark et al., 2005f; Contoli et al., 2006a), compromising the local immune response in the airway microenvironment. The lack of an antiviral response, but the clear presence of a proinflammatory response, suggest that airway fibroblasts may contribute to inflammation and asthma exacerbation. This demonstration that exogenous IFN-β protects fibroblasts against infection adds weight to the argument that treatment with exogenous IFN-β is a potential therapy against virus-induced asthma exacerbations.

4 Chapter 4: Results

4.1 Transforming Growth Factor-beta-2 (TGF-β_2) promotes Rhinovirus-1B (RV1B) replication in Primary Bronchial Epithelial Cells (PBECs) by modulating the innate immune response

Rationale

Further to the results in chapter 3, it was decided to investigate the immune-modulatory effects of TGF-β on the innate immune response of PBECs to rhinovirus infection. TGF-β has been shown to be elevated in the asthmatic airways and is a candidate for the initiation of airway remodelling in asthma (Boxall et al., 2006), (Aubert et al., 1994; Chu HW, 2008; Vignola et al., 1997). One reason for this has been suggested that in asthma there is a situation of chronic wound repair by a damaged epithelium, which in response will release pro-inflammatory and pro-fibrotic mediators such as TGF-β (Clark and Coker, 1998; Zhang et al., 1999). McCann *et al* have demonstrated that the addition of exogenous TGF-β to PBECs from healthy donors, markedly increased the replication of respiratory syncytial virus (RSV) (McCann and Imani, 2007). RSV is an enveloped virus, which like RV, causes lower respiratory tract infections in infants and is implicated in asthma exacerbations (Hansbro et al., 2008). It was decided to investigate whether similar effects of exogenous TGF-β on RV replication could be seen in PBECs from healthy and asthmatic donors. Since previous studies have shown that asthmatic subjects have elevated TGF-β in their airways, it was decided to measure baseline TGF-β in asthmatic cell cultures in order to determine whether previous observations that this cytokine is produced at higher levels in asthmatic cell cultures compared to healthy controls can be supported (Chu HW, 2008).

It was hypothesized that treatment of epithelial cells with TGF-β may cause a change into a more fibroblastic phenotype in a process called epithelial-mesenchymal transition (Cicchini et al., 2008) (Larue and Bellacosa, 2005). EMT has been associated with the increased motility and invasiveness of tumour cells (Larue and Bellacosa, 2005). Therefore, this change would cause an increase in cell survival. In the context of viral replication, where containment of viral infection depends on infected and neighbouring cells undergoing apoptosis, an increase in cell survival would promote

viral replication. In addition to phenotypic changes caused by the presence of TGF-β, it was decided to investigate the effects of this cytokine on the innate immune response against RV infection. It was also hypothesized that TGF-β may modulate the innate immune response and facilitate RV replication in PBECs. It was previously described that TGF-β can act as an anti-inflammatory cytokine, where homozygous mutations in the TGF-β_1 allele in mice resulted in a multi-focal inflammatory cell response and tissue necrosis that lead to organ failure and death (Shull et al., 1992).

4.1.1 Photomicrographs of PBEC after incubation with RV1B and TGF-β_2

PBECs from 3 healthy volunteers were used to perform initial dose response experiments, using 1-25 ng/ml TGF-β_2. Cells were incubated in starvation medium containing 1, 10 or 25 ng/ml TGF-β_2 for 24 hours. The cells were then infected with RV1B, washed and further incubated for 24 or 48 hours in the presence or absence of TGF-β_2. At 24 hours post-infection (p.i.) with RV1B, extensive cytopathic effects (CPE) were seen compared to control samples (Figure 4-1). The extent of cell death was visibly exacerbated in the presence of virus together with TGF- β_2 at 24 hours p.i. However, in the presence of TGF- β_2 alone or UV-irradiated virus with TGF- β_2, no substantial cell death was observed. By 48 hours p.i., few cells remained attached in the presence of virus with TGF- β_2, particularly at higher concentrations of TGF- β_2 (Figure 4-2). Because of the extensive cell death observed at 48 hours p.i., samples obtained at 24 hours p.i. were chosen to measure viral RNA expression, and samples obtained at 48 hours p.i. to measure infectious virus particles released using an end-point dilution assay ($TCID_{50}$/ml).

Figure 4-1. Photomicrographs of PBECs from one healthy volunteer at 24 hours post-infection with RV1B in the presence or absence of TGF- β_2 at x10 magnification.

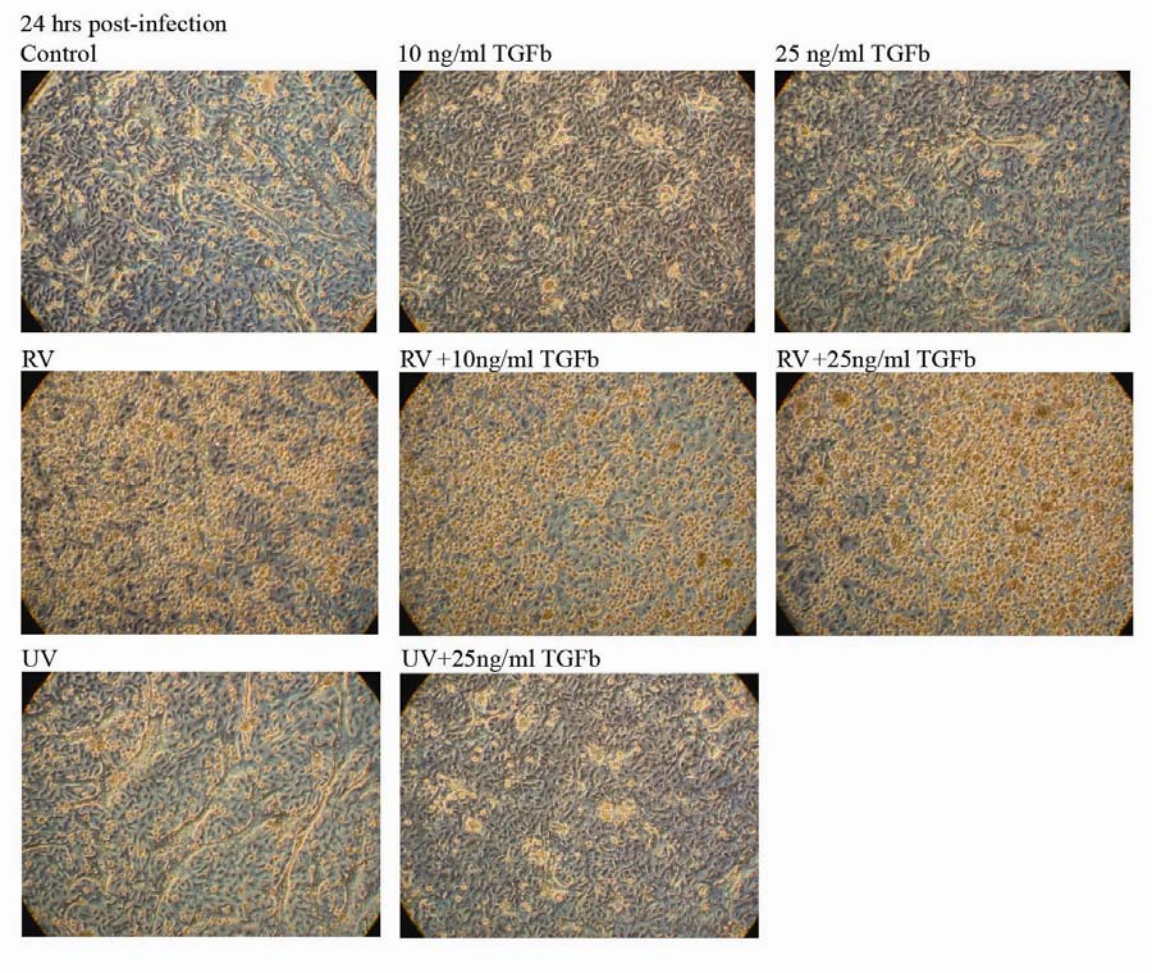

Figure 4-2. Photomicrographs of PBECs from one healthy volunteer at 48 hours post-infection with RV1B in the presence or absence of TGF- β_2 at x10 magnification.

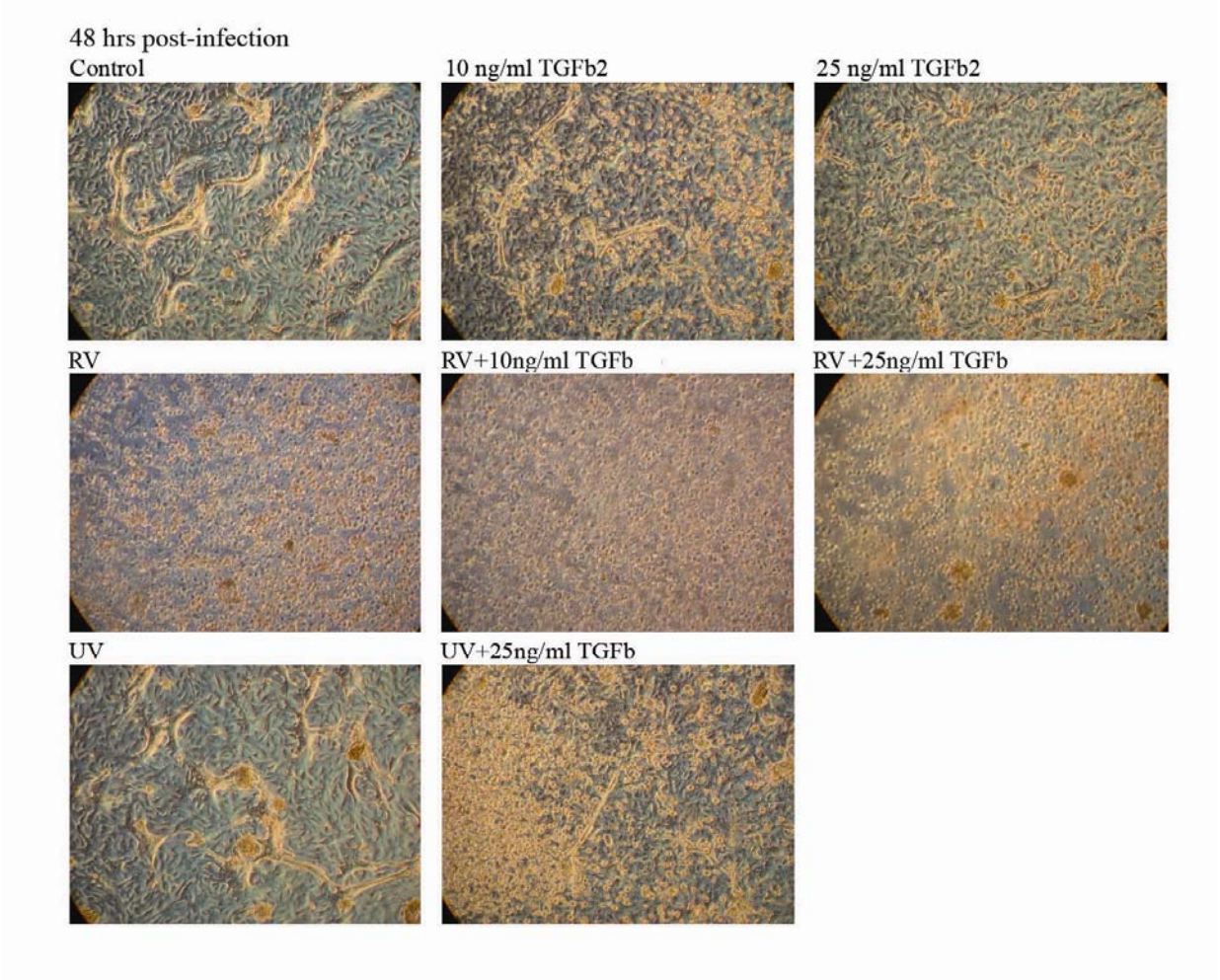

4.1.2 TGF- β_2 promotes RV1B replication in PBECs at later stages of infection

Cells from healthy control volunteers were treated as described above and incubated for 24 and 48 hours. After each time point, supernatants were removed, and stored at -80^{0}C until further analysis. Cells were harvested with TRIzol® reagent and stored at -80^{0}C until RNA extraction. Figure 4-3 shows mean data obtained from measurements of viral RNA and $TCID_{50}$/ml, obtained from 3 independent experiments performed with samples obtained from 3 different healthy donors. No statistically significant differences were observed in viral gene expression in the presence of TGF-β_2 both at 24 and 48 hours, however at 24 hours a trend towards a dose-dependent increase in viral gene expression was observed (Figure 4-3 A). Figure 4-3 B shows that at 48 hours p.i., TGF-β_2 increased viral replication both at a concentration of 10 ng/ml and 25 ng/ml, only the latter of which reached statistical significance. Although data obtained from measuring RNA provides useful information, it is not as conclusive as measuring

infectious virus particles as it does not measure the levels of viable virus shed from the cells. Therefore, for subsequent experiments conclusions were based on viral end-point dilution results. Though the data obtained with 25 ng/ml TGF-β were statistically significant, 10 ng/ml TGF-β_2 was chosen as a dose in subsequent experiments with PBECs from a large group of volunteers, as higher doses of this cytokine may have made interpretation of my data more difficult due to the extent of cell death in the presence of RV.

Figure 4-3. Viral mRNA and $TCID_{50}$/ml from PBEC infected with RV1B and treated with TGF-β. PBECs from 3 healthy volunteers were pre incubated with different concentrations of TGF-β_2 for 24 hours, followed by infection with RV1B at an MOI=0.05. Cells were then further incubated for a period of 24 and 48 hours in the presence or absence of TGF-β_2. Viral gene expression was quantified by RT-qPCR. Values are relative to housekeeping genes GAPDH and UBC and delta CT-values were calculated. Values were normalized to one patient (A). Additionally, viral supernatants were analysed using $TCID_{50}$/ml assays, see Materials and Methods (B). Graphs represent the mean values of 3 different experiments with 3 subjects, with error bars as Standard Error of the Mean.

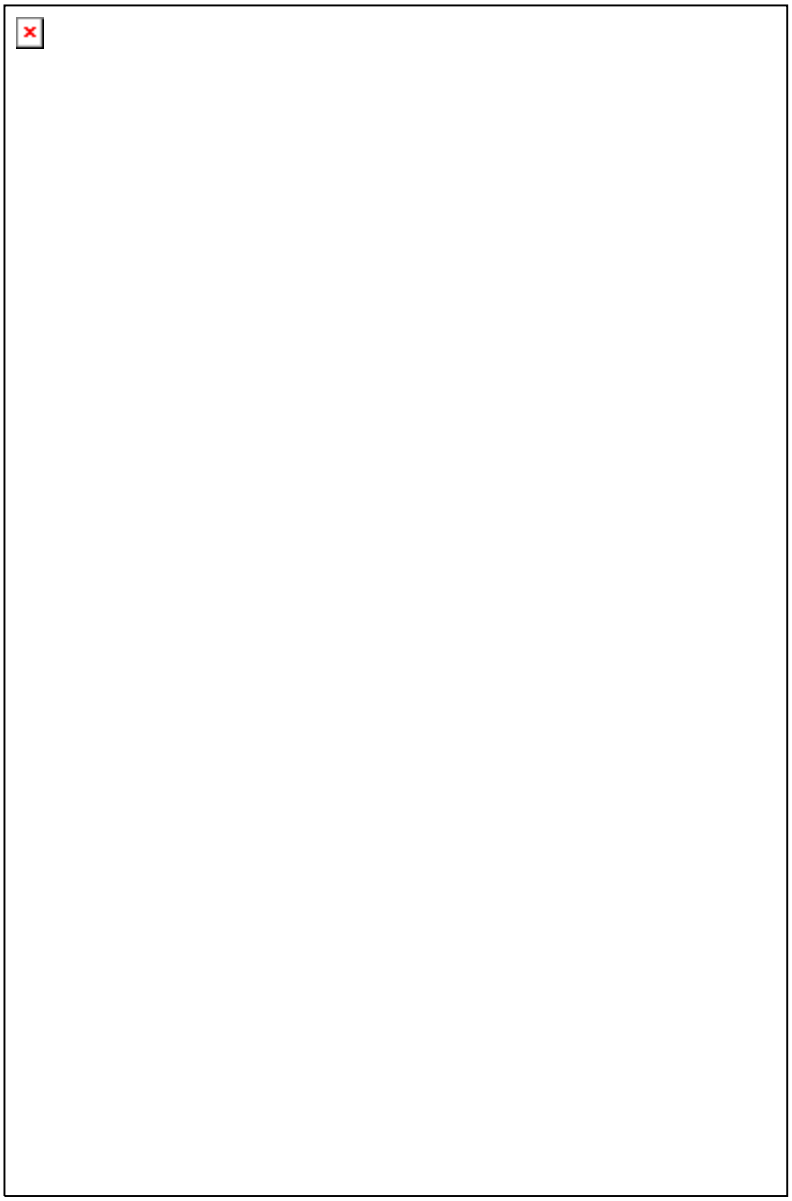

4.1.3 TGF- β_2 increases RV1B virus particle release in a larger population of healthy PBECs

Next it was investigated whether the TGF- β_2-mediated increase in RV1B replication was consistent in a larger number of samples obtained from 8 to 14 healthy volunteers. Two different doses of virus (MOI=0.01 and 0.05) were used to determine whether TGF- β_2 increased viral replication. Figure 4-4 shows no effect of TGF- β_2 on virus replication after 24 hours p.i. with either dose of virus (Figure 4-4 A and C). At 48 hours p.i., there was a significant increase in infectious virus particles released in the presence of TGF- β_2 at both doses of virus tested (Figure 4-4 B and D).

Figure 4-4. $TCID_{50}$/ml of PBECs from healthy volunteers were pre-treated for 24 hours with 10 ng/ml TGF-β_2, followed by infection with RV1B at MOI=0.01. Cells were then incubated in the presence and absence of TGF-β_2 for a period of 24 and 48 hours. The individual data points represent the $TCID_{50}$/ml values obtained from viral supernatants at 24 (A) and 48 hours post-infection (B). *p*-values were obtained by performing a Wilcoxon rank sum test. PBECs were also infected with a higher dose of virus (MOI=0.05) as above and $TCID_{50}$/ml values from samples incubated for 24 (C) and 48 hours (D) were plotted.

4.1.4 TGF- β_2 increases RV1B virus particle release in a larger population of asthmatic PBECs

In order to determine whether TGF-β_2 can increase RV replication in PBECs obtained from asthmatic patient donors the experiments were repeated as described in the previous section. A lower dose of virus (MOI=0.01) was chosen as previous titration experiments have shown a greater susceptibility of asthmatic cells to virus infection

(data not shown). Previous studies have also shown that asthmatic PBECs were more susceptible RV1B infection than normal PBEC (Wark et al., 2005g). Figure 4-5 shows no significant increase in virus replication in the presence of TGF-β_2 at 24 hours p.i. However, at 48 hours the presence of TGF-β_2 significantly increased RV replication in asthmatic PBECs (Figure 4-5).

Figure 4-5. $TCID_{50}$/ml of PBECs from asthmatic patients were pre-treated with 10 ng/ml TGF- β_2 and infected with RV1B (MOI=0.01) as described in . Data points represent $TCID_{50}$/ml obtained from viral supernatants of individual subjects at 24 (A) and 48 (B) hours.

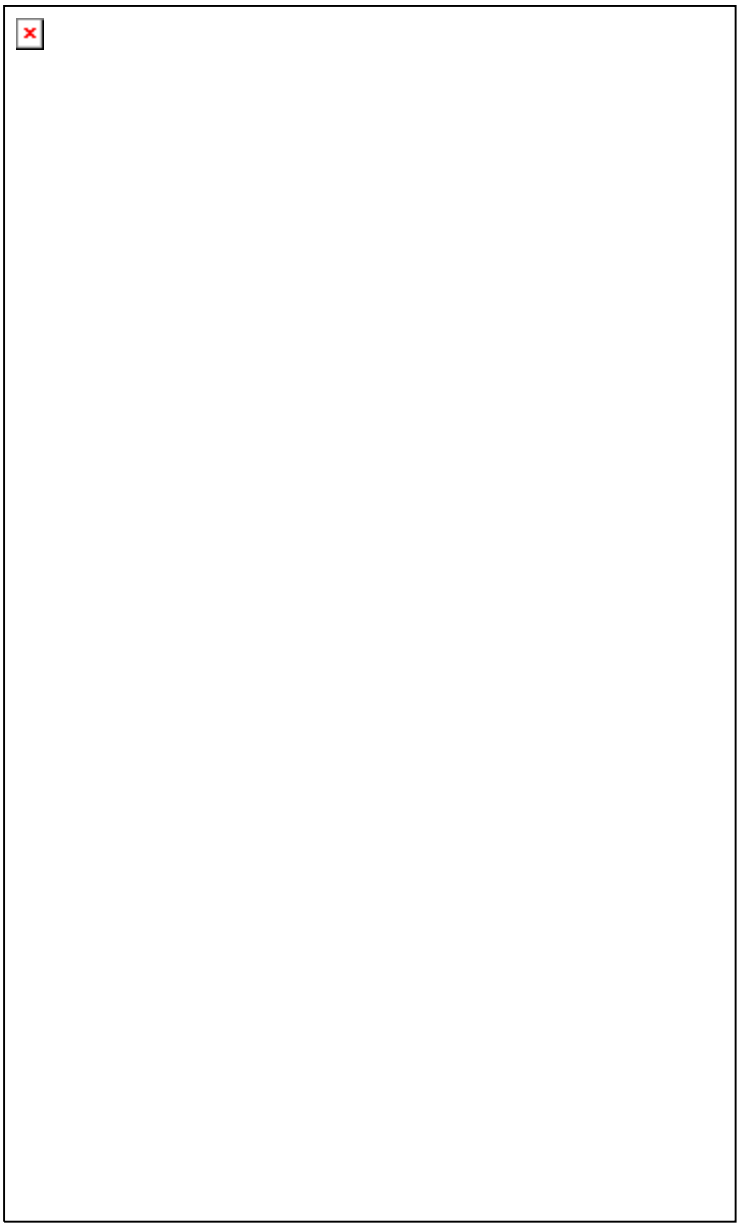

4.1.5 The effect of TGF-β on PBEC phenotype and virus induced apoptosis

In order to determine whether TGF-β was able to induce phenotypic changes in PBEC, the intracellular organization of actin was investigated. One of the hallmarks of EMT is actin reorganization, inducing cells to become more migratory (Rahimi and Leof, 2007). PBECs were seeded into collagen-coated 8-well chamber slides and cultured the cells until 80-90% confluent (see section 2.2.25 of Materials and Methods). Cells were then treated with 10 ng/ml TGF-β_2 for 72 hrs, after which they were fixed and stained with Alexa Fluor 488®-conjugated Phalloidin and Hoechst stain (Figure 4-6). Phalloidin is one of the group of toxins, also known as phallatoxins isolated from mushrooms *Amanita phalloides* (Molecular Probes product insert). It binds specifically to F-actin subunits preventing depolymerisation and is used as a tool for labelling, identifying and quantitating F-actin in tissue and cell cultures (Molecular Probes product insert). Samples were analyzed with a x20 objective on a Leica DMI6000 microscope. Images were obtained using filter cubes for the DAPI and GFP channel using the same settings for each sample. shows cells stained with phalloidin and Hoechst dye. Although no quantitative measurements were obtained, TGF-β treated cells showed a slight increase in the number of actin filaments (Figure 4-6). These may be formed as part of stress fibres caused by the presence of TGF-β which may hint at a migratory state of the cells. One of the markers of EMT is the increased expression of extracellular matrix proteins such as collagen. Collagen I gene expression was measured in cell samples obtained from one healthy subject treated with TGF-β and found increased collagen I mRNA levels in all samples that were treated with TGF-β (Figure 4-7).

Figure 4-6. Immunofluorescent staining of PBECs treated with TGF-β**.** PBECs were seeded into collagen-coated 8-well chamber slides and cultured until they were 80-90% confluent. Cells were then incubated in 10 ng/ml TGF-β_2 for 72 hrs, after which they were fixed and stained with Alexa Fluor 488®-conjugated Phalloidin and Hoechst stain.

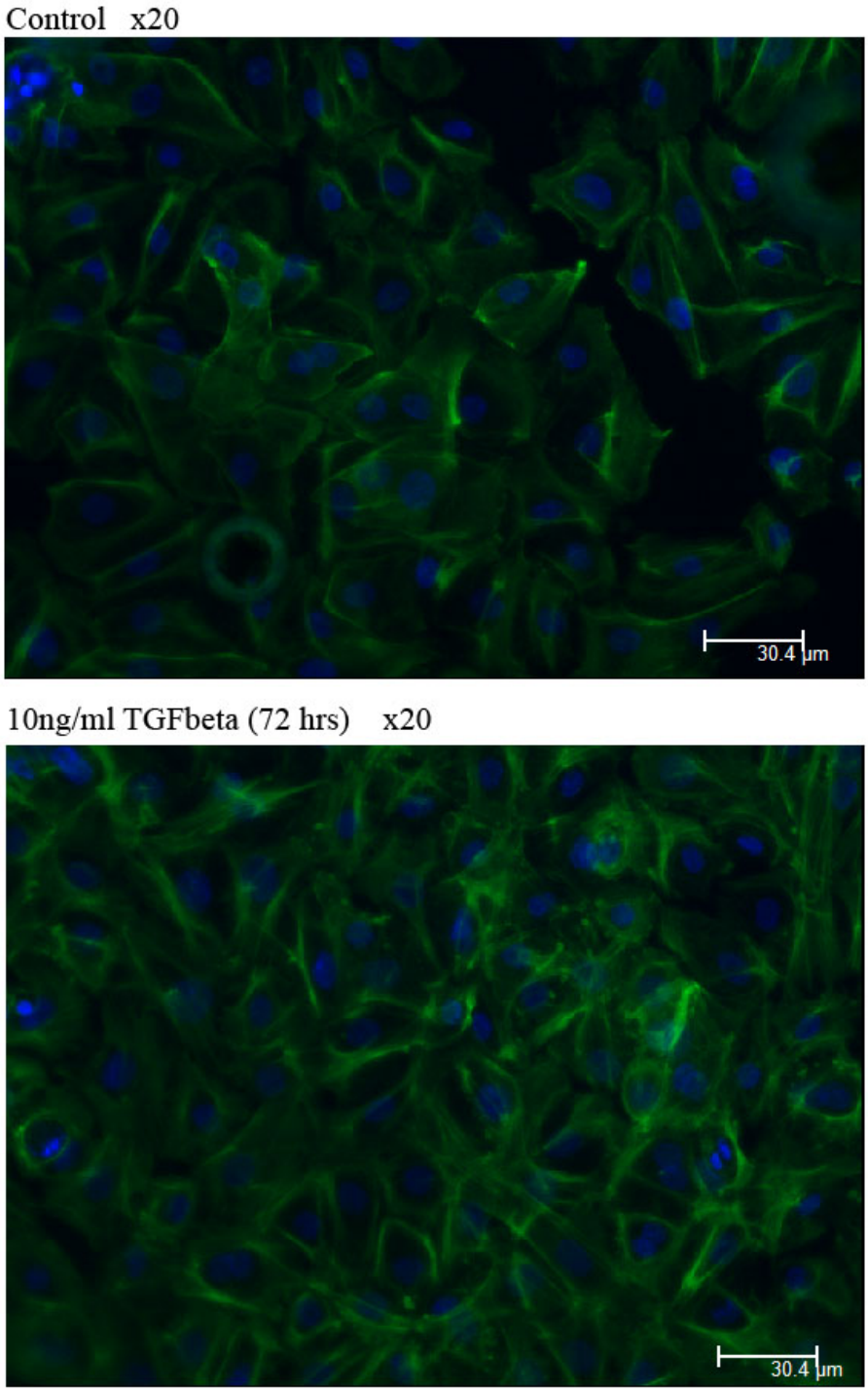

Figure 4-7. Collagen I mRNA expression in PBECs from one healthy volunteer. Cells were infected with RV (MOI=0.01) and incubated for 24 in the presence or absence of TGF-β. Collagen I gene expression was measured by RT-qPCR and CT-values were normalized first to the Geometric Mean of housekeeping genes GAPDH and UBC and then to untreated control samples by the delta-delta CT method as previously described. Graph shows relative Collagen I gene expression at 24 hours p.i.

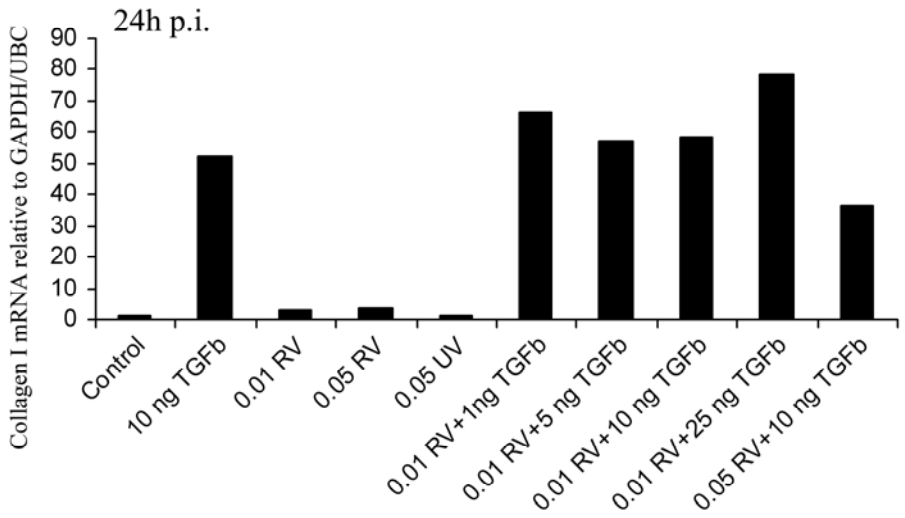

It was also decided to investigate the effects of TGF-β_2 on the apoptotic mechanisms of PBECs induced by rhinovirus. If this cytokine interfered with virus-induced apoptosis by inducing a pro-survival state, a reduction in apoptosis would be expected. Apoptosis is induced by intrinsic and extrinsic pathways. The intrinsic pathway is activated by mitochondrial membrane permeabilization to liberate cytochrome *c* to form the apoptosome together with dATP, APAF-1 and caspase-9 (Hail, Jr. et al., 2006). In contrast the extrinsic pathway is initiated by binding of death ligands to their receptors, such as Fas or TNF to their respective receptors (Hail, Jr. et al., 2006). These two pathways then converge to activate the effector caspases (Caspase-3 ,-6,-7), which are enzymes that cleave target proteins after an aspartate residue in their primary sequence and cause the morphological changes and nuclear fragmentation in the apoptotic cell (Kato et al., 2006).

PBECs from a healthy donor were seeded into collagen-coated 96-well plates at 20 000 cells per well. These were left overnight in a 37^0C incubator. Media were removed and replaced with starvation medium with or without 10 ng/ml TGF-β_2 and incubated for 24 hrs. Cells were then infected with RV stock (MOI=0.05) for 1 hour, washed, and further incubated in starvation media for 4, 8, and 24 hrs in the presence or

absence of TGF-β_2. After each time point a luminogenic caspase-3/7 substrate was added to each sample and incubated for 1 hour. Luminescence was then measured using a top count reader. Figure 4-8A shows that caspase activity was only significantly induced after infecting cell samples from one healthy subject for 24 hrs with RV. At 4 and 8 hrs post-infection, no significant difference in caspase activity was detected when compared to baseline levels. However, although there was a 7-fold difference in the amount of luminescence detected in RV-infected samples at 24 hrs p.i. compared to baseline levels, no difference in caspase 3/7 activity between TGF-β-treated and untreated samples was observed (Figure 4-8 A). Because significant caspase 3/7 activity was only detected at 24 hrs p.i., this experiment was repeated using PBECs from another healthy subject and infected for 24hrs. Mean values obtained from both experiments show a small decrease in relative caspase 3/7 activity in the presence of TGF-β (Figure 4-8B). It is likely that this assay is not sufficiently sensitive to detect differences in apoptosis between samples. Another confounding factor is that the two processes of apoptosis and necrosis are likely to occur simultaneously in the cell samples and so dissecting and quantitating one type of mechanism may be very difficult. A third factor to consider is whether caspases are involved in rhinovirus-induced apoptosis. Previous studies with the caspase inhibitor z-VAD showed controversial results with regards to cells survival and viral replication (Deszcz et al., 2005; Grassme et al., 2005; Taimen et al., 2004). Although an effect of TGF-β on the apoptotic machinery in RV-infected cells cannot be completely ruled out, it was decided to investigate other mechanisms that may explain my observations in the previous section.

Figure 4-8. Caspase 3/7 activity of RV-infected PBEC in the presence or absence of TGF-β. PBECs from a healthy donor that were seeded into collagen-coated 96-well plates and left overnight in a 37^0C incubator. Cells were then treated with or without 10 ng/ml TGF-β_2 and incubated for 24 hrs after which they were infected with RV stock (MOI=0.05) for 1 hour, washed, and further incubated in starvation media for 4, 8, and 24 hrs in the presence or absence of TGF-β_2 (A). After each time point a luminogenic caspase-3/7 substrate was added to each sample and incubated for 1 hour. Luminescence was then measured on a top count reader. Mean luminescence was also calculated from PBECs of 2 healthy subjects 24 hrs p.i. and graphed (B).

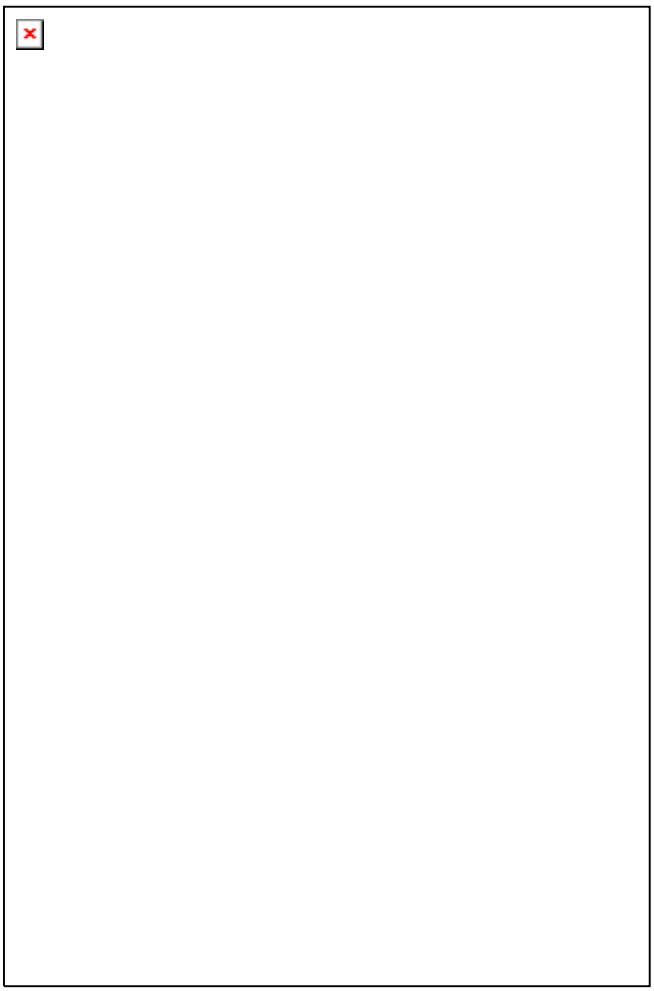

4.1.6 TGF-β reduces type I and type III interferon response to viral infection and poly I:C in healthy hbec

It was next decided to analyse the effect of TGF-β on the innate immune response to rhinovirus infection in primary bronchial epithelial cells from healthy control patient samples. A previous study has shown that the addition of exogenous TGF-β to primary bronchial fibroblasts enhanced rhinovirus replication, which was coupled by a diminished type I interferon response (Thomas et al., 2009).

IFN- β protein was measured in culture supernatants from healthy PBECs infected with rhinovirus for 48 hrs. At 48 hrs p.i., IFN-β protein levels were significantly reduced in samples treated with 10 ng/ml TGF-β_2 (p=0.027) as shown in Figure 4-9 A. In addition, IFN- β protein in cell samples treated with a synthetic dsRNA analog, polyI: polyC for 8 hours was measured, in order to ascertain that a decrease in protein levels is not due to decreased cell numbers caused by viral infection. PolyI: C is a TLR-3 ligand that stimulates IFN- β expression without causing significant cell death. An almost 60% decrease of IFN-β protein levels was observed in the presence of either 1 ng/ml or 10 ng/ml exogenous TGF-β_2 and 1 μ/ml polyIC compared to control samples where cells were treated with 1 μg/ml polyIC alone, see Figure 4-9 B (p=0.027 and p=0.026, respectively). Additionally, a statistically significant decrease in IFN-β protein when cells were treated with a higher dose of polyIC (10 μg/ml) and 10 ng/ml TGF-β was observed (p=0.028) (Figure 4-9 B).

Figure 4-9. IFN-β protein levels were measured by ELISA from RV-infected PBECs after 48 hours p.i in the presence or absence of 10 ng/ml TGF-β (A). IFN-β protein levels were also measured in PBECs obtained from 5 healthy subject donors that were stimulated with 1 and 10 μg/ml polyI:C in the presence or absence of 1 or 10 ng/ml TGF-β. Data was normalized to samples without TGF-β for each concentration of polyIC (B). The data was tested for statistical significance using a paired *t*-test or its non-parametric equivalent (Wilcoxon rank sum test).

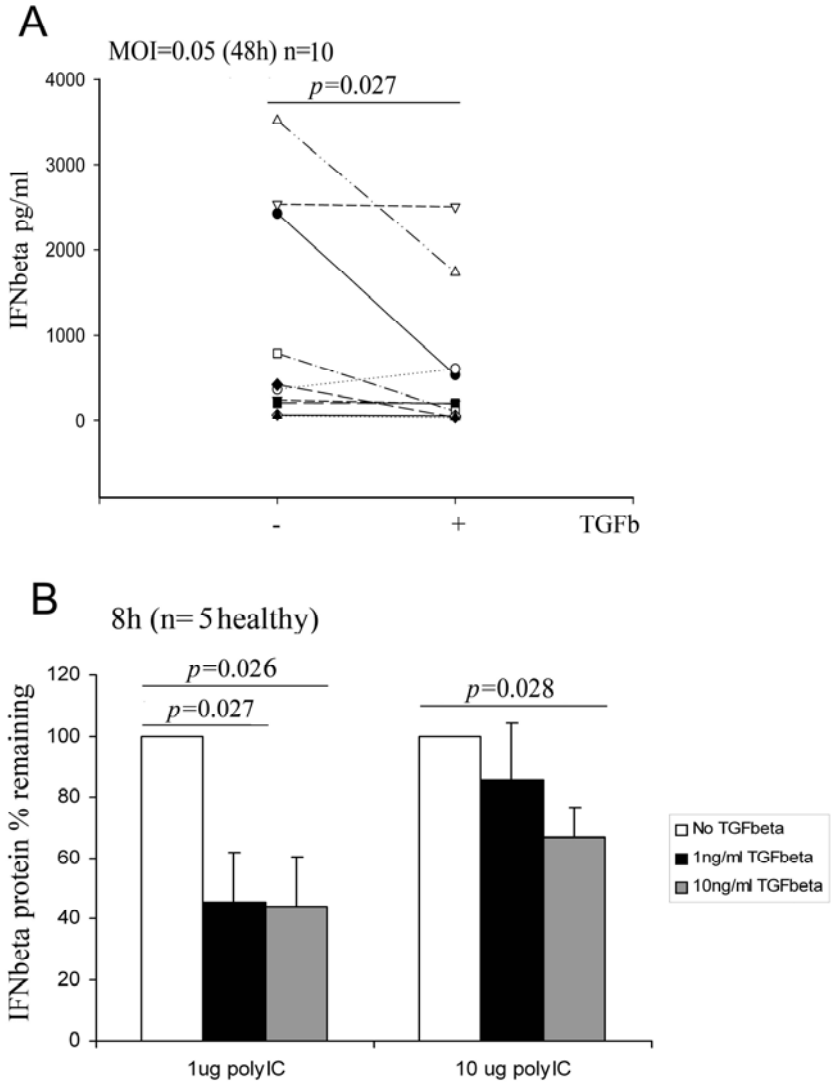

In addition, levels of IL-29, a type III interferon were also measured, in the same cell supernatant samples as described above. A similar reduction in IL-29 protein levels from virus infected cells that were pre-treated with exogenous TGF- β was observed, which was statistically significant (Figure 4-10 A), p=0.039. The same symbols for individual patients were used as in Figure 4-9. Patient samples with high levels of IFN-β also showed higher levels of IL-29. However, overall, IL-29 levels were

approximately 3 times the levels of IFN- β detected. IL-29 protein levels in cell supernatant samples that were pre-treated with TGF-β followed by stimulation for 8 hrs with polyIC were also measured. A statistical significant reduction was found after treatment with 1 and 10 ng/ml TGF-β followed by stimulation with 10 µg/ml polyIC, p=0.048 and p=0.026, respectively (Figure 4-10 B).

Figure 4-10. IL-29 protein levels were measured by ELISA from RV-infected PBECs after 48 hours p.i in the presence or absence of 10 ng/ml TGF-β (A). IL-29 protein levels were also measured in PBECs obtained from 4 healthy subject donors that were stimulated with polyI:C in the presence or absence of 1 or 10 ng/ml TGF-β. Data were normalized to samples without TGF-β for each concentration of polyIC (B). The data were tested for statistical significance using a paired *t*-test or its non-parametric equivalent (Wilcoxon rank sum test).

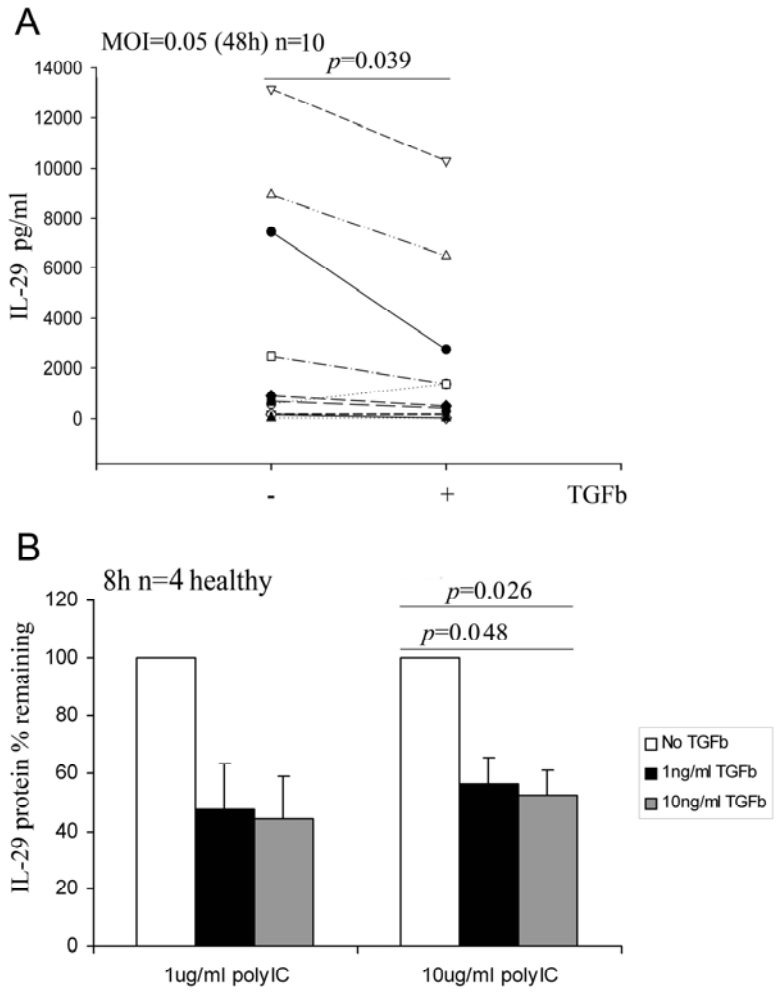

4.1.7 Higher baseline TGF- β_2 protein levels are detected in asthmatic PBEC compared to normal PBEC

Previous groups have shown an increase in TGF- β_2 immunoreactivity in the epithelium and submucosa of asthmatic bronchial biopsies (Vignola et al., 1997). Of the different TGF- β isoforms, TGF- β_2 has been previously implicated to be more important in asthma (Balzar S, 2005; Chu HW, 2008). It was, therefore, decided to compare baseline levels of secreted TGF- β_2 in normal and asthmatic PBEC cultures. Both active and total TGF- β_2 protein levels in cell culture supernatants were analysed by ELISA after cells were in starvation media for 48 hours. No significant levels of active TGF- β_2 were detected in any of the samples. Total TGF- β_2 was detected from cultures of 15 normal and 23 asthmatic PBEC by acid-treatment of the samples (Figure 4-11). Endogenous TGF- β_2 levels from asthmatic cell cultures were significantly higher compared to TGF- β_2 levels measured in healthy cell cultures (p=0.015) (Figure 4-11).

Figure 4-11. Control samples from normal and asthmatic PBEC cultures were analysed for baseline TGF- β_2. No significant levels of active TGF- β_2 were detected in the samples (data not shown). Latent TGF- β_2 was detected by acid-treatment and total TGF-β_2 was measured by ELISA and values obtained were plotted as total TGF- β_2. The Difference between the 2 groups was tested for statistical significance using a Mann-Whitney U test.

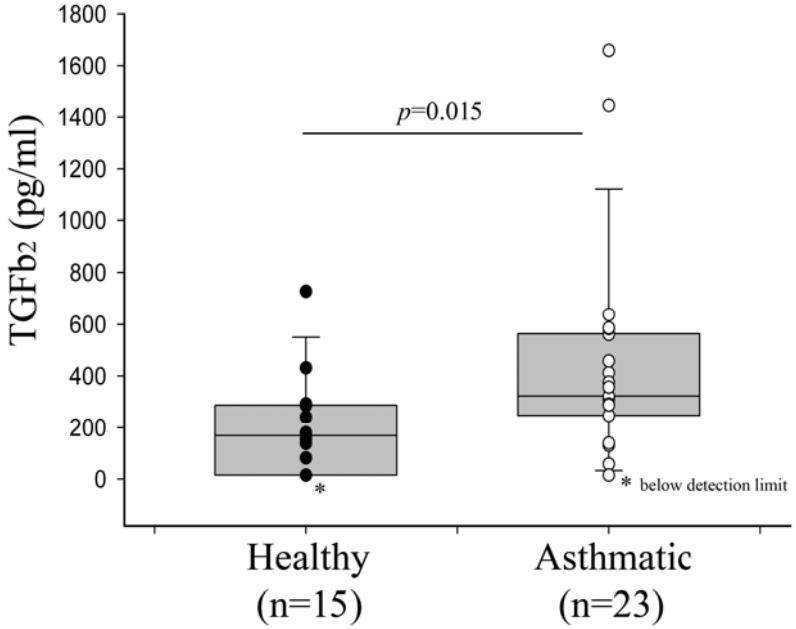

Discussion

The results in this section show that the addition of exogenous TGF-β to PBECs, increases the release RV1B virus particles into the supernatant as demonstrated by our functional studies. No significant levels of active TGF-β_2 were detected in either non-asthmatic or asthmatic cell cultures. However when total TGF-β_2 levels were measured, there were significantly higher levels of total TGF-β_2 in supernatants obtained from asthmatic cell cultures. Although these results showed that asthmatic culture produced more endogenous TGF-β_2 than cells from healthy controls, addition of exogenous TGF-β_2 to asthmatic cells still promoted virus replication suggesting that the amount of this cytokine present endogenously is not at saturating levels (Figure 4-5).

The pleiotropic effects of TGF-β *in vivo* and *in vitro* provides it with various roles in growth and development, inflammation and repair and host immunity (Clark and Coker, 1998). TGF-β is often cited as causing cell cycle arrest and apoptosis *in vitro* through complex signalling pathways involving Smad proteins (Rahimi and Leof, 2007). It is initially synthesized as a precursor protein which is then processed into an inactive form and secreted by the cell (Yang et al., 2007). Latent TGF-β complexes are normally activated by a diverse group of activators such as proteases, thrombospodin-1 (TSP-1), the integrin $\alpha_v\beta_{6,}$ reactive oxygen species (ROS), and low pH (Annes et al., 2003). It was previously published that there are higher levels of TGF-β in asthmatic tissue as shown by immunocytochemistry (Vignola et al., 1997). Supporting evidence was shown here by ELISA that asthmatic PBEC produce higher levels of TGF-β_2 even though this was predominantly the latent, inactive form.

One of the most known and characterized effect of TGF-β is cell cycle arrest and apoptosis. In epithelial cells, it has been shown to cause G1 cell cycle arrest by activation of anti-proliferative responses such as the transcriptional upregulation of the cyclin-dependent kinase (Li et al., 1994) inhibitors $p21^{Cip1/WAF1}$ and $p15^{Ink4b}$(Datto et al., 1995; Hannon and Beach, 1994; Yang et al., 2007). This upregulation is dependent on Smads as well as FoxO transcription factors (Gomis et al., 2006; Seoane, 2004; Yang et al., 2007). Interestingly it was found that the increase in p21/Waf1 after TGF-β_1 treatment of JHH-5 (Miyazaki et al., 2004) was mediated by the interferon regulatory factor-1 (IRF-1) and S100/A1, a member of the Ca^{2+}-binding S100 protein family (Miyazaki et al., 2004; Yang et al., 2007). IRF-1 is a transcription factor that is constitutively expressed and is induced by Interferon-γ (IFN- γ). Its target genes include NOS2, GBP1 and $gp91^{PHOX}$, IL12, IL15, TAP1 CDKN1A, and Caspase-1, the latter two of which are involved in controlling apoptosis (Honda and Taniguchi, 2006). Apoptosis

is a way by which cells contain virus infections since induction of cell death limits viral replication (Samuel, 2001). Thus, one might have expected to see a decrease in RV1B expression in the presence of TGF-β. A trend for decreased virus particle release, however, was only evident at 24 hours post-infection (data not shown), but this failed to reach statistical significance. In contrast, a TGF-β mediated increase in RV1B replication by 48 hours post-infection was consistent in majority of subjects tested. This increase at later time points, suggests a cumulative effect of TGF-β on this cell type.

In this section, several possible mechanisms that may be involved in the observation that the presence of TGF-β in bronchial epithelial cell cultures augments rhinovirus replication were investigated. The first hypothesis was that the addition of exogenous TGF-β causes healthy epithelial cells to acquire a more fibroblastic phenotype in a process called epithelial to mesenchymal transition (Cicchini et al., 2008), (Xu et al., 2009). EMT can occur in response to several different stimuli including tissue injury or growth factors such as TGF-β (Xu et al., 2009). It is generally characterized by the dissolution of cell to cell junction, loss of E-cadherin, and actin re-organization, making cells more migratory (Xu et al., 2009). When fluorescently labelled phalloidin was used to visualize actin filaments in TGF-β treated cell samples, a greater expression of stress fibers in the cytoplasm was observed which may be evidence of increased cell motility (Figure 4-6). Literature reviews suggest that TGF-β transforms epithelial cells from a cuboidal shape to an elongated spindle shape (Xu et al., 2009). However, it was relatively difficult to confirm this upon close inspection of our cell samples under a light microscope. It was found that prolonged treatments with TGF-β gave the cells a flat appearance with a frilled and undefined cytoplasmic membrane (data not shown).

Another characteristic of EMT is the expression of mesenchymal cytoskeletal protein, such as vimentin, collagen and fibronectin and the formation of focal adhesion kinases (Xu et al., 2009). A study suggests that TGF-mediated EMT via a src-dependent activation of focal adhesion kinases (FAK) (Cicchini et al., 2008). The importance of src kinases in rhinovirus replication will be described in the next chapter. Collagen mRNA expression was analysed in healthy PBECs treated with exogenous TGF-β by RT-qPCR and a marked increase in collagen expression was found compared to untreated samples (Figure 4-7). Since EMT is a hallmark of tumourigenesis and cell survival, this phenomenon may cause PBECs to undergo decreased apoptosis in response to rhinovirus infection and therefore increase the number of infection events (Xu et al., 2009). Apoptosis is triggered by the presence of viral RNA and IFN-β, and is

an important event in the innate immune response, that enables the host to control and contain virus infection (Takeuchi and Akira, 2007), (Deszcz et al., 2005). Therefore, the possibility that the addition of TGF-β to our cell culture system might reduce the ability of the cells to undergo apoptosis in response to rhinovirus infection by measuring caspase 3/7 activity was investigated. Caspases are a family of cyteine proteases that are activated by proteolytic cleavage of their inactive proforms (Deszcz et al., 2005). Once activated, caspases cleave a set of cellular target proteins which can cause morphological changes and DNA fragmentation (Hail, Jr. et al., 2006). Caspase-3 and -7 are effector caspases which are activated by initiator caspases such as caspases -8, -9, and -10 (Hail, Jr. et al., 2006). The assay which was used in this study is a luminescent assay that provides a proluminescent caspase-3/7 DEVD-aminoluciferin substrate and luciferase. Following cell lysis, intracellular caspases cleave the substrate, liberating aminoluciferin, which is consumed by the luciferase, generating a luminescent signal. This signal is directly proportional to caspase activity, according to the manufacturer. In this study, no difference in caspase activity was detected between the TGF-β-treated and untreated samples. Significant induction of caspase 3/7 activity was only observed by 24 hours p.i., which would have been the expected time point where differences in apoptosis might be observed, since it is only at 48 hours p.i. where an increase RV replication with TGF- β treatment was observed. This would give the host cells an additional 2-3 round of infection to accumulate virus particles. However, one issue with this assay might be its sensitivity. Therefore, small differences in caspase 3/7 activity between TGF- β treated and untreated samples may not be detected even at 24 hours p.i. Another method of assessing the ability of TGF- β to affect cell survival in our system would be to measure the amount of cytopathic effect (CPE) or cytolysis caused by viral infection. In contrast to apoptosis, cytolysis is characterized by membrane blebbing and rupture, releasing the intracellular components into the cell media (Hail, Jr. et al., 2006). One of these intracellular proteins, lactate dehydrogenase is measured as a marker of cell death, caused by rhinovirus infection. Since the presence of TGF- β causes the accumulation of infectious virus particles, it might be expected that an increased in CPE would be observed as evidenced by increased LDH detected in the supernatants of infected cells. No difference in the levels of LDH released were observed in the presence or absence of TGF-β in one experiment, however further studies would need to be done to confirm this observation.

In addition to EMT, it was also decided to investigate the effect of TGF-β on the innate immune response in rhinovirus-infected cells. Interestingly, TGF-β has been

implicated in the initial amplification of the innate immune response and the recruitment of macrophages and neutrophils (Wahl, 2007). However it seems that the current paradigm is that TGF-β can "act as a light switch: i.e. if it's on, it will turn it off; if it's off, it will turn it on (Wahl, 2007)." This description would fit the extremely pleiotropic nature of this cytokine. In these experiments, it was observed that TGF- β acts more like an anti-inflammatory cytokine by reducing both type I and type III interferon responses to virus and the synthetic dsRNA polyIC. This observation is supported by similar findings in bronchial fibroblasts where the authors found a dampening of the innate immune response against rhinovirus infection in the presence of this cytokine (Thomas et al., 2009). Though this observation of decreased innate immune response in the presence of TGF-β does not seem to be reconcilable with a lack of difference observed in the caspase 3/7 assay, it is possible that rather than having an effect on apoptosis, it could be an effect on the anti-viral machinery.

5 Chapter 5

5.1 Neutralizing endogenous TGF-β in asthmatic PBECs reduces RV replication

Rationale

In the previous section, an increase in RV replication in the presence of TGF-β in both healthy and asthmatic PBECs was observed. The data also showed that baseline expression of TGF-β in asthmatic cell cultures was higher compared to cells from healthy controls. Even though no significant levels of active TGF-β_2 were detected in either healthy an asthmatic PBEC supernatants, it does not rule out that active TGF-β is bound to its receptor in a local microenvironment and therefore not released into the supernatant. Therefore, it was decided to use a neutralizing antibody against TGF-β on asthmatic PBECs for more functional studies by blocking the active, bound form of this cytokine. PBECs were treated with this antibody and analysed its effects on RV replication and the IFN response.

Additionally, the components of TGF-β mediated cell signalling including Smad3 and p38 MAPK were also analysed to determine their role in the observed effects of TGF-β on RV replication. Smads are essential players in the Smad pathway and transcription factors that regulate gene expression in response to TGF-β. They have also been shown to be involved in TGF-β mediated EMT (Rahimi and Leof, 2007), (Ross and Hill, 2008). Smad3 is one of 5 receptor-regulated Smads, which are phosphorylated in response to different types TGF-β ligands (Ross and Hill, 2008). They are transcription factors that regulate gene expression in response to TGF-β (Ross and Hill, 2008). P38 MAPK is a member of the family of mitogen-activated protein kinases (MAPK) (Martin-Blanco, 2000). They are involved in signalling cascades in response to cytokines, growth factors or environmental stress (Martin-Blanco, 2000). McCann *et al* have shown that p38 MAPK is activated in RSV-infected cells treated with TGF-β, but have failed to show a direct link between the observed effects of TGF-β and activated p38 (McCann and Imani, 2007).

5.1.1 Neutralizing TGF-β bioactivity in asthmatic PBEC reduces RV1B replication

In order to investigate the effects of neutralizing endogenous TGF-β on RV replication in asthmatic PBECs, cells were starved for 24 hours in the presence of neutralizing anti-TGF- β antibodies, followed by infection with RV1B. Control samples

were incubated with equivalent concentrations of an IgG1 isotype control. Cells were then further incubated in the presence of the antibody for a period of 24 and 48 hours. Cell supernatant were harvested and analysed for amount of virus particles using an end-point dilution assay as described previously. No difference was observed in $TCID_{50}$/ml levels at 24 hours (Figure 5-1 A). However, a significant reduction in the release of infectious virus particles was observed in the presence of anti-TGF-β antibodies at 48 hours; p=0.012 (Figure 5-1 B).

Figure 5-1. Viral titres of infected PBECs from asthmatic patients that were pre-treated with 10 μg/ml neutralizing anti-TGF-β antibody for 24 hours. Control cells were incubated with equal concentration of isotype control. Cells were then infected with RV1B (MOI=0.01) and were incubated in the presence or absence of the antibody for a period of 24 and 48 hours. $TCID_{50}$/ml data were obtained from viral supernatant at 24 (A) and 48 (B) hours post-infection.

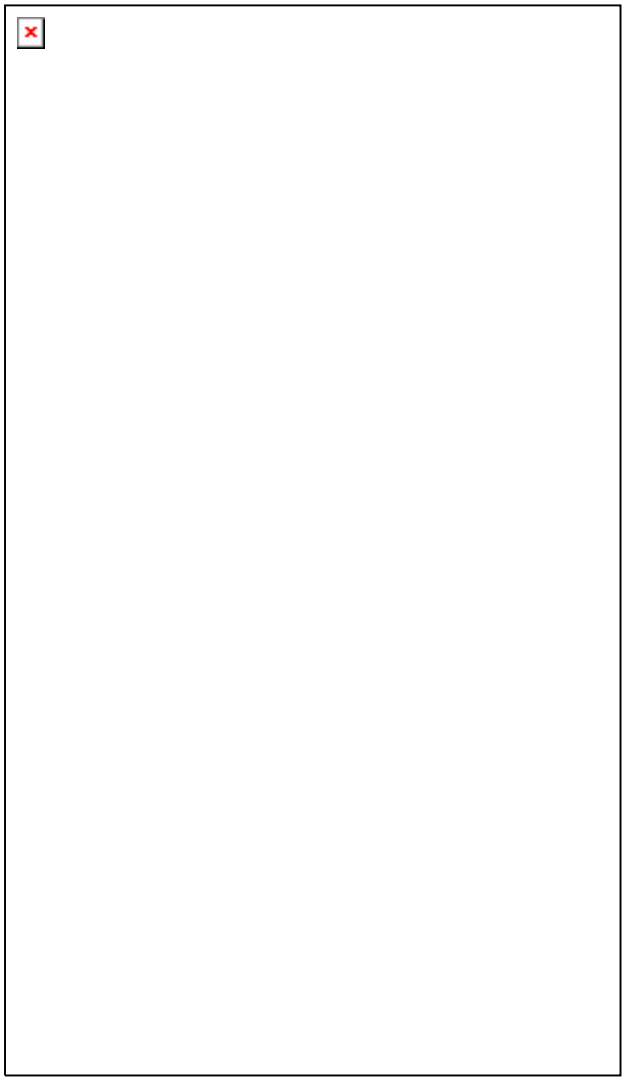

5.1.2 Photomicrographs of asthmatic PBECs after incubation with RV1B and neutralizing anti-TGF β antibody

Though a reduction in RV1B replication was seen in the previous section when asthmatic PBEC were treated with neutralizing anti-TGF-β antibodies, there were no visible difference in the amount of cell death observed in the presence or absence of neutralizing anti-TGF β antibodies both at 24 (Figure 5-2) and 48 hours (Figure 5-3). However, when LDH released into the supernatant was measured in PBECs from one asthmatic subject, there was a trend of decreased LDH at both 24 and 48h p.i. although this did not reach statistical significance (Figure 5-4).

Figure 5-2. Photomicrographs of PBEC from asthmatic patient at 24 hours post-infection with RV1B in the presence or absence of neutralizing pan anti-TGF-β antibody. Protocol is as described in Figure 5-1.

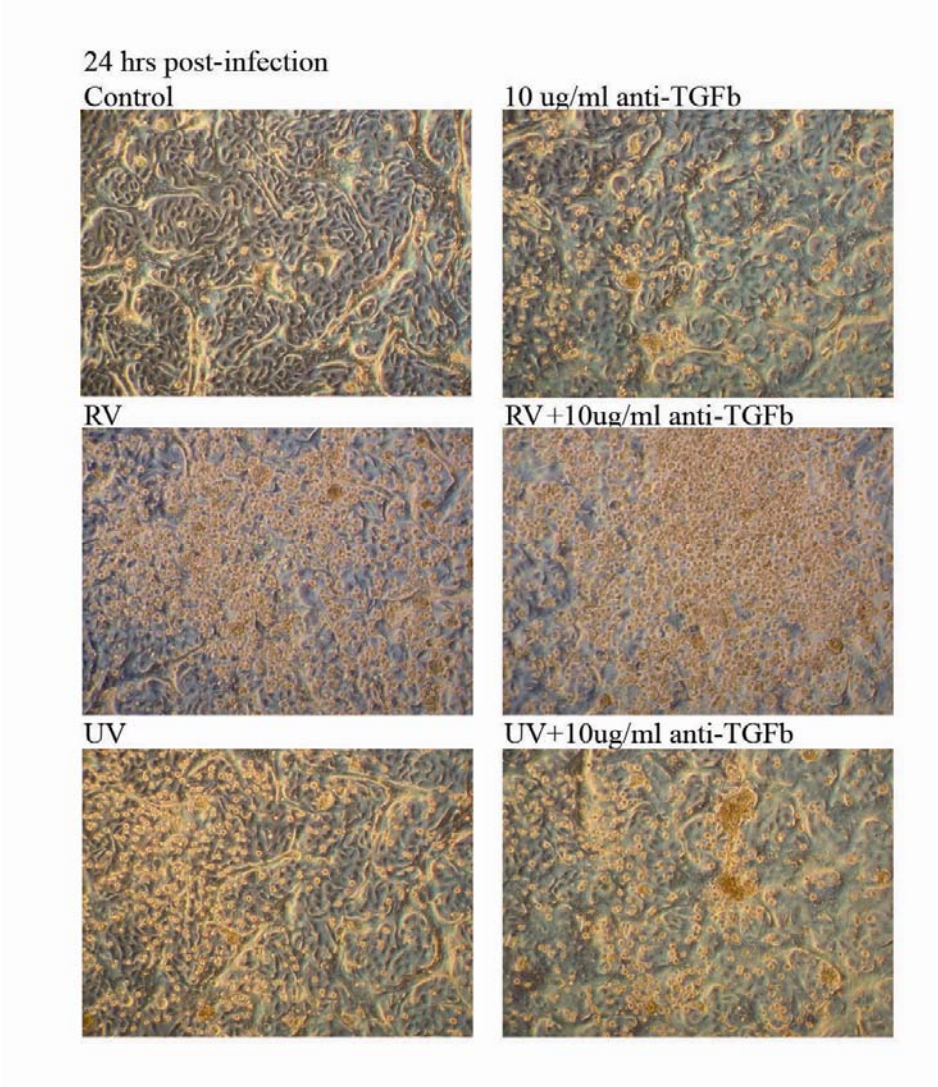

Figure 5-3. Photomicrographs of PBEC from asthmatic patient at 48 hours post-infection with RV1B in the presence or absence of neutralizing pan anti-TGF-β antibody. Protocol is as described in Figure 5-1.

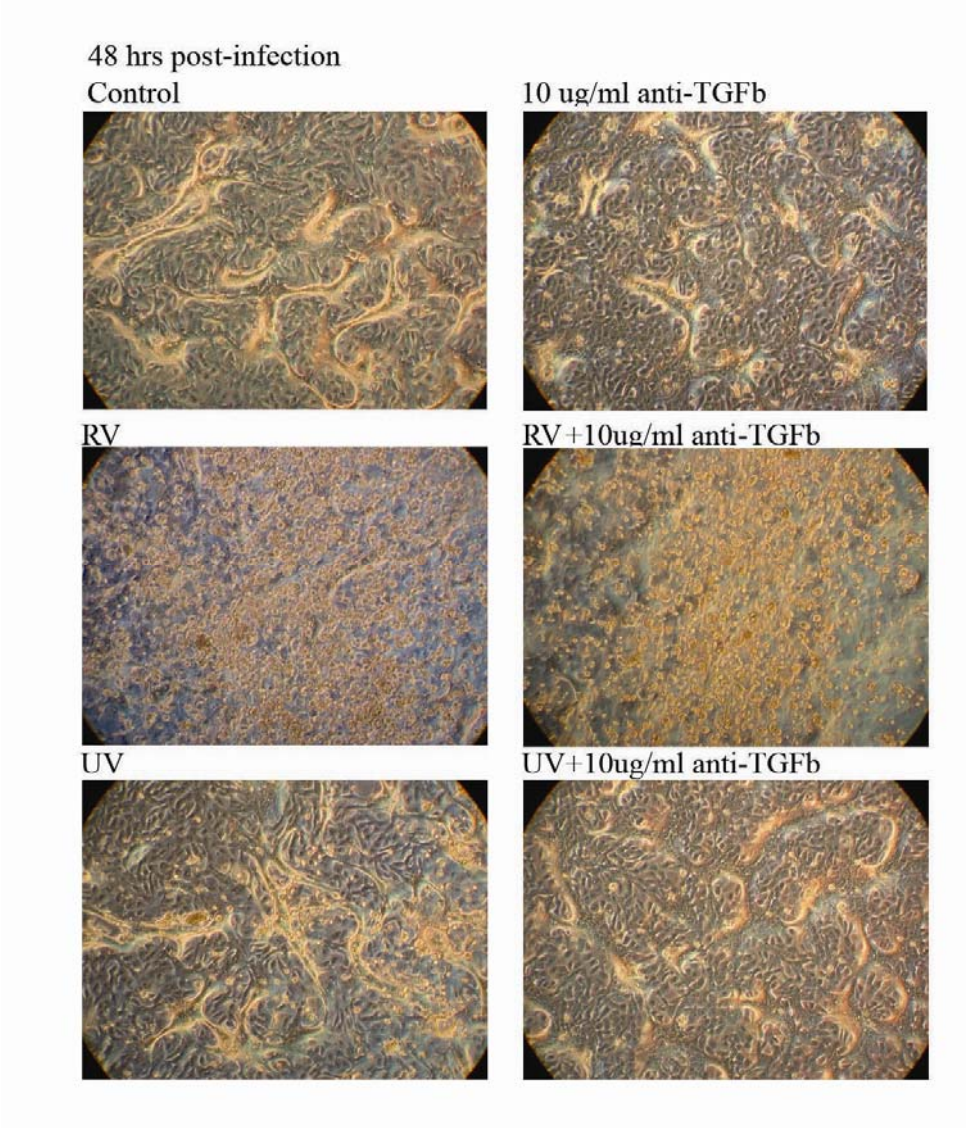

Figure 5-4. LDH Assay of PBECs from one asthmatic subject that were infected with RV (MOI=0.05) and incubated for 24 and 48 hours in the presence or absence of TGF-β or neutralizing TGF-β antibodies. Lactate dehydrogenase (Stern et al., 2007) released in culture media was measured using a Cyto Tox 96® Non-radioactive Cytotoxicity Assay and absorbance read at 492 nM. Graphs show relative optical density (OD) readings normalized to control samples obtained at 24 and 48 hours p.i.

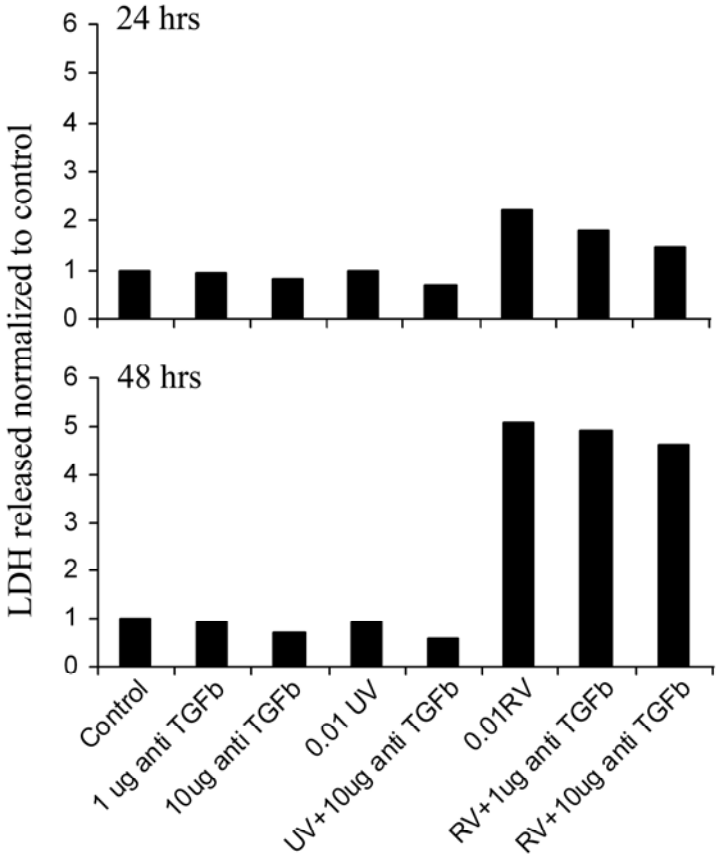

5.1.3 IFN protein levels relative to virus particles is significantly increased in the presence of anti-TGF- β antibodies in virus infected asthmatic cells and partially increased in polyI:C treated asthmatic cells

IFN-β protein levels in virus-infected cells from asthmatic patient donors that were treated with neutralizing anti-TGF-β antibodies were then measured. Virus replication is necessary for sustained induction of IFN-β, as induction of this cytokine requires a danger signal. As shown in the previous section, the presence of anti-TGF-β antibody reduced virus replication, so it was necessary to analyse IFN-β relative to the amount of virus particles when comparing the two treatment groups. Significantly more IFN-β protein in samples from cells that were treated with anti-TGF-β antibodies was

found compared to samples that were only treated with the isotype control (Figure 5-5) (p=0.012). To eliminate the confounding factor of virus replication and cell death, the effect of neutralizing TGF-β on the IFN response was tested using synthetic double-stranded RNA, polyIC as a danger signal. IFN-β and IL-29 protein levels from asthmatic PBECs that were treated with both polyIC and neutralizing anti-TGF-β antibodies were measured. It was found that the presence of the antibody augmented the levels of IFN-β to significant levels, particularly when 10 μg/ml polyIC was used (Figure 5-6 A) (p=0.031). Similar effects of the antibody on IL-29 protein levels were found, though this did not reach statistical significance (Figure 5-6 B).

Figure 5-5. IFN-β protein levels relative to virus particles measured 48h p.i. in supernatants from RV-infected asthmatic PBECs that were treated with neutralizing anti-TGF-β antibodies or an IgG1 isotype control.
The ratio of IFN-β protein (pg/ml) to virus particles ($TCID_{50}$ /ml) at 48h p.i. was obtained and plotted as a log10 value.

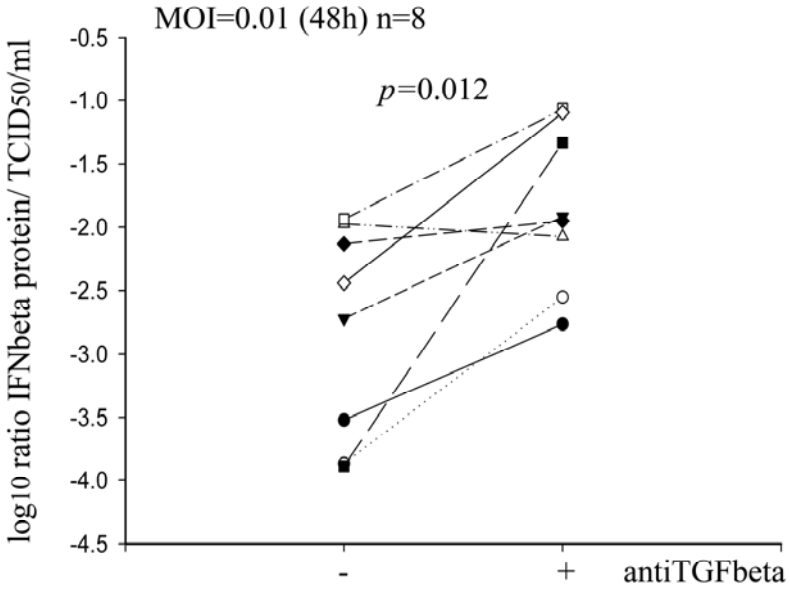

Figure 5-6. IFN-β and IL-29 protein levels of PBECs from 6 asthmatic donors that were treated with 0.1-10 μg/ml polyIC in the presence of neutralizing anti-TGF-β antibodies or an IgG isotype control and incubated for 24 hours. Supernatants were removed after 24 hours post-treatment and IFN-β protein levels (A) or IL-29 protein levels (B) were measured by ELISA.

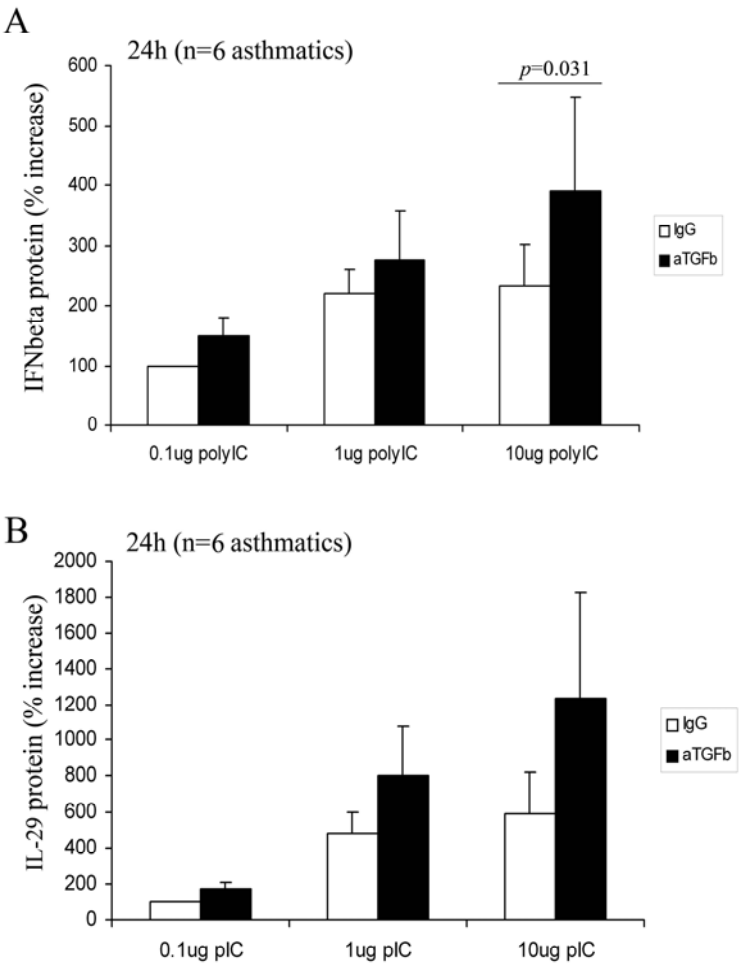

5.1.4 Chemical inhibitors of Smad-3 and p38 MAP kinase both reduce RV1B replication in asthmatic PBECs

It was decided to determine whether two components of the TGF-β signalling pathway, Smad-3 and p38 MAP kinase (p38 MAPK), were involved in the observed TGF-β-mediated effect on the innate immune response and rhinovirus replication (Figure 5-7). Asthmatic PBECs were pre-treated for 1 hour with the stated concentration of the Specific Inhibitor of Smad-3 (Jinnin et al., 2006) or the p38 MAPK inhibitor (SB203580), followed by infection with RV1B stock for 1 hour (Jinnin et al., 2006).

Cells were then washed and incubated further for 8, 24, and 48 hours with or without the inhibitors.

A dose-dependent reduction of virus titre was observed both at 24 and 48 hrs in SIS3-treated samples (Figure 5-8). RV1B mRNA levels in SIS3-treated cells were also reduced at all time points tested (Figure 5-9). IFN-β mRNA levels showed similar patterns to RV1B mRNA at 8 and 48 hours, possibly reflecting interferon induction relative to presence of viral genome (Figure 5-10). However, statistical tests showed no statistically significant correlation between IFN-β mRNA and viral RNA at 8 and 48 hours p.i. in the presence or absence of SIS3. At 24 hours p.i. there was a positive correlation between IFN- β mRNA and viral RNA in untreated samples (p=0.0251) using a Pearson correlation test. There was no correlation between the two variables when samples were treated with 1 μM SIS3. However, there was a positive correlation between IFN- β and viral mRNA when samples were treated with 5 μM SIS3 (p=0.0237). Interestingly, when values obtained for IFN- β (y-axis) were plotted against RV1B mRNA (x-axis), the gradients of the regression lines between treatment groups was greater in samples with the Smad-3 inhibitor, indicating a greater induction of IFN-β expression relative to the amount of virus present (data not shown).

Figure 5-7. The Smad3 and JNK/p38 pathway illustrating which signaling molecules we targeted using the Specific Inhibitor of Smad3 (Jinnin et al., 2006) and p38 inhibitor (SB203580). Adopted from Zhang *Cell Research* 2009 (Zhang, 2009).

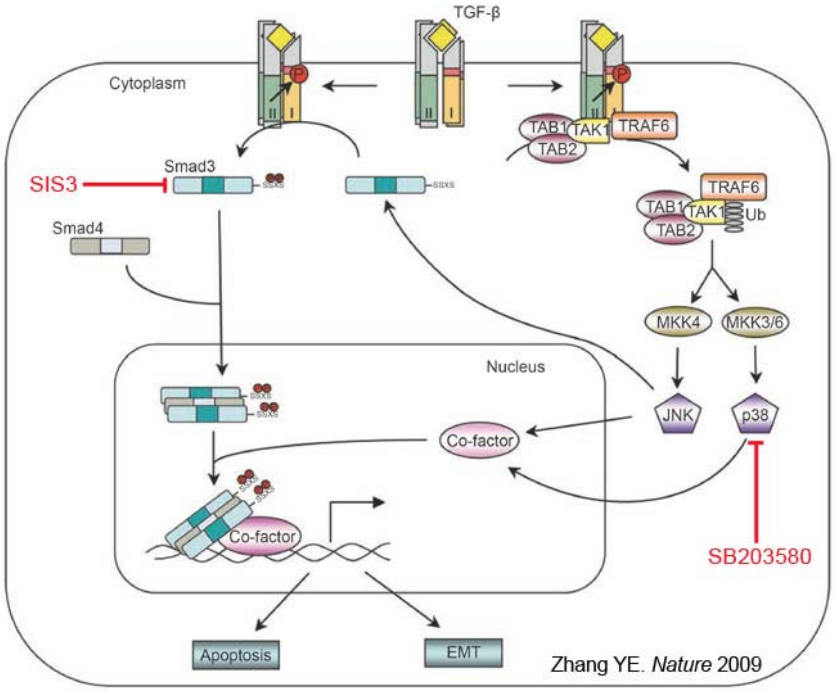

Figure 5-8. Levels of infectious virus particles measured by an end-point dilution assay ($TCID_{50}$/ml). PBECs from 3 asthmatic donors were pre-treated for 1 hour with 1 or 5 μM Smad3 inhibitor SIS3 followed by infection with RV1B (MOI=0.01). Cells were then incubated for 24 (A) or 48 hours (B) and samples were analysed for levels of virus titre. Graphs show mean values, Error bars depict Standard Errors of the Mean.

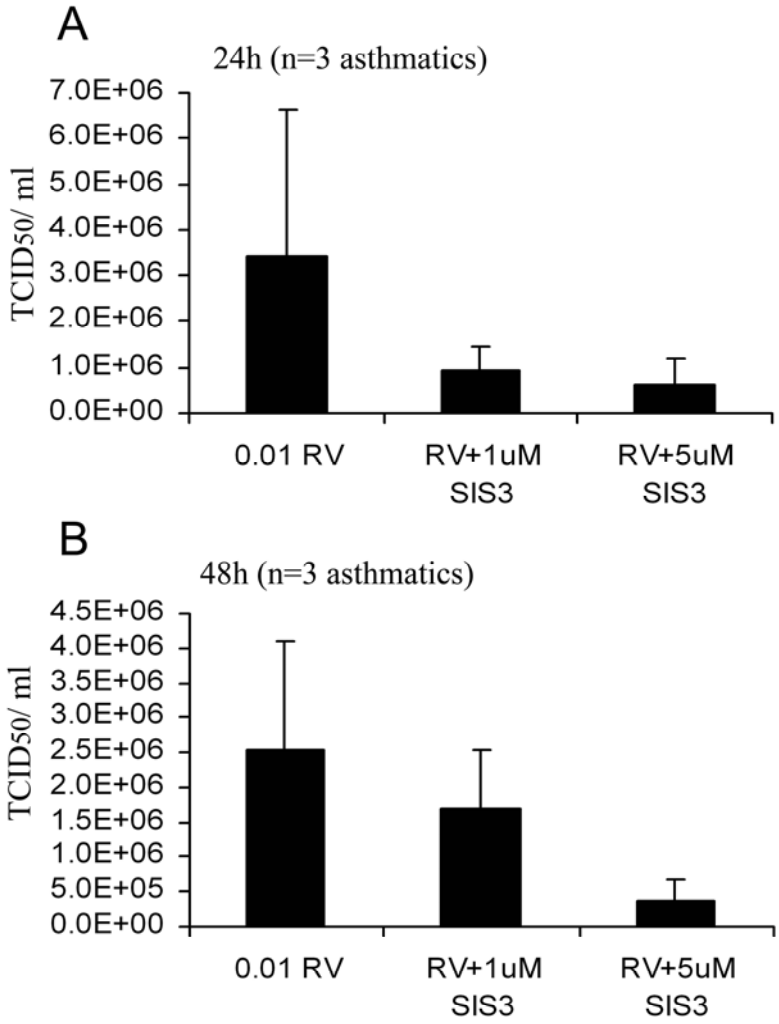

Figure 5-9. Viral RNA of PBECs from 3 asthmatic donors pre-treated with Smad-3 inhibitor (Jinnin et al., 2006) for 1 hour followed by infection with RV (MOI=0.01) and incubated for 8, 24 or 48 hours in the presence or absence of the inhibitor. DMSO was used as a vehicle control for the inhibitor. RNA was extracted from the cells and viral gene expression was measured by RT-qPCR using RV1B specific primers and probes. CT-values were normalized first to the Geometric Mean of housekeeping genes GAPDH and UBC and then to untreated control samples by the delta-delta CT method as previously described. Graph shows relative RV1B gene expression at 8 (A), 24 (B) and 48 hours (C) p.i.

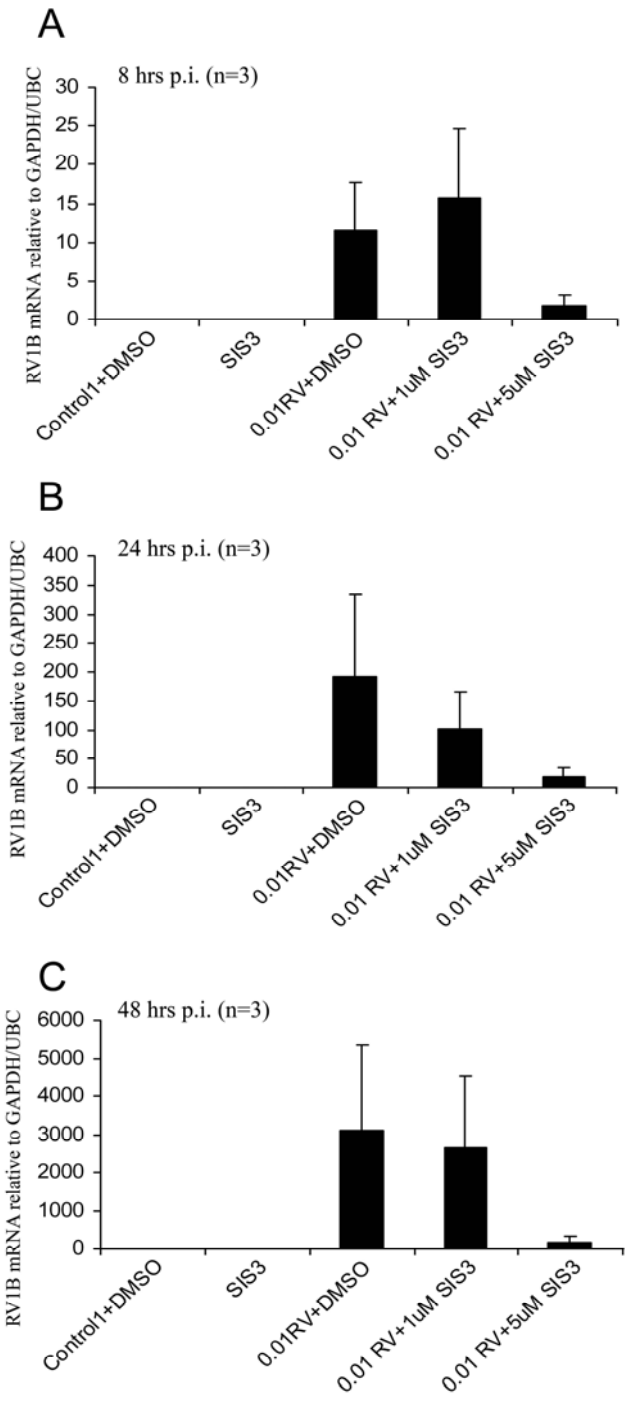

Figure 5-10. IFN-β mRNA of PBECs from 3 asthmatic donors pre-treated with Smad-3 inhibitor (Jinnin et al., 2006) for 1 hour followed by infection with RV as described in Figure 5-9. IFN-β mRNA was measured by RT-qPCR using IFN-β specific primers and probes. CT-values were normalized first to the Geometric Mean of housekeeping genes GAPDH and UBC and then to untreated control samples by the delta-delta CT method as previously described. Graph shows relative IFN-β gene expression at 8 (A), 24 (B) and 48 hours (C) p.i.

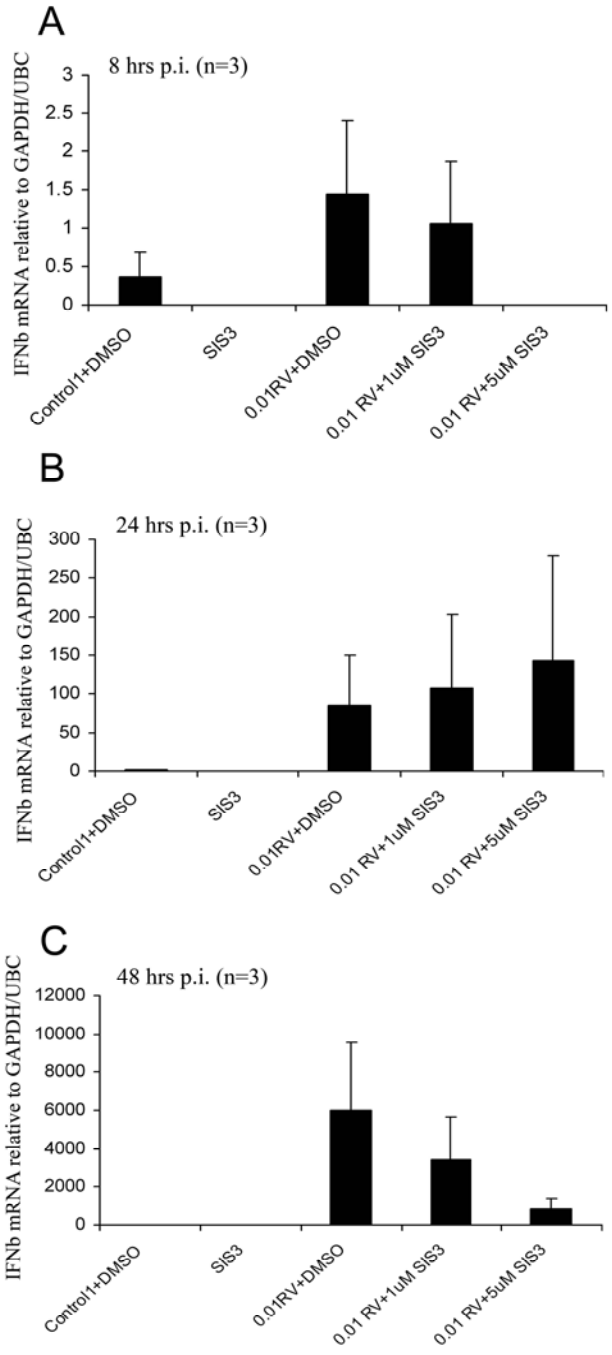

When cell samples treated with the p38 MAPK inhibitor SB203580 were analysed, a similar dose-dependent reduction in virus titre at both 24 and 48 hrs post-infection was found (Figure 5-11). Viral mRNA was also reduced in a dose-dependent manner when virus-infected cells were treated with SB203580 (Figure 5-12). Similar to my results with the Smad-3 inhibitor, a positive correlation between IFN- β and viral RNA at 24 hrs p.i. in untreated samples as well as in samples that contained 5 μM SB203580 was found (Figure 5-13). When IFN- β mRNA levels relative to viral RNA was analysed, a similar trend of increased IFN- β mRNA relative to viral RNA in the presence of the p38 MAPK inhibitor was observed (figure not shown).

Figure 5-11. Levels of infectious virus particles measured by an end-point dilution assay called $TCID_{50}$/ml from PBECs from 3 asthmatic donors were pre-treated for 1 hour with 1 or 5 μM p38 MAPK inhibitor (SB203580) followed by infection with RV1B (MOI=0.01). Cells were then incubated for 24 (A) or 48 hours (B) and samples were analysed for levels of virus titre. Graphs show mean values, Error bars depict Standard Errors of the Mean.

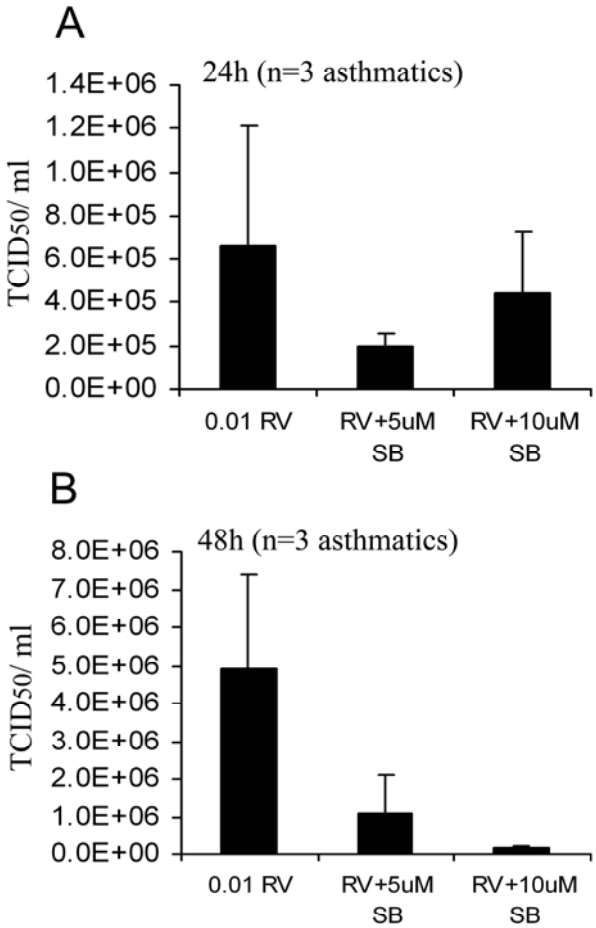

Figure 5-12. Viral mRNA of PBECs from 3 asthmatic donors pre-treated with p38 inhibitor (SB203580) for 1 hour followed by infection with RV as described in Figure 5-11. RV1B mRNA was measured by RT-qPCR using RV1B specific primers and probes. CT-values were normalized first to the Geometric Mean of housekeeping genes GAPDH and UBC and then to untreated control samples by the delta-delta CT method as previously described. Graph shows relative RV1B gene expression at 8 (A), 24 (B) and 48 hours (C) p.i.

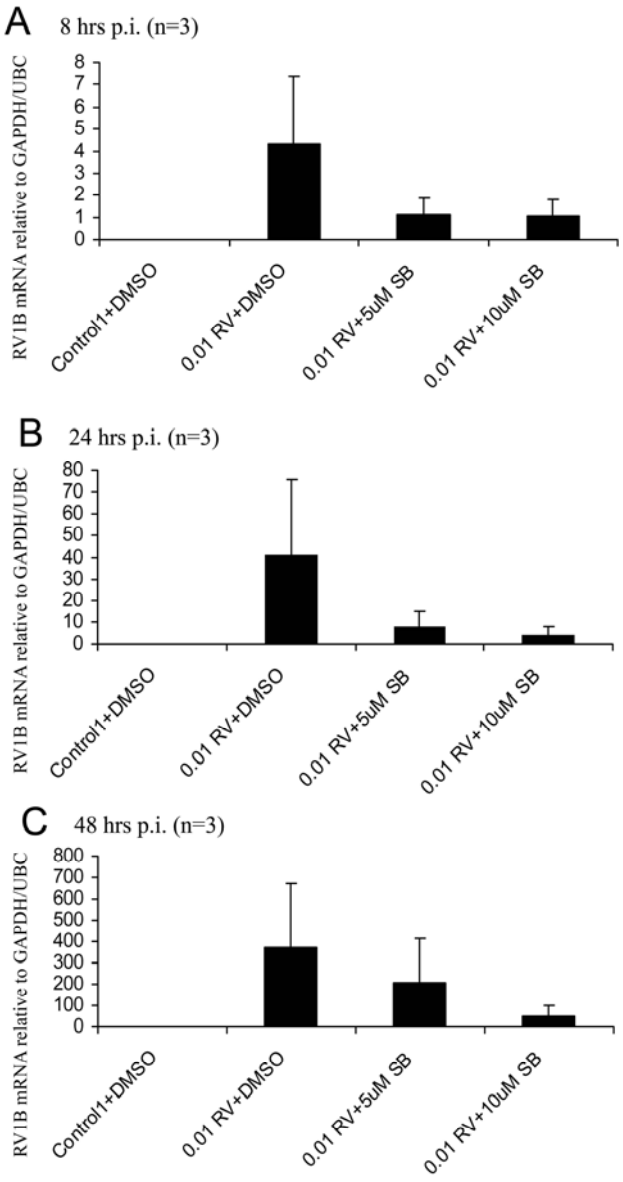

Figure 5-13. IFN-β mRNA of PBECs from 3 asthmatic donors pre-treated with p38 inhibitor (SB203580) for 1 hour followed by infection with RV as described in . IFN-β mRNA was measured by RT-qPCR using IFN-β specific primers and probes. CT-values were normalized first to the Geometric Mean of housekeeping genes GAPDH and UBC and then to untreated control samples by the delta-delta CT method as previously described. Graph shows relative IFN-β gene expression at 8 (A), 24 (B) and 48 hours (C) p.i.

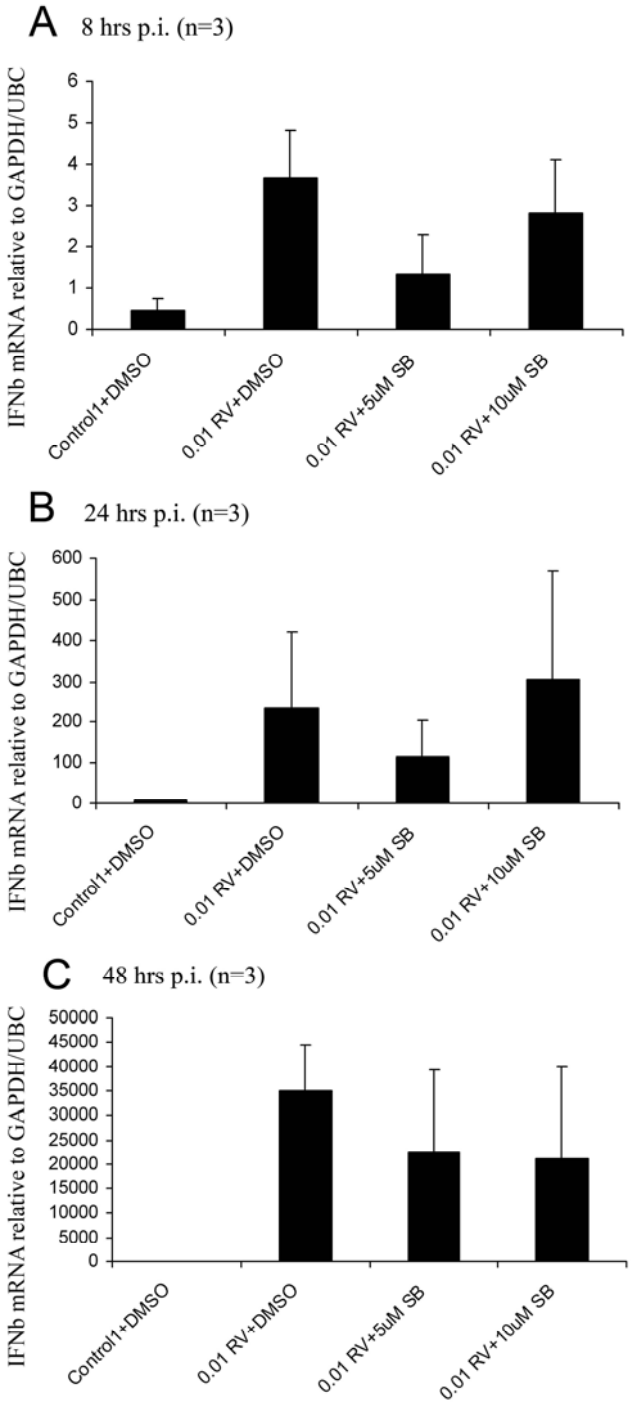

5.1.5 Chemical inhibitors of Smad-3 and p38 MAP kinase increase IFN levels in polyIC-treated PBECs from asthmatics

One of the confounding factors of analysing IFN-β expression in virus infected cells, is that its induction is dependent on the presence of viral RNA, which acts as a danger signal. Since data from the previous section showed that inhibition of Smad-3 and p38 MAPK reduced virus replication, this in itself will also affect levels of IFN-β expression. Therefore, it was decided to use polyIC as a danger signal, in order to determine whether either Smad-3 or p38 MAPK has a role in dampening the innate immune response to rhinovirus infection.

PBECs from asthmatic patient donors were pre-treated for 1 hour with either SIS3, SB203580 or DMSO as a vehicle control, followed by treatments with 0.1 μg/ml or 1 μg/ml of polyIC in the presence or absence of either inhibitor. Cells were then incubated for 24 hrs and analysed for IFN-β and IL-29 protein levels. Increased levels of IFN-β and IL-29 in the presence of SIS3 at lower doses of polyIC were observed (Figure 5-14 A and B), which reached statistical significance for IFN-β (p=0.020). The presence of the inhibitors did not increase IFN-β levels when cells were treated with a higher dose of polyIC (1 μg/ml), suggesting that this concentration is at saturating levels for the cells to be able to respond to the addition of the inhibitors (Figure 5-14 A). Significant decreases in IL-29 protein in presence of the p38 MAPK inhibitor were also observed (Figure 5-14 B). However, the observation that SIS-3 was able to augment both the IFN-β and the IL-29 response in polyIC-stimulated cells, indicates that Smad-3 is likely to be more important in the TGF-β-mediated effect on the innate immune response.

Figure 5-14. IFN-β protein (A) and IL-29 protein levels (B) of PBECs from 5 asthmatic donors pre-treated with 5 μM SIS3 or SB203580 for 1 hour followed by treatment with polyIC at a concentration of 0.1 or 1 μg/ml and incubated for 24 hours. DMSO was used as a vehicle control for the inhibitors. Supernatants were removed after 24 hours post-treatment and IFN-β and IL-29 protein levels were measured by ELISA. Data were normalized to value obtained from samples treated with 0.1 μg/ml polyIC only. Graphs show mean values, Error bars depict Standard Errors of the Mean. Data were tested for significant using a Wilcoxon rank sum test.

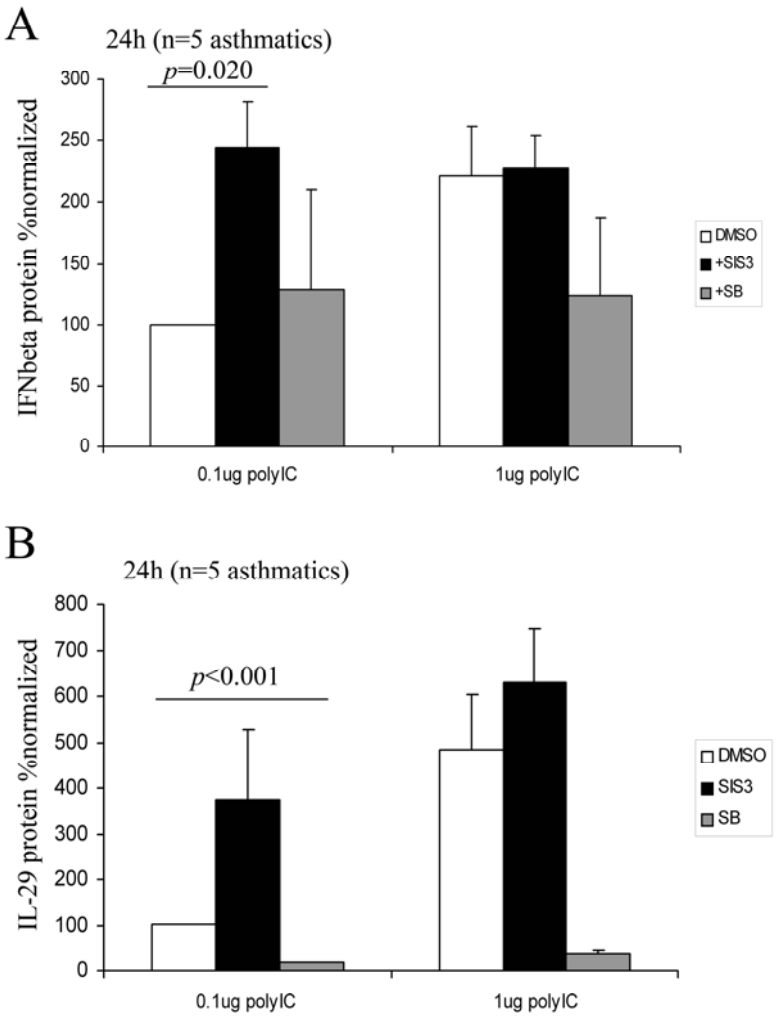

5.1.6 Analysis of the effects of TGF-β on STAT-1 and PIAS-1 protein interaction

Although it was shown in the previous section, that Smad-3 may play a role in TGF-β-mediated dampening of the innate immune response, questions about the mechanism of this process remained open. Previous published data have shown that TGF-β regulates the interaction between Protein Inhibitor of Activated STAT-1 (PIAS-1) and STAT-1 (Reardon and McKay, 2007). In this paper, it was shown in pull-down experiments experiments that pre-treatment of Hep-2 cells with TGF-β prior to stimulation with IFN-γ increased the interaction of PIAS-1 with STAT-1 (Reardon and McKay, 2007). In another study, MAPK has been implicated in increasing the binding of PIAS-1 to STAT-1 in a SUMO-dependent manner (Vanhatupa et al., 2008). The observations made in this study, showed a TGF-β-mediated increase in RV replication, coupled with a decrease in IFN response occurring at later time points (48h). This observation points to TGF-β-mediated effect on the secondary induction of the IFN response, involving the STAT pathway, rather than the primary IFN response, showen by the relatively slow kinetics of the TGF-β effect.

It was, therefore decided to investigate whether in this system, the presence of TGF-β in PBEC cultures, contributes to an increased interaction of PIAS-1 and STAT-1, thereby reducing the amplification of the IFN response. In order to ascertain STAT-1 activation was taking place during polyIC treatment, despite treatment with inhibitors or anti-TGF-β antibodies, a portion of cell lysates in RIPA buffer were analysed by SDS-PAGE and immunoblotted for phosphorylated STAT-1^{Tyr701}. It found that STAT-1 was phosphorylated in the presence of either dose of polyIC, regardless of the presence of the inhibitors or anti-TGF-β antibodies (Figure 5-15 A).

To determine whether the TGF-β mediated inhibitory role of PIAS-1 in polyIC-treated PBECs from asthmatic donors, cells from 3 asthmatic donors were pre-treated with antibodies for 24 hrs, followed by stimulation with polyIC at 0.1 and 1 μg/ml polyIC for 8 hrs. Samples that were treated with either the Smad-3 or the p38 MAPK inhibitor were also included, in order to see whether either of these signalling molecules was involved in the PIAS-1/STAT-1 interaction. Cells were harvested with RIPA buffer and pull-down experiments were conducted using an anti-PIAS-1 antibody (see Materials and Methods). Lysates were then analysed by SDS-PAGE, electroblotted and membranes probed with an anti-STAT-1 antibody (Figure 5-15 B). This experiment was repeated in PBECs from 2 other asthmatic subjects. When the STAT-1 to PIAS-1 ratio

was determined, no significant differences between samples that were treated with anti-TGF-β antibodies and samples that were only treated with an IgG1 control were observed (Figure 5-16). Slight decreases in co-immunoprecipitated STAT-1 in samples that were pre-treated with the p38 MAPK and Smad-3 inhibitor, particularly in samples that were then stimulated with 0.1 μg/ml polyIC were observed, though this did not reach statistical significance (Figure 5-16).

Although, no significant differences in levels of co-immunoprecipitated STAT-1 was observed in asthmatic PBECs, we decided to repeat experiments in cells from one non-asthmatic subject. PBECs from a healthy control volunteer were pre-treated with 10 ng/ml TGF-β for 24 hrs, followed by stimulation with 0.1 and 1 μg/ml polyIC. Pulled-down samples were immunoblotted and probed for STAT-1 levels as described (Figure 5-17 A). Membranes were also stripped and re-probed with anti-PIAS-1 antibodies as an internal control (Figure 5-17 A). STAT-1 and PIAS-1 protein bands were then quantified by densitometry using Image J software and values plotted as a ratio of STAT-1 to PIAS-1 (Figure 5-17 B). No significant differences in pulled-down STAT-1 levels between polyIC-treated samples and control samples were observed, although asmall increase in STAT-1 was observed in samples pre-treated with TGF-β and stimulated with 0.1 μg/ml polyIC (Figure 5-17 B).

Figure 5-15. Co-immuneprecipitation of STAT-1 protein with anti PIAS-1 antibodies using asthmatic PBECs treated with neutralizing anti-TGF-β antibodies or and isotype control.

Cells from asthmatic volunteers were pre-treated with 10 μg/ml anti-TGF-β antibodies followed by stimulation with 0.1 and 1 μg/ml polyIC for 8 hrs. Aliquots of cell lysates used in pull-down experiments were analysed by SDS-PAGE for phosphorylated STAT-1 (Tyrosine 701). Membranes were then stripped and re-probed with pan-STAT-1 antibodies (A). Co-immuneprecipitation experiments were conducted as decribed in Figure 4-28. Samples from the pull-down lysates were probed for STAT-1 and PIAS-1 protein (B).

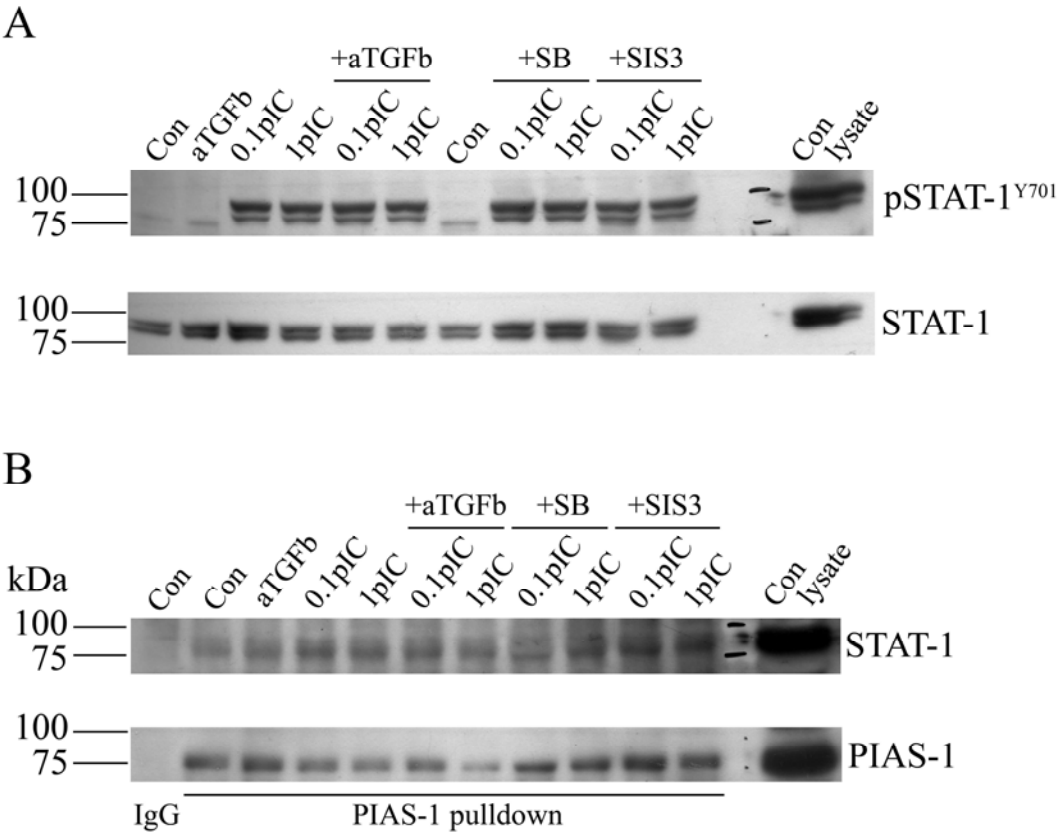

Figure 5-16. STAT-1 and PIAS-1 protein bands from Figure 5-15 were quantified by densitometry and plotted as a ratio of STAT-1 to PIAS-1.

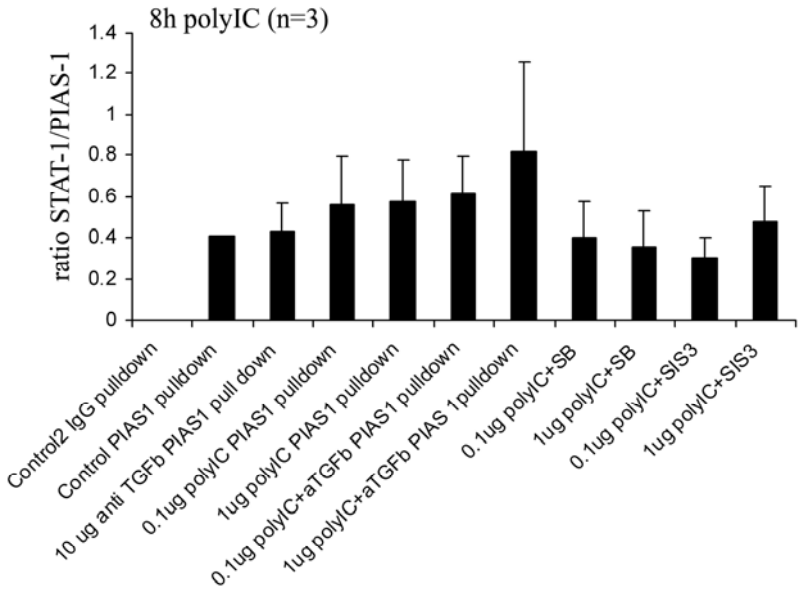

Figure 5-17. Co-immuneprecipitation of STAT-1 protein with anti PIAS-1 antibodies using non-asthmatic PBECs treated with exogenous TGF-β_2.

Cells from healthy control volunteers were pre-treated with 10 ng/ml TGF-β for 24 hrs followed by stimulation with 0.1 and 1 μg/ml polyIC for 8 hrs. Goat anti-PIAS-1 antibodies were used for pull-down experiments followed by detection with rabbit anti-STAT-1 antibodies. Membranes were then stripped and re-probed with rabbit anti-PIAS-1 antibodies (A). STAT-1 and PIAS-1 protein bands were quantified by densitometry and plotted as a ratio of each other (B).

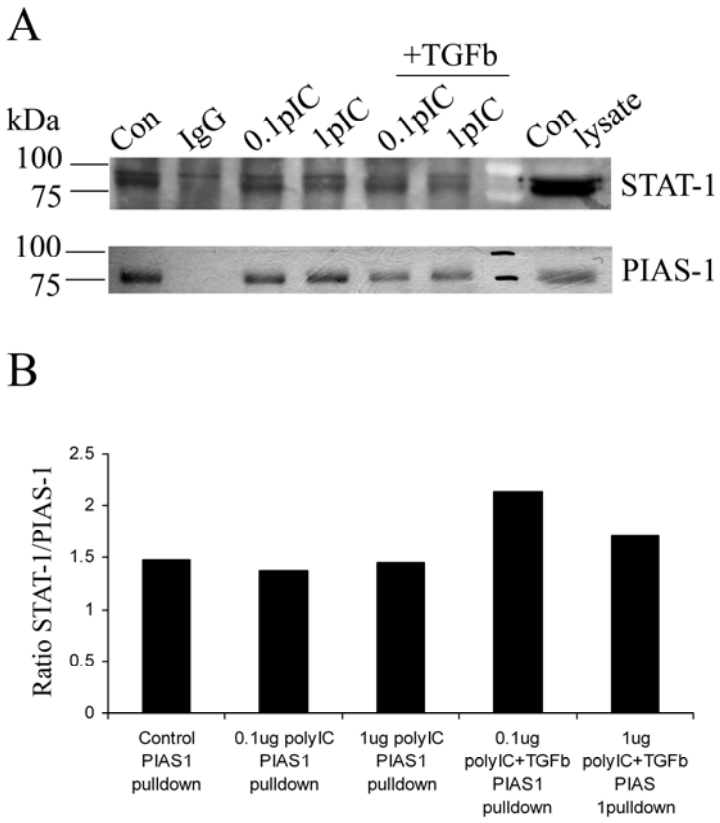

Discussion

In the previous section it was shown that when PBECs were treated with exogenous TGF-β_2, RV replication was promoted to significantly higher levels. This section demonstrated that this effect can be reversed in asthmatic epithelial cell cultures by blocking endogenous TGF-β activity with a neutralizing antibody. When neutralizing antibodies to TGF-β were added to asthmatic epithelial cell cultures, the amount of RV1B released from infected cells was reduced significantly. These findings suggest that the presence of higher levels of TGF-β in the airways of asthmatic subjects may contribute to virus-induced exacerbation. From the photomicrographs, no significant differences were seen in terms of cell death in the presence or absence of the antibody. As the presence of the antibody decreased the virus titre in RV1B infected cells at 48 hours (Figure 5-1), it might have been expected that less cytopathic cell death due to viral infection would be observed. However, the photomicrographs and LDH data shown in Figure 5-2 to Figure 5-4 that neutralizing antibodies against TGF-β had no effect on the amount of virus-induced cytopathic effect in these cells.

When IFN-β protein levels were analysed relative to virus particles from infected cells it was found that the presence of anti-TGF-β antibody in the presence RV promoted expression of IFN-β protein significantly more compared to RV alone samples. This was also true when cells were stimulated with synthetic double-stranded RNA. These findings support results from the previous section, where it was observed that exogenous TGF-β suppressed the IFN response, suggesting that this cytokine might play a role in dampening the innate immune response.

In order to determine the mechanism by which TGF- β modulates the innate immune response, the roles of Smad-3 and p38 MAPK in TGF-β mediated modulation of the innate immune response were also investigated. Chemical inhibitors to both molecules inhibited viral replication and SIS3 was able to augment IFN-β in polyIC-treated asthmatic cells, suggesting that Smad-3 might be more important in TGF-β-mediated modulation of the innate immune response. In previous studies, it has been suggested TGF-β increases the interaction of STAT-1 (Signal Transducer and Activator of Transcription) and PIAS-1 (a protein inactivator of Stat-1), thereby preventing transcriptional activity of STAT-1 (Reardon and McKay, 2007; Liu and Shuai, 2008). This was suggested to be mediated by Smad-signalling and not via p38 MAPK (Reardon and McKay, 2007). PIAS proteins also exhibit SUMO-E3 ligase activity, and in a separate study it was demonstrated that PIAS-mediated SUMO-1 modification of STAT-1 was dependent on p38 MAPK activity (Vanhatupa et al., 2008). Attempts to

address the question whether the presence of TGF-β promoted the interaction of PIAS-1 and STAT-1 and thereby decreasing the IFN response were made. It was hypothesized that the presence of anti-TGF-β antibodies would decrease this interaction and therefore the amount of STAT-1 pulled down with anti-PIAS-1 antibodies. In these studies, it was demonstrated that the presence of anti-TGF-β antibodies did not cause a significant change in the amount of STAT-1 detected in co-immuneprecipitation experiments when cells were stimulated with polyIC for 8 hrs. Indeed no significant differences between unstimulated and polyIC-stimulated cells were detected at 8 hrs post-treatment, suggesting perhaps that longer stimulation is required to mount a negative feedback. It would, therefore, be interesting to analyse STAT-1-PIAS-1 interactions after 24 or 48 hrs stimulation with polyIC. It would also make sense to add additional control cells treated with IFN-γ to ascertain previous observations of STAT-1-PIAS-1 interactions in the context of IFN- γ treated cells (Reardon and McKay 2007). Since PIAS-1 regulates STAT-1 transcriptional activity, another way to pursue these studies is to conduct gel shift assays and determine whether TGF-β increases PIAS-1 association to IFN-β promoters via STAT-1. Another possibility is that it is PIAS-2, encoded by the *PIAS-x* gene, that may be more important in negative regulation of the IFN response. PIAS-2 will bind to activated STAT-2, and therefore might be more important in the context of IFN-β signalling, which involves STAT-1/STAT-2 heterodimerization (Rytinki et al., 2009; Takaoka and Yanai, 2006).

Although PIAS-1 has been described as a SUMO E3 ligase, it is doubtful that SUMO is associated with the PIAS-1-STAT-1 complex (Palvimo, 2007b). SUMO or small ubiquitin –related modifier, are small proteins, which can be attached to target protein in a specific and regulated manner in order to regulate cellular processes (Rytinki et al., 2009). Unlike ubiquitin, SUMO modification is reversible and like its relative it is able to form chains on target proteins (Rytinki et al., 2009). It is believed that PIAS-1 represses STAT-1 activity in a SUMO-independent manner (Chung et al., 1997; Palvimo, 2007a). It was shown by Western Blotting that STAT-1 is phosphorylated at Y701 when PBECs are treated with polyIC in the presence or absence of TGF-β antibodies. It is possible that the STAT-1-PIAS-1 interaction is a dynamic process and that the small difference induced by the presence of TGF-β may not be detectable in our system. It is also likely that TGF-β may exert dampening activity on the IFN response through a number of different mechanisms which may or may not involve PIAS-1.

Another possibility is that TGF-β may affect accessibility of IFN-β promoters by

regulating histone deacetylases (HDACs). In one study it was shown that trichostatin A (TSA), an HDAC inhibitor, was able to inhibit TGF-β induced myofibroblastic changes in human skin skin fibroblasts (Glenisson et al., 2007). It would, therefore, be interesting in future studies conduct experiments analysing IFN-β promoter accessibility by PCR-amplification of restriction digests spanning this site.

The data presented in this section provide an interesting point as to why asthmatics are more prone exacerbation following rhinovirus infection. Previous published data have shown that asthmatics are likely to produce less interferon against RV infection, and thus become more susceptible to this virus (Wark et al., 2005a), (Contoli et al., 2006b). It is possible that the environment in the asthmatic airways, which includes the expression of high levels of endogenous TGF-β, may contribute to this decreased innate immune response to virus infection.

6 Chapter 6: Results

6.1 Small molecule chemical inhibitors of src kinases inhibit rhinovirus replication through possible modulation of the innate immune response

Rationale

In the previous chapter, the possible mechanisms involved in TGF-β-mediated enhancement of rhinovirus replication in PBECs were investigated. As part of this investigation, it was decided to determine whether this observation involves the activation of focal adhesion kinase (FAK) protein by src kinases, which was shown in a previous study to be mediated by TGF-β (Cicchini et al., 2008). The aim of this chapter was to apply a more biochemical approach in elucidating TGF-β mediated signalling, the involvement of src protein tyrosine kinases and their effect on RV replication. During this investigation, a range of src inhibitors were tested, including PP2, src kinase inhibitor 1 (SKI-1) and SU6656 on RV-infected PBECs and viral replication and the IFN responses were measured as described in previous chapters.

6.1.1 Evidence of intracellular localization of beta 1 integrins following TGF-β treatment

FAK and cellular-src (c-src) are signalling proteins, which, when activated can alter cellular behaviour via a group of receptors called integrins (Mitra and Schlaepfer, 2006). Integrins are transmembrane receptors that link the extracellular matrix (ECM) to the intracellular actin cytoskeleton at point of cell to substratum interaction, called focal adhesion (Mitra and Schlaepfer, 2006). Integrin clustering can promote cell proliferation, survival and migration in normal and tumour cells (Mitra and Schlaepfer, 2006). Initial attempts were made to stain PBEC cell monolayers that were incubated with or without TGF-β (10 ng/ml) with an anti-beta1-integrin antibody coupled with a FITC-labelled secondary antibody (Figure 6-1). Figure 6-1 shows that in untreated control cell monolayers, beta1-integrin is more localized on the cell surface, whereas after 48 hrs of TGF-β treatment (10 ng/ml), this protein becomes more cytoplasmic implying perhaps a change in cellular phenotype, such as, for example cell motility.

Figure 6-1. PBECs from a healthy donor were grown in collagen-coated 8-well chamber slides. Cells were treated with 10 ng/ml TGF-β_2 for 48 hours and fixed with 4% paraformaldehyde. Cells were stained for beta-1 integrin using a mouse monoclonal beta 1 integrin antibody (clone P5D2) followed by incubation with a secondary anti-mouse antibody labeled conjugated to fluorescein isthocyanate (FITC). Cells were counterstained with TOPR3 nuclear dye. Images were taken at x20 magnification using the GFP and CY5 channels and overlayed.

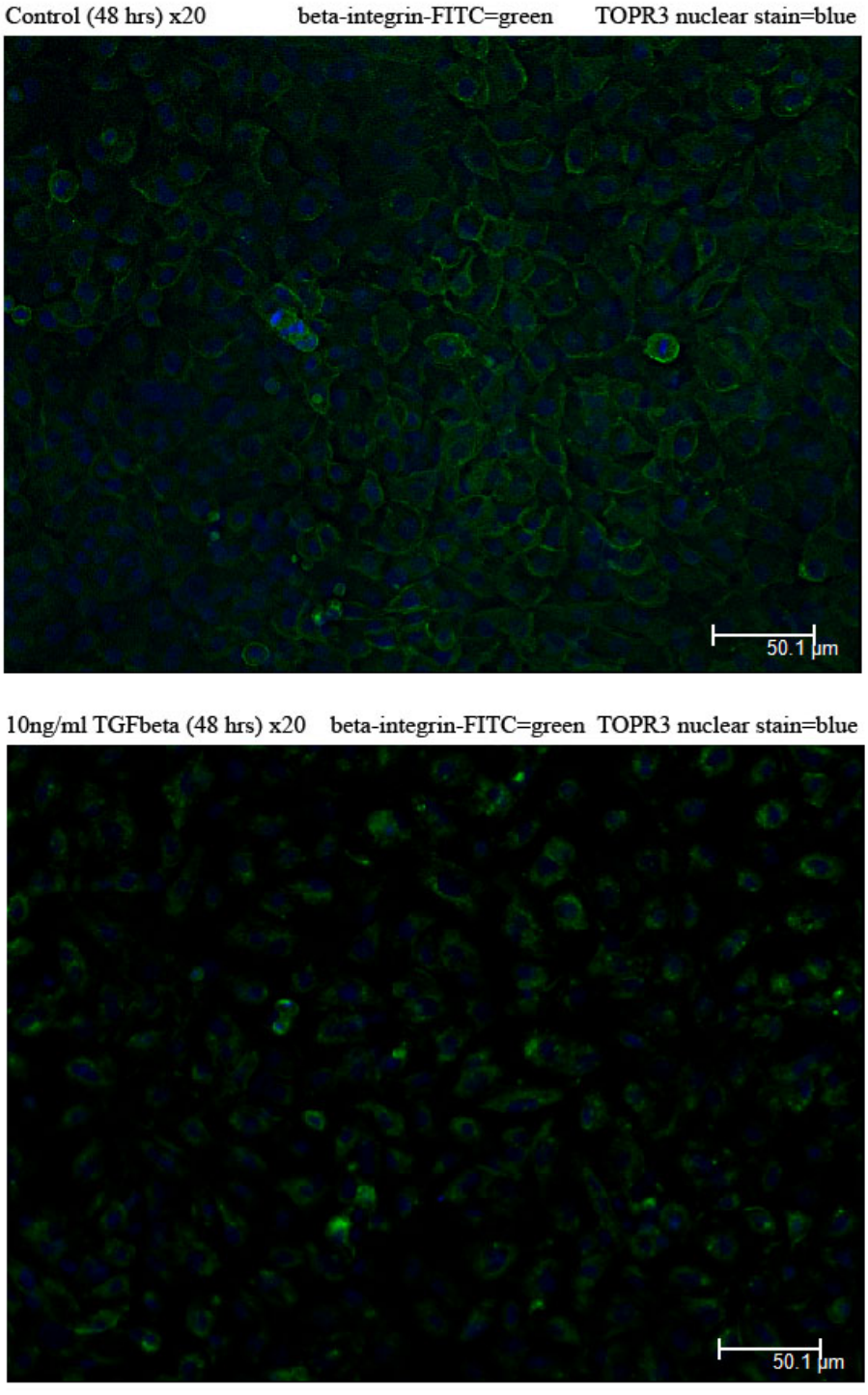

6.1.2 Inhibition of src family protein tyrosine kinases results in significant reduction of infectious virus particles from rhinovirus-infected HBEC

Src is a member of the protein tyrosine kinase (PTK) family and contains a NH_2-terminal domain required for membrane attachment, known as the Src homology (SH) 4 region (Figure 6-2 A). It is followed by SH3 and SH2 domains which are regulatory domains that bind proline-rich and phosphotyrosyl regions, respectively (Okutani et al., 2006), (Alvarez et al., 2006) (Figure 6-2 A). Upregulation of Src PTK activity occurs after phosphorylation of the tyrosine in the catalytic region (Tyr^{416} or Tyr^{419}) and is negatively regulated by phosphorylation of the tyrosine in the COOH-terminal tail (Tyr^{527} or Tyr^{530}) (Okutani et al., 2006), (Alvarez et al., 2006) (Figure 6-2 B). Cellular src (c-src) is a protooncogene known for its ability to regulate cell cycle and cause tumor formation (Alvarez et al., 2006). Apart from its involvement in signal transduction pathways, src has also been implicated in cell adhesion, focal adhesion assembly and cell migration (Thomas and Brugge, 1997). Recent studies have shown a requirement for the protein tyrosine kinase src in the induction rhinovirus-induced IL-8 (Bentley et al., 2007), as well as the induction of TNF-α, RANTES and IL-1β by Japanese encephalitis virus (Raung et al., 2007). A group has also reported that double stranded RNA (dsRNA)-induced IFN-β activation was reduced when src was inhibited (Johnsen et al., 2006). Thus, it seems that src inhibition would be detrimental to the innate immune response against rhinovirus infection. However, further studies with enveloped viruses have shown that HBx, a non-structural regulatory protein of the Hepatitis B virus (HBV) stimulates src tyrosine kinases which are required for viral reverse transcription (Klein et al., 1999). Furthermore, Hirsch *et al* have demonstrated that inhibition of src interfered with the viral assembly West-Nile Virus in infected cells and caused an increase in ER-associated virus particles (Hirsch et al., 2005). Another enveloped virus, the dengue virus, was also shown to require c-src for efficient virion assembly (Chu and Yang, 2007). As no studies to date have been conducted with non-enveloped viruses and src, we decided to investigate the effects of src inhibition on the rhinovirus life cycle and to explore the possibilities of a new target for therapy.

Figure 6-2. The linear structure of c-src.

Numbers above the linear molecule denote amino acid residues in sequence from the N terminus (N) to the C terminus (C). C-src has 7 domains (SH1-SH7), which are depicted in different colours (A). This figure shows c-Src regulation. Src is maintained in an inactive conformation (center) with SH2 domain engaged with the tyrosine (Tyr) residue Tyr^{530}, the SH3 somain engaged with the SH2-kinase linker, and Tyr^{416} dephosphorylated (B). Dephosphorylation of Tyr^{530} by protein tyrosine phosphatase (PTP) action (right) disrupts intramolecular interaction between the SH2 domain and Tyr^{530}; Tyr^{416} can become autophosphorylated, resulting in Src activation. Phosphorylation of Tyr^{530} by c-Src kinase (CSK) allows this interaction to reform, resulting in Src inaction (Alvarez et al., 2006). Modified from Alvarez et al. *Cancer* 2006 (Alvarez et al., 2006).

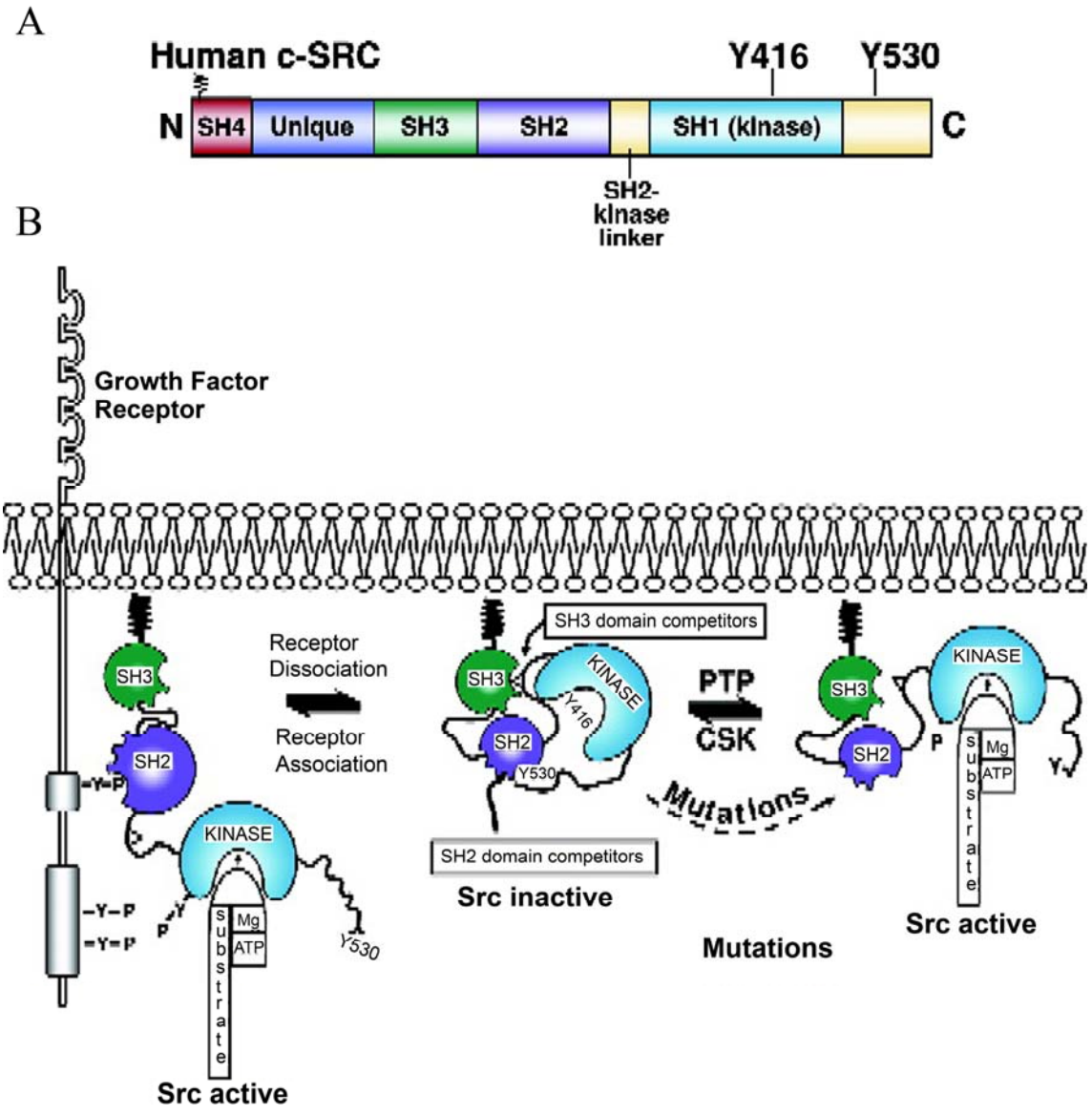

Small, cell-permeable inhibitors to protein kinases have been developed for cancer therapy, as well to investigate the physiological roles of protein kinases in signalling pathways (Bain et al., 2007; Okutani et al., 2006). PP1 and PP2 are inhibitors that have been widely used, but will also inhibit other protein tyrosine kinases such as Eph-A2 and FGF-R1 (Bain et al., 2007). Both inhibitors act by binding to the ATP-binding site of the kinase (Okutani et al., 2006). Additional chemical inhibitors that have been studied for their relative potencies against members of the src family of protein tyrosine kinases include SU6656 and src kinase inhibitor 1 (SKI1) (Table 6.1-1) (Bain et al., 2007; Okutani et al., 2006). In this study the inhibitors PP2, SU6656 and SKI 1 were used to study of the role of c-src in rhinovirus replication in primary bronchial epithelial cells.

Table 6.1-1. Modified from (Bain et al., 2007)

Potencies of compounds developed as Raf and Src inhibitors towards a variety of protein kinases

IC_{50} values were determined from assays carried out at ten different inhibitor concentrations.

Compound	Protein kinase	IC_{50} (μM)	[ATP] in assay (μM)
SU 6656	Src	0.10	50
	Lck	0.15	50
	Aurora B	0.019	20
	Aurora C	0.017	5
	BRSK2	0.10	50
	MST2	0.11	50
	AMPK	0.11	50
Src-I1	Src	0.18	50
	RIP2	0.026	100
PP2	Src	0.036	50
	Lck	0.031	50
	RIP2	0.019	100
	CK1δ	0.041	20

In initial studies, the effects of PP2 and SU6656 on RV1B replication in primary bronchial epithelial cells (PBECs) were studied. PBECs from a group of 6 healthy and 9 asthmatic subjects were obtained and infected with RV1B stock at MOI=0.01 and analysed. Cells were then incubated for a period of 24 and 48 hours and viral supernants were assessed for viral titre using the $TCID_{50}$ assay as described previously. The summary data were graphed as the mean $\log_{10}$ $TCID_{50}$/ml in . SU6656 reduced virus titre by 4 $\log_{10}$ scales after 24 hrs of infection and almost 5 $\log_{10}$ scales by 48 hrs (Figure 6-3 A and B). PP2 did not significantly reduce the virus titre, even though this inhibitor was tested at the same concentration as SU6656, suggesting that this inhibitor is not as potent as the latter in our system (Figure 6-3). Previous published data using West-Nile Virus (WNV)-infected Vero showed that 5 μM PP2 was sufficient in inhibiting virus replication up to 4 $\log_{10}$, although interestingly, it had no effect on Herpex Simplex Virus (HSV) replication (Hirsch et al., 2005).

Figure 6-3. Cell supernatants from infected cells were measured for virus titre using the end-point dilution assay as described in materials and methods and mean values graphed as $TCID_{50}$/ml.
Error bars represent standard errors of the mean. Samples were obtained from 6 healthy and 9 asthmatic subjects and infected for 24 (A) and 48 hours (B) with RV1B at MOI=0.01 in the presence or absence of the named src kinase inhibitors. DMSO was used as a vehicle control. ***p*<0.01 vs RV only

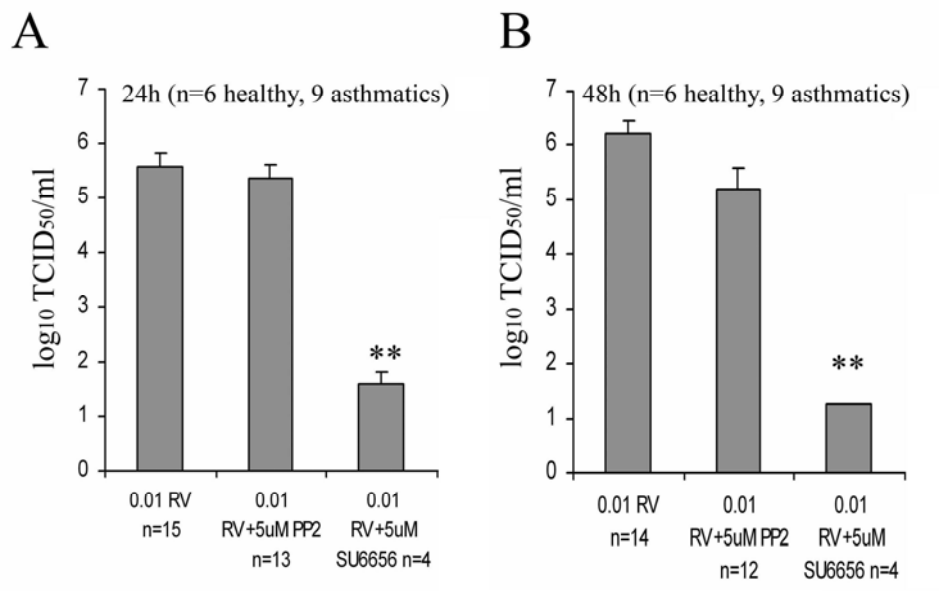

Additionally, the Src kinase inhibitor 1 (SKI1) compound was tested at concentrations of 10 and 20 μM in cells from 4 and 9 subjects respectively and compared it to the efficacy of SU6656. It was found that both concentrations of SKI1 significantly inhibited viral replication at 24 and 48 hours post-infection ($p<0.01$) (Figure 6-4). However, even at twice the concentration, SKI1 was not as effective in inhibiting viral replication as SU6656 (Figure 6-4). A previous study, systematically studying the potencies of difference protein kinase inhibitors, showed in a biochemical assay that SU6656 has a half maximal inhibitory concentration (IC_{50}) to that for SKI1 (Bain et al., 2007). It was, therefore, decided to use the highest concentrations tested for SU6656 (10μM) and SKI1 (20 μM) in subsequent experiments, as they have different potencies.

Figure 6-4. Virus titre of RV-infected PBECs in the presence or absence of src kinase inhibitors. Cell supernatants from infected cells were measured for virus titre using the end-point dilution assay as described in materials and methods and mean values graphed as $TCID_{50}$/ml. Error bars represent standard errors of the mean. Samples were obtained from 6 healthy and 9 asthmatic subjects and infected for 24 (A) and 48 hours (B) with RV1B at MOI=0.01 in the presence or absence of the named src kinase inhibitors. DMSO was used as a vehicle control. **p<0.01 vs RV only

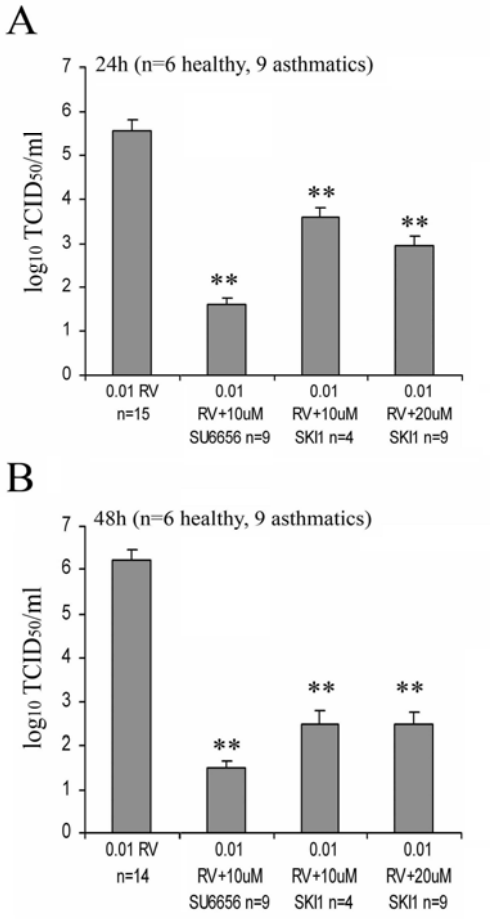

In order to determine whether these inhibitors were effective at inhibiting RV replication when cells were infected at a higher dose of virus, PBECs were infected with RV at MOI=0.05, treated with SKI1 and SU6656 and incubated for 24 and 48 hours. Both inhibitors reduced the release of infectious virus particles significantly at 24 hours post-infection (Figure 6-5 A). However, at 48 hours only the SKI1 compound reduced virus replication to statistical significant levels (Figure 6-5 B). For one of the subjects, SU6656 had no effect on virus replication, which contributed to overall increase in the mean $TCID_{50}$/ ml values (Figure 6-5 B). However, this may be an experimental error as SU6656 was effective against virus replication in all other experiments.

In order to test whether src inhibitors can be added as late as 6 hrs post-infection and reduce virus replication, SKI 1 and SU6656 were tested at higher doses in cells infected with MOI=0.01 RV1B. Cells from 2 healthy and 2 asthmatic subjects were infected with RV1B and inhibitors were added 1, 4, and 6 hrs p.i. The presence of both inhibitors significantly reduced virus titre at both 24 and 48 hrs p.i. regardless whether they were added at an early or later stage of infection (Figure 6-6 A and B). Photos taken of PBEC monolayers infected with high doses of virus (MOI=0.1, 0.5) and incubation in the presence or absence of SU6656 reflect the extent of protection provided by this inhibitor by reducing the amount of virus-induced CPE (Figure 6-7).

To rule out the possibility that the addition of src inhibitors interferes with the entry of viruses into the cells a GFP-tagged HRV construct transfected into HeLa cells was tested for responses to the inhibitors. A pUCT7-HRV16 vector plasmid vector (kindly provided by Dr. Tobias Tuthill) was linearized with the *SacI* enzyme. Digested DNA was then purified (see Methods) and T7 transcripts containing the RV16 genome generated *in vitro*. RNA transcripts were then electroporated into HeLa cells and incubated in the presence of SKI1. At 12 hour post-transfection less green fluorescent cells were visible in the presence of SKI1 compared to vehicle-treated samples (Figure 6-8). The SU6656 compound was not used in these experiments, because of substantial autofluorescence by this inhibitor.

Figure 6-5. Virus titre of RV-infected PBECs in the presence or absence of src kinase inhibitors. Cell supernatants from infected cells were measured for virus titre using the end-point dilution assay as described in materials and methods and mean values graphed as $TCID_{50}$/ml.

Error bars represent standard errors of the mean. Samples obtained from 6 healthy and 1 asthmatic subject were infected with RV1B at MOI=0.05 and incubated for 24 (A) and 48 (B) hours in the presence or absence of various src kinase inhibitors. * $p<0.05$ vs RV only.

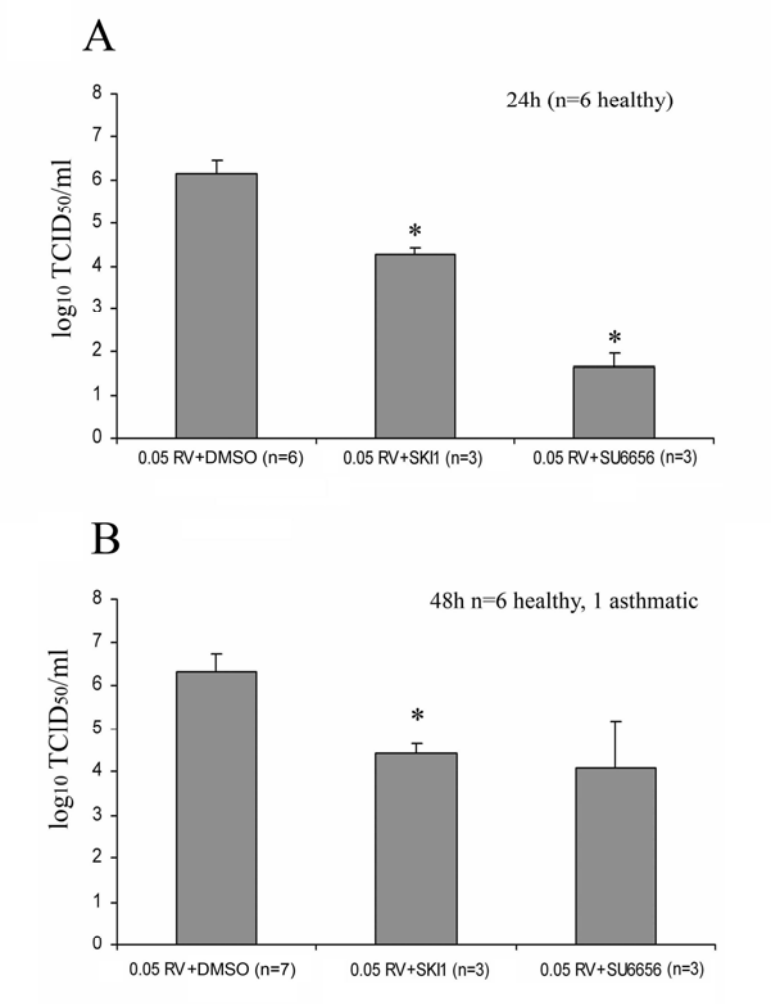

Figure 6-6. Virus titre of RV-infected PBECs in the presence or absence of src kinase inhibitors. Cell supernatants from infected cells were measured for virus titre using the end-point dilution assay as described in materials and methods and mean values graphed as $TCID_{50}$/ml.

Error bars represent standard errors of the mean. Cell samples infected with 0.01 MOI RV1B were incubated for 1, 4, or 6 hours before the addition src kinase inhibitors and further incubated for 24 (A) or 48 (B) hours. *p<0.05 vs RV only

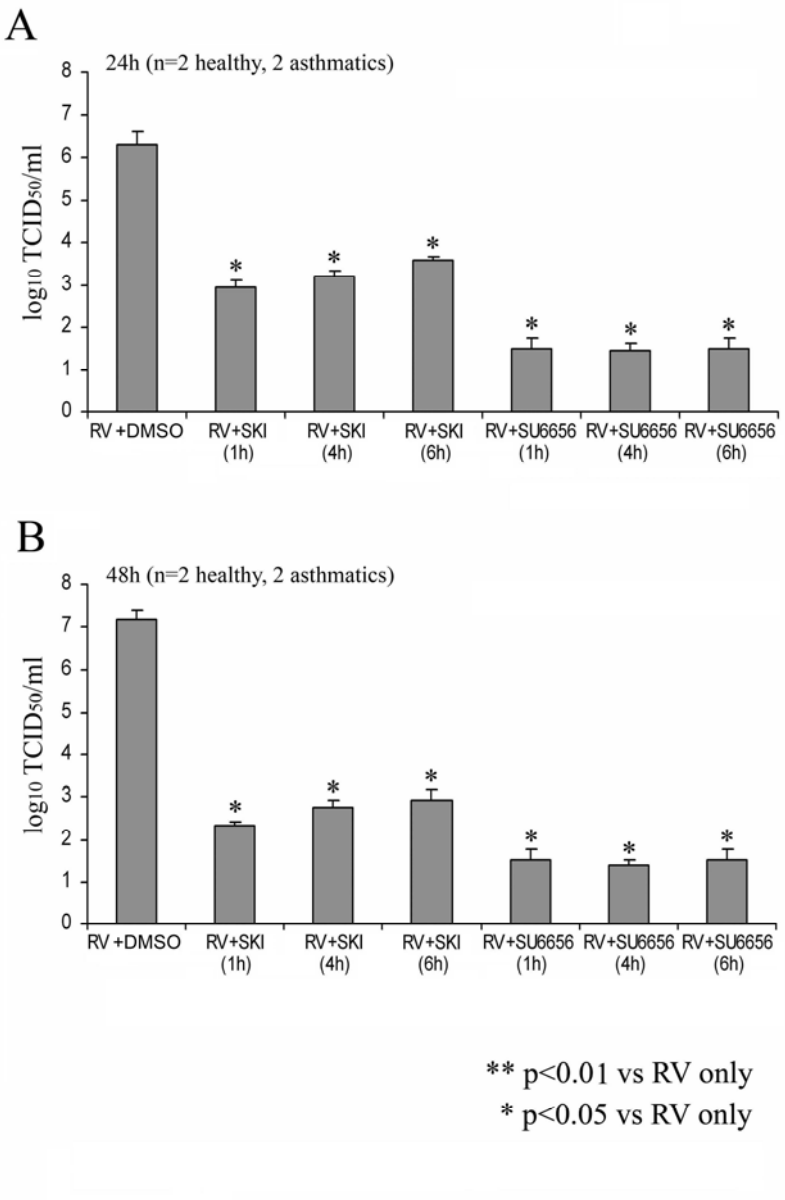

Figure 6-7. Photomicrographs of RV-infected PBECs in the presence or absence of src kinase inhibitor. Cells were infected with 0.1-0.5 MOI RV1B and incubated with 10µM SU6656 or DMSO was used as a vehicle control. Cells were incubated for 8 hours at 37^0C, 5% CO_2.

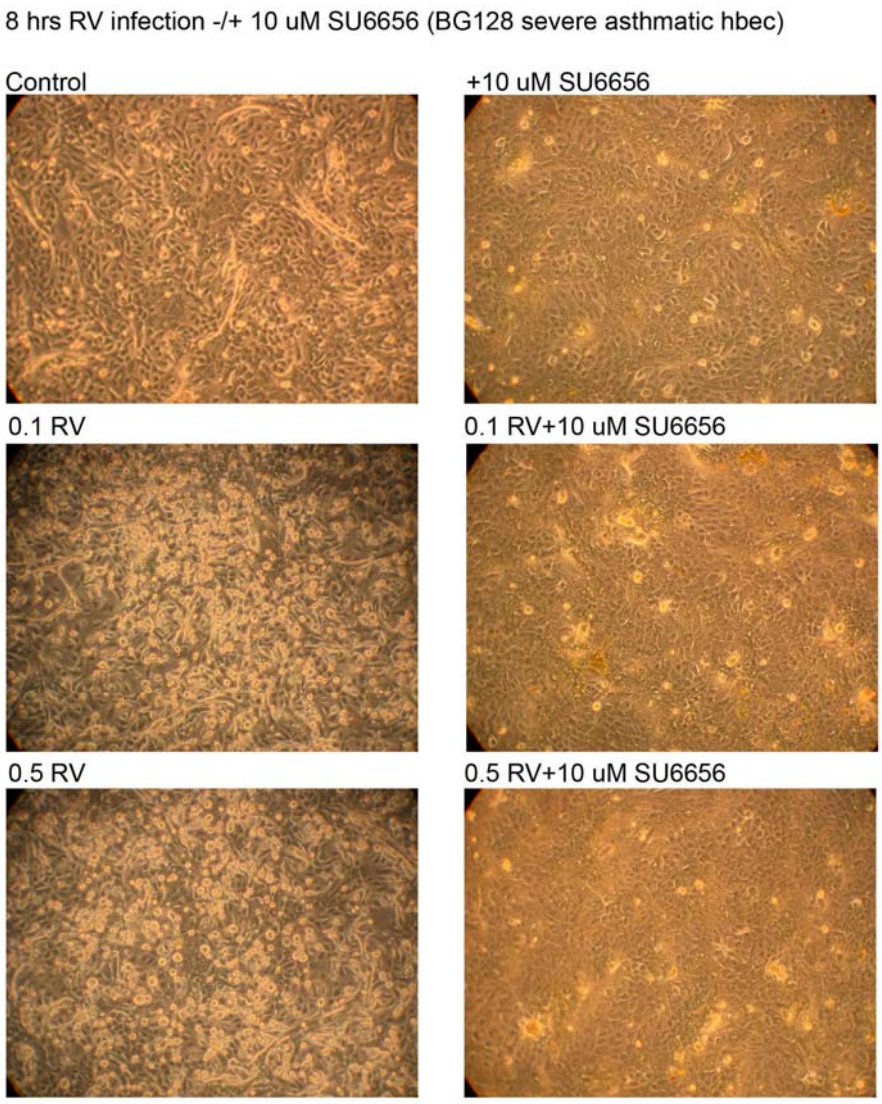

Figure 6-8. Ohio Hela cells were electroporated with RNA transcripts generated from an *in vitro* T7 transcription reaction of a GFP-tagged HRV construct.
Cells and incubated in the presence of SKI1 for 12 hours. DMSO was used as a vehicle control. Cells were analyzed with a fluorescence microscope using the GFP channel.

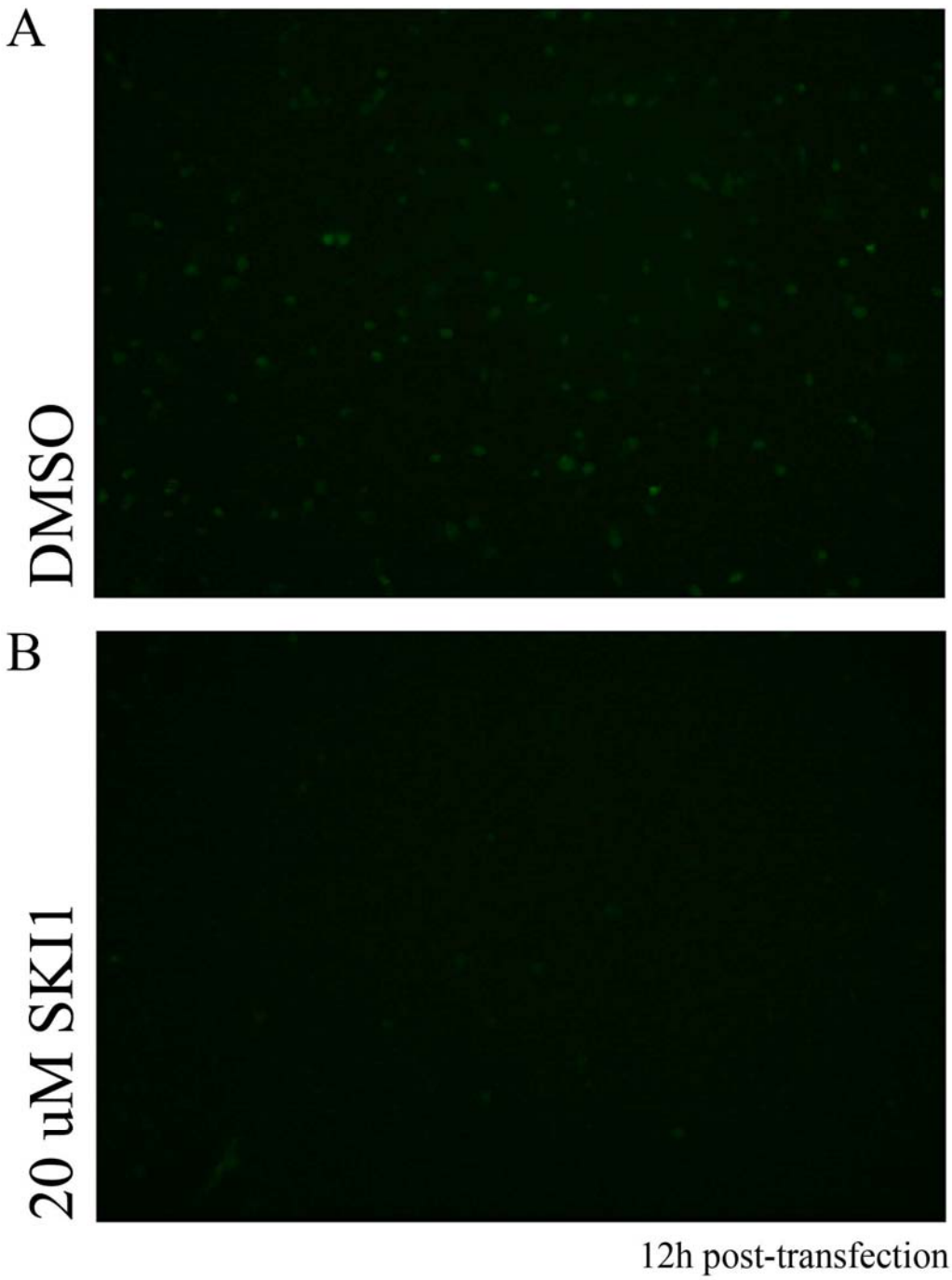

6.1.3 Src inhibition causes substantial viral mRNA degradation in rhinovirus-infected HBEC

Next, viral mRNA from RV1B-infected cells treated with SU6656 at 8 hrs p.i. was measured. Remarkable decreases in levels of viral mRNA compared to control samples were observed. This was also true for cells infected with higher doses of virus and incubated with the inhibitor (Figure 6-9A). The presence SU6656 decreased viral mRNA in a dose dependent manner (0.1-10 μM), although only samples treated with the highest concentration of 10 μM SU6656 reached a statistically significant reduction (Figure 6-9 B). RV1B mRNA from virus-infected cells treated with inhibitor 1, 4, and 6 hrs p.i. were also measured and found to be significantly reduced at 8, 24 and 48 hrs p.i. to almost non-detectable levels (Figure 6-10). This observation pointed to RNA degradation, possibly due to increased active RNAseL in the presence of inhibitors. Furthermore, it was found that the addition of SU6656 even at 16 hrs pi provided some protection against further virus-induced cytopathic cell death (Figure 6-11). This was accompanied by decreased levels of viral mRNA as observed previously (Figure 6-12 A).

Due to the potency of the src inhibitors against RV replication, it was decided to analyse IFN levels in the presence and absence of the inhibitors. IFN-β mRNA levels for samples treated with the vehicle DMSO only reflected for the most part viral mRNA levels (Figure 6-12 B), confirming previous observations that viral mRNA will induce IFN-β mRNA. However, interestingly, in the presence of the inhibitor, this relationship is lost, in that even when viral mRNA is decreased significantly compared to DMSO-treated samples, increases in IFN-β mRNA levels were still observed, suggesting that the SU6656 compound may somehow modulate the induction of IFN.

Figure 6-9. Viral RNA from RV-infected PBECs in the presence or absence of src kinase inhibitor SU6656. Cells from 2 healthy and two asthmatic subject were infected with RV1B (MOI=0.01-0.5) and incubated for 8 hours in the presence or absence of SU6656.

DMSO was used as a vehicle control. Cells were harvested and RNA extracted as described in Materials and Methods. Viral RNA was measured by RT-qPCR using RV1B-specific primers and probes and normalized to the Geometric Mean of the housekeeping genes GAPDH and UBC. The graph represents mean values of different subject, and error bars the standard error of the mean.

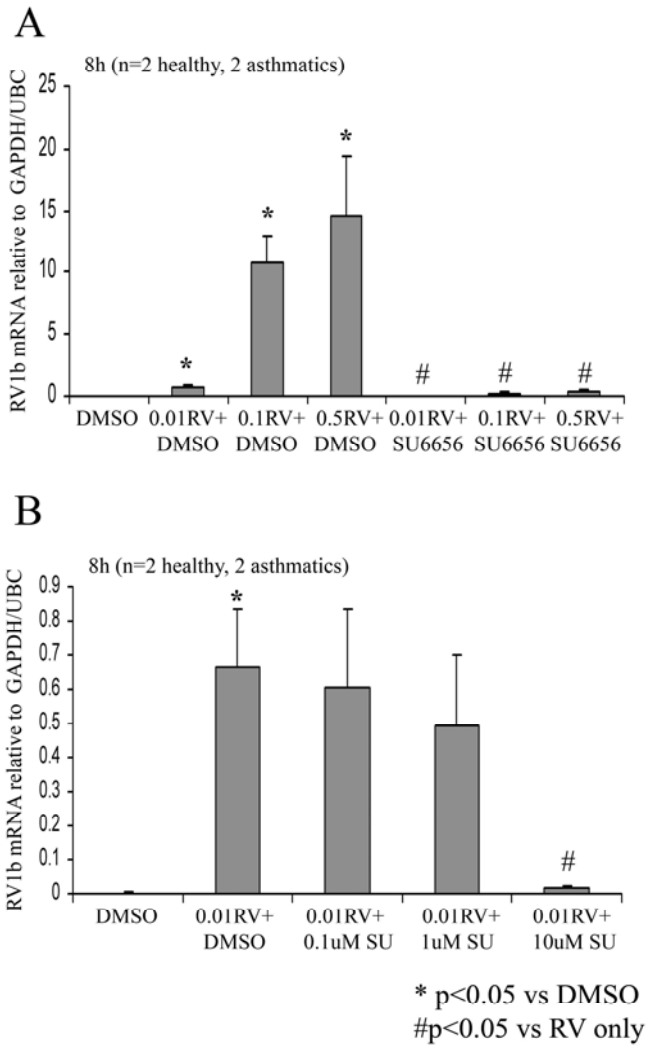

Figure 6-10. Viral RNA from RV-infected PBECs in the presence or absence of src kinase inhibitors. Cells from 2 healthy and two asthmatic subject were infected with RV1B (MOI=0.01-0.5) and incubated for 1, 4, or 6 hours followed by treatment with the inhibitors SKI1 or SU6656.

DMSO was used as a vehicle control. Cells were then further incubated for a period of 24 or 48 hours. Cells were harvested and RNA extracted as described in Materials and Methods. Viral RNA was measured by RT-qPCR using RV1B-specific primers and probes and normalized to the Geometric Mean of the housekeeping genes GAPDH and UBC. The graph represents mean values of different subject, and error bars the standard error of the mean.

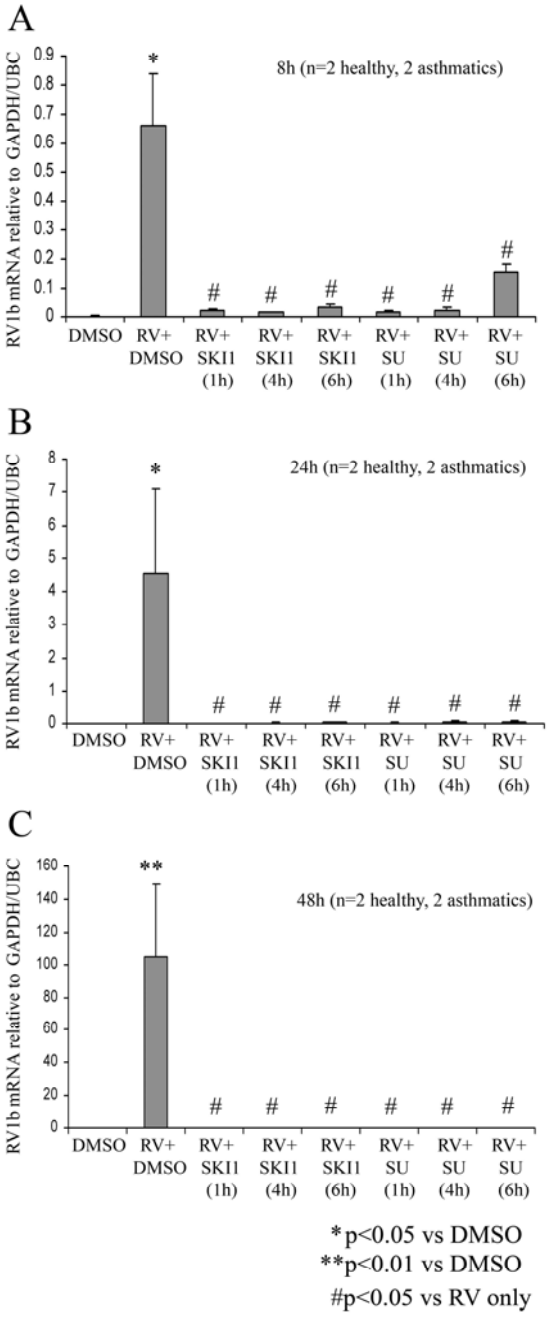

Figure 6-11. Photomicrographs of PBECs were infected with RV1B at MOI=0.01-0.1 and incubated for 16 hours.
10 µM SU6656 was added to cells. DMSO was used as a vehicle control. Cells were then incubated further for 24 hours.

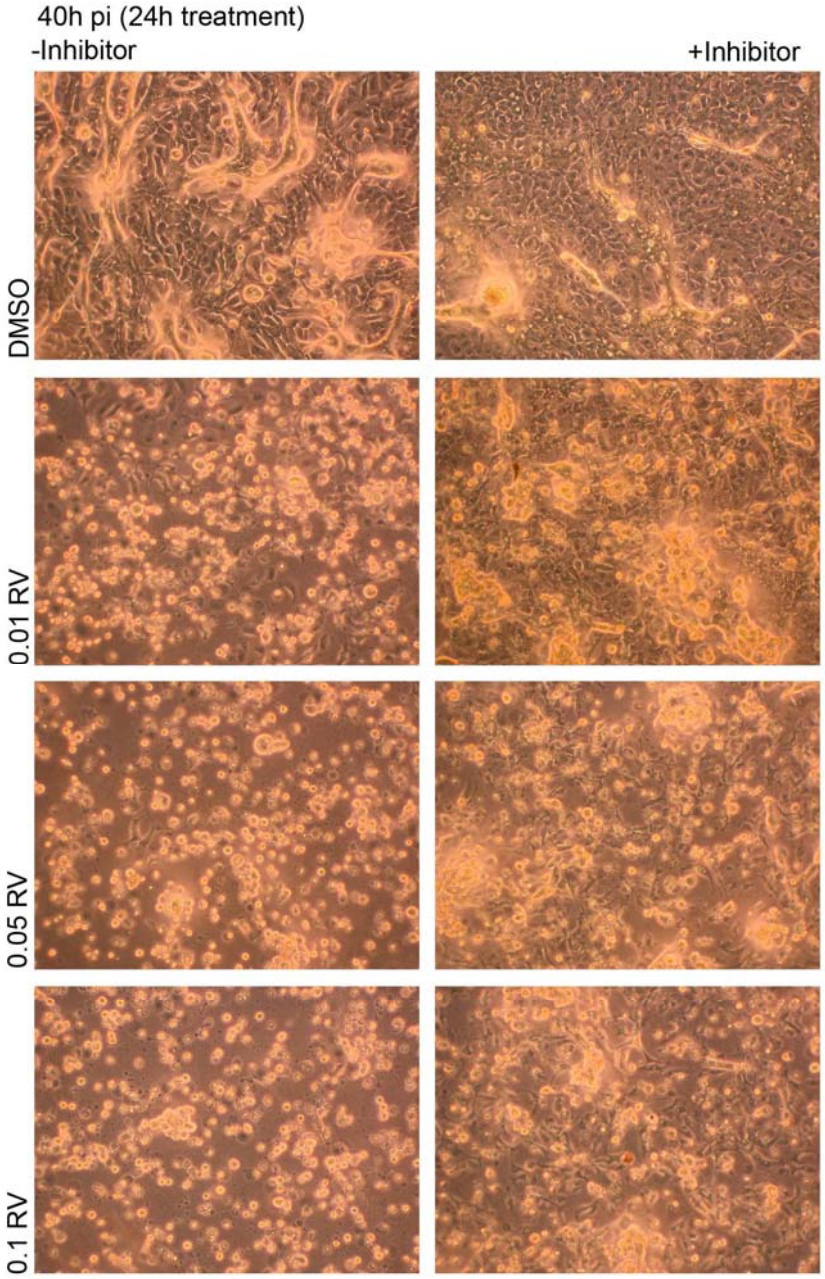

Figure 6-12. RV1B and IFN-β mRNA from RV-infected PBECs in the presence or absence of SU6656. Cells from three asthmatic subject were infected with RV1B (MOI=0.01-0.1) and incubated for 16 hours followed by treatment with the inhibitor SU6656 at a concentration of 10 μM.

DMSO was used as a vehicle control. Cells were then further incubated for a period of 24 hours. Cells were harvested and RNA extracted as described in Materials and Methods. Viral RNA (A) and IFN-β mRNA (B) was measured by RT-qPCR using RV1B-specific primers and probes and normalized to the Geometric Mean of the housekeeping genes GAPDH and UBC. The graph represents mean values of different subjects, and error bars the standard error of the mean.

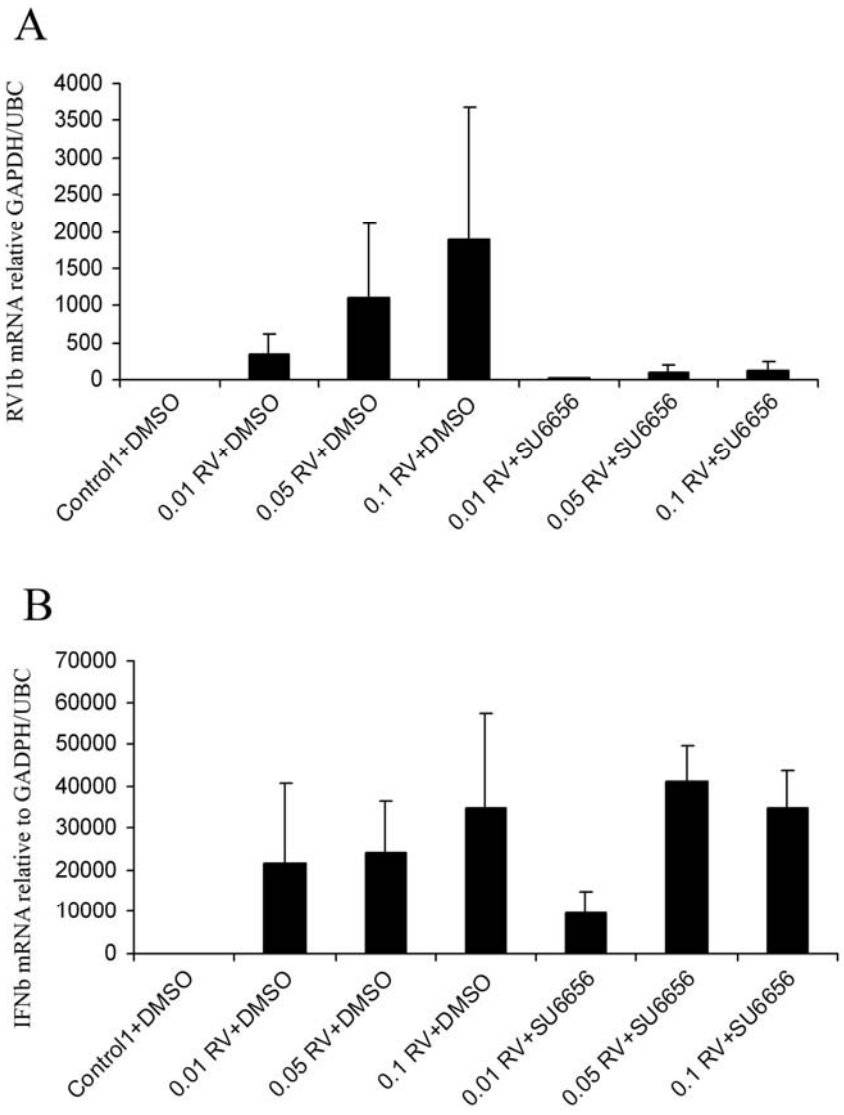

6.1.4 Inhibition of src kinases promotes virus-induced IFN-β production

It was decided to further investigate the possibility that the potent inhibition of RV replication by src kinase inhibitors, particularly SU6656, is due to the modulation of the IFN response against RV infection. Previous published data have shown that c-src is required for double stranded RNA (dsRNA)-mediated IFN-β induction in human monocyte-derived dendritic cells (Johnsen et al., 2006). Contrary to Johnsen *et al*, we found that SU6656 significantly increased virus induced IFN-β mRNA levels compared to vehicle- treated samples after 8 hrs infection $p<0.05$ (Figure 6-13 A). The other src kinase inhibitors PP2 and SKI1 did not significantly induce IFN-β levels in the presence of RV (Figure 6-13 A). When cells were treated with SU6656 after infection with higher doses of RV1B (MOI=0.1 and 0.5), IFN-β mRNA levels were significantly increased in the presence of the inhibitor compared to rhinovirus alone $p<0.05$ (Figure 6-13 B). Increased induction of IFN-β with SU6656 was in a dose-dependent manner (0.1-10 μM SU6656), although only treatment with 10 μM SU6656 reached statistical significance (Figure 6-13 C). IFN-β was not induced by the presence of the inhibitor alone (data not shown).

In order to test whether the SU6656 compound augmented the IFN-β response independently of virus replication, similar experiments with PBEC were conducted, but using a synthetic ds RNA polyI:polyC (polyI:C), a known TLR-3 ligand and inducer of type I IFNs and lower dose of SU6656 (5 μM). It was observed that in the presence of both polyI:C and 5 μM SU6656, IFN-β mRNA was significantly enhanced at 2 and 4 hrs post-treatment (Figure 6-14 A), although only data obtained at 4 hrs post-treatment with 0.1 μg/ml polyIC reached statistical significance. IFN-β protein levels were measured after 24 hrs of treatment with both polyIC and SU6656. It was found that in 6 subjects tested, IFN-β protein levels were significantly induced in the presence of the inhibitor when cells were treated with both 0.1 and 1 μg/ml polyIC, $p=0.032$ and $p=0.021$ (Figure 6-14 B).

Figure 6-13. IFN-β mRNA of RV-infected PBECs in the presence or absence of src kinase inhibitors. Cells from two healthy and two asthmatic subject were infected with RV1B (MOI=0.01-0.5) and incubated for 1, 4, or 6 hours followed by treatment with the inhibitors SKI1 or SU6656.

DMSO was used as a vehicle control. Cells were then further incubated for a period of 24 or 48 hours. Cells were harvested and RNA extracted as described in Materials and Methods. IFN-β mRNA was measured by RT-qPCR using IFN-β -specific primers and probes and normalized to the Geometric Mean of the housekeeping genes GAPDH and UBC. The graph represents mean values of different subject, and error bars the standard error of the mean.

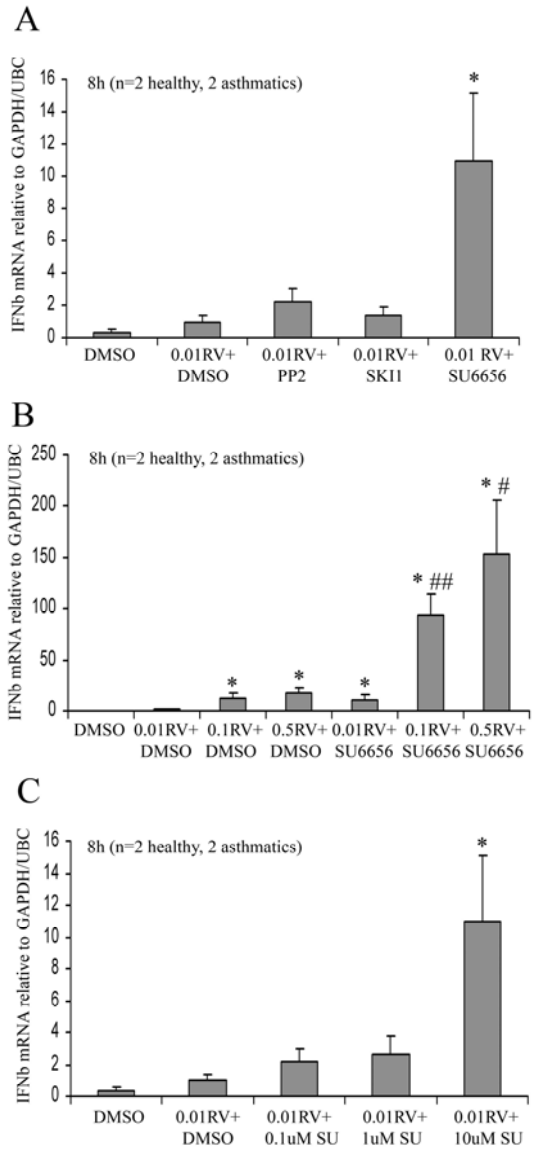

* p<0.05 vs DMSO
#p<0.05 vs RV only
##p<0.05 vs RV only

Figure 6-14. IFN-β mRNA and protein levels in polyIC-treated PBECs treated with SU6656 or DMSO. Cells from three asthmatic subjects were treated with synthetic double stranded RNA polyI:polyC (polyI:C) at 0.1 or 1 μg/ml, in the presence or absence of 5 μM SU6656.

DMSO was used as a vehicle control. Cells were incubated for 2 and 4 hours, harvested, and RNA extracted as described in Materials and Methods. IFN-β was measured by RT-qPCR using IFN-β -specific primers and probes and normalized to the Geometric Mean of the housekeeping genes GAPDH and UBC. The graph represents mean values of different subject, and error bars the standard error of the mean (A). PBECs treated with polyI:C and SU6656 as described and incubated for 24 hours, and cell supernatants were assayed for IFN-β protein by ELISA. The graph represents mean values of 6 different subjects, and error bars the standard error of the mean (B).

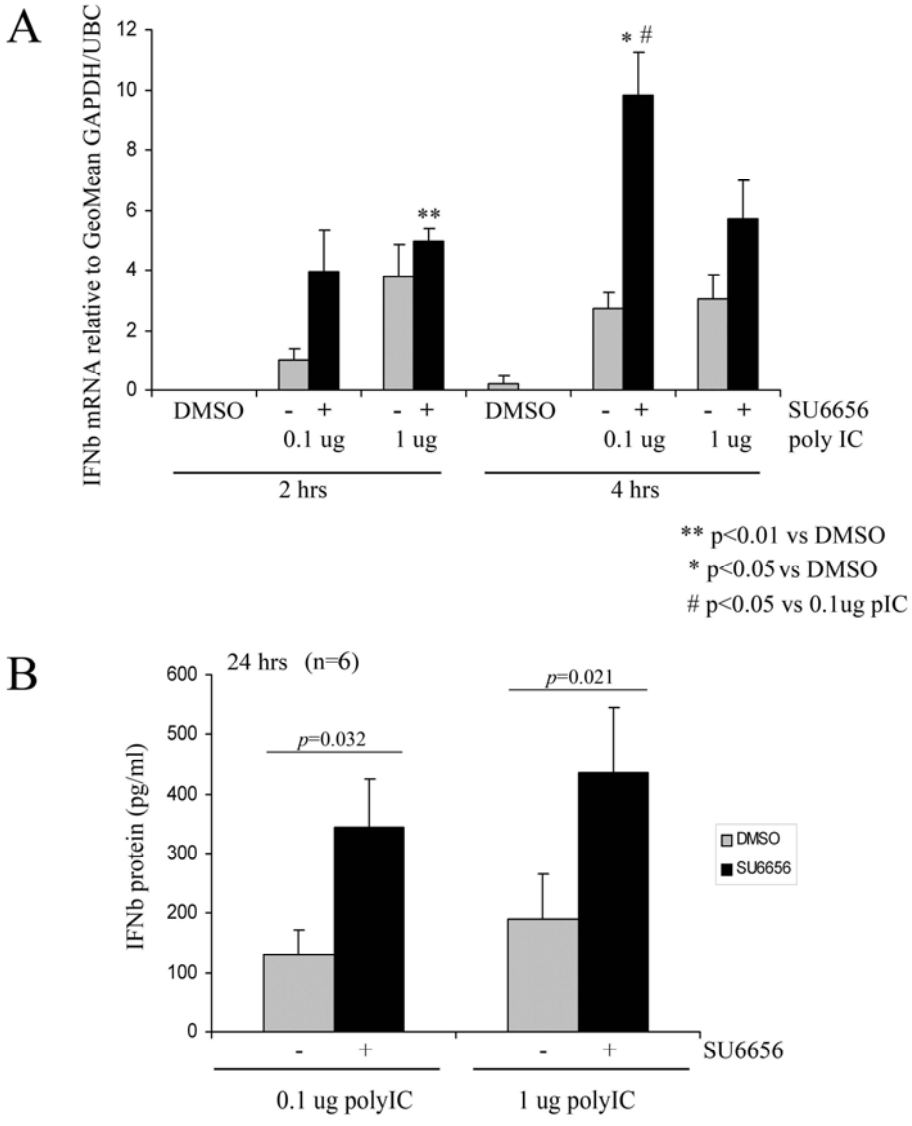

6.1.5 SU6656 does not significantly affect src (Y416) phosphorylation

In order to determine whether treatment the SU6656 compound affected the phosphorylation status of src kinase, we treated PBECs from healthy and asthmatic patient donors with 10 μM SU6656 for 1 hour, followed by infection with RV1B (MOI=10) in the presence or absence of the inhibitor. The cells were then incubated for a period of 10, 20, 30, 60, 90 and 120 minutes and harvested with SDS-PAGE sample buffer. Samples were analysed by SDS-PAGE gel electrophoresis as described in Materials and Methods, followed by Western blotting. Membranes were then incubated with an antibody raised against phosphorylated src kinase at Tyrosine residue 416 (Figure 6-15). As a loading control, the same membranes were then stripped with stripping buffer and re-incubated with a pan-src antibody (Figure 6-15). Protein bands were then quantified by densitometry and graphed as shown in Figure 6-16. Virus on its own did not increase src phosphorylation compared to uninfected control cells. There was a trend towards increased src phosphorylation in samples from the healthy control volunteer during the first 20 minutes of virus infection in the presence of the inhibitor points however this difference became insignificant at later times point (Figure 6-15 A and A). There were no significant changes in the presence of the inhibitor when cells from an asthmatic volunteer were infected with RV1B (Figure 6-15 B and Figure 6-16 B).

Figure 6-15. Phosphorylation status of src protein kinase in RV-infected PBECs in the presence or absence of SU6656. Western blot analysis of the phosphorylation status of src at Tyrosine reside 416 in PBEC infected with RV1B and treated with 10 μM SU6656.

Cells from a healthy (A) and asthmatic (B) patient donor were pre-treated with 10 μM SU6656, followed by infection with RV1B (MOI=10) for a period of 10, 20, 40, 60, 90, and 120 mins in the presence or absence of SU6656. Cells were harvested with SDS-PAGE sample buffer and probed with an anti-phospho src (Y416) antibody. Membranes were then stripped and re-probed with a pan-src antibody as a loading control.

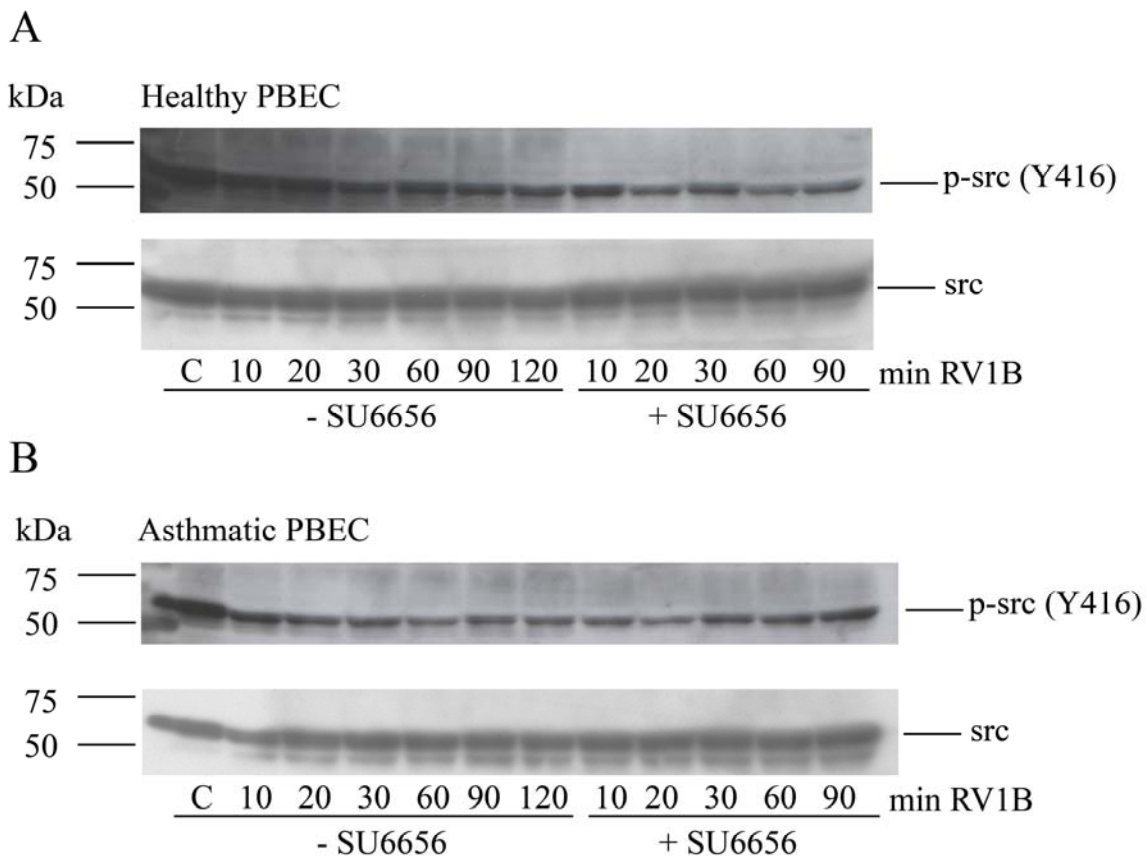

Figure 6-16. Protein bands from Figure 6-15 were quantified by densitometry using Image J analysis software.

The ratio of phosphor-src (Y416) to pan-src were calculated and plotted. This graph shows the results obtained from samples of a healthy volunteer (A) and an asthmatic patient donor (B).

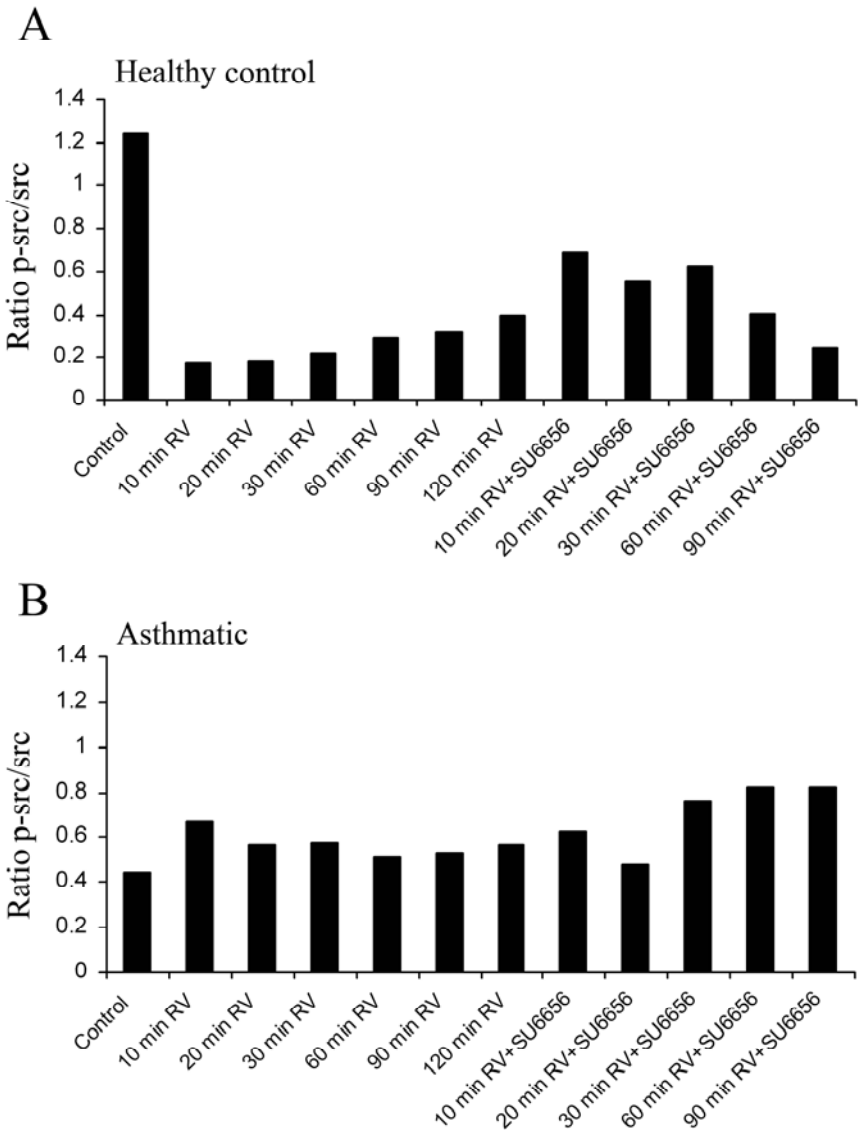

6.2 Possible mechanisms by which the src kinase inhibitor SU6656 modulates the innate immune response

Rationale:

In the previous section, a marked reduction in RV replication was observed when infected PBECs were treated with the src kinase inhibitor SU6656. Three different inhibitors to src kinase were compared, and it was shown that the PP2 compound was the least effective at inhibiting RV replication, even though it was shown to be effective against other viruses (Hirsch et al., 2005). Western blot data from the previous section showed no significant increase in src phosphorylation in RV-infected PBECs compared to un-infected cells. This is in contrast to previous data where it was shown that RV-39, a major group virus was able to induce src phosphorylation in 16HBE cells (Bentley et al., 2007). This was then shown to be inhibited by treatment with src inhibitors (Bentley et al., 2007). In order to determine whether the observed anti-viral effects of the src inhibitors on RV replication is due to a role of src in virus replication or due to off-target effects of this inhibitor, as the data suggests, it was decided to use small interfering RNAs (siRNAs) to knock-down the *src* gene and to determine whether this would have an effect on RV replication. SiRNAs are widely-used tools for selectively silencing gene transcription. It is a naturally occurring phenomenon first discovered in *Caenorhabditis elegans* and *Drosophila* (Moss, 2001). The classical pathway in *Drosophila* involves double-stranded RNA (dsRNA) being processed by R2D2/Dicer heterodomers into siRNAs (Figure 6-17) (Dykxhoorn and Lieberman, 2005). The duplexed siRNA is unwound, leaving one strand, the guide strand to be taken up by the RNA-inducing silencing complex (RISC) (Figure 6-17) (Dykxhoorn and Lieberman, 2005). The single stranded siRNA guides the endonuclease activity of the activated RISC to the homologous site on the mRNA, cleaving the mRNA (Figure 6-17) (Dykxhoorn and Lieberman, 2005).

The next question was how the SU6656 compound induces its antiviral effect. In the previous section, data were presented that showed a marked degradation of viral RNA in the presence of this inhibitor. Degradation of viral mRNA occurs via 2',5'-oligoadenylate (2-5A)/ RNase L system (Silverman, 2007). 2-5A or [p_χ5' A (2'p5' A)$_n$; x = 1 to 3; $n \geq 2$] are nucleic acid species that contain 2' to 5' phosphodiester bonds (Silverman, 2007). The trimeric and tetrameric species [(2'-5')p_3A_3 and (2'-5')p_3A_4] are the principal forms of 2-5A produced in iFN-treated, virus infected cells (Silverman, 2007). Rhinoviruses will produce a double-stranded RNA (dsRNA) as a replicative

intermediate, which activates the pathogen recognition receptor 2-5A synthetase (OAS), resulting in the production 2-5A (Silverman, 2007). This molecule then activates catalytically latent RNAseL, which cleaves within single-stranded regions of RNA (Silverman, 2007). We postulated that one of the mechanisms by which the SU6656 compound may exert its anti-viral activity is by enhancing the RNaseL activity and degrading viral mRNA. We postulated that by inducing IFN levels src kinase inhibitors may increase OAS activity and therefore the production of 2', 5'-oligoadenylates (2-5As) to activate latent RNAseL, that results in increased degradation of viral RNA. To test this hypothesis, we used siRNAs targeting the *RNaseL* gene and to determine whether this inhibitor is still able to reduce viral replication despite knocking-down RNAseL.

Figure 6-17. The classical RNA interference (RNAi) pathway in Drosophila.
This figure was obtained from Dykxhoorn D.M. and Lieberman J. *Annu. Rev. Med.* 2005. 56:401-23.

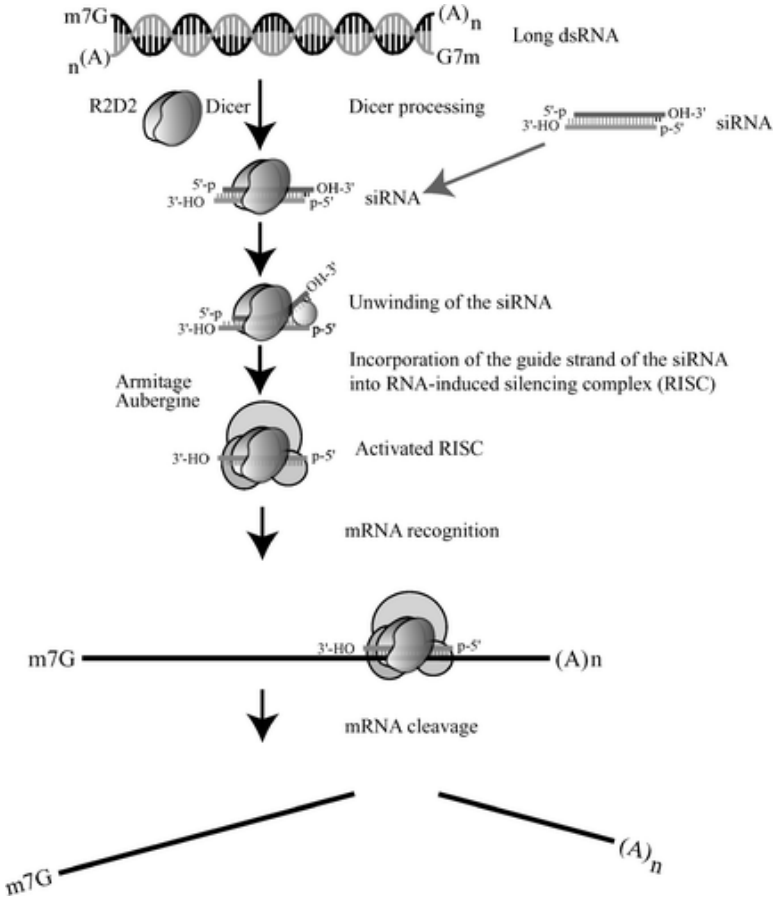

6.2.1 Optimizing transfection of src and RNaseL siRNAs into PBECs

In order to determine the optimum conditions for transfecting siRNAs into PBECs, it was decided to first use siRNA labelled with the CY3 fluorophore and targeted to Cyclophilin B as a positive silencing control, purchased from Dharmacon (siGLO Cyclophilin B Control siRNA). The transfection efficiency was tested by using the transfection reagent X-treme Gene siRNA. PBECs were seeded into 24-well plates as described in the Materials and Methods section and were incubated until they were 60-80% confluent. SiGLO Cyclophilin B was then transfected into PBEC at a final concentration of 15, 30, and 60 nM (see Materials and Methods). Untransfected cells were included as a negative control. Cells were then incubated at 37^0C, 5% CO_2 for a period of 24 and 48 hours. Hoechst nuclear stain was then added to live cells for 30 mins, before cells were analysed under a fluorescence microscope. Figure 6-18 shows merged images of the phase-control, DAPI (nuclei) channel and CY3 (siRNA) channel. Fluorescence in the CY3 channel was observed when cells were transfected with the lowest concentration of siRNA (15nM) at both 24 and 48 hours. Cells transfected with 30 nM siRNA showed no CY3 fluorescence after 24 hrs transfection. However, at 48 hrs post-transfection some cells showed some red fluorescence in the perinuclear region. The greatest number of fluorescent cells in the CY3 channel was observed, when they were transfected with the highest concentration of siRNA (60 nM) for 24 hours (Figure 6-18). Interestingly, when *cyclophilin B* gene expression was analysed in the transfected cells, the greatest knock-down of *cyclophilin B* mRNA was observed at 48 hours post-transfection with 30 nM siRNA (Figure 6-19 B). No significant changes in cyclophilin B mRNA were observed between treatment groups after 24 hours transfection with siRNA (Figure 6-19 B). Therefore, it was decided to transfect siRNAs targeted to our genes of interest for 48 hours before infection with virus, as preliminary experiments showed optimum knock-down of target genes after 48 hours transfection with siRNA.

Figure 6-18. Immunofluorescent photographs of PBEC from a healthy control volunteer. Cells were incubated with Hoechst 33342 nuclear stain and visualized with the DAPI channel (blue). Cells transfected with CY3-labelled Cyclophilin B siRNA were visualized with the CY3 channel. Photos show merged snapshots of phase-contrast, DAPI and CY3 channel at x20 magnification.

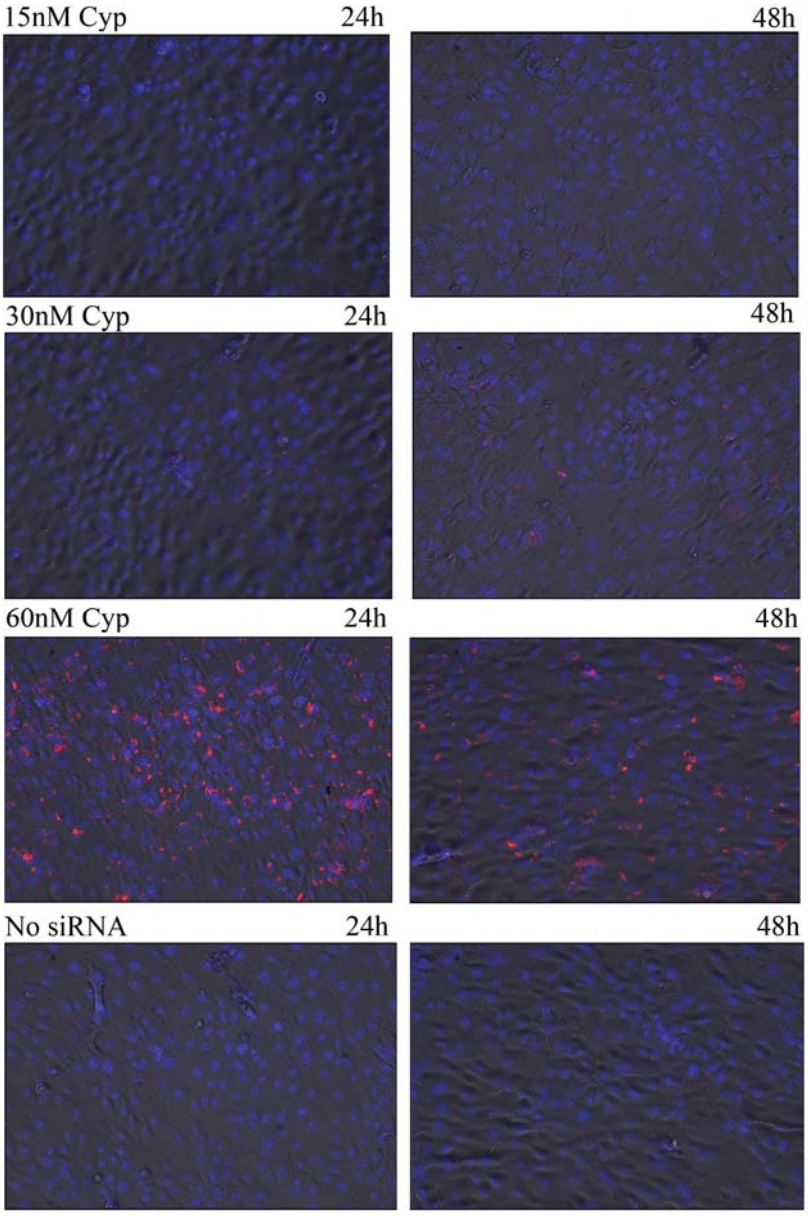

Figure 6-19. PBECs from a healthy volunteer were transfected with siRNA targeted against Cyclophilin B and incubated for 24 (A) and 48 (B) hours. Cells were harvested with Trizol reagent and total RNA was extracted as described in Materials and Methods section. Cyclophilin B mRNA was measured by RT-qPCR as previously described and normalized to housekeeping genes GAPDH/UBC. Graphs represent mean values of duplicate wells from one experiment and cells from one patient donor.

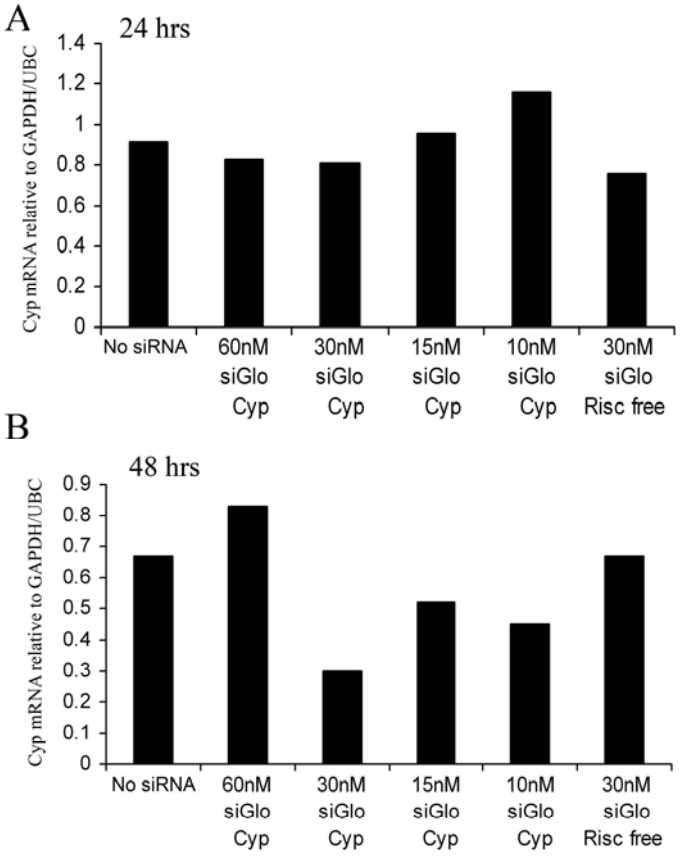

6.2.2 RV replication in PBECs transfected with siRNAs against src using X-treme gene transfection reagent

In order to determine the effects of *src* knock-down on RV replication, PBECs from 2 asthmatic patients were transfected with 100 nM src or control pool siRNA and incubated for 48 hours. Previous experiments did not show significant knockdown of *src* mRNA levels using low concentration of siRNA (data not shown). When transfected PBECs were analysed for *src* mRNA levels, an almost 50% knockdown was observed in *src* mRNA level was observed (Figure 6-20) compared to cells transfected with a scrambled control pool siRNA. Transfected cells were then infected with RV1B for 1

hour and then incubated for 8 and 24 hours as described in the Materials and Methods section.

Figure 6-20. PBEC from two asthmatic patient donors were transfected with siRNA targeted against src and incubated for 48 hours. Cells were harvested with Trizol reagent and total RNA was extracted as described in Materials and Methods section. Src and RNaseL mRNA was measured by RT-qPCR as previously described and normalized to housekeeping genes GAPDH/UBC. Graphs represent mean values of triplicate wells from two separate experiments.

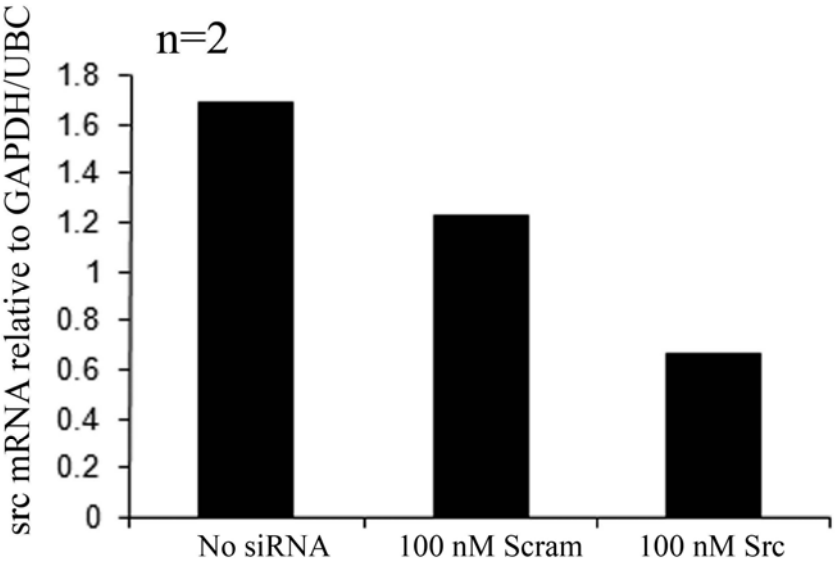

No significant differences in RV1B mRNA levels were found when cells that were transfected with src siRNA were compared to cells that were transfected with a control pool siRNA **(**Figure 6-21A). It has to be taken into account that src mRNA levels were only reduced to 50% following transfection with siRNA. So it is possible that the lack of an effect on RV replication may be due to residual src RNA and protein levels. There was a significant reduction in RV1B mRNA in all infected samples that contained the src inhibitor SU6656, regardless whether they were transfected with siRNA or not (Figure 6-21 A). The same was true when viral titres were measured by $TCID_{50}$/ml, in that the presence of SU6656 inhibited viral replication to significant levels, regardless whether they were transfected with siRNA or not (Figure 6-21 B). IFN-β mRNA levels were also measured in the same cell samples as used in the previous section after 8 hours post-infection. Since siRNA are essentially short dsRNA, there is always the possibility that this duplex molecule will elicit an IFN-β by binding

directly to its receptor TLR-3. Low levels of IFN-β induction were observed in samples transfected with siRNA alone **(**Figure 6-22 A). This may partly explain why we saw lower RV1B mRNA levels in samples that have been transfected with siRNA prior to RV1B infection, compared cells that were not transfected (Figure 6-21 A). The presence of the SU6656 compound greatly enhanced IFN-β at 8 hours post-infection compared to samples that were treated with the vehicle control DMSO (Figure 6-22 A). This observation supports previous data in Figure 6-13, where the presence of this compound augmented the type I IFN response.

Figure 6-21. PBEC from two asthmatic patient donors were transfected with siRNA targeted against src and incubated for 48 hours, followed by infection with RV1B at MOI=0.01 for 8 hours. Cells were harvested with Trizol reagent and total RNA was extracted as described in Materials and Methods section. RV1B mRNA was measured by RT-qPCR as previously described and normalized to housekeeping genes GAPDH/UBC (A). Supernatants from infected PBECs were used to re-infect HeLa cells, in a standard virus titration assay as described in the Materials and Methods section (B). Graphs represent mean values of triplicate wells from two separate experiments.

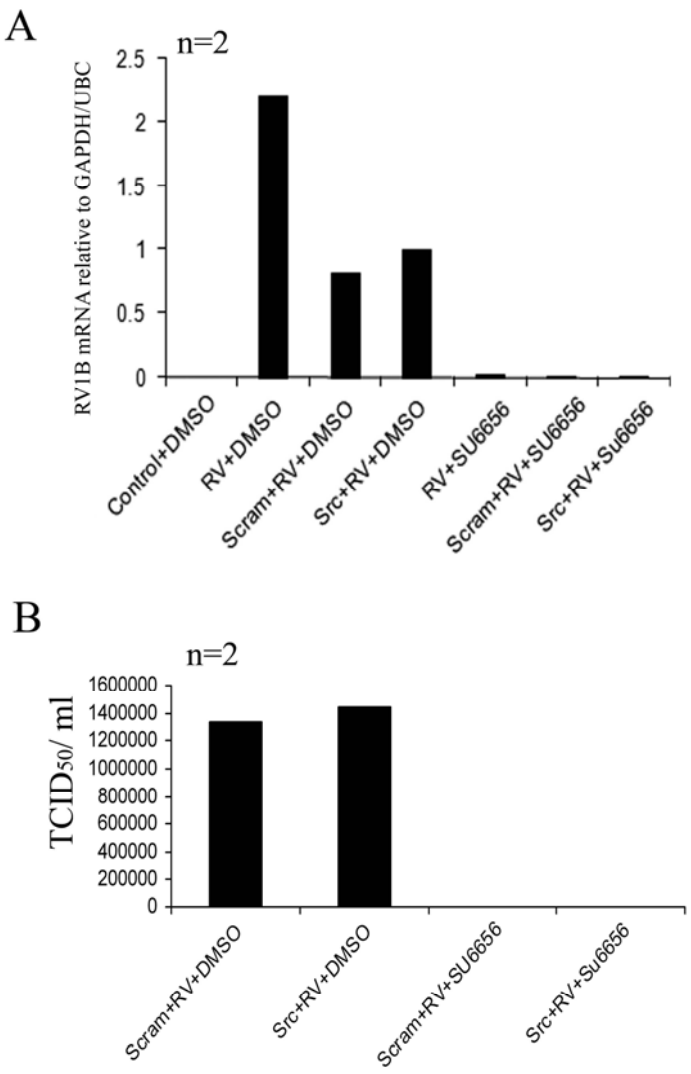

Figure 6-22. IFN-β mRNA of PBECs transfected with src siRNA in the presence or absence of RV and/or SU6656. PBEC from two asthmatic patient donors were transfected with siRNA targeted against src for 48 hours, followed by infection with RV1B at MOI=0.01 for 8 hours. Cells were harvested with Trizol reagent and total RNA was extracted as described in Materials and Methods section. IFN-β mRNA was measured by RT-qPCR as previously described and normalized to housekeeping genes GAPDH/UBC. Graphs represent mean values of triplicate wells from one experiment.

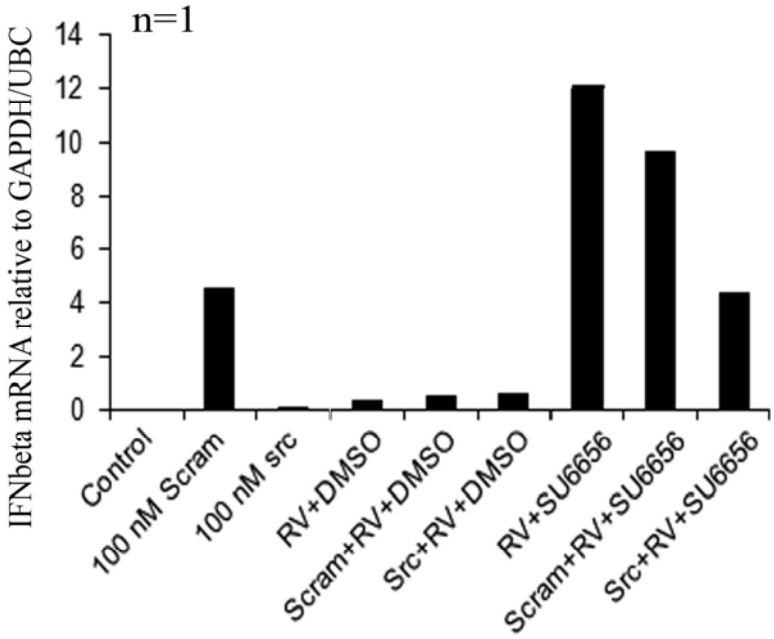

6.2.3 RV replication in PBECs transfected with siRNAs against src using Oligofectamine transfection reagent

Since results in section 6.2.2 showed only a 50% knock-down in *src* mRNA levels it was decided to test a different transfection reagent for transfection of src siRNA into PBECs. Oligofectamine reagent was used to transfect 100 nM src siRNA into PBECs from 2 asthmatic and 1 healthy subject. RNaseL siRNA was included as a control to measure the effect of siRNA transfection on src protein levels by Western blotting. However, RNAseL siRNA was not included in subsequent RV infection experiments. 50% knockdown of src protein in one subject after transfection of src siRNA was observed (Figure 6-23). However, in subsequent experiments, only 10% knockdown of src protein was observed (data not shown). Knockdown of *src* mRNA levels was perhaps more consistent in the three subjects tested. Knockdown of *src* mRNA was down to 50% after 48 and 72 hours post-transfection, and therefore not a big improvement from experiments using the X-treme Gene siRNA (Figure 6-24 A and B). This was regardless whether samples were infected with RV1B or not. No significant difference in RV1B mRNA levels was observed after transfection with src siRNA, although, as shown previously, the presence of siRNAs did not change the marked potency of SU6656 (Figure 6-25 A). There was a trend towards increased RV1B mRNA expression in the presence of src siRNA, however this was not significant (Figure 6-25 A). It was also observed that there was a similar increase in IFN-β mRNA in the presence of SU6656 regardless whether cells were transfected with src siRNA or the control pool, although no significant differences were observed between samples that were transfected with src or control pool siRNA (B). Closer analysis of IFN-β mRNA levels in SU6656-treated samples showed that there was a slight trend towards decrease in the presence of src siRNA (Figure 6-25 C). In previous studies it has been shown that src is involved in dsRNA-mediated IFN-β expression (Johnsen et al., 2006). It is possible that this is also true for RV-induced IFN-β, as IFN-β mRNA analysis of siRNA-transfected samples without the inhibitor, showed a slight decrease in the presence of src siRNA (Figure 6-25 B). However, the observation that in the SU6656-treated samples, this decrease in IFN-β in the presence of src siRNA is not substantial, points to another off-target effect of SU6656 that facilitated IFN-β production. It is also important to consider that residual src levels due to insufficient knock-down may also cause the lack of a difference between the samples.

When viral titres were analysed, it was observed that there was a decrease in titre when cells were transfected with src siRNA and infected with RV1B, compared to cells that were transfected with control pool siRNA (Figure 6-26). Although this did not reach statistical significance, this would mimic the effect of the SU6656 compound of inhibiting virus replication. Although it is unclear whether src itself is required for RV replication, intuition would suggest that cell proliferation and survival would be in the interest of the virus, as this would promote the production of progeny virus. Therefore, one would expect that a reduction in src expression, one would decrease RV replication. However, further work would be needed in order to ascertain that src protein levels were sufficiently reduced to obtain a reliable phenotype.

Figure 6-23. Src protein levels in PBECs after transfection with siRNAs targeted to src kinase protein.

Transfected PBECs lysates were analysed by SDS-PAGE and immunoblotted using anti-src antibodies and anti-actin antibodies (A). Protein bands were subsequently quantified by densitometry using Image J software and the ratio of src protein to actin protein were obtained (B).

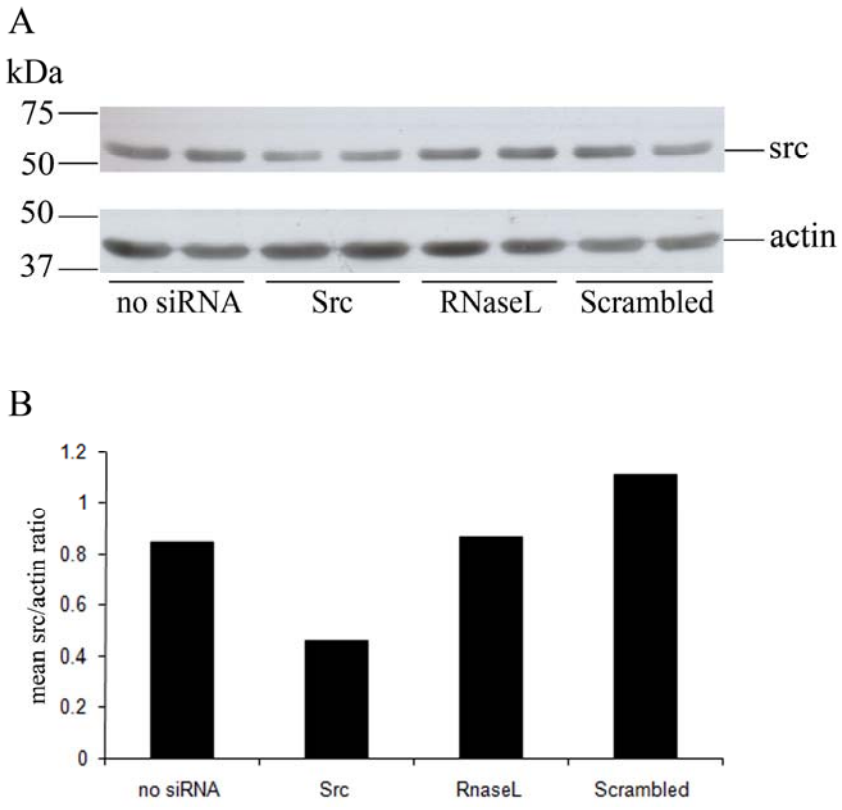

Figure 6-24. Src mRNA levels from 3 subjects after transfection with src siRNA and RV1B infection.

PBECs from 2 asthmatic and 1 healthy subjects were transfected with src siRNA and incubated for 48 hours. Cells were then infected with RV1B (MOI=0.01) and incubated for 8 (A) and 24 hours (B). *Src* mRNA was measured by RT-qPCR and analysed relative to house-keeping genes GAPDH and UBC by the delta-delta Ct method. Graphs show mean value and Standard errors.

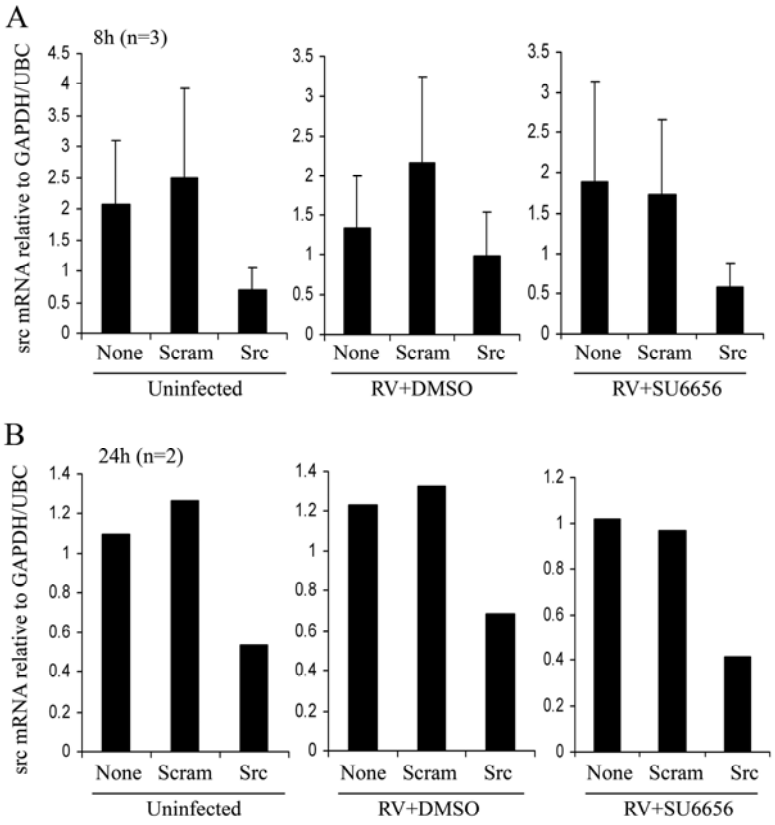

Figure 6-25. RV1B and IFN-β mRNA levels from 3 subjects after transfection with src siRNA and RV1B infection.

PBECs from 2 asthmatic and 1 healthy subjects were transfected with src siRNA and infected with RV1B as described in Figure 6-21. *RV1B* mRNA (A) and IFN-β mRNA (B) were measured by RT-qPCR and analysed relative to house-keeping genes GAPDH and UBC by the delta-delta Ct method. Graphs show mean value and Standard errors. The data obtained for src siRNA-transfected samples infected with RV1B in the presence or absence of SU6656 were plotted on a different scaled graph to observe potential difference in more detail (C).

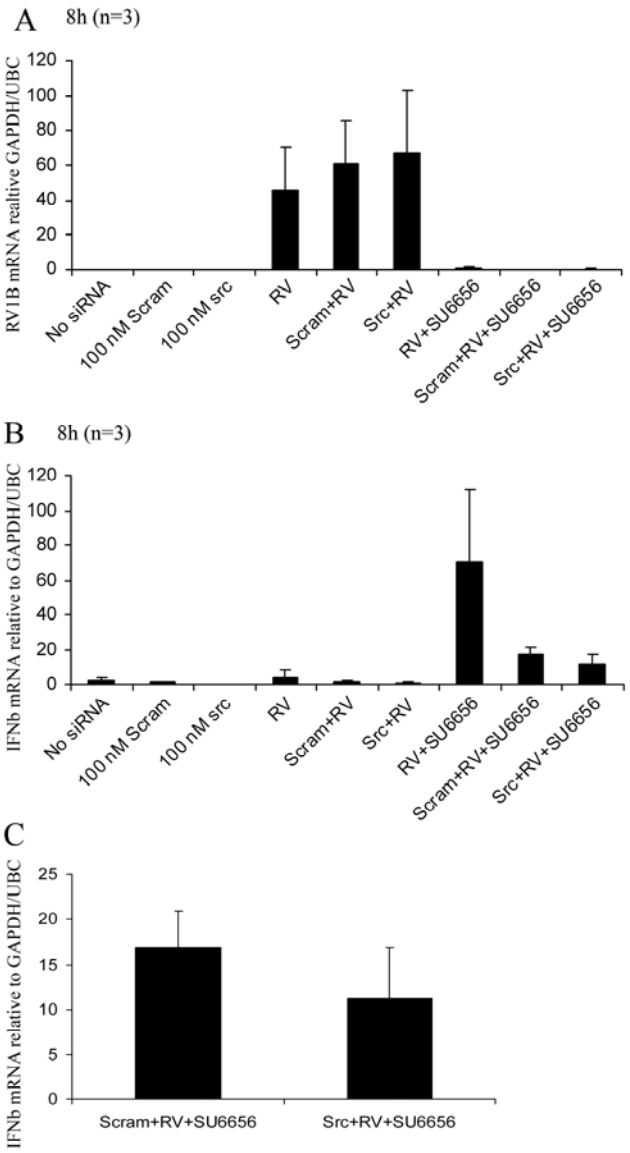

Figure 6-26. Viral titres from PBECs transfected with src siRNA and infected with RV1B.

PBECs from 4 subjects were transfected with src siRNA for 48 hours followed by infection with RV1B and incubated for 24 hours. Viral supernatants were measured using $TCID_{50}$/ml assay. Graphs show mean values and Standard errors.

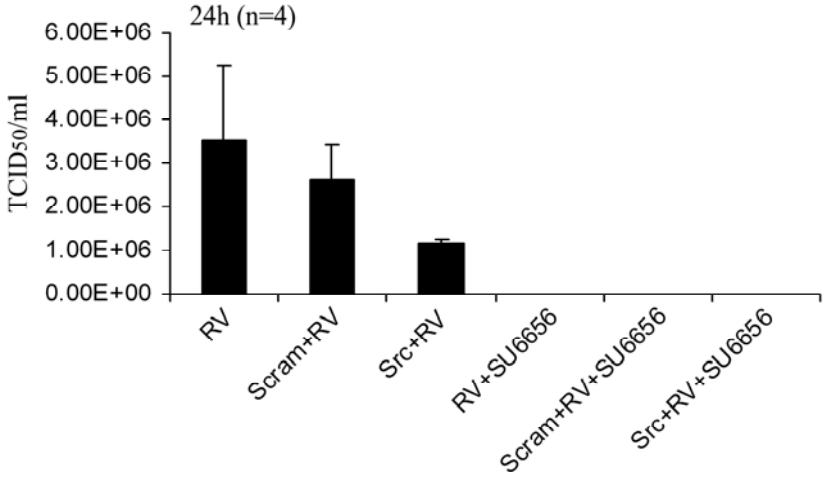

6.2.4 RV replication in PBECs transfected with siRNAs against RNAseL using X-treme gene transfection reagent

Although it is likely that the SU6656-mediated increase in IFN and therefore increased OAS/RNaseL activity may not be the only explanation to the potent antiviral effects of SU6656, especially as this potency is also observed after the addition of inhibitor 6 hours p.i., it was decided to investigate further the observed degradation of viral RNA. Since the data presented in section 6.1.3 showed evidence of RV1B mRNA degradation in the presence of SU6656, it was decide to investigate whether this degradation was mediated through increased activity of RNAseL in the presence of this inhibitor. PBECs from 2 asthmatic patients were transfected with 100 nM RNaseL or control pool siRNA as described in the previous section and incubated for 48 hours. Cells transfected with src siRNA were also analysed for *RNaseL* levels as an additional control. Cells transfected with RNAseL siRNA showed an approximate 60% knockdown in *RNAseL* mRNA levels compared to cells transfected with the scrambled control siRNA and src siRNA (Figure 6-27). When viral RNA was measured, it was found that cells that were transfected with RNAseL siRNA had slightly higher levels of RV1B mRNA (Figure 6-28 A). RNaseL siRNA-transfected cells also produced a much

higher virus titre compared to cells that were transfected with control pool siRNA (Figure 6-28 B). These results are what was expected, as knocking down this enzyme which is part of the antiviral defense mechanism one would expect a greater chance of virus replication. It was initially postulated that SU6656 exerts its antiviral activity by enhancing RNaseL activity, however even with reduced levels of *RNaseL* mRNA, the potency of this inhibitor did not change (Figure 6-28).

Figure 6-27. *RNaseL* mRNA levels from 2 subjects after transfection with src siRNA and RV1B infection.

PBECs from 2 asthmatic subjects were transfected with RNaseL siRNA and incubated for 48 hours. Cells were then infected with RV1B (MOI=0.01) and incubated for 8 (A) and 24 hours (B). *RNaseL* mRNA was measured by RT-qPCR and analysed relative to house-keeping genes GAPDH and UBC by the delta-delta Ct method. Graphs show mean value and Standard errors.

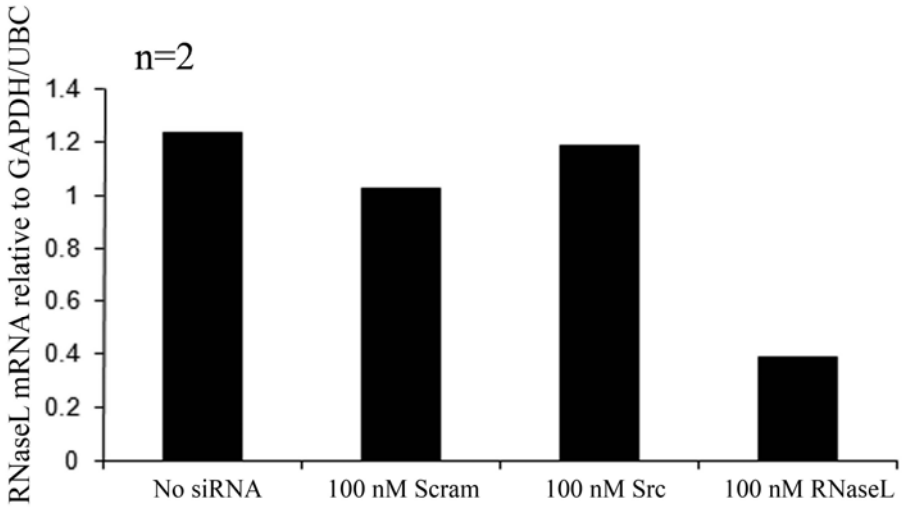

Figure 6-28. PBEC from two asthmatic patient donors were transfected with siRNA targeted against RNaseL and incubated for 48 hours, followed by infection with RV1B at MOI=0.01 for 8 hours. Cells were harvested with Trizol reagent and total RNA was extracted as described in Materials and Methods section. RV1B mRNA was measured by RT-qPCR as previously described and normalized to housekeeping genes GAPDH/UBC (A). Supernatants from infected PBECs were used to re-infect HeLa cells, in a standard virus titration assay as described in the Materials and Methods section (B). Graphs represent mean values of triplicate wells from two separate experiments.

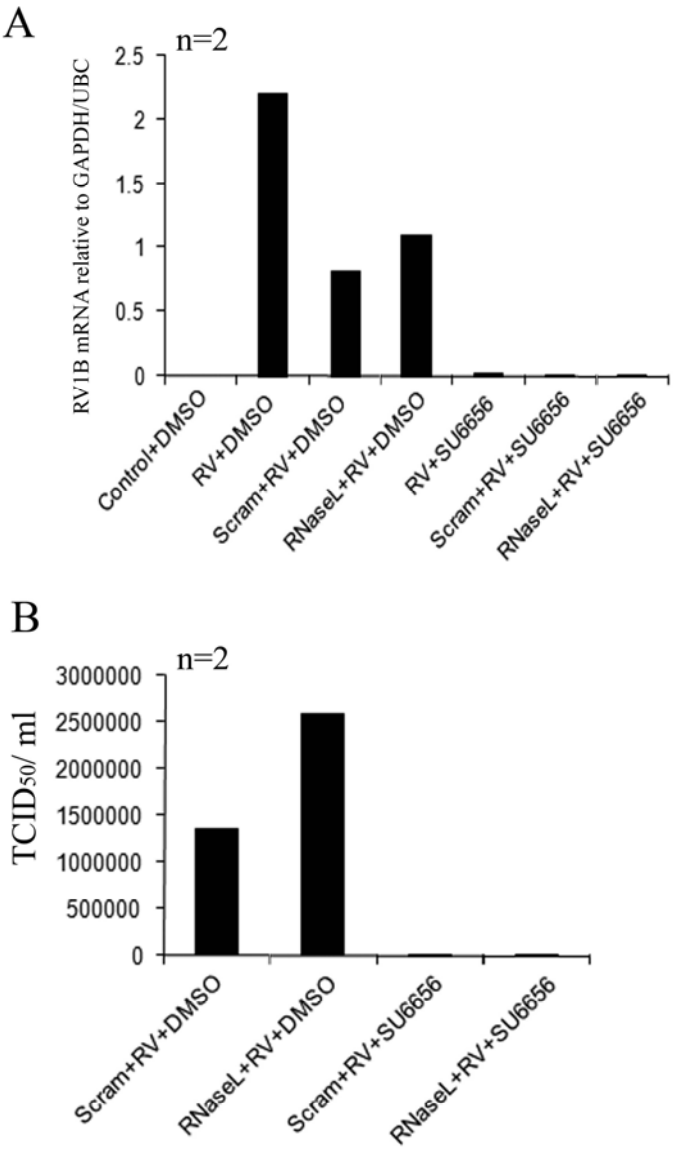

Discussion

Previous groups have shown a specific requirement for src in viral replication and assembly of enveloped viruses. However, no induction of src phosphorylation was observed in the presence of rhinovirus, suggesting that src on its own may not be as important in the rhinovirus life cycle. The data presented in this section demonstrate potent inhibition of RV replication in the presence of src inhibitors, suggesting that these compounds may act on multiple targets. Of the panel of src inhibitors that were tested, the SU6656 compound was the most effective at reducing viral mRNA levels and infectious virus particles released from bronchial epithelial cells. This inhibition was as potent even when the inhibitor was added after one round of infection, as late as 6 hrs post-infection. Reduced levels of viral mRNA in the presence of the inhibitor points to RNA degradation by possible increased RNAse L activity.

The mechanism by which src inhibitors act on the replication of unenveloped viruses may be different to that of enveloped viruses as experiments with dengue and West-Nile virus have shown a block at the post-translation level such virus assembly and maturation (Chu and Yang, 2007; Hirsch et al., 2005). A significant induction in IFN-β mRNA levels by the SU6656 compound was also observed in the presence of virus during the early phase of infection. These increases were maintained by the presence of a danger signal in the form of ds RNA (Figure 6-14). It was found previously that the c-src is required for ds RNA-mediated IFN-β activation in dendritic cells (Johnsen et al., 2006), however we do not know whether this is a cell type-specific event. Another question is whether localization of c-src is important for its role in specific signal transduction events. Although Johnsen *et al* have shown co-localization of src with TLR-3 in endosomes of dendritic cells (Johnsen et al., 2006), Bentley *et al* suggest that src functions upstream of Akt and is localized in lipid rafts, where it is required for the induction of IL-8 (Bentley et al., 2007).

Since similar inductions of IFN-β in the presence of other src kinase inhibitors tested were not observed, it is possibly this property is specific to SU6656 and that the inhibitory mechanisms of the other compounds are slightly different. It would be interesting to investigate whether endogenous cellular src has specific roles in viral replication as shown in HBV (Bouchard et al., 2006) or mRNA stability (Bromann et al., 2005).

Additionally, the aim was to test the hypothesis that src kinases have a role in

RV replication based on previous observation that src kinase inhibitor SU6656 causes viral RNA degradation and reduced virus titre to significant levels. If src kinase was important in RV replication, it would be expected that similar reduction in RV replication would take place in cells transfected with siRNA targeted to the *src* gene. One of the problems was that we were only able to knockdown *src* mRNA levels to about 50% of control. It may be that residual *src* RNA transcripts were sufficient enough to compensate for any effects of the knock-down. Another question is whether the protein has a sufficiently low turn-over in order to negate any effects of mRNA degradation. Significant protein knockdown was only observed in one out of three experiments by Western blotting. It is possible that one would need to optimize the ratio of transfection reagent to siRNA, however due to time constraints this was not done. Additionally, it might be necessary to test other transfection reagents such as Lipofectamine.

By abolishing src kinase expression, one would have expect a higher degree of cell death, as one of its major roles is in cell proliferation (Thomas and Brugge, 1997). However, no major differences were seen between cells that were transfected with the src siRNA and cells that were transfected with control siRNA based on cell phenotype and the amount of cell death (data not shown).

No significant effects on RV replication was observed after knocking down RNaseL mRNA, although the problems may be similar as to the ones cited above, where the amount knocked-down was not sufficient to affect RV replication. Slightly higher levels of RV virus titre was observed in cells that were transfected with RNaseL siRNA. It may be that an increase in the number of experiments and subjects, this difference will reach more significant levels. Regardless of the amount of RNaseL and src mRNA knocked down in these experiments, a significant inhibition of RV replication in the presence of SU6656 was still observed. Although it was originally postulated that this compound affects RNaseL activity, it is likely that the src inhibitor is exerting its activity through multiple pathways, which account for its potency.

7 Chapter 6

7.1 Final Discussion and Future Work

Human rhinoviruses (HRV) are infectious agents that normally do not cause more than a common cold in healthy individuals. However, in people with asthma, an infection with this respiratory virus can often lead them into suffering an exacerbation and death. Recent advances in the scientific field meant that we are now a few steps closer to understanding the nature of rhinovirus-induced asthma exacerbation and how the immune response plays a key role in this observed phenomenon. Clinical studies have now shown that bronchial biopsies obtained from subjects with asthma were more likely to stain positive for HRV than healthy controls (Wos et al., 2008). In children the presence of rhinovirus in nasopharyngeal and throat swabs was positively correlated with asthma exacerbations (Khetsuriani et al., 2007). Even when bronchial epithelial cells from asthmatics were isolated and cultured *in vitro* they maintained their permissiveness to RV infection, and allow more efficient replication compared to normal cells (Wark et al., 2005a). It has now been found that measuring the inflammatory mediator IFN-gamma induced protein 10 (IP-10) in serum, can be used as a marker for virus-induced asthma (Wark et al., 2007a).

It has been shown previously that ICAM-1, the cellular receptor utilized by major group rhinoviruses to bind to its host and trigger intracellular uptake is elevated in asthma (Manolitsas et al., 1994). Therefore, one would have expected that this may increase the susceptibility of asthmatics infection at least for major group rhinoviruses. However, in a subsequent clinical study, where RV infection was monitored and compared between asthmatic and healthy control subjects who were in a co-habiting relationship, no difference was found in the frequency of infection (Corne et al., 2002). It was found, however that people with asthma were more likely to suffer from lower respiratory tract (LRT) infection and have more sever and longer-lasting LRT symptoms (Corne et al., 2002). It seems, therefore, that the difference between the two subject groups lies in the inability to clear the infection rather than the likelihood of infection. In two further studies that followed, it was shown PBEC isolated from asthmatic subjects had an innate inability to mount a sufficient interferon response against rhinoviruses and combat the infection (Contoli et al., 2006b; Wark et al., 2005a).

The next obvious question would be why do asthmatics have a defective interferon response? Is it a genetic or epigenetic trait that develops from early childhood? What are the underlying mechanisms? It has been shown in a study in

Wisconsin, that children who were sensitized with aeroallergens by age 3, were more likely to develop rhinovirus wheezing illness, compared to those who were not sensitized (Jackson et al., 2008). Infection with rhinovirus accompanied by wheeziness in early childhood has been linked to a greater risk of developing asthma in adulthood (Martinez, 2009). It has also been shown that children who later developed chronic wheezing had low IFN-γ responses by peripheral blood mononuclear cells in the first years of their life (Stern et al., 2007). Though it is difficult to pinpoint causality, as Martinez notes in his review, it is possible that "a genetically mediated impairment to rhinovirus infection may increase the susceptibility to airway obstruction and that this susceptibility may be due to an altered inflammatory response to viral infections" (Martinez, 2009).

In this project, this question of genetic predisposition was addressed by looking at the responses of other cells in the airway, which, if true, would respond in a similar way to bronchial epithelial cells, i.e. an impaired immune response to rhinovirus infection. When an infection model was established with primary bronchial fibroblasts, it was found that these cells were very sensitive to RV infection. This was accompanied by a lack of an interferon response, even at early time points when cell death was not yet as significant. Since this observation would not allow a comparison between disease-related differences in rhinovirus-induced interferon production, it was decided to use a synthetic analog of double-stranded RNA (dsRNA) polyI:C. It was found that although bronchial fibroblasts were able to produce IFN in response to dsRNA, there were no asthma-related differences in their response. In contrast, treatment of PBECs with polyI:C, have shown that the cells obtained from asthmatic subjects produce significantly less IFN-β, which supports the original study by Wark et al using rhinovirus infection experiments (Uller *et al* unpublished data, (Wark et al., 2005a). It is difficult to determine whether the lack of disease-specific differences in the response of bronchial fibroblasts is due to a lack of a genetic defect, since polyI:C treatment cannot be used as a substitute for virus infection in *in vitro* experiments. DsRNA can be recognized by different intracellular sensors such as Protein kinase R (PKR), Mda-5, Rig-I and TLR-3 (Edwards et al., 2007). PKR is a serine/threoning protein kinase and although its role in IFN signalling is controversial, it has been shown that fibroblasts from PKR knock-out mice were unable to produce type I IFN (Edwards et al., 2007). Rig-I and Mda-5 have been implicated as sensors for viral ds RNA, although it is suggested that during infection with picornaviruses, Mda-5 seems to be more important (Kato et al., 2006). In fibroblasts and epithelial cells, TLR3 signalling usually occurs

intracellularly via the endosome, although it has been shown that anti-human TLR3 antibodies can inhibit polyI:C-induced IFN-β production in fibroblasts, indicating that TLR3 on the cell surface may play some role in the recognition process (Itoh et al., 2008; Matsumoto et al., 2002a). One can, therefore, not be certain how much of the polyI:C enters the endosome in these experiments, and how much binds to the cell surface of fibroblasts. If the polyI:C predominantly signals via the cell surface TLR3, the question is how relevant this is to virus infection, where one would expect signalling to occur intracellularly. However, if in fibroblasts TLR3 is predominantly located on the cell surface, this would explain why no significant IFN-β induction was seen when the cells were infected with virus. Any dsRNA produced as a replicative intermediate from virus infection of epithelial cells would have to be released from infected cells in order to be able to bind to TLR3 on the cell surface of underlying fibroblasts. These experiments with bronchial fibroblasts produced some interesting data, which led to some important conclusions about the possible role of these cells in the airway of asthmatics during rhinovirus infection. However, because of their differences to epithelial cells in their cellular architecture, epithelial cells were chosen to be utilized in subsequent experiments.

In order to understand why asthmatics do not mount an efficient innate immune response to rhinovirus infection, the contribution of other cytokines that are known to play a role in the diseased state of asthma were analysed. One such cytokine is TGF-β, which is known to be particularly elevated in asthma and it has been accepted as a major contributing factor to airway remodelling in chronic asthma (Batra et al., 2004; Boxall et al., 2006; Redington et al., 1997). Interestingly, genetic polymorphism in the TGF-β gene has also been shown to be linked to asthma severity (Pulleyn et al., 2001). Due to its complex and pleiotropic nature, it is not surprising that it can have a variety (and often opposing) of functions (Sanchez-Capelo, 2005; Wahl, 2007). However, in recent studies it was found that TGF-β can promote the replication of respiratory viruses and contribute to the dampening of the innate immune response (McCann and Imani, 2007; Thomas et al., 2009). Similar results were obtained when RV-infected PBEC were treated with TGF-β, in that it promoted viral replication. The opposite effect was achieved when asthmatic PBECs were treated with neutralizing antibodies against this cytokine. However, in the quest to understand the mechanisms behind these observations, several hypotheses were tested, one of them being that this cytokine modulates the survival of infected cells causing them to become “incubators” for viral replication. The most convincing evidence, however, was that the presence of TGF-β

modulates the innate immune response by dampening both type I and type III interferon responses to RV infection. Since previous data imply that the asthmatic airway contains elevated TGF-β, this would create an environment favourable to virus replication, possibly leading to exacerbation. It is still somewhat unclear what the molecular mechanisms are behind TGF-β-dependent modulation of the innate immune response. The answer to this question was pursued by using chemical inhibitors to several components of the TGF-β signalling pathway. Both the Smad3 and the p38 MAPK inhibitors inhibited viral replication in asthmatic PBECs. However, it was observed that Smad3 plays a more important role, since the Smad3 inhibitor was able to increase both IFN-β and IL-29 in polyI:C-treated PBECs, thereby reversing the TGF-β effect. One of the suggestions in the literature is that Smad3 is involved in a TGF-β mediated regulation of the protein inhibitor of activated STAT-1 (PIAS-1) (Reardon and McKay, 2007). PIAS-1 is a negative regulator of the innate immune response by binding directly to NF-κB and STAT-1, leading to the inhibition of their transcriptional activity (Liu et al., 1998; Liu et al., 2004; Liu and Shuai, 2008). This raises the question whether the presence of TGF-β in our PBEC cultures enhances the interaction of PIAS-1 and STAT-1, thereby negatively regulating the amplification of the interferon response. This would fit with the observation that the effect of this cytokine on RV replication occurs at later timepoints (48 hours), suggesting that the observed effect of this cytokine on the interferon response is cumulative, rather than immediate. This raises the question whether the presence of TGF-β enhances the interaction of STAT-1 and PIAS-1, and whether this interaction can be abrogated by neutralizing antibodies to TGF-β or treatment with the SIS-3 and p38 MAPK inhibitors. Results from experiments that were conducted suggest that TGF-β does not greatly affect PIAS-1/STAT-1 interaction after PBECs were stimulated with polyIC for 8 hours. However, it is possible that it is necessary to stimulate for a longer time period in order to mount a negative feedback. Therefore, further experiments would include stimulation with polyIC for 24 or 48 hours in the presence of neutralizing antibodies to TGF-β. It is also possible that TGF-β regulates other components that negatively regulate IFN induction such as suppressors of cytokine signalling (SOCS). A previous study showed that TGF-β induces SOCS-3 expression in macrophage precursors (Fox et al., 2003). SOCs are a secondary response family of genes that interrupt signal transmission and maintain immune homeostasis (Bonjardim et al., 2009). These proteins interact with the cytoplasmic moieties of both TLR-3 and cytokines receptors (Bonjardim et al., 2009). For example, SOCS1 interacts with the TLR-2 and TLR-4 adapter molecule Mal (Myd88-adapter like)/ TIRAP. This

interaction is followed by Mal polyubiquitination and subsequent degradation, and thus suppressing the innate immune response (Bonjardim et al., 2009). It should also be noted that the previous studies by Reardon et al. used IFN-γ rather than IFN-β in their STAT-1/PIAS-1 pulldown experiments (Reardon and McKay 2007).

In order to understand the mechanism of TGF-β induced augmentation of RV replication, the possibility of the involvement of src kinases was explored. Src kinases have been previously shown to be involved in TGF-β mediated activation of focal adhesion kinases (FAK), which are thought to have a functional role in TGF-β epithelial-to-mesenchymal transition (Cicchini et al., 2008). Several chemical inhibitors (PP2, src kinase inhibitor I, and SU6656) against src kinase were used and were found to be different in terms of their potencies they inhibited RV replication regardless of the addition of exogenous TGF-β. This suggested the possible involvement of src kinases in virus replication. However, when short interfering RNAs (siRNAs) were used to knock-down *src* gene expression in PBECs, it was found that it did not greatly affect RV replication. One of the problems that was encountered was that the extent of *src* knockdown of mRNA and protein was 50% at the most, which may not be sufficient to achieve a different cellular phenotype. A great variability in siRNA potencies was also observed between cell samples obtained from different patients. Since results from only three subjects were obtained, it might be worth increasing the subject number and perhaps test more potent siRNAs, in order to arrive at a more satisfying conclusion.

The three src kinase inhibitors used in these experiments varied greatly in their potencies, with PP2 being the least potent and SU6656 being the most potent. It was therefore postulated that the latter was acting via several mechanisms, which was the reason for its effectiveness as an inhibitor. When the IFN-β levels in virus-infected PBECs that were treated with SU6656 were analysed, it was found that it was significantly induced in the presence of the inhibitor. This was also true when cells were treated with the synthetic dsRNA polyI:C. However, it is likely that that its antiviral activities is due entirely to its ability to induce interferon, since pilot experiments where cells were treated with both the inhibitor and neutralizing antibodies to IFN-β, a marked protection by SU6656 was still observed (data not shown). It may be that in addition to IFN-β it is necessary to neutralize the type III interferons in order reverse the inhibitory effect of SU6656, which may be done in future experiments.

It is difficult to determine whether the antiviral property of SU6656 is due to its direct effect on RNaseL activity, as seen in the increased viral RNA degradation, or whether RNAseL activity is indirectly induced by increased IFN levels. In either case, it

was postulated that the compound's antiviral activity is dependent on RNaseL. It was hypothesised that knocking down *RNAseL* with siRNAs would affect the antiviral activity of SU6656. However, similar problems as mentioned above were encountered, in that the potency of the siRNA targeted against RNaseL was not very good. Another question is how stable this enzyme is as a protein, and whether knocking it down at mRNA level would greatly affect its protein level. One would likely have to consider incubating cells with siRNA for longer than 48 hours.

Though the inhibitory property of the src kinase inhibitor SU6656 still needs to be fully understood from a mechanistic level, the discovery of this compound as a potent inhibitor of rhinovirus replication still has important implications from a therapeutic perspective. It should be noted that the doses used in these experiments greatly exceeded the inhibitory concentrations 50 (IC_{50}) calculated in *in vitro* experiments (Bain et al., 2007). It is therefore possibly that at these high concentrations, this inhibitor would have off-target effects and therefore account for its remarkable potencies. Nevertheless, current work is currently being conducted involving the design of compounds that are similar in structure to SU6656 with the intention of modulating type I and type III interferon responses. This type of approach would possibly eliminate confounding factors, such as issues of dose, stability and half-life when giving IFN-β directly to asthmatic patients. Assuming that this src kinase inhibitor or similar compounds can be given to asthmatic patients with no fear of adverse effects, the expectation is that triggering the body's own defence against respiratory viral infection might provide a more effective means of preventing asthma exacerbations.

Several studies with animal models have been conducted to elucidate the mechanisms of virus-induced exacerbation in asthma. One such model showed that in RSV infection in mice, airway inflammation and the development of airway hyperresponsiveness are dependent on the presence of Th2 cytokines (IL-5 and IL-13) and not IFN-γ, a Th1 cytokine induced by virus infection (Schwarze et al., 1999; Tauro et al., 2008; Tekkanat et al., 2001). In this review, Tauro *et al.* suggests that virus-induced reactive airway disease may be driven by Type 2 cytokine producing $CD8^+$ T cells (Tauro et al., 2008). Additionally, it was shown in another study that infection with respiratory viruses results in the expansion of mature lung dendritic cells resulting in a strong immunogenicity of an otherwise non-immunogenic antigen (Brimnes et al., 2003). As the author of the review notes, these studies together suggest that prolonged

infection with respiratory viruses increases antigen presentation in the airways resulting in T-cell to responses not only to the virus but also to unrelated antigens including allergens (Tauro et al., 2008). In order to understand the interaction of allergen sensitization and viral infection, studies have been conducted in animals sensitized to different allergens and then infected with respiratory viruses, a model that mimics viral exacerbation of asthma in sensitized individuals (Tauro et al., 2008). One such study was conducted in guinea pigs, where the animals were sensitized with ovalbumin (OVA) and challenged with RSV. Those that underwent both treatments had more severe symptoms of AHR and inflammation (Robinson et al., 1997) (Figure 7-1). Although this interaction of allergen sensitization and viral-induced respiratory symptoms is present, it is difficult to define the causal relationship between both factors. Is early exposure to allergen during childhood a contributing factor to increased susceptibility to respiratory virus infection or vice versa?

Figure 7-1. Immunological effects of viral infection in atopic lung. Figure was obtained from a review written by Tauro et al 2008 Microbes and Infection (Tauro et al., 2008).

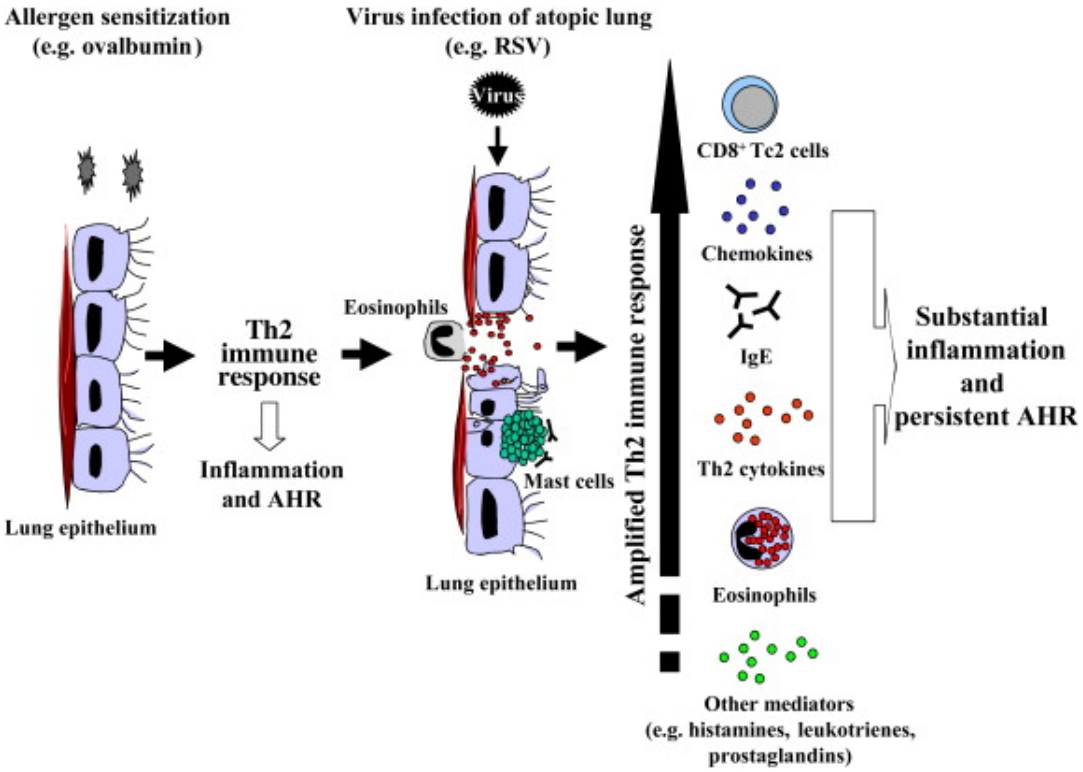

It is recognized that there are probably numerous factors contributing to later development of virus induced asthma exacerbation in adults. It is important to consider this problem in context in order to understand the various mechanisms involved. A

current model of asthma pathogenesis is that structural cells in the airways that make up the epithelial mesenchymal trophic unit (EMTU) play a central role in the "chronic wound repair" that is characteristic of asthma (Holgate, 2008) The epithelial cell layer contains tight junction proteins, which make up a highly regulated and impermeable barrier (Holgate, 2008). However, some allergens are known to exert proteolytic activity and can degrade tight junctions of the epithelium (Wan et al., 1999). In one of the studies conducted in our lab, immunofluorescence staining of bronchial biopsies obtained from an asthmatic subject showed increased disruption of tight junction proteins compared to samples obtained from a healthy control subject (Xiao *et al*. unpublished data). Further studies in our group have also shown that infection of epithelial cells also disrupt tight junction (Xatzipsalti *et al* unpublished data). The results in chapter 3 suggest that bronchial fibroblasts may contribute to increased inflammation following virus infection. I*n vivo*, these cells may be susceptible to virus infection due to a defective epithelial barrier. The loss of epithelial barrier integrity may allow infection to penetrate into the submucosa causing the release of inflammatory mediators and recruitment of inflammatory cells. This still begs the fundamental question of why epithelial cells are unable to mount a sufficient interferon response against rhinovirus infection. The results presented in this thesis provide one of many possible explanations, in that it is possible that it is a deficiency in amplification of the interferon response which may contribute to virus-induced exacerbation. Early studies have shown an association of TGF-β_1 polymorphism with asthma (Pulleyn et al., 2001). However, more recent genetic studies have also associated TGF-β_2 polymorphism to childhood asthma (Hatsushika et al., 2007). Previous data show that cell samples from asthmatics show elevated TGF-β_2 levels. Indeed the data presented here show that TGF-β_2 increases rhinovirus replication and decreases the innate immune response. Although, no significant levels of TGF-β_1 protein levels were detected in PBEC cultures, similar experiments may need to be conducted using exogenous TGF-β_1 to determine whether the TGF-β-mediated increase in RV replication is isotype-dependent. *In vivo* aberrant production of both TGF-β isotypes by different cell types in the airways may lead to an even greater chance of RV-induced exacerbation in asthmatics. Similar data was published recently in primary bronchial fibroblasts (Thomas et al., 2009), however the authors suggest that TGF-β act on initial interferon signalling, as the TGF-β_2-induced reduction in interferon production was overcome by the addition of exogenous interferon (Thomas et al., 2009). Interestingly, however, they only show a significant increase in virus titre following TGF-β_2 treatment, after 72 hours post-infection

(Thomas et al., 2009), which mirrors our observation that TGF-β mediated increase in virus replication occurs at later time points.

Figure 7-2 shows a summary of the different aspects of this project which centers around understanding the mechanisms contributing to the deficient innate immune response to RV infection in asthmatics. During the attempt to address the question of genetic predisposition and establishing an infection model in bronchial fibroblasts, an inability of these cells to mount an IFN response against RV infection but a strong capability for a proinflammatory response was observed. In the context of the EMTU, it makes sense that the cellular architecture of bronchial fibroblasts would not allow them to respond to RV infection directly. As they lie underneath an epithelial cell layer, infection of epithelial cells would induce enough interferon protein to protect the underlying mesenchymal layer in a normal environment. However, in an asthmatic environment a disrupted epithelial cell barrier and defective interferon response might allow penetration into the mesenchymal layer where infection of bronchial fibroblasts would cause a substantial proinflammatory response which may contribute to asthma exacerbations.

Figure 7-2. A summary of the different studies pursued during this project.

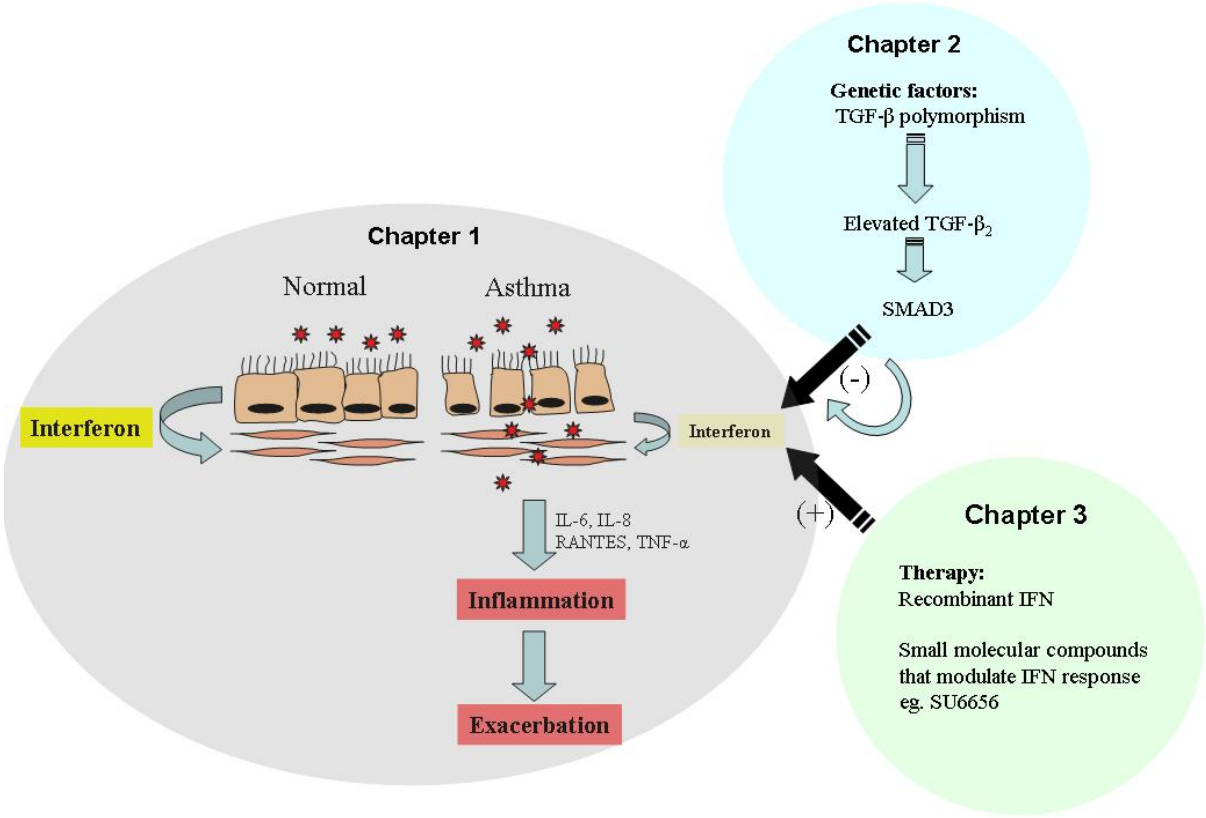

Since the observation that bronchial fibroblasts do not produce detectable levels of interferon in response to RV infection making them not an ideal cell model to study RV replication, it was decided to continue using primary bronchial epithelial cells (PBECs) as done by previous research groups. Since TGF-β is an anti-inflammatory cytokine and has been shown to be elevated in asthmatic tissue, it was decided to investigate whether this cytokine might be an important player in RV-induced asthma exacerbation. Significant increases in RV replication in the presence of this cytokine in PBECs from healthy volunteers was observed, which was coupled with a decreased innate immune response. In Figure 7-2, I postulated that the TGF-β mediated effect on the IFN response might be mediated through Smad-3, a signalling molecule of the TGF-β pathway, and that this molecule might mediate the interaction of the Protein Inhibitor of Activated STAT-1 (PIAS-1) and STAT-1, to decrease the amplification of the IFN response.

In this project, I also discovered that the src kinase inhibitor SU6656 is a potent inhibitor of RV replication and that this inhibition was accompanied by a substantial IFN response. SU6656 or SU6656-like compounds might therefore be a good candidates for and alternative therapy against RV-induced asthma exacerbation. Current work is being conducted to design chemical compounds that are similar in structure as SU6656 and possess similar anti-viral and IFN-inducing activity.

Reference List

Alvarez RH, Kantarjian HM, Cortes JE, 2006. The role of Src in solid and hematologic malignancies: development of new-generation Src inhibitors. Cancer 107: 1918-1929.

Andrejeva J, Childs KS, Young DF, Carlos TS, Stock N, Goodbourn S, Randall RE, 2004. The V proteins of paramyxoviruses bind the IFN-inducible RNA helicase, mda-5, and inhibit its activation of the IFN-beta promoter. Proc. Natl. Acad. Sci. U. S. A 101: 17264-17269.

Ank N, West H, Bartholdy C, Eriksson K, Thomsen AR, Paludan SR, 2006. Lambda interferon (IFN-lambda), a type III IFN, is induced by viruses and IFNs and displays potent antiviral activity against select virus infections in vivo. J Virol. 80: 4501-4509.

Annes JP, Munger JS, Rifkin DB, 2003. Making sense of latent TGFbeta activation. J Cell Sci. 116: 217-224.

Aubert JD, Dalal BI, Bai TR, Roberts CR, Hayashi S, Hogg JC, 1994. Transforming growth factor beta 1 gene expression in human airways. Thorax 49: 225-232.

Bach EA, Aguet M, Schreiber RD, 1997. The IFN gamma receptor: a paradigm for cytokine receptor signaling. Annu. Rev. Immunol 15: 563-591.

Bain J, Plater L, Elliott M, Shpiro N, Hastie CJ, McLauchlan H, Klevernic I, Arthur JS, Alessi DR, Cohen P, 2007. The selectivity of protein kinase inhibitors: a further update. Biochem. J 408: 297-315.

Balzar S CHSPCMTJSMWS. Increased TGF-beta2 in severe asthma with eosinophilia. J Allergy Clin Immunol 115, 110-117. 2005.
Ref Type: Generic

Batra V, Musani AI, Hastie AT, Khurana S, Carpenter KA, Zangrilli JG, Peters SP, 2004. Bronchoalveolar lavage fluid concentrations of transforming growth factor (TGF)-beta1, TGF-beta2, interleukin (IL)-4 and IL-13 after segmental allergen challenge and their effects on alpha-smooth muscle actin and collagen III synthesis by primary human lung fibroblasts. Clin Exp. Allergy 34: 437-444.

Bentley JK, Newcomb DC, Goldsmith AM, Jia Y, Sajjan US, Hershenson MB, 2007. Rhinovirus activates interleukin-8 expression via a Src/p110beta phosphatidylinositol 3-kinase/Akt pathway in human airway epithelial cells. J Virol. 81: 1186-1194.

Berghall H, Siren J, Sarkar D, Julkunen I, Fisher PB, Vainionpaa R, Matikainen S, 2006. The interferon-inducible RNA helicase, mda-5, is involved in measles virus-induced expression of antiviral cytokines. Microbes. Infect. 8: 2138-2144.

Bluyssen AR, Durbin JE, Levy DE, 1996. ISGF3 gamma p48, a specificity switch for interferon activated transcription factors. Cytokine Growth Factor Rev. 7: 11-17.

Boero S, Sabatini F, Silvestri M, Petecchia L, Nachira A, Pezzolo A, Scarso L, Rossi GA, 2007. Modulation of human lung fibroblast functions by ciclesonide: evidence for its conversion into the active metabolite desisobutyryl-ciclesonide. Immunol. Lett. 112: 39-46.

Bonjardim CA, Ferreira PC, Kroon EG, 2009. Interferons: signaling, antiviral and viral evasion. Immunol Lett. 122: 1-11.

Bouchard MJ, Wang L, Schneider RJ, 2006. Activation of focal adhesion kinase by hepatitis B virus HBx protein: multiple functions in viral replication. J Virol. 80: 4406-4414.

Boxall C, Holgate ST, Davies DE, 2006. The contribution of transforming growth factor-beta and epidermal growth factor signalling to airway remodelling in chronic asthma. Eur. Respir. J 27: 208-229.

Brimnes MK, Bonifaz L, Steinman RM, Moran TM, 2003. Influenza virus-induced dendritic cell maturation is associated with the induction of strong T cell immunity to a coadministered, normally nonimmunogenic protein. J Exp. Med. 198: 133-144.

Bromann PA, Korkaya H, Webb CP, Miller J, Calvin TL, Courtneidge SA, 2005. Platelet-derived growth factor stimulates Src-dependent mRNA stabilization of specific early genes in fibroblasts. J Biol. Chem. 280: 10253-10263.

Brooks GD, Buchta KA, Swenson CA, Gern JE, Busse WW, 2003. Rhinovirus-induced interferon-gamma and airway responsiveness in asthma. Am J Respir. Crit Care Med. 168: 1091-1094.

Burgess JK, 2009. The role of the extracellular matrix and specific growth factors in the regulation of inflammation and remodelling in asthma. Pharmacol. Ther. 122: 19-29.

Chakir J, Shannon J, Molet S, Fukakusa M, Elias J, Laviolette M, Boulet LP, Hamid Q, 2003. Airway remodeling-associated mediators in moderate to severe asthma: effect of steroids on TGF-beta, IL-11, IL-17, and type I and type III collagen expression. J Allergy Clin Immunol 111: 1293-1298.

Chen C, Huang X, Sheppard D, 2006. ADAM33 is not essential for growth and development and does not modulate allergic asthma in mice. Mol. Cell Biol. 26: 6950-6956.

Chi B, Dickensheets HL, Spann KM, Alston MA, Luongo C, Dumoutier L, Huang J, Renauld JC, Kotenko SV, Roederer M, Beeler JA, Donnelly RP, Collins PL, Rabin RL, 2006. Alpha and lambda interferon together mediate suppression of CD4 T cells induced by respiratory syncytial virus. J Virol. 80: 5032-5040.

Chu HW BSSGWJTJSPWSE. Transforming growth factor-beta2 induces bronchial epithelial mucin expression in asthma. Am J Pathol 165[4], 1097-1106. 2008.
Ref Type: Generic

Chu JJ, Yang PL, 2007. c-Src protein kinase inhibitors block assembly and maturation of dengue virus. Proc. Natl. Acad. Sci. U. S. A 104: 3520-3525.

Chu WM, Ostertag D, Li ZW, Chang L, Chen Y, Hu Y, Williams B, Perrault J, Karin M, 1999. JNK2 and IKKbeta are required for activating the innate response to viral infection. Immunity. 11: 721-731.

Chung CD, Liao J, Liu B, Rao X, Jay P, Berta P, Shuai K, 1997. Specific inhibition of Stat3 signal transduction by PIAS3. Science 278: 1803-1805.

Cicchini C, Laudadio I, Citarella F, Corazzari M, Steindler C, Conigliaro A, Fantoni A, Amicone L, Tripodi M, 2008. TGFbeta-induced EMT requires focal adhesion kinase (FAK) signaling. Exp. Cell Res. 314: 143-152.

Clark DA, Coker R, 1998. Transforming growth factor-beta (TGF-beta). Int. J Biochem. Cell Biol. 30: 293-298.

Cohn L, Elias JA, Chupp GL, 2004. Asthma: mechanisms of disease persistence and progression. Annu. Rev. Immunol 22: 789-815.

Contoli M, Message SD, Laza-Stanca V, Edwards MR, Wark PA, Bartlett NW, Kebadze T, Mallia P, Stanciu LA, Parker HL, Slater L, Lewis-Antes A, Kon OM, Holgate ST, Davies DE, Kotenko SV, Papi A, Johnston SL, 2006b. Role of deficient type III interferon-lambda production in asthma exacerbations. Nat. Med. 12: 1023-1026.

Contoli M, Message SD, Laza-Stanca V, Edwards MR, Wark PA, Bartlett NW, Kebadze T, Mallia P, Stanciu LA, Parker HL, Slater L, Lewis-Antes A, Kon OM, Holgate ST, Davies DE, Kotenko SV, Papi A, Johnston SL, 2006a. Role of deficient type III interferon-lambda production in asthma exacerbations. Nat. Med. 12: 1023-1026.

Cooney MK, Kenny GE, 1977. Demonstration of dual rhinovirus infection in humans by isolation of different serotypes in human heteroploid (HeLa) and human diploid fibroblast cell cultures. J Clin Microbiol. 5: 202-207.

Corne JM, Marshall C, Smith S, Schreiber J, Sanderson G, Holgate ST, Johnston SL, 2002. Frequency, severity, and duration of rhinovirus infections in asthmatic and non-asthmatic individuals: a longitudinal cohort study. Lancet 359: 831-834.

Corrigan CJ, Hartnell A, Kay AB, 1988. T lymphocyte activation in acute severe asthma. Lancet 1: 1129-1132.

Dahlen SE, Hedqvist P, Hammarstrom S, Samuelsson B, 1980. Leukotrienes are potent constrictors of human bronchi. Nature 288: 484-486.

Darnell JE, Jr., Kerr IM, Stark GR, 1994. Jak-STAT pathways and transcriptional activation in response to IFNs and other extracellular signaling proteins. Science 264: 1415-1421.

Datto MB, Li Y, Panus JF, Howe DJ, Xiong Y, Wang XF, 1995. Transforming growth factor beta induces the cyclin-dependent kinase inhibitor p21 through a p53-independent mechanism. Proc. Natl. Acad. Sci. U. S. A 92: 5545-5549.

Decker T, Lew DJ, Mirkovitch J, Darnell JE, Jr., 1991. Cytoplasmic activation of GAF, an IFN-gamma-regulated DNA-binding factor. EMBO J 10: 927-932.

Deszcz L, Gaudernak E, Kuechler E, Seipelt J, 2005. Apoptotic events induced by human rhinovirus infection. J Gen. Virol. 86: 1379-1389.

Dharmage SC, Erbas B, Jarvis D, Wjst M, Raherison C, Norback D, Heinrich J, Sunyer J, Svanes C, 2009. Do childhood respiratory infections continue to influence adult respiratory morbidity? Eur. Respir. J 33: 237-244.

Dougherty RH, Fahy JV, 2009. Acute exacerbations of asthma: epidemiology, biology and the exacerbation-prone phenotype. Clin Exp. Allergy 39: 193-202.

Dreschers S, Dumitru CA, Adams C, Gulbins E, 2007. The cold case: are rhinoviruses perfectly adapted pathogens? Cell Mol. Life Sci. 64: 181-191.

Dykxhoorn DM, Lieberman J, 2005. The silent revolution: RNA interference as basic biology, research tool, and therapeutic. Annu. Rev. Med. 56: 401-423.

Edwards MR, Slater L, Johnston SL, 2007. Signalling pathways mediating type I interferon gene expression. Microbes. Infect. 9: 1245-1251.

Fanta CH, 2009. Asthma. N. Engl. J Med. 360: 1002-1014.

Feltis BN, Wignarajah D, Reid DW, Ward C, Harding R, Walters EH, 2007. Effects of inhaled fluticasone on angiogenesis and vascular endothelial growth factor in asthma. Thorax 62: 314-319.

Fitzgerald KA, McWhirter SM, Faia KL, Rowe DC, Latz E, Golenbock DT, Coyle AJ, Liao SM, Maniatis T, 2003. IKKepsilon and TBK1 are essential components of the IRF3 signaling pathway. Nat. Immunol 4: 491-496.

Flood-Page PT, Menzies-Gow AN, Kay AB, Robinson DS, 2003. Eosinophil's role remains uncertain as anti-interleukin-5 only partially depletes numbers in asthmatic airway. Am J Respir. Crit Care Med. 167: 199-204.

Fox SW, Haque SJ, Lovibond AC, Chambers TJ, 2003. The possible role of TGF-beta-induced suppressors of cytokine signaling expression in osteoclast/macrophage lineage commitment in vitro. J Immunol 170: 3679-3687.

Galli SJ, Tsai M, Piliponsky AM, 2008. The development of allergic inflammation. Nature 454: 445-454.

Gern JE, French DA, Grindle KA, Brockman-Schneider RA, Konno S, Busse WW, 2003. Double-stranded RNA induces the synthesis of specific chemokines by bronchial epithelial cells. Am. J Respir. Cell Mol. Biol. 28: 731-737.

Ghildyal R, Dagher H, Donninger H, de Silva D, Li X, Freezer NJ, Wilson JW, Bardin PG, 2005. Rhinovirus infects primary human airway fibroblasts and induces a neutrophil chemokine and a permeability factor. J Med. Virol. 75: 608-615.

Glenisson W, Castronovo V, Waltregny D, 2007. Histone deacetylase 4 is required for TGFbeta1-induced myofibroblastic differentiation. Biochim. Biophys. Acta 1773: 1572-1582.

Gomis RR, Alarcon C, Nadal C, Van PC, Massague J, 2006. C/EBPbeta at the core of the TGFbeta cytostatic response and its evasion in metastatic breast cancer cells. Cancer Cell 10: 203-214.

Grandvaux N, tenOever BR, Servant MJ, Hiscott J, 2002. The interferon antiviral response: from viral invasion to evasion. Curr. Opin. Infect. Dis. 15: 259-267.

Grassme H, Riehle A, Wilker B, Gulbins E, 2005. Rhinoviruses infect human epithelial cells via ceramide-enriched membrane platforms. J Biol. Chem. 280: 26256-26262.

Hail N, Jr., Carter BZ, Konopleva M, Andreeff M, 2006. Apoptosis effector mechanisms: a requiem performed in different keys. Apoptosis. 11: 889-904.

Haller O, Kochs G, Weber F, 2006. The interferon response circuit: induction and suppression by pathogenic viruses. Virology 344: 119-130.

Hannon GJ, Beach D, 1994. p15INK4B is a potential effector of TGF-beta-induced cell cycle arrest. Nature 371: 257-261.

Hansbro NG, Horvat JC, Wark PA, Hansbro PM, 2008. Understanding the mechanisms of viral induced asthma: new therapeutic directions. Pharmacol. Ther. 117: 313-353.

Hatsushika K, Hirota T, Harada M, Sakashita M, Kanzaki M, Takano S, Doi S, Fujita K, Enomoto T, Ebisawa M, Yoshihara S, Sagara H, Fukuda T, Masuyama K, Katoh R, Matsumoto K, Saito H, Ogawa H, Tamari M, Nakao A, 2007. Transforming growth factor-beta(2) polymorphisms are associated with childhood atopic asthma. Clin Exp. Allergy 37: 1165-1174.

Heymann PW, Carper HT, Murphy DD, Platts-Mills TA, Patrie J, McLaughlin AP, Erwin EA, Shaker MS, Hellems M, Peerzada J, Hayden FG, Hatley TK, Chamberlain R, 2004. Viral infections in relation to age, atopy, and season of admission among children hospitalized for wheezing. J Allergy Clin Immunol 114: 239-247.

Hirsch AJ, Medigeshi GR, Meyers HL, DeFilippis V, Fruh K, Briese T, Lipkin WI, Nelson JA, 2005. The Src family kinase c-Yes is required for maturation of West Nile virus particles. J Virol. 79: 11943-11951.

Hiscott J, Nguyen TL, Arguello M, Nakhaei P, Paz S, 2006. Manipulation of the nuclear factor-kappaB pathway and the innate immune response by viruses. Oncogene 25: 6844-6867.

Hiscott J, Pitha P, Genin P, Nguyen H, Heylbroeck C, Mamane Y, Algarte M, Lin R, 1999. Triggering the interferon response: the role of IRF-3 transcription factor. J Interferon Cytokine Res. 19: 1-13.

Holgate ST, 2008. The airway epithelium is central to the pathogenesis of asthma. Allergol. Int. 57: 1-10.

Holgate ST, Church M.K., Lichtenstein L.M. Allergy. 2006a. Mosby Elsevier.
Ref Type: Generic

Holgate ST, Davies DE, Powell RM, Howarth PH, Haitchi HM, Holloway JW, 2007. Local genetic and environmental factors in asthma disease pathogenesis: chronicity and persistence mechanisms. Eur. Respir. J 29: 793-803.

Holgate ST, Yang Y, Haitchi HM, Powell RM, Holloway JW, Yoshisue H, Pang YY, Cakebread J, Davies DE, 2006b. The genetics of asthma: ADAM33 as an example of a susceptibility gene. Proc. Am Thorac. Soc. 3: 440-443.

Honda K, Taniguchi T, 2006. IRFs: master regulators of signalling by Toll-like receptors and cytosolic pattern-recognition receptors. Nat. Rev. Immunol 6: 644-658.

Ihle JN, Kerr IM, 1995. Jaks and Stats in signaling by the cytokine receptor superfamily. Trends Genet. 11: 69-74.

Isaacs A, Lindenmann J, 1957. Virus interference. I. The interferon. Proc. R. Soc. Lond B Biol. Sci. 147: 258-267.

Itoh K, Watanabe A, Funami K, Seya T, Matsumoto M, 2008. The clathrin-mediated endocytic pathway participates in dsRNA-induced IFN-beta production. J Immunol 181: 5522-5529.

Iwasaki A, Medzhitov R, 2004. Toll-like receptor control of the adaptive immune responses. Nat. Immunol 5: 987-995.

Jackson DJ, Gangnon RE, Evans MD, Roberg KA, Anderson EL, Pappas TE, Printz MC, Lee WM, Shult PA, Reisdorf E, Carlson-Dakes KT, Salazar LP, DaSilva DF, Tisler CJ, Gern JE, Lemanske RF, Jr., 2008. Wheezing rhinovirus illnesses in early life predict asthma development in high-risk children. Am J Respir. Crit Care Med. 178: 667-672.

Jinnin M, Ihn H, Tamaki K, 2006. Characterization of SIS3, a novel specific inhibitor of Smad3, and its effect on transforming growth factor-beta1-induced extracellular matrix expression. Mol. Pharmacol. 69: 597-607.

Johnsen IB, Nguyen TT, Ringdal M, Tryggestad AM, Bakke O, Lien E, Espevik T, Anthonsen MW, 2006. Toll-like receptor 3 associates with c-Src tyrosine kinase on endosomes to initiate antiviral signaling. EMBO J 25: 3335-3346.

Johnson PR, Burgess JK, Ge Q, Poniris M, Boustany S, Twigg SM, Black JL, 2006. Connective tissue growth factor induces extracellular matrix in asthmatic airway smooth muscle. Am J Respir. Crit Care Med. 173: 32-41.

Johnson PR, Burgess JK, Underwood PA, Au W, Poniris MH, Tamm M, Ge Q, Roth M, Black JL, 2004. Extracellular matrix proteins modulate asthmatic airway smooth muscle cell proliferation via an autocrine mechanism. J Allergy Clin Immunol 113: 690-696.

Johnston SL, 2005. Overview of virus-induced airway disease. Proc. Am Thorac. Soc. 2: 150-156.

Johnston SL, Pattemore PK, Sanderson G, Smith S, Lampe F, Josephs L, Symington P, O'Toole S, Myint SH, Tyrrell DA, ., 1995. Community study of role of viral infections in exacerbations of asthma in 9-11 year old children. BMJ 310: 1225-1229.

Jordan WJ, Eskdale J, Boniotto M, Rodia M, Kellner D, Gallagher G, 2007. Modulation of the human cytokine response by interferon lambda-1 (IFN-lambda1/IL-29). Genes Immun. 8: 13-20.

Kanaoka Y, Boyce JA, 2004. Cysteinyl leukotrienes and their receptors: cellular distribution and function in immune and inflammatory responses. J Immunol 173: 1503-1510.

Kato H, Takeuchi O, Sato S, Yoneyama M, Yamamoto M, Matsui K, Uematsu S, Jung A, Kawai T, Ishii KJ, Yamaguchi O, Otsu K, Tsujimura T, Koh CS, Reis e Sousa, Matsuura Y, Fujita T, Akira S, 2006. Differential roles of MDA5 and RIG-I helicases in the recognition of RNA viruses. Nature 441: 101-105.

Kaul P, Biagioli MC, Singh I, Turner RB, 2000. Rhinovirus-induced oxidative stress and interleukin-8 elaboration involves p47-phox but is independent of attachment to intercellular adhesion molecule-1 and viral replication. J Infect. Dis. 181: 1885-1890.

Kawai T, Akira S, 2006. Innate immune recognition of viral infection. Nat. Immunol 7: 131-137.

Kawai T, Akira S, 2007c. Antiviral signaling through pattern recognition receptors. J Biochem. (Tokyo) 141: 137-145.

Kay AB, 2001. Allergy and allergic diseases. First of two parts. N. Engl. J Med. 344: 30-37.

Kessler DS, Veals SA, Fu XY, Levy DE, 1990. Interferon-alpha regulates nuclear translocation and DNA-binding affinity of ISGF3, a multimeric transcriptional activator. Genes Dev. 4: 1753-1765.

Khetsuriani N, Kazerouni NN, Erdman DD, Lu X, Redd SC, Anderson LJ, Teague WG, 2007. Prevalence of viral respiratory tract infections in children with asthma. J Allergy Clin Immunol 119: 314-321.

Klein NP, Bouchard MJ, Wang LH, Kobarg C, Schneider RJ, 1999. Src kinases involved in hepatitis B virus replication. EMBO J 18: 5019-5027.

Knight D, 2002. Increased permeability of asthmatic epithelial cells to pollutants. Does this mean that they are intrinsically abnormal? Clin Exp. Allergy 32: 1263-1265.

Knight DA, Holgate ST, 2003. The airway epithelium: structural and functional properties in health and disease. Respirology. 8: 432-446.

Kotla S, Peng T, Bumgarner RE, Gustin KE, 2008. Attenuation of the type I interferon response in cells infected with human rhinovirus. Virology 374: 399-410.

Kulkarni AB, Huh CG, Becker D, Geiser A, Lyght M, Flanders KC, Roberts AB, Sporn MB, Ward JM, Karlsson S, 1993. Transforming growth factor beta 1 null mutation in mice causes excessive inflammatory response and early death. Proc. Natl. Acad. Sci. U. S. A 90: 770-774.

Larue L, Bellacosa A, 2005. Epithelial-mesenchymal transition in development and cancer: role of phosphatidylinositol 3' kinase/AKT pathways. Oncogene 24: 7443-7454.

Leckie MJ, ten BA, Khan J, Diamant Z, O'Connor BJ, Walls CM, Mathur AK, Cowley HC, Chung KF, Djukanovic R, Hansel TT, Holgate ST, Sterk PJ, Barnes PJ, 2000. Effects of an interleukin-5 blocking monoclonal antibody on eosinophils, airway hyper-responsiveness, and the late asthmatic response. Lancet 356: 2144-2148.

Levy DE, Marie I, Smith E, Prakash A, 2002. Enhancement and diversification of IFN induction by IRF-7-mediated positive feedback. J Interferon Cytokine Res. 22: 87-93.

Li R, Waga S, Hannon GJ, Beach D, Stillman B, 1994. Differential effects by the p21 CDK inhibitor on PCNA-dependent DNA replication and repair. Nature 371: 534-537.

Lin R, Heylbroeck C, Pitha PM, Hiscott J, 1998. Virus-dependent phosphorylation of the IRF-3 transcription factor regulates nuclear translocation, transactivation potential, and proteasome-mediated degradation. Mol. Cell Biol. 18: 2986-2996.

Liu B, Liao J, Rao X, Kushner SA, Chung CD, Chang DD, Shuai K, 1998. Inhibition of Stat1-mediated gene activation by PIAS1. Proc. Natl. Acad. Sci. U. S. A 95: 10626-10631.

Liu B, Mink S, Wong KA, Stein N, Getman C, Dempsey PW, Wu H, Shuai K, 2004. PIAS1 selectively inhibits interferon-inducible genes and is important in innate immunity. Nat. Immunol 5: 891-898.

Liu B, Shuai K, 2008. Targeting the PIAS1 SUMO ligase pathway to control inflammation. Trends Pharmacol. Sci. 29: 505-509.

Lundgren R, Soderberg M, Horstedt P, Stenling R, 1988. Morphological studies of bronchial mucosal biopsies from asthmatics before and after ten years of treatment with inhaled steroids. Eur. Respir. J 1: 883-889.

Lynch KR, O'Neill GP, Liu Q, Im DS, Sawyer N, Metters KM, Coulombe N, Abramovitz M, Figueroa DJ, Zeng Z, Connolly BM, Bai C, Austin CP, Chateauneuf A, Stocco R, Greig GM, Kargman S, Hooks SB, Hosfield E, Williams DL, Jr., Ford-Hutchinson AW, Caskey CT, Evans JF, 1999. Characterization of the human cysteinyl leukotriene CysLT1 receptor. Nature 399: 789-793.

Makinde T, Murphy RF, Agrawal DK, 2007. The regulatory role of TGF-beta in airway remodeling in asthma. Immunol. Cell Biol. 85: 348-356.

Manolitsas ND, Trigg CJ, McAulay AE, Wang JH, Jordan SE, D'Ardenne AJ, Davies RJ, 1994. The expression of intercellular adhesion molecule-1 and the beta 1-integrins in asthma. Eur. Respir. J 7: 1439-1444.

Marie I, Durbin JE, Levy DE, 1998b. Differential viral induction of distinct interferon-alpha genes by positive feedback through interferon regulatory factor-7. EMBO J 17: 6660-6669.

Martin JG, Siddiqui S, Hassan M, 2006. Immune responses to viral infections: relevance for asthma. Paediatr. Respir. Rev. 7 Suppl 1: S125-S127.

Martin-Blanco E, 2000. p38 MAPK signalling cascades: ancient roles and new functions. Bioessays 22: 637-645.

Martinez FD, 2009. The origins of asthma and chronic obstructive pulmonary disease in early life. Proc. Am Thorac. Soc. 6: 272-277.

Massague J, Wotton D, 2000. Transcriptional control by the TGF-beta/Smad signaling system. EMBO J 19: 1745-1754.

Matsukura S, Kokubu F, Kurokawa M, Kawaguchi M, Ieki K, Kuga H, Odaka M, Suzuki S, Watanabe S, Takeuchi H, Kasama T, Adachi M, 2006. Synthetic double-stranded RNA induces multiple genes related to inflammation through Toll-like receptor 3 depending on NF-kappaB and/or IRF-3 in airway epithelial cells. Clin Exp. Allergy 36: 1049-1062.

Matsumoto M, Kikkawa S, Kohase M, Miyake K, Seya T, 2002a. Establishment of a monoclonal antibody against human Toll-like receptor 3 that blocks double-stranded RNA-mediated signaling. Biochem. Biophys. Res. Commun. 293: 1364-1369.

McCann KL, Imani F, 2007. Transforming growth factor beta enhances respiratory syncytial virus replication and tumor necrosis factor alpha induction in human epithelial cells. J. Virol. 81: 2880-2886.

Menzies-Gow A, Flood-Page P, Sehmi R, Burman J, Hamid Q, Robinson DS, Kay AB, Denburg J, 2003. Anti-IL-5 (mepolizumab) therapy induces bone marrow eosinophil maturational arrest and decreases eosinophil progenitors in the bronchial mucosa of atopic asthmatics. J Allergy Clin Immunol 111: 714-719.

Mitra SK, Schlaepfer DD, 2006. Integrin-regulated FAK-Src signaling in normal and cancer cells. Curr. Opin. Cell Biol. 18: 516-523.

Miyazaki M, Sakaguchi M, Akiyama I, Sakaguchi Y, Nagamori S, Huh NH, 2004. Involvement of interferon regulatory factor 1 and S100C/A11 in growth inhibition by transforming growth factor beta 1 in human hepatocellular carcinoma cells. Cancer Res. 64: 4155-4161.

Montefort S, Roberts JA, Beasley R, Holgate ST, Roche WR, 1992. The site of disruption of the bronchial epithelium in asthmatic and non- asthmatic subjects. Thorax 47: 499-503.

Moss EG, 2001. RNA interference: it's a small RNA world. Curr. Biol. 11: R772-R775.

Nakao K, Nakata K, Yamashita M, Tamada Y, Hamasaki K, Ishikawa H, Kato Y, Eguchi K, Ishii N, 1999. p48 (ISGF-3gamma) is involved in interferon-alpha-induced suppression of hepatitis B virus enhancer-1 activity. J Biol. Chem. 274: 28075-28078.

Newcomb DC, Sajjan U, Nanua S, Jia Y, Goldsmith AM, Bentley JK, Hershenson MB, 2005. Phosphatidylinositol 3-kinase is required for rhinovirus-induced airway epithelial cell interleukin-8 expression. J Biol. Chem. 280: 36952-36961.

Novick D, Cohen B, Rubinstein M, 1994. The human interferon alpha/beta receptor: characterization and molecular cloning. Cell 77: 391-400.

Okutani D, Lodyga M, Han B, Liu M, 2006. Src protein tyrosine kinase family and acute inflammatory responses. Am J Physiol Lung Cell Mol. Physiol 291: L129-L141.

Oliver BG, Johnston SL, Baraket M, Burgess JK, King NJ, Roth M, Lim S, Black JL, 2006. Increased proinflammatory responses from asthmatic human airway smooth muscle cells in response to rhinovirus infection. Respir. Res. 7: 71.

Padgett RW, Reiss M, 2007. TGFbeta superfamily signaling: notes from the desert. Development 134: 3565-3569.

Palvimo JJ, 2007a. PIAS proteins as regulators of small ubiquitin-related modifier (SUMO) modifications and transcription. Biochem. Soc. Trans. 35: 1405-1408.

Papadopoulos NG, Moustaki M, Tsolia M, Bossios A, Astra E, Prezerakou A, Gourgiotis D, Kafetzis D, 2002. Association of rhinovirus infection with increased disease severity in acute bronchiolitis. Am J Respir. Crit Care Med. 165: 1285-1289.

Peters-Golden M, Henderson WR, Jr., 2007. Leukotrienes. N. Engl. J Med. 357: 1841-1854.

Pichlmair A, Schulz O, Tan CP, Naslund TI, Liljestrom P, Weber F, Reis e Sousa, 2006. RIG-I-mediated antiviral responses to single-stranded RNA bearing 5'-phosphates. Science 314: 997-1001.

Pohunek P, Warner JO, Turzikova J, Kudrmann J, Roche WR, 2005. Markers of eosinophilic inflammation and tissue re-modelling in children before clinically diagnosed bronchial asthma. Pediatr. Allergy Immunol 16: 43-51.

Prockop DJ, Kivirikko KI, 1995. Collagens: molecular biology, diseases, and potentials for therapy. Annu. Rev. Biochem. 64: 403-434.

Proetzel G, Pawlowski SA, Wiles MV, Yin M, Boivin GP, Howles PN, Ding J, Ferguson MW, Doetschman T, 1995. Transforming growth factor-beta 3 is required for secondary palate fusion. Nat. Genet. 11: 409-414.

Puddicombe SM, Polosa R, Richter A, Krishna MT, Howarth PH, Holgate ST, Davies DE, 2000. Involvement of the epidermal growth factor receptor in epithelial repair in asthma. FASEB J. 14: 1362-1374.

Pulleyn LJ, Newton R, Adcock IM, Barnes PJ, 2001. TGFbeta1 allele association with asthma severity. Hum. Genet. 109: 623-627.

Puxeddu I, Pang YY, Harvey A, Haitchi HM, Nicholas B, Yoshisue H, Ribatti D, Clough G, Powell RM, Murphy G, Hanley NA, Wilson DI, Howarth PH, Holgate ST, Davies DE, 2008. The soluble form of a disintegrin and metalloprotease 33 promotes angiogenesis: implications for airway remodeling in asthma. J Allergy Clin Immunol 121: 1400-6, 1406.

Rahimi RA, Leof EB, 2007. TGF-beta signaling: a tale of two responses. J Cell Biochem. 102: 593-608.

Raung SL, Chen SY, Liao SL, Chen JH, Chen CJ, 2007. Japanese encephalitis virus infection stimulates Src tyrosine kinase in neuron/glia. Neurosci. Lett. 419: 263-268.

Reardon C, McKay DM, 2007. TGF-beta suppresses IFN-gamma-STAT1-dependent gene transcription by enhancing STAT1-PIAS1 interactions in epithelia but not monocytes/macrophages. J Immunol 178: 4284-4295.

Redington AE, Madden J, Frew AJ, Djukanovic R, Roche WR, Holgate ST, Howarth PH, 1997. Transforming growth factor-beta 1 in asthma. Measurement in bronchoalveolar lavage fluid. Am J Respir. Crit Care Med. 156: 642-647.

Ribbene A, Bucchieri F, Wark PA, Andrews A-L, Puddicombe SM, Zummo G, Holgate S.T., Davies D.E., 2007. Epithelial-Mesenchymal Communication Following Rhinovirus Infection Of Asthmatic Bronchial Epithelial Cells. Am J Resp Crit Care Med 175: A479.

Robinson PJ, Hegele RG, Schellenberg RR, 1997. Allergic sensitization increases airway reactivity in guinea pigs with respiratory syncytial virus bronchiolitis. J Allergy Clin Immunol 100: 492-498.

Ross S, Hill CS, 2008. How the Smads regulate transcription. Int. J Biochem. Cell Biol. 40: 383-408.

Rytinki MM, Kaikkonen S, Pehkonen P, Jaaskelainen T, Palvimo JJ, 2009. PIAS proteins: pleiotropic interactors associated with SUMO. Cell Mol. Life Sci.

Samuel CE, 2001. Antiviral actions of interferons. Clin Microbiol. Rev. 14: 778-809, table.

Sanchez-Capelo A, 2005. Dual role for TGF-beta1 in apoptosis. Cytokine Growth Factor Rev. 16: 15-34.

Sanford LP, Ormsby I, Gittenberger-de Groot AC, Sariola H, Friedman R, Boivin GP, Cardell EL, Doetschman T, 1997. TGFbeta2 knockout mice have multiple developmental defects that are non-overlapping with other TGFbeta knockout phenotypes. Development 124: 2659-2670.

Sato M, Suemori H, Hata N, Asagiri M, Ogasawara K, Nakao K, Nakaya T, Katsuki M, Noguchi S, Tanaka N, Taniguchi T, 2000. Distinct and essential roles of transcription factors IRF-3 and IRF-7 in response to viruses for IFN-alpha/beta gene induction. Immunity. 13: 539-548.

Sato S, Sugiyama M, Yamamoto M, Watanabe Y, Kawai T, Takeda K, Akira S, 2003. Toll/IL-1 receptor domain-containing adaptor inducing IFN-beta (TRIF) associates with TNF receptor-associated factor 6 and TANK-binding kinase 1, and activates two distinct transcription factors, NF-kappa B and IFN-regulatory factor-3, in the Toll-like receptor signaling. J Immunol 171: 4304-4310.

Schafer SL, Lin R, Moore PA, Hiscott J, Pitha PM, 1998. Regulation of type I interferon gene expression by interferon regulatory factor-3. J Biol. Chem. 273: 2714-2720.

Schiller M, Javelaud D, Mauviel A, 2004. TGF-beta-induced SMAD signaling and gene regulation: consequences for extracellular matrix remodeling and wound healing. J Dermatol. Sci. 35: 83-92.

Schwarze J, Cieslewicz G, Hamelmann E, Joetham A, Shultz LD, Lamers MC, Gelfand EW, 1999. IL-5 and eosinophils are essential for the development of airway hyperresponsiveness following acute respiratory syncytial virus infection. J Immunol 162: 2997-3004.

Seoane J, 2004. p21(WAF1/CIP1) at the switch between the anti-oncogenic and oncogenic faces of TGFbeta. Cancer Biol. Ther. 3: 226-227.

Seth RB, Sun L, Ea CK, Chen ZJ, 2005. Identification and characterization of MAVS, a mitochondrial antiviral signaling protein that activates NF-kappaB and IRF 3. Cell 122: 669-682.

Sharma S, tenOever BR, Grandvaux N, Zhou GP, Lin R, Hiscott J, 2003. Triggering the interferon antiviral response through an IKK-related pathway. Science 300: 1148-1151.

Shull MM, Ormsby I, Kier AB, Pawlowski S, Diebold RJ, Yin M, Allen R, Sidman C, Proetzel G, Calvin D, ., 1992. Targeted disruption of the mouse transforming growth factor-beta 1 gene results in multifocal inflammatory disease. Nature 359: 693-699.

Siegel PM, Massague J, 2003. Cytostatic and apoptotic actions of TGF-beta in homeostasis and cancer. Nat. Rev. Cancer 3: 807-821.

Silverman RH, 2007. Viral encounters with 2',5'-oligoadenylate synthetase and RNase L during the interferon antiviral response. J Virol. 81: 12720-12729.

Stark GR, Kerr IM, Williams BR, Silverman RH, Schreiber RD, 1998. How cells respond to interferons. Annu. Rev. Biochem. 67: 227-264.

Stern DA, Guerra S, Halonen M, Wright AL, Martinez FD, 2007. Low IFN-gamma production in the first year of life as a predictor of wheeze during childhood. J Allergy Clin Immunol 120: 835-841.

Suhara W, Yoneyama M, Kitabayashi I, Fujita T, 2002. Direct involvement of CREB-binding protein/p300 in sequence-specific DNA binding of virus-activated interferon regulatory factor-3 holocomplex. J Biol. Chem. 277: 22304-22313.

Tager AM, Luster AD, 2003. BLT1 and BLT2: the leukotriene B(4) receptors. Prostaglandins Leukot. Essent. Fatty Acids 69: 123-134.

Taimen P, Berghall H, Vainionpaa R, Kallajoki M, 2004. NuMA and nuclear lamins are cleaved during viral infection--inhibition of caspase activity prevents cleavage and rescues HeLa cells from measles virus-induced but not from rhinovirus 1B-induced cell death. Virology 320: 85-98.

Takaoka A, Yanai H, 2006. Interferon signalling network in innate defence. Cell Microbiol. 8: 907-922.

Takeuchi O, Akira S, 2007. Recognition of viruses by innate immunity. Immunol Rev. 220: 214-224.

Taniguchi T, Takaoka A, 2001. A weak signal for strong responses: interferon-alpha/beta revisited. Nat. Rev. Mol. Cell Biol. 2: 378-386.

Tauro S, Su YC, Thomas S, Schwarze J, Matthaei KI, Townsend D, Simson L, Tripp RA, Mahalingam S, 2008. Molecular and cellular mechanisms in the viral exacerbation of asthma. Microbes. Infect. 10: 1014-1023.

Tekkanat KK, Maassab HF, Cho DS, Lai JJ, John A, Berlin A, Kaplan MH, Lukacs NW, 2001. IL-13-induced airway hyperreactivity during respiratory syncytial virus infection is STAT6 dependent. J Immunol 166: 3542-3548.

Theofilopoulos AN, Baccala R, Beutler B, Kono DH, 2005. Type I interferons (alpha/beta) in immunity and autoimmunity. Annu. Rev. Immunol 23: 307-336.

Thomas BJ, Lindsay M, Dagher H, Freezer NJ, Li D, Ghildyal R, Bardin PG, 2009. Transforming Growth Factor-{beta} Enhances Rhinovirus Infection by Diminishing Early Innate Responses. Am J Respir. Cell Mol. Biol.

Thomas SM, Brugge JS, 1997. Cellular functions regulated by Src family kinases. Annu. Rev. Cell Dev. Biol. 13: 513-609.

Uze G, Lutfalla G, Gresser I, 1990. Genetic transfer of a functional human interferon alpha receptor into mouse cells: cloning and expression of its cDNA. Cell 60: 225-234.

Uze G, Monneron D, 2007. IL-28 and IL-29: newcomers to the interferon family. Biochimie 89: 729-734.

Van EP, Little RD, Dupuis J, Del Mastro RG, Falls K, Simon J, Torrey D, Pandit S, McKenny J, Braunschweiger K, Walsh A, Liu Z, Hayward B, Folz C, Manning SP, Bawa A, Saracino L, Thackston M, Benchekroun Y, Capparell N, Wang M, Adair R, Feng Y, Dubois J, FitzGerald MG, Huang H, Gibson R, Allen KM, Pedan A, Danzig MR, Umland SP, Egan RW, Cuss FM, Rorke S, Clough JB, Holloway JW, Holgate ST, Keith TP, 2002. Association of the ADAM33 gene with asthma and bronchial hyperresponsiveness. Nature 418: 426-430.

Vanhatupa S, Ungureanu D, Paakkunainen M, Silvennoinen O, 2008. MAPK-induced Ser727 phosphorylation promotes SUMOylation of STAT1. Biochem. J 409: 179-185.

Vignola AM, Chanez P, Chiappara G, Merendino A, Pace E, Rizzo A, la Rocca AM, Bellia V, Bonsignore G, Bousquet J, 1997. Transforming growth factor-beta expression in mucosal biopsies in asthma and chronic bronchitis. Am J Respir. Crit Care Med. 156: 591-599.

von ME, 2009. Gene-environment interactions in asthma. J Allergy Clin Immunol 123: 3-11.

Wahl SM, 2007. Transforming growth factor-beta: innately bipolar. Curr. Opin. Immunol 19: 55-62.

Walker C, Kaegi MK, Braun P, Blaser K, 1991. Activated T cells and eosinophilia in bronchoalveolar lavages from subjects with asthma correlated with disease severity. J Allergy Clin Immunol 88: 935-942.

Wan H, Winton HL, Soeller C, Tovey ER, Gruenert DC, Thompson PJ, Stewart GA, Taylor GW, Garrod DR, Cannell MB, Robinson C, 1999. Der p 1 facilitates transepithelial allergen delivery by disruption of tight junctions. J Clin Invest 104: 123-133.

Wan YY, Flavell RA, 2007. Regulatory T cells, transforming growth factor-beta, and immune suppression. Proc. Am Thorac. Soc. 4: 271-276.

Wark PA, Bucchieri F, Johnston SL, Gibson PG, Hamilton L, Mimica J, Zummo G, Holgate ST, Attia J, Thakkinstian A, Davies DE, 2007a. IFN-gamma-induced protein 10 is a novel biomarker of rhinovirus-induced asthma exacerbations. J Allergy Clin Immunol 120: 586-593.

Wark PA, Johnston SL, Bucchieri F, Powell R, Puddicombe S, Laza-Stanca V, Holgate ST, Davies DE, 2005a. Asthmatic bronchial epithelial cells have a deficient innate immune response to infection with rhinovirus. J Exp. Med. 201: 937-947.

Wathelet MG, Lin CH, Parekh BS, Ronco LV, Howley PM, Maniatis T, 1998. Virus infection induces the assembly of coordinately activated transcription factors on the IFN-beta enhancer in vivo. Mol. Cell 1: 507-518.

Weaver BK, Kumar KP, Reich NC, 1998. Interferon regulatory factor 3 and CREB-binding protein/p300 are subunits of double-stranded RNA-activated transcription factor DRAF1. Mol. Cell Biol. 18: 1359-1368.

Wos M, Sanak M, Soja J, Olechnowicz H, Busse WW, Szczeklik A, 2008. The presence of rhinovirus in lower airways of patients with bronchial asthma. Am J Respir. Crit Care Med. 177: 1082-1089.

Wu P, Dupont WD, Griffin MR, Carroll KN, Mitchel EF, Gebretsadik T, Hartert TV, 2008. Evidence of a causal role of winter virus infection during infancy in early childhood asthma. Am J Respir. Crit Care Med. 178: 1123-1129.

Xepapadaki P, Psarras S, Bossios A, Tsolia M, Gourgiotis D, Liapi-Adamidou G, Constantopoulos AG, Kafetzis D, Papadopoulos NG, 2004. Human Metapneumovirus as a causative agent of acute bronchiolitis in infants. J Clin Virol. 30: 267-270.

Xu J, Lamouille S, Derynck R, 2009. TGF-beta-induced epithelial to mesenchymal transition. Cell Res. 19: 156-172.

Yang Z, Mu Z, Dabovic B, Jurukovski V, Yu D, Sung J, Xiong X, Munger JS, 2007. Absence of integrin-mediated TGFbeta1 activation in vivo recapitulates the phenotype of TGFbeta1-null mice. J Cell Biol. 176: 787-793.

Yoneyama M, Kikuchi M, Natsukawa T, Shinobu N, Imaizumi T, Miyagishi M, Taira K, Akira S, Fujita T, 2004. The RNA helicase RIG-I has an essential function in double-stranded RNA-induced innate antiviral responses. Nat. Immunol 5: 730-737.

Yoneyama M, Suhara W, Fukuhara Y, Fukuda M, Nishida E, Fujita T, 1998. Direct triggering of the type I interferon system by virus infection: activation of a transcription factor complex containing IRF-3 and CBP/p300. EMBO J 17: 1087-1095.

Zhang S, Smartt H, Holgate ST, Roche WR, 1999. Growth factors secreted by bronchial epithelial cells control myofibroblast proliferation: an in vitro co-culture model of airway remodeling in asthma. Lab Invest 79: 395-405.

Zhang YE, 2009. Non-Smad pathways in TGF-beta signaling. Cell Res. 19: 128-139.

Zhao J, Takamura M, Yamaoka A, Odajima Y, Iikura Y, 2002. Altered eosinophil levels as a result of viral infection in asthma exacerbation in childhood. Pediatr. Allergy Immunol 13: 47-50.

Academic Thesis: Declaration Of Authorship

I, Nicole Bedke declare that this thesis and the work presented in it are my own and has been generated by me as the result of my own original research.

The molecular mechanisms involved in rhinovirus-induced asthma exacerbation and its potential therapy

I confirm that:

1. This work was done wholly or mainly while in candidature for a research degree at this University;
2. Where any part of this thesis has previously been submitted for a degree or any other qualification at this University or any other institution, this has been clearly stated;
3. Where I have consulted the published work of others, this is always clearly attributed;
4. Where I have quoted from the work of others, the source is always given. With the exception of such quotations, this thesis is entirely my own work;
5. I have acknowledged all main sources of help;
6. Where the thesis is based on work done by myself jointly with others, I have made clear exactly what was done by others and what I have contributed myself;
7. Either none of this work has been published before submission, or parts of this work have been published as:

Bedke N et al. Contribution of bronchial fibroblasts to the antiviral response in asthma. J Immunol. 2009 Mar 15;182(6):3660-7.

Signed: .....

Date: 01. June 2010